



Universidad de Concepción
Dirección de Postgrado
Facultad de Ciencias Biológicas
Programa de Doctorado en Ciencias Biológicas Mención Microbiología

DETERMINACIÓN DE LOS TIPOS DE INTERACCIÓN ENTRE *HELICOBACTER PYLORI* Y *CANDIDA ALBICANS*



Tesis para optar al grado de Doctor en Ciencias Biológicas
Mención Microbiología

SIXTA LILIANA PALENCIA LUNA
CONCEPCIÓN-CHILE
2020

Profesor Guía: Dra. Apolinaria García Cancino
Dpto. de Microbiología, Facultad de Ciencias Biológicas
Universidad de Concepción

Esta tesis ha sido realizada en el Departamento de Microbiología de la Facultad de Ciencias Biológicas, Universidad de Concepción.

Profesores integrantes Comisión Evaluadora:

Dra. Apolinaria García Cancino
Facultad de Ciencias Biológicas
Universidad de Concepción

Dr. Carlos González Correa
Facultad de Ciencias Biológicas
Universidad de Concepción

Dr. Manuel Meléndrez Castro
Facultad de Ingeniería
Universidad de Concepción

Dr. Patricio Godoy Martínez
Profesor Evaluador Externo
Universidad Austral de Chile

Dr. Víctor Campos Araneda
Director Programa Doctorado
Facultad de Ciencias Biológicas
Universidad de Concepción



**Tesis financiada por
CONICYT-PCHA/ Doctorado Nacional/2017-21170513**



AGRADECIMIENTOS

A Dios por su amor...

La autora agradece a las siguientes entidades y personas que de una u otra forma hicieron posible desarrollar totalmente el presente trabajo de investigación.

Comisión Nacional de Investigación Científica y Tecnológica CONICYT, por el financiamiento de mis estudios doctorales durante el periodo (2017-2019) y la beca de apoyo a la realización de tesis doctoral. Por medio de este apoyo incondicional del Gobierno de Chile fue posible realizar de manera satisfactoria mi formación doctoral en la Universidad de Concepción.

Escuela de Graduados de la Universidad de Concepción, por la beca de arancel y estipendio durante el periodo (2015-2016) y por la beca de arancel dada a final de mis estudios (2020).

A la **Dra. Apolinaria García Cancino** por la buena disposición y permitirme realizar mi trabajo de investigación bajo su dirección, además de sus valiosos aportes académicos.

Al **Dr. Manuel Palencia Luna** por sus valiosas asesorías en los diferentes componentes de la química, lo cual permitió desarrollar un trabajo interdisciplinario, además de permitirme realizar mis pasantías en el Laboratorio de Ciencias con Aplicaciones Tecnológicas y Bioinorgánica del grupo GI-CAT, de la Universidad del Valle, Cali- Colombia.

A los doctores **Manuel Meléndrez Castro**, **Carlos González Correa** y **Patricio Godoy Martínez** miembros de la comisión encargada de evaluar esta tesis, por sus sugerencias, tiempo y disposición.

A la **Dra. Verónica Madrid Valdebenito** por su disposición y palabra de ánimo que nunca faltaron.

Al personal integrante del Laboratorio de investigación en Ciencias con aplicaciones tecnológicas GI-CAT, del departamento de Ciencias Química de la Universidad del Valle, Cali- Colombia, en especial a **MSc Tulio Lerma**, **MSc María E. Berrios**, **MSc. Viviana Garcés** y **MSc Mayra Mora**.

A la secretaria del programa de doctorado en microbiología **Sra. Margareth Santana Jaramillo**, por sus palabras llenas de fe, energía y positivismo que me reconfortaron en los malos y buenos momentos.

A esos amigos que siempre aportaron un apoyo emocional de manera incondicional y sincera. Por su confianza y amistad: **Carla Daza Castro, Valeria García Castillo, Jandira Tomas y Adolay Sobarzo Escares.**

A mis hijos **Emily, Máximo y Anagabriel**, por ser mis tres tesoros que le dan luz a mi vida y la razón para nunca desfallecer.

A mí querida familia Saida, Víctor, Manuel, Andrea, Manuel D, Daniel, Alice y Helen.

A mi esposo **Cristian Gabriel Rojas Vergara**, por su amor, amistad, comprensión y respaldo absoluto, siendo esencial para alcanzar un peldaño más en mi vida profesional.



CONTENTS

Resumen	7
Abstract	10
Prologo	13
1. CHAPTER I. Introduction	16
2. CHAPTER II. General background	18
2.1 Article 1. Fungi-bacterium interactions: <i>Helicobacter pylori</i> - <i>Candida albicans</i>	
2.2 Article 2. Polymicrobial Biofilms: Fundamentals, diseases, and treatments – A review	
3. CHAPTER III. Hypothesis, General objective and Specific objectives	90
4. CHAPTER IV. Mid-infrared vibrational spectrum characterization of outer surface of <i>Candida albicans</i> by Functionally-Enhanced Derivative Spectroscopy (FEDS)	91
5. CHAPTER V. Vibrational spectrum characterization of outer surface of <i>Helicobacter pylori</i> biofilms by Functionally-Enhanced Derivative Spectroscopy (FEDS)	112
6. CHAPTER VI. Multiple surface interaction mechanisms direct the anchoring, co-aggregation and formation of polymicrobial biofilm between <i>Candida albicans</i> and <i>Helicobacter pylori</i>	132
7. CHAPTER VII. Study of the promotion of the interconversion between coccoid and bacillary forms resulting of <i>Helicobacter pylori</i> and <i>Candida albicans</i> interaction	167
8. CHAPTER VIII. Discussion	181
9. CONCLUSIONS	185
10. PERSPECTIVES	186

RESUMEN

Las interacciones microbiológicas en los organismos y la naturaleza se consideran estrategias esenciales para asegurar la supervivencia, colonización y equilibrio de los diferentes ecosistemas, que generan un amplio espectro de situaciones asociadas a la patogenicidad, nutrición, adquisición de genes, transporte, construcción de nichos y estructuras comunitarias, entre otros; mediada por diversos parámetros físicos, biológicos y químicos. Comúnmente el estudio de los microorganismos, sean bacterias u hongos, se realiza mediante procedimientos axénicos, es decir, a partir de poblaciones de microorganismos aislados, provenientes de una sola célula. Sin embargo, es claro que este tipo de cultivo son muy extraños en la naturaleza ya que, el crecimiento de los microorganismos en ambientes naturales como aguas, suelos, o el cuerpo humano son de naturaleza mixta (es decir, diferentes poblaciones de microorganismos, de diferentes especies y con diferente origen que comparten el mismo entorno de crecimiento). Es importante indicar que el crecimiento de los microorganismos fenotípicamente está codificado por dos estados, un estado planctónico que lo presenta el 1% de los microorganismos, y un estado sésil o de biofilm que lo posee el 99% de los microorganismos. Se ha reportado que los hongos y las bacterias forman consorcios con propiedades diferentes respecto a la de las poblaciones de origen, siendo, las interacciones hongo-bacteria importantes en una variedad de campos, como la agricultura, industria de alimentos, industrias farmacéuticas, medicina y biotecnología.

H. pylori, desde 1994 fue reconocida por el Organismo Internacional de Investigación sobre el Cáncer y la Organización Mundial de la Salud (OMS) como carcinógeno de categoría I. La presencia de *H. pylori* en la mucosa gástrica humana, se asocia como un factor predisponente para el desarrollo de patologías gástricas como gastritis, úlceras pépticas, adenocarcinoma gástrico no cardíaco y linfoma malt gástrico MALT. Sin embargo, se puede considerar como parte del microbioma gástrico humano transitorio, ya que es capaz de permanecer décadas interactuando con la mucosa gástrica sin daño aparente (portadores asintomáticos), pero se sabe que en el 100% de los casos causa una gastritis. Por lo tanto, la comprensión de los factores que afectan a su virulencia y prevalencia es un objetivo importante para avanzar en su control y tratamiento.

Por otro lado, *C. albicans* es el hongo más comúnmente detectado que forma parte de la microbiota intestinal y de las superficies de la mucosa humana; sin embargo, se convierte en

un microorganismo patógeno oportunista en individuos inmunocomprometidos bajo una variedad de condiciones, pero también, a partir de las vistas generales médicas y económicas, es un serio desafío de salud pública, debido a su impacto negativo como consecuencia de las altas tasas de mortalidad y aumento significativo de los costos de atención y hospitalización. A menudo se asocia con una variedad de especies de bacterias patógenas como *Escherichia coli*, *Pseudomonas aeruginosa*, *Staphylococcus aureus*, *Staphylococcus epidermidis*, *Acinetobacter baumannii* y *Lactobacillus rhamnosus*.

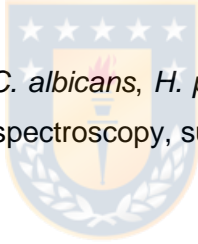
De acuerdo a lo anterior, la presencia de bacterias y hongos en un mismo entorno sugiere la existencia de interacciones bióticas que pueden contribuir a la prevalencia de enfermedades o infecciones relacionadas con estos microorganismos. Es importante indicar que, en el caso particular de *C. albicans* y *H. pylori*, los datos referentes a las distintas interacciones bióticas posibles, su relación con factores abióticos del entorno de crecimiento y su efecto sobre la patogenicidad bacteriana son escasos, no estando completamente definidos y entendidos. Según el contexto anterior, el objetivo de este trabajo fue determinar los tipos de interacción *in vitro* entre *H. pylori* y *C. albicans*.

Para el desarrollo de este objetivo, la estrategia metodológica se centró en emplear no sólo análisis microscópico o ensayos microbiológicos convencionales, o clásicos, sino que se quiso implementar técnicas espectrales debido a una mayor sensibilidad, menor subjetividad, rapidez, simplicidad del análisis y ausencia de pretratamiento. Sin embargo, los problemas inherentes como solapamiento, ensanchamiento de señales y ausencia de una metodología estándar, llevó a que estos problemas fueran abordados. Por lo tanto, se sintetizó y modificó químicamente superficies de celulosa que pudieran activarse espectralmente mediante el anclaje covalente de las cadenas laterales de isocianato produciendo una señal característica en el infrarrojo (IR) de fácil monitorización y ser utilizadas como soporte para las biocapas de los microorganismos en estudio (*C. albicans* y *H. pylori*). Se desarrolló un sistema de análisis por espectroscopia de infrarrojo para biocapas de microorganismos, mediante esta técnica. El paso siguiente fue hacer la caracterización espectral de los microorganismos individuales y sus co-cultivos, para ello, se utilizó la herramienta analítica de espectroscopía derivada funcionalmente mejorada (FEDS), por ser un método simple para obtener la deconvolución espectral y el aumento de la resolución espectral de señales, lo que permitió una mejor identificación, clasificación y análisis de señales significativas que se encontraban solapadas en el espectro de espectroscopia IR de los microorganismos en estudio. Además, se utilizaron métodos adicionales para contrastar los resultados como

dispersión dinámica de la luz, ángulo de contacto, electroforesis de gel de agarosa y amplificación genética. Paralelamente se realizó microscopía óptica, microscopía electrónica de barrido (SEM), microscopía electrónica de transmisión (TEM), microscopía de inmunofluorescencia y prueba de viabilidad (kit BacLigh, Invitrogen, EE. UU). Los resultados evidenciaron que múltiples mecanismos de interacción superficial dirigen el anclaje, la co-agregación y la formación de biopelícula polimicrobiana entre *C. albicans* y *H. pylori*: (i) interacciones hidrofóbicas entre cadenas de péptidos no polares y estructuras lipídicas, (ii) enlaces de hidrógeno entre componentes superficiales de levadura y bacteria e (iii) interacciones superficiales mediadas por el grupo funcional thiol. No se evidenció pruebas de internalización e interacciones electrostáticas. Además, se sugiere una interconversión del estado cocoide al estado bacilar, producto de la interacción entre cepas específicas de *H. pylori* y *C. albicans* (ATCC 43504 y ATCC 14053, respectivamente).

Se concluye que la interacción entre las superficies de *H. pylori* y *C. albicans*, establecen un sistema mixto sistemático, iniciado por el proceso de la co-agregación y su posterior anclaje, mediado por los mecanismos anteriormente mencionados.

Keywords: Types of interaction, *C. albicans*, *H. pylori*, co-aggregation, polymicrobial biofilm, Functionally-Enhanced derivative spectroscopy, surface properties.



ABSTRACT

Microbiological interactions in organisms and nature are considered essential strategies to ensure the survival, colonization and balance of the different ecosystems, which generate a wide spectrum of situations associated with pathogenicity, nutrition, gene acquisition, transport, construction of niches and community structures, among others; mediated by various physical, biological and chemical parameters. Commonly, the study of microorganisms, whether bacteria or fungi, is carried out by axenic procedures, that is, from populations of isolated microorganisms, from a single cell. However, it is clear that this type of culture is very strange in nature since, the growth of microorganisms in natural environments such as water, soil, or the human body are of mixed nature (that is, different populations of microorganisms, of different species and with different origin that share the same growing environment). It is important to indicate that the growth of microorganisms is phenotypically encoded by two states, a planktonic state that is present in 1% of microorganisms, and a sessile or biofilm state that is possessed by 99% of microorganisms. It has been reported that fungi and bacteria form consortiums with different properties compared to their populations of origin, being the fungus-bacteria interactions important in a variety of fields, such as agriculture, food industry, pharmaceuticals industry, medicine and biotechnology.

H. pylori, since 1994 was recognized by the International Agency for Research on Cancer and the World Health Organization (WHO) as a category I carcinogen.

The presence of *H. pylori* in the human gastric mucosa is associated as a predisposing factor for the development of gastric pathologies such as gastritis, peptic ulcers, non-cardiac gastric adenocarcinoma, and MALT gastric malt lymphoma. However, it can be considered as part of the transitory human gastric microbiome since it is capable of remaining for decades interacting with the gastric mucosa without causing harm to the host (asymptomatic carriers). but it is known that in 100% of cases it causes gastritis. Therefore, understanding the factors that affect its virulence and prevalence is an important goal to advance its control and treatment.

On the other hand, *C. albicans* is the most commonly detected fungus that is part of the intestinal microbiota and the surfaces of the human mucosa; however, it becomes an opportunistic pathogenic microorganism in immunocompromised individuals under a variety of conditions, but also, from medical and economic overviews, it is a serious public health challenge, due to its negative impact as a consequence of high mortality rates and significant

increase in the costs of care and hospitalization. It is often associated with a variety of pathogenic bacteria species such as *Escherichia coli*, *Pseudomonas aeruginosa*, *Staphylococcus aureus*, *Staphylococcus epidermidis*, *Acinetobacter baumannii*, and *Lactobacillus rhamnosus*.

According to the above, the presence of bacteria and fungi in the same environment suggests the existence of biotic interactions that can contribute to the prevalence of diseases or infections related to these microorganisms. It is important to indicate that, in the particular case of *C. albicans* and *H. pylori*, the data referring to the different possible biotic interactions, their relationship with abiotic factors in the growth environment and their effect on bacterial pathogenicity are scarce, not being completely defined and understood. According to the previous context, the objective of this work was to determine the types of *in vitro* interaction between *H. pylori* and *C. albicans*.

For the development of this objective, the methodological strategy focused on employing not only microscopic analysis or conventional microbiological tests, or classical ones, but it was wanted to implement spectral techniques due to greater sensitivity, less subjectivity, speed, simplicity of the analysis and absence of pretreatment. However, inherent problems such as overlap, signal broadening and the absence of a standard methodology led to these problems being addressed. Therefore, cellulose surfaces were synthesized and chemically modified that could be spectrally activated by the covalent anchoring of the isocyanate side chains, producing a characteristic signal in the infrared (IR) that is easy to monitor and be used as a support for the biofilms of microorganisms. under study (*C. albicans* and *H. pylori*), an infrared spectroscopy analysis system for biofilms of microorganisms was developed, using this technique, the next step was to make the spectral characterization of the individual microorganisms and their co-cultures, to Therefore, the powerful functionally enhanced derived spectroscopy (FEDS) analytical tool was used as it is a simple method to obtain spectral deconvolution and increased spectral resolution of signals, which allowed better identification, classification and analysis of significant signals that were overlapping in the spectroscopy spectrum IR of the microorganisms under study, in addition, additional methods were used to contrast the results such as dynamic light scattering, contact angle, agarose gel electrophoresis and genetic amplification. In parallel, light microscopy, scanning electron microscopy (SEM), transmission electron microscopy (TEM), immunofluorescence microscopy and viability test (BacLigh kit, Invitrogen, USA) were performed.

The results showed that multiple surface interaction mechanisms direct the anchoring, co-aggregation and the formation of polymicrobial biofilm between *C. albicans* and *H. pylori*: (i) hydrophobic interactions between nonpolar peptide chains and lipid structures, (ii) hydrogen bonds between surface components of yeast and bacteria and (iii) surface interactions mediated by the thiol functional group. There was no evidence of internalization and electrostatic interactions. Furthermore, an interconversion from the coccoid state to the bacillary state is suggested, as a result of the interaction between specific strains of *H. pylori* and *C. albicans* (ATCC 43504 and ATCC 14053, respectively).

It is concluded that the interaction between the surfaces of *H. pylori* and *C. albicans* establish a systematic mixed system, initiated by the process of co-aggregation and its subsequent anchoring, mediated by the aforementioned mechanisms.

Keywords: Types of interaction, *C. albicans*, *H. pylori*, co-aggregation, polymicrobial biofilm, Functionally-Enhanced derivative spectroscopy, surface properties.



Prólogo

Esta tesis se circunscribe en la determinación de los tipos de interacción entre *H. pylori* y *C. albicans*. Se centra en estos dos microorganismos por tratarse de un factor predisponentes para el desarrollo de cancer gástrico, además de encontrarse colonizando un 50 % de la población humana para el caso de la bacteria, mientras que *C. albicans* es una levadura patógena oportunista que hace parte de la microbiota humana.

En particular, se ha descrito la coexistencia entre *C. albicans* y *H. pylori* desde el estómago, y varios investigadores han propuesto un efecto sinérgico sobre la patogénesis de la úlcera.

Para abordar esto, el estudio se centró en tres componentes principales: desarrollo de una metodología espectroscópica para el estudio de interacciones superficiales, determinar los tipos de interacción, y establecer el efecto de la coexistencia entre estos dos microorganismos, con principal énfasis en la viabilidad bacteriana.

El capítulo 1, consiste en una breve descripción del tema, objetivos y metodología implementada para dicho estudio.

El capítulo 2, corresponde a los antecedentes generales, respaldado por dos manuscritos de revisión, con el objetivo de contextualizar respecto a las interacciones entre levaduras y bacterias, su importancia para el entendimiento de los distintos procesos que se desencadenan entre estos microorganismos, y la complejidad que surge por la presencia de estas interacciones hace que sea necesario describirlas en diferentes niveles (biológicos, fisicoquímicos y bioquímicos) que en muchas ocasiones son interdependientes. En el caso particular de las interacciones entre *C. albicans* y *H. pylori*, no se dispone de una descripción completa sobre las interacciones que pueden tener lugar; además, los mecanismos de interacción que se han reportado son débilmente entendidos.

El capítulo 3, realiza la formulación de la hipótesis, objetivo general, seguido los objetivos específicos, como lineamiento para el desarrollo de la tesis doctoral.

Los capítulos 4 y 5, dan respuesta al objetivo 1.

El capítulo 4, hace referencia a la caracterización del espectro vibratorio del infrarrojo medio de la superficie exterior de *C. albicans* mediante espectroscopia derivada funcionalmente

mejorada (FEDS). El objetivo de este trabajo fue evaluar la capacidad del algoritmo FEDS para la caracterización de la superficie de microorganismos, específicamente *Candida albicans*, mediante espectroscopía de IR medio, y utilizando la técnica de superficie sensora de celulosa. Este trabajo es una etapa clave en el estudio de las interacciones célula-célula y célula-superficie entre microorganismos, incluido el estudio de biopelículas polimicrobianas.

El capítulo 5, trata sobre la caracterización del espectro vibratorio de la superficie exterior de las biopelículas de *Helicobacter pylori* mediante espectroscopía derivada funcionalmente mejorada (FEDS). El objetivo de este trabajo es caracterizar la superficie exterior de dos cepas *H. pylori* por IR+FEDS. Este trabajo es una etapa clave para el estudio de las interacciones células celulares y de células-superficie entre microorganismos, así como para caracterizaciones de biopelículas polimicrobianas donde están involucradas las especies de *H. pylori*. Para ello, las biopelículas bacterianas artificiales, o biocapas bacterianas, se depositaron en membranas de celulosa de ultrafiltración que fueron previamente modificadas por la inserción covalente de un marcador espectral y utilizadas como superficie de detección para el análisis de biocapas de bacterias. Los biocapas se analizaron utilizando un espectrofotómetro infrarrojo con ATR y los datos fueron analizados por procedimientos clásicos y por deconvolución basada en la transformación FEDS.

El capítulo 6, consiste en los múltiples mecanismos de interacción de superficies que dirigen el anclaje, coagregación y formación de biopelículas polimicrobianas entre *C. albicans* y *H. pylori*. El objetivo de este trabajo fue avanzar en el conocimiento de la interacción superficial entre *H. pylori* y *C. albicans* para la formación de biopelículas polimicrobianas. Los estudios de superficies microbianas tanto de bacterias, levaduras y mezclas de ellas se llevaron a cabo mediante espectroscopía infrarroja y análisis de deconvolución.

El capítulo 7, consiste en el estudio de la promoción de la interconversión entre formas cocoides y bacilares resultante de la interacción de *H. pylori* y *C. albicans*. El objetivo de este trabajo fue establecer el efecto de la interacción entre *H. pylori* y *C. albicans* en la interconversión recíproca de la forma cocoide al estado bacilar de la bacteria para avanzar en la comprensión de las interacciones microbianas entre estos dos seres humanos patógenos.

Capítulo 8. esta sección corresponde a las discusiones que correlaciona los resultados obtenidos en cada artículo. Luego se comentan las conclusiones generales, que hacen principal énfasis en estudiar los microorganismos como parte de comunidades de especies mixtas en lugar de forma aislada, Además de las señales típicas asociadas con el espectro IR de microorganismos, por FEDS, se puede realizar una mejor y detallada descripción de la membrana externa de las biopelículas de *H. pylori* y *C. albicans*. Además de la combinación de diferentes mecanismos a nivel de superficie: interacciones hidrofóbicas entre cadenas de aminoácidos no polares y estructuras lipídicas, formación de enlaces de hidrógeno y anclaje covalente a través de la formación de enlaces disulfuro participan en la interacción de *H. pylori* y *C. albicans*. Y por último sugieren la interacción entre cepas específicas para restablecer el cambio de un estado cocoide a un estado bacilar.

Proyecciones

El conocimiento de los mecanismos involucrados en las interacciones entre *C. albicans* y *H. pylori* ayudará a comprender de mejor forma la patogénesis microbiana, además de vislumbrar nuevas estrategias para el control de la infección por esta bacteria.



CAPITULO I. INTRODUCCIÓN

Los microorganismos en los diferentes ecosistemas (agua, suelo, aire) rara vez se establecen en poblaciones constituidas por una sola especie, debido a que requieren mantener una constante interacción con su entorno y entre sí, como estrategia de supervivencia y adaptación para garantizar su cohabitación y afrontar los posibles cambios que se puedan generar. Estas interacciones, involucran el reconocimiento ambiental, donde intervienen factores fisicoquímicos como la temperatura, el pH humedad, salinidad, compuestos bioactivos (metabolitos), fitohormonas etc., así como la transferencia de información molecular y genética [1-2], que se ha descrito en los tipos de interacciones microbianas producto de las asociaciones biológicas, ejemplo, formación de biopelículas mixtas, sistema de detección de quórum, intercambio de sideróforos y metabolitos. Además de la amplia gama de interacciones descritas entre bacterias con otros organismos como plantas, humanos, animales, protozoos y hongos, logrando establecer asociaciones simbióticas que pueden ser endosimbiótica o ectosimbiótica [3], mutualistas [4], competitivas [5], antagónicas [6], patógenas y parasitarias [7], cuyos patrones interactivos dentro de estas redes pueden ser, positivas (ganar), negativas (pérdida) o neutrales donde no hay ningún efecto en las especies que interactúan [2].

Aunque los mecanismos moleculares implicados en las interacciones a menudo no se comprenden completamente, un aspecto que puede facilitar la comprensión de las asociaciones entre bacterias y levaduras es la clasificación de las interacciones según su “naturaleza”, interacciones biológicas, fisicoquímicas y bioquímicas [3].

Las interacciones entre hongos y bacterias (BFI) son de gran importancia en el funcionamiento de numerosos ecosistemas, son miembros fundamentales de las comunidades que impulsan los ciclos bioquímicos [8], y contribuyen tanto a la salud como a la enfermedad en los seres humanos [9-11], plantas [12-14] y animales [15-17]. Las bacterias y los hongos a menudo se encuentran juntos en diferentes ecosistemas, especialmente en biopelículas, donde permanecen adheridas a superficies sólidas e interactúan a través de diferentes procesos de señalización. A pesar del lapso de tiempo de su coexistencia, la investigación basada en la exploración de las interrelaciones entre bacterias y hongos, especialmente en el contexto de múltiples infecciones, sigue siendo mínima. Sin embargo, las descripciones de muchas relaciones interactivas de amplio alcance entre los hongos patógenos como *Candida albicans* y diferentes patógenos bacterianos, como *Pseudomonas*

aeruginosa [18-20], *Staphylococcus aureus* [21-22], *Streptococcus gordonii* [23-25] están aumentando de forma rutinaria [26], por ejemplo, en la cavidad oral, la respiración rápida de *C. albicans* y otras especies de *Candida* crean un nicho anaeróbico al reducir el nivel de oxígeno disuelto. Esto favorece a las bacterias anaeróbicas y antagoniza las bacterias aeróbicas, lo que influye directamente en la composición del microbioma, ya que la respiración aeróbica se ve facilitada por la estructura de las biopelículas de *Candida* y la inhibición de la respiración. Los metabolitos bacterianos como las fenazinas [27] inhiben la formación de biopelículas por el hongo [28-29]. Por el contrario, la producción de etanol por *C. albicans* estimula la producción de fenazina por *P. aeruginosa* y la formación de biofilms por parte de las bacterias a través de un circuito de retroalimentación, que teóricamente aumenta la virulencia de ambos microorganismos [8,30].

Durante las últimas décadas se han desarrollado diversas técnicas moleculares como: Enfoques basados en secuencias, Metagenómica, Genómica unicelular, Metatranscriptómica, Fluorescente *in situ* Hibridación (FISH), PCR cuantitativa, Microarrays, Metaproteómica y Metabolómica [31] para el Estudio del microbioma, que se define como un conjunto formado por microorganismos, sus genes y sus metabolitos en un nicho ecológico determinado [32]. Sin embargo, las técnicas anteriores por sí solas no brindan información específica, refiriéndose a la "naturaleza" de las interacciones [3], existe un gran vacío en la comprensión de los mecanismos. De acuerdo a lo anterior, el objetivo principal del presente trabajo se circunscribe en determinar a nivel *in vitro* los tipos de interacción entre *H. pylori* y *C. albicans*, a través de técnicas espectroscópicas, en donde su principio se centra en la radiación IR para producir cambios de estados vibracionales a nivel molecular sin requerir de la alteración química de las muestras. En particular, la espectroscopia IR es un método no destructivo, rápido, fácil de usar y muy sensible. Que utilizada en conjunto con el método de espectroscopía derivada funcionalmente mejorada (FEDS) permite obtener la deconvolución espectral y el aumento de la resolución espectral de señales que presenten una alta superposición y el ensanchamiento de las señales adyacentes, además de un mejor análisis de los espectros de diferentes microorganismos, que presentan una alta similitud, lo cual permite identificar y caracterizar las principales propiedades estructurales, moleculares y funcionales de la membrana externa que contribuyen con la interacción de los microorganismos en estudio.

CAPÍTULO II. GENERAL BACKGROUND

Paper 1:

Fungi-bacterium interactions: *Helicobacter pylori* - *Candida albicans*

Sixta Palencia¹, Gisela Lagos¹, Apolinaria García¹ *

¹ *Bacterial Pathogenicity Laboratory, Department of Microbiology, Faculty of Biological Sciences, University of Concepción, Concepción, Chile*

Corresponding author: apgarcia@udec.cl

Journal of Science with Technological Applications

<https://doi.org/10.34294/j.jsta.16.1.5> | ISSN 0719-8647 | www.jsta.cl

Paper 2:

Polymicrobial Biofilms: Fundamentals, diseases, and treatments – A review

Arturo Espinosa¹, Manuel Palencia^{1*}, Sixta Palencia², Apolinaria García²

¹*Departament of Chemistry, Faculty of Natural and Exact Sciences, Universidad del Valle, Cali – Colombia.*

² *Bacterial Pathogenicity Laboratory, Department of Microbiology, Faculty of Biological Sciences, University of Concepción, Concepción, Chile*

Corresponding author: manuel.palencia@correounivalle.edu.co

Journal of Science with Technological Applications

<https://doi.org/10.34294/j.jsta.20.8.54> | ISSN 0719-8647 | www.jsta.cl

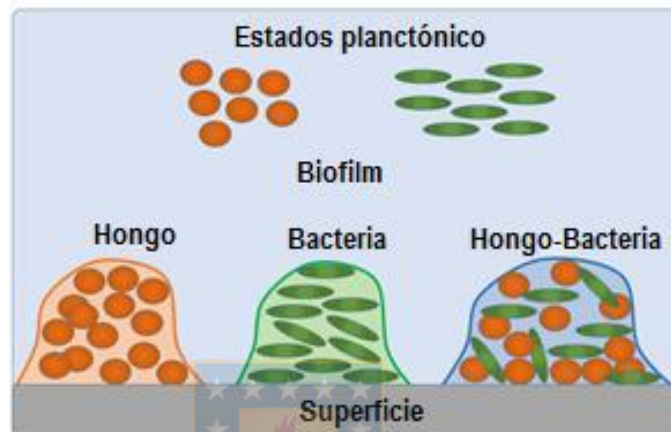
Fungi-bacterium interactions: *Helicobacter pylori* - *Candida albicans*

Sixta Palencia¹, Gisela Lagos¹, Apolinaria García¹ *

¹ Bacterial Pathogenicity Laboratory, Department of Microbiology, Faculty of Biological Sciences, University of Concepción, Concepción, Chile

Corresponding author: apgarcia@udec.cl

Graphical abstract



Abstract

Candida albicans is the most commonly fungus found on the surfaces of human mucosa, it is often associated with a variety of species of pathogenic bacteria such as *Escherichia coli*, *Pseudomonas aeruginosa* and *Staphylococcus aureus*. Therefore, the presence of bacteria and fungi in the same environment suggests the existence of biotic interactions that may contribute to the prevalence of diseases and infections related to these microorganisms. It is important to note that, in the case of *Candida albicans* and *Helicobacter pylori*, the data concerning to the possible interactions, and their relationship with growth factors of the environment and effects on bacterial pathogenicity are scarce, not completely defined and understood. Therefore, the aim of this this review is to describe the main mechanisms of interactions between bacteria and yeast, and, in particular, between *Candida albicans* and *Helicobacter pylori*.

Keywords

Interaction mechanisms, Biofilm, *Candida albicans*, *Helicobacter pylori*

Content

1. Introduction
2. Interactions between bacteria and fungi

- 2.1 Biological interactions
 - 2.1.1 Mixed communities of fungi and bacteria
 - 2.1.2 Trophic interactions
 - 2.1.3 Symbiotic interactions
- 2.2 Physicochemical interactions
 - 2.2.1 Contact and adhesion interactions
 - 2.2.2 Modification of the physicochemical properties of the environment
 - 2.2.3 Coaggregation
- 2.3 Biochemical interactions
 - 2.3.1 Antibiosis or chemical interaction
 - 2.3.2 Signal-mediated interactions
 - 2.3.3 Interactions by chemotaxis
 - 2.3.4 Cooperative metabolism
 - 2.3.5 Interactions mediated by protein secretion and gene transfer
- 2.4 Mechanisms of contact interaction
 - 2.4.1 Lectin binding
 - 2.4.2 Protein-protein binding
- 3. *Candida albicans*
 - 3.1 General
 - 3.2 Interaction with other microorganisms
- 4. *Helicobacter pylori*
 - 4.1 General
 - 4.2 Interaction with other microorganisms
- 5. Interaction between *C. albicans* and *H. pylori*
- 6. Conclusions
- Acknowledgments
- Interest conflict
- References



1. Introducción

Commonly, the study of microorganisms, whether bacteria or fungi, is carried out by axenic procedures, that is, from populations of isolated microorganisms, from a single cell. However, it is clear that this type of culture is very strange in nature since, the growth of microorganisms in natural environments such as waters, soils, or the human body are of mixed nature (that is, different populations of microorganisms, of different species and with

different origin share the same growth environment) [1, 2]. This way of conducting microbiological studies ignores the fact that, in many environments, bacteria and fungi coexist and interact. Fungi and bacteria have been reported to form consortiums with different properties than their populations of origin, with fungus-bacteria interactions being important in a variety of fields ranging from agriculture to medicine and biotechnology. In general terms, it can be stated that the combination of physical associations and molecular interactions between bacteria and fungi produces a wide spectrum of situations associated with pathogenicity, nutrition, gene acquisition, transport, construction of niches and community structures, among others [1].

As a result of the interactions, effects may occur on:

- *The development of the fungus*: Bacteria can affect, positively or negatively, the production of spores and the development of the fungus. This can occur, for example, by inhibiting or increasing sporulation or by the production of metabolites that promote the growth of the fungus.
- *Pathogenicity*: This effect can be both positive and negative. Several low molecular weight molecules produced by bacteria have been shown to have an effect on the morphological transitions of fungi, from yeast to filamentous form, which is a critical aspect in the context of the pathogenicity of the fungus, such as, for example, Mutanobactin A and fatty acids derived from lactic acid).
- *The physiology of both the bacteria and the fungus*: This effect can be appreciated mainly at the level of biofilm formation since, due to the small size of the bacterial cells, the observation of the effects of the fungus on the bacteria is associated with great difficulty. Biofilm formation leads to the generation of different ecological niches within which the bacterium exhibits physiological differences such as antibiotic resistance, stress and altered expression of gene virulence compared to free bacteria.
- *Survival characteristics (Dispersion, colonization of microorganisms)*: This effect has been observed in a reciprocal way between fungi and bacteria. The fungus can act as a vector and thus the colonization of sites initially inaccessible to microorganisms can be promoted.
- *Provision of heritable changes*: This effect is not well understood, and it is suggested that it must be linked to certain special circumstances that lead to the transfer of genes between bacteria and fungi, or the presence of intrahiphal bacteria.
- *The complexity of life cycles*: Although it requires observations over long periods of time, it has been described for different micro-organisms.

The foregoing shows how the dynamic relationships between bacteria and fungi, both beneficial and harmful, depend on the environment and the characteristics of the microorganisms (see Table 1) [1]. Thus, it is clear that the mechanistic identification of the different behaviors resulting from these interactions represents the first step for the control and manipulation of microorganisms in more realistic conditions than those existing in different fields, such as, for example, medicine.

Table 1. Examples of the effects resulting from fungus-bacteria interactions [1]

Effect	Microorganism		Description
	Fungus	Bacterium	
Development of the fungus	<i>Phytophthora alni</i>	Unidentified	Stimulation of spore germination
	<i>Amanita muscaria</i>	<i>Streptomyces ssp.</i>	Effect on the organization of the cytoskeleton
Pathogenicity	<i>Agaricus bisporus</i>	<i>Pseudomonas putida</i>	Induction in the production of the fungus
	<i>Fusarium oxysporum</i>	Unidentified	Adoption of a pathogenic and invasive growth
	<i>Botrytis cinerea</i>	<i>Leaf bacteria</i>	Inhibition of spore germination
	<i>Botrytis cinerea</i>	<i>Chrysanthemum</i>	
	<i>Botrytis cinerea</i>	Soil bacteria	The degradation of oxalic acid inhibits the pathogenicity of the fungus
	<i>Candida albicans</i>	<i>Streptococcus mutan</i>	Inhibition of morphological transition
Physiology of microorganisms	<i>Aspergillus fumigatus</i>	<i>Pseudomonas aeruginosa</i>	Inhibition of biofilm formation
	<i>Gigaspora margarita</i>	<i>Endobacterias</i>	Physiological changes of the fungus
Dispersion and colonization	<i>Candida hyphae</i>	<i>Staphylococcus aureus</i>	Enhancement of biofilm formation
Provision of inheritable changes	<i>Rhizopus microsporus</i>	<i>Endobacterias</i>	Resistance to endobacterial rhizoxin toxin
	<i>Saccharomyces cerevisiae</i>	alphaproteobacterias	Sulfatase-encoding gene transfer
	<i>Saccharomyces bayanus</i>	alphaproteobacterias	Sulfatase-encoding gene transfer
Complexity over life cycles	<i>Agaricus bisporus</i>	<i>Pseudomonas putida</i>	The production of the fungus is dependent on the presence of the bacteria

2. Interactions between bacteria and fungi

Recently Frey-Klett *et al.* (2011) [1] have made a classification of the interactions between fungi and bacteria, consisting of two large categories: (i) Complexes or physical groupings and (ii) Molecular and communication interactions. However, the Frey-Klett *et al.* Classification is based, in its most general form, on associations between microorganisms and not on the nature of the interaction.

For the sake of a more mechanistic approach, this review proposes another classification based on the nature of the interaction: biological, physicochemical and biochemical interactions. However, the specific categories of both classifications is the same. In the first

case, *Complexes or Physical Groupings*, those interactions are included where there is contact between microorganisms, for example, adhesion phenomena, biofilm formation of a mixed nature, ecto-symbiotic interactions (that is, where the bacterium remains outside the the plasma membrane of the fungus) and endosymbiotic (that is, the bacteria is located inside the fungal cell) [1]. These types of clusters are found in a variety of very diverse environments such as the lungs of patients with cystic fibrosis, the human oral cavity, cheeses, wines, agricultural environments and forests [3-7].

In the second case, *Molecular and Communication Interactions*, they include: Interactions via antibiosis, interactions through signals, interactions through modulation of the physicochemical environment, interactions through chemotaxis and cell contact, trophic interactions, interactions based on cooperative metabolism, interactions through protein secretion and interactions through gene transfer [1].

2.1. Biological interactions

Bacteria and fungi can carry out groupings that can range from disordered polymicrobial communities to specific symbiotic associations [1]. This category includes the formation of mixed communities, trophic interactions and symbiosis (ecto- and endosymbiotic interactions). These are briefly described below:

2.1.1 Mixed communities of fungi and bacteria: Mixed biofilms, formed by bacteria and fungi, have been reported, which have been considered as a more intimate level of association, where communities have been formed by an extracellular matrix of macromolecules derived from microorganisms that have physical and physiological properties different from those observed. for single cells [1]. In this sense, it has been concluded that two or more fungi can act as biotic support for the establishment of a bacterial biofilm [8-10]. Clearly, the formation of these communities implies the occurrence of physical and chemical processes that lead to the achievement of this type of communities (Figure 1).

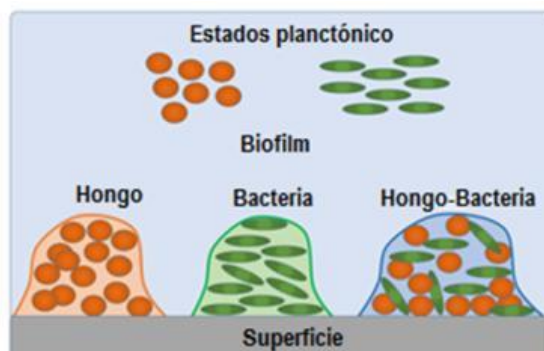


Figure 1. Illustration of the interaction through the formation of mixed communities

2.1.2 Symbiotic interactions: Ectosymbiotic interactions, where the bacteria remain outside the plasma membrane of the fungus, and endosymbiotic interactions, in which the bacteria are located inside the fungus cell are a clear example of symbiotic situations between fungi and bacteria [16- 21]. These interactions, as in the case of mixed communities, imply the occurrence of physical and chemical processes that are framed in other types of interactions (see Figure 2).

2.1.3 Trophic interactions: The nutritional interactions between fungi and bacteria are very important. Trophic competition between fungi and bacteria has been well documented in the rhizospheric environment, where competition for nutrients such as carbon, nitrogen and iron can be an effective control mechanism against pathogenic root fungi [7, 11-15].

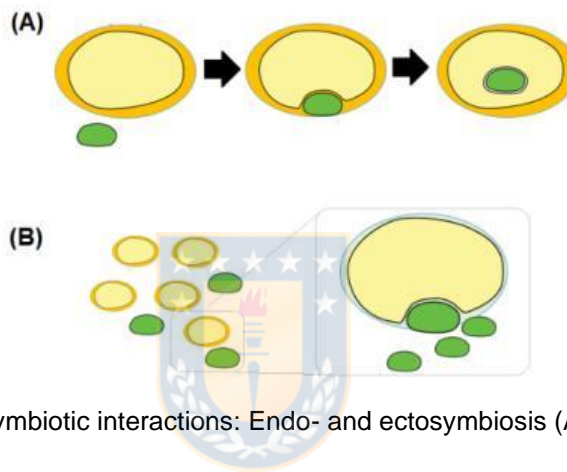


Figure 2. Illustration of symbiotic interactions: Endo- and ectosymbiosis (A and B, respectively)

2.2 Physicochemical interactions

In this type of interactions are those that are associated with physical phenomena (such as contact and adhesion) and physicochemical (such as changes in pH and viscosity). These types of interactions include: Contact and adhesion interactions and interactions mediated by the modification of the physicochemical properties of the environment.

2.2.1 Contact and adhesion interactions: The contact between the cells of the fungi and the bacteria and the adhesion phenomena are the most important aspects in the process of formation of mixed biofilm of bacteria and fungi, also, the contact is a first stage of the ecto- and endosymbiotic interactions. A degree of specificity has been identified in these types of interactions, for example, *Pseudomona aeruginosa* is capable of colonizing hyphae, but not the yeast-like form of *C. albicans*. In the clinical environment, this type of interaction is of great importance since it is associated with the prevalence of certain infections, as well as the colonization of catheters, prostheses and other biomedical devices [8, 22-23]. Thus, for example, the presence of *C. albicans* is favored by the formation of *Staphylococcus aureus* biofilm. The adhesion of microorganisms on surfaces is usually described as a function of

different interaction regimes, and they are described by two models: one thermodynamic and one physicochemical [24, 25] (see Figure 3).

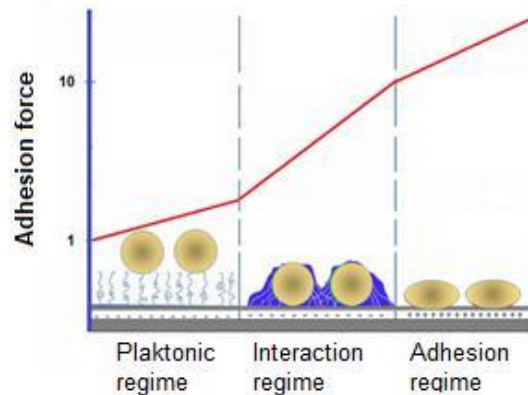


Figure 3. Bacterial adhesion regimes: (1) Planktonic regime (extremely weak forces), (2) Interaction regime (the microbial response to its adherence increases with increasing its adhesion force and (3) adhesion regime (the Adhesion forces are very strong, commonly occurs with positively charged surfaces, and can lead to bacterial adherence or death [24, 25].

On the other hand, cellular contact between fungi and bacteria can result in important changes in their physiology and interactions. These interactions can also be modulated by the environment, for example, it has been identified that nutritional supplements can modulate the cohesion between *C. albicans* and oral bacteria [26]. However, the molecular nature of the contact between fungi and bacteria has been studied in very few systems, where it has been concluded, the importance of the membranes. For example, the anchorage of *Acinetobacter baumannii* on *C. albicans* is mediated by the main membrane proteins OmpA, while the contact between *Streptococcus gordonii* and *C. albicans* is partially mediated by the proteins of the bacterial cell wall (SspA and SspB) and hyphal proteins (Als3) [27]. It should be noted that interactions based on contact between bacteria and fungi are not only adhesive. Contact can be made through the secretion of certain substances at the surface level, for example, an arginase secreted by fungi has been reported to act as a lectin. Thus, the binding of arginase to a polygalactosylated receptor is analogous to the symbiosis formed between algae and fungi [28].

2.2.2 Modification of the physical-chemical properties of the environment: One of the most common effects is the promotion of pH changes, since some microorganisms such as *Streptococcus*, *Lactobacillus* and *Candida*, can inhabit environments with a broad spectrum of acidity, most are susceptible to pH lower than 4. Therefore, changes in pH can affect microbial communities by inhibiting growth. For example, the growth of bacterial strains with

lower tolerance to acidity may be favored by the production of alkaline metabolites as a result of lactate metabolism. Similarly, the presence of alkalizing yeasts such as *Geotrichum candidum* enhances the growth of Salmonella on the tomato surface. In addition to promoting or inhibiting growth, changes in the pH of the medium can influence the kinetics of the synthesis of secondary metabolites (eg, the production of aflotoxin by *Aspergillus parasiticus* is greater under acidic growing conditions) [29, 30].

2.2.3 Coaggregation: Coaggregation is defined as the process by which genetically distinct bacteria [31] bond with each other through specific molecules. Four microscopic methods, turbidimetry, and radioactive assays have been described in bacterial coaggregation studies. Adhesive interactions between yeast and bacteria, to date, have not been extensively studied compared to adhesive interactions between bacteria, due in part to experimental difficulties [32]. A clear distinction has recently been made between bacterial coaggregation and coadhesion [33, 34]. It has been proposed that the word coaggregation is used exclusively for the interaction between two microbial pairs when both parts are planktonic, while coadhesion is the suggested expression for sessile interaction [32].

Previous research developed by Sandin *et al.* (1982) and Lee and King (1983), suggest that the mannose component present on the surface of *C. albicans* and epithelial cells act as mediators of adherence to the human epithelium. The pre-incubation of buccal and uroepithelial epithelial cells with strains that have fimbriae, such as *Escherichia coli* and *Klebsiella pneumoniae* increase the subsequent binding of *C. albicans* to epithelial cells, all this process is inhibited by the action of mannose [35]. These data suggest that certain bacteria possess ligands that bind to both *Candida* and epithelial cells, mediating yeast adhesion through a "bridging" action of intermicrobial binding, important in the formation of dental plaque [36].

2.3 Biochemical interactions

These types of interactions include interactions associated with chemical substances generated by the metabolism of micro-organisms, which can produce or trigger different effects. These include: Antibiosis or chemical interactions, signal-mediated interactions (quorum sensing), cooperative metabolism, and chemotaxis.

2.3.1 Interaction of antibiosis or chemicals: It is a form of biochemical interaction that can be classified as a "chemical warfare" consisting of the diffusion of molecules, commonly chemically complex, between microorganisms. In more formal terms, antibiosis is the association between two micro-organisms in which at least one of them is affected by the release of metabolites or components secreted by the cell. Opportunistic pathogenic

microorganisms are located at specific sites in the human body that induce infections when the host's immune system is deficient. The persistence of any species at the site of infection is determined both by its ability to interact with the host and its success in competition with other microbes. The ability to participate in synergistic relationships, such as co-degradation of complex substrates or cross-feeding of growth factors, and to inhibit antagonistic interactions, including those mediated by antibiotics and extracellular enzymes, that contribute to the survival of an organism within a microbial community [37]. An example of this mechanism is penicillin, which was developed by antibiosis of a contaminating *Penicillium* mold from a *Staphylococcus* culture [38]. Different mechanisms are associated with this interaction: inhibition of key cellular functions such as cellular respiration, transport systems, impairment of the integrity of cell membranes, among others.

Burns, *et al.*, Demonstrated that *P. aeruginosa* has the ability to limit the establishment of infections caused by *C. albicans*, inhibiting its filamentous form through the action of molecules such as N-3-oxo-C12 homoserine lactone that allows the cell-cell signaling and compounds containing a 12-carbon backbone, including dodecanol [4], which repress the filamentation pattern of the fungus without altering its growth rate, at a concentration of 200 mM. *Klebsiella aerogenes* supplies dopamine, which can be used for melanization by *Cryptococcus neoformans* [39]. Pigmentation protects microorganisms not only against environmental stress, but also against immune defense [22].

Explaining in this way the transition mechanism of the morphology of the fungus in the presence of certain molecules secreted by bacteria. There are different mechanisms of action of antibiotics in the established interactions between fungi and bacteria. These include the inhibition of key cellular functions such as cellular respiration (eg hydrogen cyanide and fusaric acid), cell wall synthesis (eg penicillin and butyric acid) transport systems, and (eg, β -phenylethanol), while others can compromise the integrity of cell membranes (eg, hydrolytic enzymes, cyclic lipopeptides, and polymyxin B) [40].

2.3.2 Signal-mediated interactions: Although they are also the result of molecules generated by microorganisms, these are not generated as chemical weapons to try to guarantee the prevalence of the species. Some molecules are produced, by fungi or bacteria, to act as chemical sensors. For example, it has been reported that bacterial peptidoglycan induces the growth of hyphae of *Candida albicans*, likewise, the presence of farnesol (metabolite of *C. albicans*) can modulate the expression of virulence genes in *Pseudomonas aeruginosa* by "quorum sensing" [41, 42].

2.3.3 Interactions by chemotaxis: Chemotaxis is understood to be the movement of bacteria and other cells of uni- and multicellular organisms, in response to the concentration

of certain chemical substances in their environment. This directed movement has been demonstrated in different instances, for example, the chemotactic response of the biocontrol strain *Pseudomonas fluorescens* WCS365, of fusaric acid from *Fusarium oxysporum* has been identified as an important chemotactic signal originating from the fungus [43].

2.3.4 Cooperative metabolism: Cooperative metabolism is an extension of the concept of using specific metabolisms. In this mechanism, one of the species helps to meet the general growth requirements of the other. In this scenario, the exchange of metabolites results in the formation or degradation of a molecule that neither can produce individually. Examples in food production are the manufacture of cheeses and wines, where each species contributes to the synthesis of substances that determine the organo-oleptic qualities of the final product. For example, in cheese ripening, the interaction between *Kluyveromyces lactis* and *Brevibacterium linens* results in an altered profile of volatile aromatic sulfur compounds.

2.3.5. Interactions mediated by protein secretion and gene transfer: In addition to the transfer of nutritive metabolites, antibiotics, and signaling molecules, the exchange of other biomolecules between bacteria and fungi can also occur. Thus, many bacteria possess molecule secretion systems, such as proteins and DNA, in the vicinity of cells and in the extracellular vicinity. In Gram-negative bacteria, for example, these secretion systems can range from simple transporters to multi-component protein complexes. These have been classified into nine secretion systems ranging from T1SS to T9SS (see Table 2). (Note: Currently 10 secretion systems are described).

Table 2. Description of bacterial secretion systems [1]

Secretion system	Type of substance secreted	Description
T1SS y T2SS	Lipases Proteases Beta glucanases	They produce antifungal activity in different bacterial species, and in some cases, they can act synergistically with secondary metabolites of bacteria
T3SS y T4SS	Direct release of bacterial proteins or DNA into the host cytoplasm	These systems have been studied in the context of bacterial virulence towards eukaryotic cells
T5SS y T6SS	Secretion of proteins, toxins and enzymes	In the case of T5SS, proteins have the ability to insert into the membrane and allow the peptide to reach the outside of the cell. On the other hand, T6SS systems involve a protein injection system and virulence factors.

2.4 Mechanisms of contact interaction

Among the main mechanisms of contact between bacteria and yeasts are lectin binding (proteins that bind to sugars with high specificity) and protein-protein binding.

2.4.1 Lectin binding: The main role of lectins is that of recognition at both the cellular and molecular level, thus, for example, some bacteria use lectins to attach to the cells of the host

organism during infection. Bacterial surface lectins recognize a particular sugar on the phagocytic cell surface and mediate phagocytosis of bacteria. Cells with which bacteria interact through their surface lectins include different classes of phagocytes, such as human polymorpho-nuclear leukocytes [44-46] and peritoneal macrophages of mice [47-48], rats [3], and human beings. Fungi are recognized by a series of immune receptors among which Dectin-1 has arisen, as the key to phagocytosis and destruction by myeloid phagocytes. Dectin-1 is a C-type lectin receptor that recognizes beta-1,3-glucans found in the cell walls of almost all fungi [49]. Dectin-1 activates intracellular signals through CARD9 that lead to the production of inflammatory cytokines and the induction of T helper 17 (Th17) in immune responses [50-51].

Recently, Medina *et al.* (2014) have reported that the fixation process of *Arcobacter butzleri* and *Acanthamoeba castellanii* involves the participation of mannose-binding proteins and membrane-associated receptors of glucose and galactose present in amoebae, while, in their internalization, actin polymerization in the protozoan plays an active role [52] in the interaction.

2.4.2 Protein-protein binding: Proteins are responsible for most of the biological processes that occur in cells, either individually or in coordination with other macromolecules. Outside of cells, proteins and their interactions promote cell-to-cell communication, millions of micro- and macromolecular interactions are required to maintain the normal functional and structural architecture of a cell at any given time [40].

Adhesion proteins function in confined regions between cell membranes and the extracellular matrix or in adjacent cells. However, the binding mechanisms of adhesion proteins, associated affinities, and adhesion energies are normally based on investigations of the binding between soluble fragments and recombinant membrane proteins [53].

3. *Candida albicans*

3.1 General

Candida albicans is a pleomorphic fungus that commonly exists as a commensal of the skin and mucosal tissues of the oral, urogenital, and gastrointestinal cavity. Its pathogenesis is facilitated by environmental changes, including modifications of the resident microbiota, modification of physiology and alterations of immune defense [54] (see Figure 4).

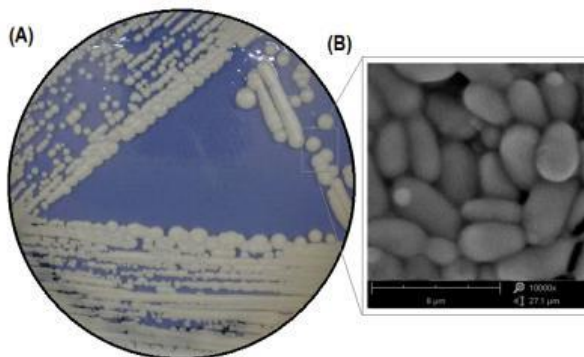


Figure 4. Photo of *Candida albicans* grown *in vitro* (A) and electron micrograph (B) (Courtesy of the Research Group in Sciences with Technological Applications, GI-CAT, Universidad del Valle, Cali-Colombia).

Similar to *Saccharomyces cerevisiae*, the yeast cell surface contains four important components (i) mannoproteins, (ii) β (1,6) -glycans, (iii) β (1,3) -glycans and (iv) chitin; however, the cell wall of *C. albicans* contains considerably more β (1,6) -glucans, implying that the β (1,6) -glucan molecules are more numerous or contain more glucose residues or both.

The above suggests that these molecules can strongly influence the surface interaction of yeast with any substance or entity in the environment. In addition, the mannans of the cell wall side chains contain numerous phosphodiester bonds, causing *C. albicans* cells to have an isoelectric point between 2-3 [55]. In this sense, such a low isoelectric point suggests that the surface of yeast in most of the environments of its common habitat will find a negative surface charge, leading to their behaving as ion exchangers; consequently, this ion exchanger characteristic would only be absent in extremely acidic environments such as the stomach [56]. The presence of negative surface charge density makes, in particular, the yeast surface susceptible to the ionic strength of the medium, thus, changes in the ionic strength could be associated with a decrease in the ability of the yeast to adsorb on tissues or other surfaces, as well as changes in surface hydration that it may present.

The above suggests that these molecules can strongly influence the surface interaction of yeast with any substance or entity in the environment. In addition, the mannans of the cell wall side chains contain numerous phosphodiester bonds, causing *C. albicans* cells to have an isoelectric point between 2-3 [55]. In this sense, such a low isoelectric point suggests that the surface of yeast in most of the environments of its common habitat will find a negative surface charge, leading to their behaving as ion exchangers; consequently, this ion exchanger characteristic would only be absent in extremely acidic environments such as the stomach [56]. The presence of negative surface charge density makes, in particular, the yeast surface susceptible to the ionic strength of the medium, thus, changes in the ionic strength

could be associated with a decrease in the ability of the yeast to adsorb on tissues or other surfaces, as well as changes in surface hydration that it may present.

In addition, mannans, a type of mannoproteins, form a capsule-like structure on the cell surface of yeast that can be shed during tissue infection. Bacteria have been reported to associate with the sugars in this capsule-shaped layer through lectin-like activity [57]. Yeast mannoproteins are also involved in lectin interactions with human epithelial cells through molecular recognition of epithelial cell sugars. Likewise, these mannoproteins can serve as receptors for protein-protein interactions between yeast and bacteria; however, to date there are few data regarding protein-protein interactions between yeast and bacteria [40]. Cell wall proteins can play a role in maintaining structural integrity and mediating adhesion, either to host microbes, or they can have enzymatic functions, eg proteolysis. Additional factors that may influence these proteins are the morphology of the yeast cells, pseudohyphae, and hyphae and the maintenance of either a planktonic state or a sessile lifestyle [58].

3.2 Interaction with other microorganisms

Bacteria and fungi can establish a wide range of physical associations between polymicrobial communities or highly specific symbiotic associations. In addition, these bacterial and fungal communities create environmental conditions that promote or control the growth of other microorganisms; studies have shown that during respiration of *C. albicans* oxygen tension levels are reduced and provides

Streptococcal stimulating factors in the oral environment, while the second micro-organism provides nutrients that promote the growth of the fungus. In contrast, commensal bacteria that inhabit the female reproductive tract, such as *Lactobacillus* spp., potentially inhibit the growth and virulence of *C. albicans* through the secretion of organic acids and the production of hydrogen peroxide (H₂O₂). Supporting these findings in vitro, it has been shown that 96% of healthy women generate *Lactobacillus* H₂O₂ species as part of their microbiota, on the other hand, these bacterial populations are lower in women suffering from vaginosis [57].

These interactions are dependent on physiological and cellular development; for example, *Pseudomonas aeruginosa* is able to colonize hyphae, but not the yeast form of *C. albicans* [40]. Symbioses can be classified as an ectosymbiotic or endosymbiotic relationship, which are characterized by the fact that the bacteria remain on the outside of the fungal plasma membrane or the bacteria are within the fungal cell, respectively. Additionally, *C. albicans* has been reported to have the ability to congregate with various species of oral streptococci [59]. A description of the different interactions of *C. albicans* with different microorganisms is summarized in Table 3.

Table 3. Description of different interactions between *C. albicans* and different bacteria

Fungus	Bacterium	Description
<i>Candida albicans</i>	<i>Pseudomonas aeruginosa</i>	Colonizes hyphae, but not the yeast form Modulation of gene virulence expression Glycan-mediated contact-dependent hyphal death Transformation of a secondary metabolite of bacterial origin (pyocyanin) Enhancement of individual infection (co-infection)
	<i>Staphylococcus aureus</i>	<i>C. albicans</i> enhances biofilm formation and vancomycin resistance Enhancement of individual infection (co-infection) Inhibits the yeast-hyphae transition of <i>C. albicans</i>
	<i>Streptococcus mutans</i>	Inhibition of the transition between yeast and filamentous forms by fatty acids and mutanobactin A
	<i>Acinetobacter baumannii</i>	Attaches to the surface of <i>C. albicans</i> by outer membrane proteins (OmpA)
	<i>Streptococcus gordonii</i>	It is anchored to the surface of <i>C. albicans</i> by proteins (SspA and SspB) of the outer membrane, and to the hyphae by proteins of the wall (Als3)
	<i>Escherichia coli</i>	Enhancement of individual infection (co-infection) Resistance to oral antiseptics
	<i>Staphylococcus epidermidis</i>	Mixed biofilm formation

4. *Helicobacter pylori*

4.1 General

H. pylori is a Gram negative bacteria, spiral shaped, 2.5 to 5.0 long and 0.5 to 1.0 mm wide, has 4 to 6 flagella, is slow growing and microaerophilic. It inhabits the acidic environment of the human stomach [60, 61]. For its colonization and survival in this environment, it expresses multiple subunits of the enzyme urease [62, 63].

On the other hand, *H. pylori* promotes the development of gastrointestinal diseases characterized by infiltration of polymorphonuclear cells [64]; due to the fact that, when the bacteria enter the body, it adheres and starts the colonization of the gastric epithelium, which induces the activation of defense mechanisms to neutralize the infection, such as cell exfoliation, regenerative changes, cellular and humoral immune responses. the bacterial products promote the secretion of proinflammatory mediators and the secretion of IL-8, this being a potent neutrophil chemoattractant. In this process, a small percentage of individuals manages to neutralize the infection, but another large number of the population remains

infected for many years, causing damage and changes in the morphology of gastric epithelial cells [65, 66].

Currently, the metabolic pathways used by *H. pylori* are not fully known. However, studies by Mendz and Hazell have made it possible to elucidate the metabolic pathways used by this bacterium. *H. pylori* isolates show glucose kinase activity that is associated with the bacterial cell membrane. Furthermore, the activity of the enzyme is characteristic of the pentose phosphate pathway. Therefore, *H. pylori* may possibly be able to catabolize D-glucose, which warrants the presence of physical D-glucose transporters. It appears that some characteristics of this glucose transport system are unique to this bacterium [68]. *H. pylori* exhibits urea cycle activity as well as the Entner-Doudoroff pathway. Fumarate reductase is an essential component of its metabolism and, as such, constitutes a possible target for therapeutic intervention. [69]. *H. pylori* can metabolize amino acids by fermentation pathways similar to anaerobic bacteria, and cytochrome has also been reported to be involved in the termination of its respiratory chain [68]. *H. pylori* contain polyphosphate granules, which can function as a reserve energy source in bacteria associated with a degenerated epithelium, where an exogenous energy source may be absent, it also needs high levels of CO₂ for its growth in vitro, due to in part to the activity of the enzyme acetyl coenzyme A carboxylase [69]. A photograph of *H. pylori* is shown in Figure 5.

4.2 Interaction with other microorganisms

Recently Siavoshi *et al* (2013) reported that *H. pylori*, the most common causative agent of bacterial infections worldwide, affects 50% of the world's human population. It has a unique symbiotic relationship with yeast of the genus *Candida*. Which protects *H. pylori* against adverse environmental conditions [70]. *H. pylori* penetrates yeast and resides in a *Candida* vacuole, where it can survive heat (100 ° C for 15 minutes), dehydration (37 ° C for 3 months), and chlorination (2 ppm). This symbiotic relationship can prolong the viability of the bacteria [71].

5. Interactions between *C. albicans* and *H. pylori*

Several studies have suggested that both *C. albicans* and *H. pylori* are inhabitants of the human stomach and that they establish an association, in which *H. pylori* is internalized in the *C. albicans* vacuole [72, 73, 74]. Cavalier-Smith (2002), described that the vacuoles of eukaryotic cells represent a unique and sophisticated niche in which endosymbiotic bacteria could survive and promote a persistent association with the host cell. However, the

importance of their mutual interaction in the development of gastric diseases such as gastritis and peptic ulcers is not clearly understood. It is not known whether concomitant infection with *C. albicans* and *H. pylori* in the stomach could exacerbate the clinical outcome compared with infection with a single organism [75]. In fact, a considerable number of studies have described the involvement of yeast in gastric diseases through microscopic observations of yeast cells in histopathology samples stained in gastric biopsies, especially in *H. pylori*-negative patients [76, 77, 78].

The approach to an endosymbiotic interaction between *C. albicans* and *H. pylori* is based on different studies that, indirectly, have compiled evidence that suggests the internalization of *H. pylori* in the vacuoles of *C. albicans*.

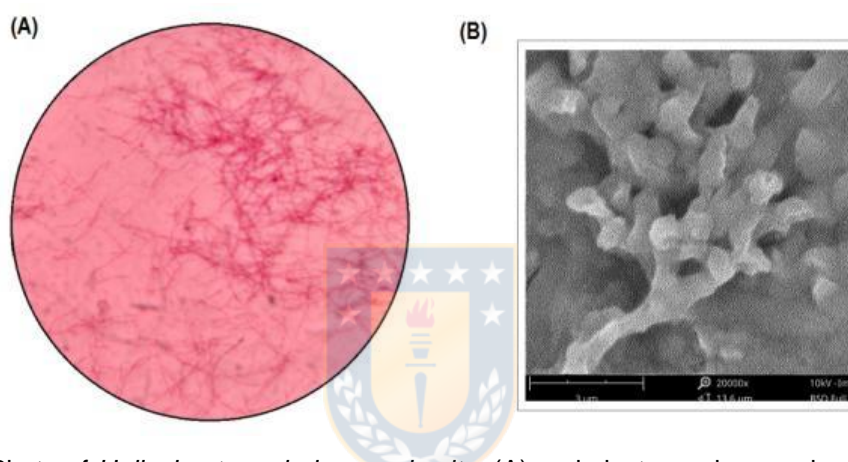


Figure 5. Photo of *Helicobacter pylori* grown *in vitro* (A) and electron micrograph of *H. pylori* biofilm on reactive polymeric surfaces (Courtesy of the Research Group in Sciences with Technological Applications, GI-CAT, Universidad del Valle, Cali-Colombia).

6. Conclusions

The interactions between yeasts and bacteria are of great importance for the understanding of the different processes that are triggered between these microorganisms, in real conditions of habitat and colonization. The complexity that arises from the presence of these interactions makes it necessary to describe the interactions at different levels (biological, physicochemical and biochemical) that are often interdependent. Furthermore, it is clear that the interactions must be described in terms of each pair or group of species. In the particular case of the interactions between *C. albicans* and *H. pylori*, a complete description of the interactions that may take place is not available; Furthermore, the interaction mechanisms that have been reported are poorly understood and are based only on the description of experimental observations by a relatively small number of authors. Finally, it is concluded that progress

should be made in the study of interactions, and the development of new strategies for such studies, as far as possible of general applicability.

Acknowledgments. To Dr. Manuel Palencia of the Research Group in Sciences with Technological Applications (GI-CAT), of the Department of Chemistry of the Universidad del Valle (Cali-Colombia), for the advice provided in the preparation of the document. Authors thank the Program for Scientific Knowledge Diffusion of Mindtech s.a.s. (PSKD 2016-2020) for funds associated with publication costs.

Interest conflict. The authors declare no conflict of interest.

References

- [1] P. Frey-Klett, P. Burlinson, A. Deveau, M. Barret, M. Tarkka, A. Sarguinet. Bacterial-Fungal Interactions: Hyphens between Agricultural, Clinical, Environmental, and Food Microbiologists. *Microbiol. Molecular Biol. Rev.* 75 (2011) 583–609.
- [2] M. T. Tarkka, A. Sarniguet, P. Frey-Klett. Inter-kingdom encounters: recent advances in molecular bacterium-fungus interactions. *Curr. Genet.* 55 (2009) 233–243.
- [3] A. Bauernfeind, G. Hörl, R. Jungwirth, C. Petermüller, B. Przyklenk, C. Weisslein-Pfister, R. M. Bertele, K. Harms. Qualitative and quantitative microbiological analysis of sputa of 102 patients with cystic fibrosis. *Infection* 15 (1987) 270–277.
- [4] M. Avila, D. M. Ojcius, O. Yilmaz. The oral microbiota: living with a permanent guest. *DNA Cell Biol.* 28 (2009) 405–411.
- [5] B. J. B Wood. *Microbiology of fermented foods*, 2nd ed. Springer, Berlin, Germany. (1998).
- [6] P. Frey-Klett, J. Garbaye, M. Tarkka. The mycorrhiza helper bacteria revisited. *New Phytol.* 176 (2007) 22–36.
- [7] J. M. Whipps. Microbial interactions and biocontrol in the rhizosphere. *J. Exp. Bot.* 52 (2001) 487–511.
- [8] D. A. Hogan, M. J. Wargo, N. Beck. Bacterial biofilms on fungal surfaces. In S. Kjelleberg and M. Givskov (ed.), *The biofilm mode of life: mechanisms and adaptations*. Horizon Scientific Press, Norfolk, United Kingdom. (2007) 235–245.
- [9] R. M. Donlan, J. W. Costerton. Biofilms: survival mechanisms of clinically relevant microorganisms. *Clin. Microbiol. Rev.* 15 (2002) 167–193.
- [10] G. Seneviratne, J. S. Zavahir, W. M. M. S. Bandara, M. L. M. A. W. Weerasekara. Fungal-bacterial biofilms: their development for novel biotechnological applications. *World J. Microbiol. Biotechnol.* 24 (2008) 739–743.
- [11] Y. Elad, R. Baker. The role of competition for iron and carbon 602 Frey-Klett *et al.* *Microbiol. Mol. Biol. Rev.* in suppression of chlamyospore germination of *Fusarium* spp. by *Pseudomonas* spp. *Phytopathology* 75 (1985) 1053-1059.
- [12] M. S. Finstein, M. Alexander. Competition for carbon and nitrogen between *Fusarium* and bacteria. *Soil Sci.* 94 (1962) 334–339.
- [13] P. Lemanceau, P. A. Bakker, W. J. De Kogel, C. Alabouvette, B. Schippers. Antagonistic effect of nonpathogenic *Fusarium oxysporum* Fo47 and pseudobactin 358 upon pathogenic *Fusarium oxysporum* f. sp. dianthi. *Appl. Environ. Microbiol.* 59 (1993) 74–82.
- [14] K. C. Marshall, M. Alexander. Competition between soil bacteria and fusarium. *Plant Soil* 12 (1960) 143–153.
- [15] P. Lemanceau, P. A. Bakker, W. J. De Kogel, C. Alabouvette, B. Schippers. Effect of pseudobactin 358 production by *Pseudomonas putida* WCS358 on suppression of fusarium wilt of carnations by nonpathogenic *Fusarium oxysporum* Fo47. *Appl. Environ. Microbiol.* 58 (1992) 2978-2982.

- [16] M. Kluge. A fungus eats a cyanobacterium: the story of the *Geosiphon pyriformis* endocyanosis. *Biol. Environ.* 102 (2002) 11-14.
- [17] J. Rikkinen, I. Oksanen, K. Lohtander. Lichen guilds share related cyanobacterial symbionts. *Science* 297 (2002) 357.
- [18] A. A. Pinto-Tomas, M. A. Anderson, G. Suen, D. M. Stevenson, F. S. Chu, W. W. Cleland, P. J. Weimer, C. R. Currie. Symbiotic nitrogen fixation in the fungus gardens of leaf-cutter ants. *Science* 326 (2009) 1120-1123.
- [19] M. Grube, G. Berg. Microbial consortia of bacteria and fungi with focus on the lichen symbiosis. *Fungal Biol. Rev.* 23 (2009) 72–85.
- [20] M. Grube, M. Cardinale, J. V. de Castro, Jr., H. Muller, G. Berg. Species-specific structural and functional diversity of bacterial communities in lichen symbioses. *ISME J.* 3 (2009) 1105-1115.
- [21] M. Naumann, A. Schussler, P. Bonfante. The obligate endobacteria of arbuscular mycorrhizal fungi are ancient heritable components related to the Mollicutes. *ISME J.* 4 (2010) 862–871.
- [22] T. Baena-Monroy, V. Moreno-Maldonado, F. Martínez, B. Aldape-Barrios, G. Quindós, LO. Sánchez-Vargas. *Candida albicans*, *Staphylococcus aureus* and *Streptococcus mutans* colonization in patients wearing dental prosthesis. *Med. Oral Patol. Oral Cir.* (2005) 10 (Suppl. 1): E27-E39.
- [23] G. E. Pierce. *Pseudomonas aeruginosa*, *Candida albicans*, and devicerelated nosocomial infections: implications, trends, and potential approaches for control. *J. Ind. Microbiol. Biotechnol.* 32 (2005) 309–318.
- [24] H. Busscher, H. van der Mei. How Do Bacteria Know They Are on a Surface and Regulate Their Response to an Adhering State? *Plos Pathogens* 8 (2012) 1–3.
- [25] D. Absolom, F. Lamberti, Z. Policova, W. Zingg, C. van Oss, A. Wilhelm. Surface Thermodynamics of Bacterial Adhesion. *Appl. Environ. Microb.* 1 (1983) 90–97.
- [26] H. Nikawa. *et al.* Alteration of the coadherence of *Candida albicans* with oral bacteria by dietary sugars. *Oral Microbiol. Immunol.* 16 (2001) 279–283.
- [27] R. J. Silverman, A. H. Nobbs, M. M. Vickerman, M. E. Barbour, H. F. Jenkinson. Interaction of *Candida albicans* cell wall Als3 protein with *Streptococcus gordonii* SspB adhesin promotes development of mixed-species communities. *Infect. Immun.* 78 (2010) 4644–4652.
- [28] E. M. Diaz, M. Sacristan, M. E. Legaz, C. Vicente. Isolation and characterization of a cyanobacterium-binding protein and its cell wall receptor in the lichen *Peltigera canina*. *Plant Signal. Behav.* 4 (2009) 598–603.
- [29] A. M. Calvo, R. A. Wilson, J. W. Bok, and N. P. Keller. Relationship between secondary metabolism and fungal development. *Microbiol. Mol. Biol. Rev.* 66 (2002) 447-459.
- [30] M. A. Penalva, H. N. Arst, Jr. Regulation of gene expression by ambient pH in filamentous fungi and yeasts. *Microbiol. Mol. Biol. Rev.* 66 (2002) 426-446.
- [31] C. V. Bamford, A. d'Mello, A. H. Nobbs, L.C. Dutton, M. M. Vickerman, H. F. Jenkinson. *Streptococcus gordonii* modulates *Candida albicans* biofilm formation through intergeneric communication. *Infect. Immun.* 77 (2009) 3696–3704.
- [32] W. M. Bandara, G. Seneviratne, S. A. Kulasooriya. Interactions among endophytic bacteria and fungi: effects and potentials. *J. Biosci.* 31 (2006) 645–650.
- [33] E. Barbieri, P. Ceccaroli, R. Saltarelli, C. Guidi, L. Potenza, M. Basaglia, F. Fontana, E. Baldan, S. Casella, O. Ryahi, A. Zambonelli, V. Stocchi. New evidence for nitrogen fixation within the Italian white truffle *Tuber magnatum*. *Fungal Biol.* 114 (2010) 936–942.
- [34] J. M. Barea, G. Andrade, V. Bianciotto, D. Dowling, S. Lohrke, P. Bonfante, F. O'Gara, C. Azcon-Aguilar. Impact on arbuscular mycorrhiza formation of *Pseudomonas* strains used as inoculants for biocontrol of soil-borne fungal plant pathogens. *Appl. Environ. Microbiol.* 64 (1998) 2304-2307.
- [35] J. M. Barea, R. Azcon, C. Azcon-Aguilar. Mycorrhizosphere interactions to improve plant fitness and soil quality. *Antonie Van Leeuwenhoek* 81 (2002) 343–351.
- [36] J. M. Barke, R. F. Seipke, S. Grüşchow, D. Heavens, N. Drou, M. J. Bibb, R. JM. Goss, W. Yu. Douglas, M. I Hutchings. A mixed community of *actinomycetes* produces multiple antibiotics for the fungus farming ant *Acromyrmex octospinosus*. *BMC Biol.* 8: 109. doi: 10.1186 / 1741-7007-8-109. (2010).
- [37] T. J. Aspray, P. Frey-Klett, J. E. Jones, J. M. Whipps, J. Garbaye, G. D. Bending. Mycorrhization helper bacteria: a case of specificity for altering ectomycorrhiza architecture but not ectomycorrhiza formation. *Mycorrhiza* 16 (2006) 533–541.

- [38] A. Fleming. On the antibacterial action of cultures of a *Penicillium*, with special reference to their use in the isolation of *B. influenzae*. Br. J. Exp. Pathol. 10 (1929) 226-236.
- [39] P. A. Backman, R. A. Sikora. Endophytes: an emerging tool for biological control. Biol. Control 46 (2008) 1–3.
- [40] H. Alexandre, P. J. Costello, F. Remize, J. Guzzo, M. Guilloux-Benatier. *Saccharomyces cerevisiae*-*Oenococcus oeni* interactions in wine: current knowledge and perspectives. Int. J. Food Microbiol. 93 (2004) 141–154.
- [41] C. Cugini, M. W. Calfee, J. M. Farrow 3rd, D. K. Morales, E. C. Pesci, D. A. Hogan. Farnesol, a common sesquiterpene, inhibits PQS production in *Pseudomonas aeruginosa*. Mol. Microbiol. 65 (2007) 896–906.
- [42] C. Cugini, D. K. Morales, D. A. Hogan. *Candida albicans* produced farnesol stimulates *Pseudomonas* quinolone signal production in LasR-defective *Pseudomonas aeruginosa* strains. Microbiology 156 (2010) 3096–3107.
- [43] S. de Weert, I. Kuiper, E. L. Lagendijk, G. E. Lamers, B. J. Lugtenberg. Role of chemotaxis toward fusaric acid in colonization of hyphae of *Fusarium oxysporum* f. sp. radicis-lycopersici by *Pseudomonas fluorescens* WCS365. Mol. Plant Microbe Interact. 17 (2004) 1185-1191.
- [44] F. Bastian, C. Alabouvette. Lights and shadows on the conservation of a rock art cave: the case of Lascaux Cave. Int. J. Speleol. 38 (2009) 55–60.
- [45] F. Bastian, C. Alabouvette, V. Jurado, C. Saiz-Jimenez. Impact of biocide treatments on the bacterial communities of the Lascaux Cave. Naturwissenschaften 96 (2009) 863–868.
- [46] F. Bastian, V. Jurado, A. Novakova, C. Alabouvette, C. Saiz-Jimenez. The microbiology of Lascaux Cave. Microbiology 156 (2010) 644–652.
- [47] S. T. Bates, G. W. Cropsey, J. G. Caporaso, R. Knight, and N. Fierer. Bacterial communities associated with the lichen symbiosis. Appl. Environ. Microbiol. 77 (2011) 1309–1314.
- [48] T. Bauchop, D. O. Mountfort. Cellulose fermentation by a rumen anaerobic fungus in both the absence and the presence of rumen methanogens. Appl. Environ. Microbiol. 42 (1981) 1103-1110.
- [49] B. Baurhoo, F. Goldflus, X. Zhao. Purified cell wall of *Saccharomyces cerevisiae* increases protection against intestinal pathogens in broiler chickens. Int. J. Poult. Sci. 8 (2009) 133–137.
- [50] C. V. Benedict, J. A. Cameron, S. J. Huang. Polycaprolactone degradation by mixed and pure cultures of bacteria and a yeast. J. Appl. Polym. Sci. 28 (1983) 335-342.
- [51] G. Berg, Plant-microbe interactions promoting plant growth and health: perspectives for controlled use of microorganisms in agriculture. Appl. Microbiol. Biotechnol. 84 (2009) 11–18.
- [52] G. Berg, A. Krechel, M. Ditz, R. A. Sikora, A. Ulrich, J. Hallmann. Endophytic and ectophytic potato-associated bacterial communities differ in structure and antagonistic function against plant pathogenic fungi. FEMS Microbiol. Ecol. 51 (2005) 215–229.
- [53] A. Bernalier, G. Fonty, F. Bonnemoy, P. Gouet. Degradation and fermentation of cellulose by the rumen anaerobic fungi in axenic cultures or in association with cellulolytic bacteria. Curr. Microbiol. 25 (1992) 143-148.
- [54] A. S. Adams, C. R. Currie, Y. Cardoza, K. D. Klepzig, K. F. Raffa. Effects of symbiotic bacteria and tree chemistry on the growth and reproduction of bark beetle fungal symbionts. Dog. J. Forest Res. 39 (2009) 1133-1147.
- [55] E. Addis, G. H. Fleet, J. M. Cox, D. Kolak, T. Leung. The growth, properties and interactions of yeasts and bacteria associated with the maturation of Camembert and blue-veined cheeses. Int. J. Food Microbiol. 69 (2001) 25–36.
- [56] M. F. Adesina, R. Grosch, A. Lembke, T. D. Vatchev, K. Smalla. *In vitro* antagonists of *Rhizoctonia solani* tested on lettuce: rhizosphere competence, biocontrol efficiency and rhizosphere microbial community response. FEMS Microbiol. Ecol. 69 (2009) 62–74.
- [57] P. E. Aho, R. J. Seidler, H. J. Evans, P. N. Raju. Distribution, enumeration, and identification of nitrogen-fixing bacteria associated with decay in living white fir trees. Phytopathology 64 (1974) 1413-1420.
- [58] M. A. Al-Fattani, L. J. Douglas. Penetration of *Candida* biofilms by antifungal agents. Antimicrob. Agents Chemother. 48 (2004) 3291–3297.
- [59] M. Barret. P. Frey-Klett, M. Boutin, A. Y. Guillerm-Erckelboudt, F. Martin, L. Guillot, A. Sarniguet. The plant pathogenic fungus *Gaeumannomyces graminis* var. tritici improves bacterial growth and triggers early gene regulations in the biocontrol strain *Pseudomonas fluorescens* Pf29Arp. New Phytol. 181 (2009) 435–447.

- [60] C. S. Goodwin, R. K. McCulloch, J. A. Armstrong, S. H. Wee. Unusual cellular fatty acids and distinctive ultrastructure in a new spiral bacterium (*Campylobacter pyloridis*) from the human gastric mucosa. *J. Med. Microbiol.* 19 (1987) 257-267.
- [61] M. Rohder, J. Puls, R. Buhrdorf, W. Fischer, R. Haas, A. novel Sheathed surface organelle of the *Helicobacter pylori* cag type IV secretion system, *Mol. Microbiol.* 49 (2003) 219-234.
- [62] A. Covacci, J. L. Telford, G. Del Giudice, J. Parsonnet, R. Rappuoli. *Helicobacter Pylori* virulence and genetic geography, *Science* 284 (1999) 13281–333.
- [63] H. L. Mobley, The role of *Helicobacter pylori* urease in the pathogenesis of gastritis and peptic ulceration, *Aliment. Pharmacol. Ther.* 1 (1996) 576–4.
- [64] M. J. Blaser. Hypotheses on the pathogenesis and natural history of *Helicobacter pylori*-induced inflammation. *Gastroenterology* 102 (1992) 720–727.
- [65] B. J. Marshall, Armstrong JA, McGeachie DB, Glancy RJ. Attempt to fulfil Koch's postulates for *pyloric Campylobacter*. *Med J Aust.* 142 8 (1985) 436-9.
- [66] J. R. Warren. Gastric pathology associated with *Helicobacter pylori*. *Gastroenterol Clin North Am.* 29 3 (2000) 705–751.
- [67] E. Bruce, Dunn, H. Cohem, M. J. Blaser. *Helicobacter pylori*. *Clinical Microbiology Reviews.* (1997) 720-774.
- [68] G. L. Mendz, S. L. Hazell, S. Srinivasan. Fumarate reductase: a target for therapeutic intervention against *Helicobacter pylori*. *Arch. Biochem. Biophys.* 321 (1995) 153-159.
- [69] B. P. Burns, S. L. Hazell, G. L. Mendz. Acetyl-CoA carboxylase activity in *Helicobacter pylori* and the requirement of increased CO₂ for growth. *Microbiology* 1418 (1995) 3113-3118.
- [70] P. Saniee, F. Siavoshi, N. Broujeni, M. Khormali, A. Sarrafnejad, R. Malekzadeh. Localization of *H. pylori* within the Vacuole of *Candida* Yeast by Direct Immunofluorescence Technique. *Arch Iran Med.* 16 12 (2013) 705–710.
- [71] G. D. Eslick. *Helicobacter pylori* infection transmitted sexually via oral-genital contact: a hypothetical model. *Sex Transm Inf.* 76 (2000) 489–492.
- [72] C. E. Alvarez-Martinez, P. J. Christie. Biological diversity of prokaryotic type IV secretion systems. *Microbiol. Mol. Biol. Rev.* 73 (2009) 775-808.
- [73] V. Ansanay, S. Dequin, C. Camarasa, V. Schaeffer, J. P. Grivet, B. Blondin, J. M. Salmon, P. Barre. Malolactic fermentation by engineered *Saccharomyces cerevisiae* as compared with engineered *Schizosaccharomyces pombe*. *Yeast* 12 (1996) 215–225.
- [74] W. L. Araujo, W. Jr. Maccheroni, C. L. Aguilar-Vildoso, P. A. Barroso, H. O. Saridakis, J. L. Azevedo. Variability and interactions between endophytic bacteria and fungi isolated from leaf tissues of citrus rootstocks. *Dog. J. Microbiol.* 47 (2001) 229-236.
- [75] K. Arfi, M. N. Leclercq-Perlat, H. E. Spinnler, P. Bonnarme. Importance of curd-neutralizing yeasts on the aromatic potential of *Brevibacterium linens* during cheese ripening. *Int. Dairy J.* 15 (2004) 883–891.
- [76] N. K. Arora, M. J. Kim, S. C. Kang, D. K. Maheshwari. Role of chitinase and beta-1,3-glucanase activities produced by a *fluorescent pseudomonad* and *in vitro* inhibition of *Phytophthora capsici* and *Rhizoctonia solani*. *Dog. J. Microbiol.* 53 (2007) 207–212.
- [77] V. Artursson. Bacterial-fungal interactions highlighted using microbiomics: potential application for plant growth enhancement. Ph.D. thesis. Swedish University of Agricultural Sciences, Uppsala, Sweden. (2005).
- [78] D. Aruscavage, K. Lee, S. Miller, J. T. LeJeune. Interactions affecting the proliferation and control of human pathogens on edible plants. *J. Food Sci.* 71 (2006) R89-R99.

Polymicrobial Biofilms: Fundamentals, diseases, and treatments – A review

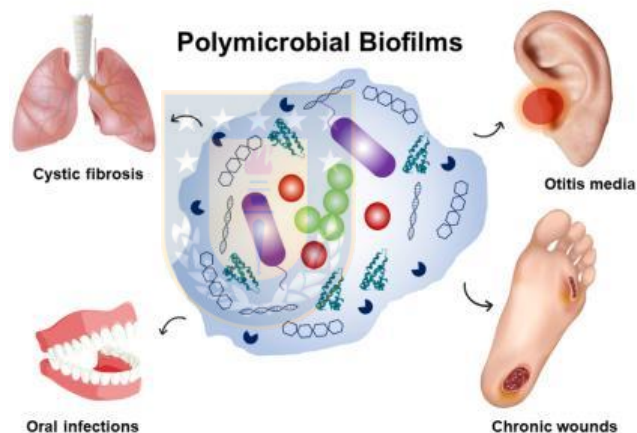
Arturo Espinosa¹, Manuel Palencia^{1*}, Sixta Palencia², Apolinaria García²

¹Departament of Chemistry, Faculty of Natural and Exact Sciences, Universidad del Valle, Cali – Colombia.

² Bacterial Pathogenicity Laboratory, Department of Microbiology, Faculty of Biological Sciences, University of Concepción, Concepción, Chile

*corresponding author: manuel.palencia@correounivalle.edu.co

Graphical abstract



Abstract

Microbes microorganisms grow in two states, biofilm and planktonic cell, in the case of biofilms. When planktonic cells adhere to a surface, they exhibit behaviors described as “reversible” and “irreversible” patterns, being the cell adhesion a key point for the formation of biofilms. It estimates that 80 % of human infections are caused by biofilms and 65 % of nosocomial infections are generated by the growth of these microcolonies in biomedical devices and human tissues. Polymicrobial biofilms are responsible of pathologies in higher living organisms, plants, animals and humans. Polymicrobial biofilms are understood to be those microbial communities that have high resistance and tolerance to antibiotics, formed by microbial groups made up of more than one type of microorganisms, which, among them, develop different symbiotic mechanisms to coexist in a common space. Although research

about alternative treatments such as nanoparticles, natural products, phage therapy and vaccines have taken on relevance in the biomedical field, the area of "polymicrobial biofilms" can still be considered new, because there are mechanisms of their growth and interaction that are not yet understood. This review aims to contribute with concepts and studies that promote these investigations, with the aim of being closer to an effective treatment that allows reducing the impact generated by polymicrobial biofilms on human health, food and biotechnology industries, among others.

Keywords: Polymicrobial biofilm, biofilm, co-infections, chronic, diseases, treatments.

Content

1. Introduction
2. Fundamentals
 - 2.1 Biofilm formation
 - 2.2 Metagenomics
 - 2.3 Polymicrobial interactions
 - 2.3.1 Quorum detection systems (QS)
 - 2.3.2 Synergistic interactions
 - 2.3.3 Competitive interactions
 - 2.4 Extracellular matrix
 - 2.4.1 Composition of Extracellular matrix
 - 2.4.2 Physical and chemical properties of extracellular matrix
 - 2.4.3 Functions of extracellular matrix
 - 2.5 Biofilm habitats
 - 2.5.1 Biotic habitats
 - 2.5.2 Abiotic habitats
3. Study methods of biofilms
 - 2.1 In vitro models
 - 2.1.1 Static models
 - 2.1.2 Dynamic models
 - 2.1.3 Microcosm
 - 2.2 In vivo models
 - 2.3 Measurement and identification
3. Diseases associated with polymicrobial biofilms
 - 3.1 Diagnostics



- 3.2 Chronic wounds
- 3.3 Lung infections in patients with cystic fibrosis
- 3.4 Oral diseases
- 3.5 Otitis media
- 3.6 Biofilm infections acquired by medical devices
- 4. Novel treatments
 - 4.1 Nanoparticle-based treatments
 - 4.2 Treatment with natural products
 - 4.3 Phage therapy
 - 4.4 Vaccines
- 5. Conclusions and perspectives
- 6. References

1. Introduction

The growth of microorganisms is determined by two phenotypes: planktonic cells (i.e., individual biological entities or single-cells that may float or swim in a liquid medium) or sessile aggregates or biofilms (i.e., collective of cells adhered to each other or some surface). However, it has been evidenced microbial cells are mainly organized in complex biofilms communities, so they are rarely found as individual cells in their natural environment. Polymicrobial biofilms are defined as the set of multiple microorganisms remaining protected in a matrix created by themselves, being more resistant and tolerant to host defenses and antibiotics compared with planktonic cells. These microbial communities generally interact collectively with the aim to be stronger and surviving hostile environments such as natural surroundings, abiotic surfaces and even in the human body (Bjarnsholt, 2013; Elias and Banin, 2012; Peters *et al.*, 2012; Orazi and O'Toole, 2019).

Biofilms are found in a wide variety of environments and ecosystems, taking advantage of any nutrient source to initiate adhesion, metabolic processes and ensure their survival. The closeness between microorganisms allows their interaction, contributing to the exchange, distribution and accumulation of metabolic products such as polysaccharides, glycolipids, proteins, enzymes and extracellular DNA, among others, strengthening their resistance (Azeredo *et al.*, 2017; Bjarnsholt, 2013; Flemming and Wingender, 2010). Although these communities were already known since the end of the twentieth century, advances in study methods, accompanied by technological progress, have been demonstrated the influence of biofilms on diseases and infections such as cystic fibrosis,

caries, periodontitis, otitis and their responsibility of the chronicity of wounds. In fact, the National Institutes of Health estimates that 80 % of human infections are caused by biofilms. In addition, the Centers for Disease Control and Prevention (CDC) established that 65 % of infections acquired in a hospital are generated by the growth of these microcolonies in biomedical devices and human tissues, being the main contamination in hospital environments (Elias and Banin, 2012; Lebeaux *et al.*, 2013; Orazi and O'Toole, 2019; Percival, 2017; Short *et al.*, 2014).

The importance of biofilms in the field of medicine, lies in the resistance that this level of biological organization confers on antibiotics, chemical disinfection, and the host's immune response. It has been estimated that approximately 200,000 deaths occur annually in the United States caused by chronic infections associated with microorganisms, so studies of the interactions and behavior of these communities have increased in the last two decades, with the aim of developing successful therapies and treatments (Elias and Banin, 2012; Lebeaux *et al.*, 2013; Orazi and O'Toole, 2019; Short *et al.*, 2014).

This review aims to present the multiple studies of formation, interaction, and behavior of polymicrobial biofilms, describing various environments that can colonize and exhibiting the main causes of their resistance as components of the matrix and synergy between microorganisms. In addition, study techniques will be established, explaining their use to diagnose the multiple infections and diseases caused by these communities. Infections, such as caries, chronic wounds, cystic fibrosis, and otitis will be exposed along with advances in studies focused on treating these conditions, such as research with nanoparticles, natural products and therapies based on vaccines and bacteriophages.

2. Fundamentals

Since the time of Pasteur, it is a basic knowledge that microorganisms are found everywhere, to a greater or lesser degree, every natural environment has unicellular or multicellular microscopic entities. Since then, much of microbiological research has focused on the study of microbes individually and in isolation. In 1683, Antoni van Leeuwenhoek described "animals" in the plaque on his teeth, however, these microbial aggregations were not relevant until 1977, when Nils Hoiby determined that these consortia were related to chronic infection in patients with cystic fibrosis. In 1987, the term "biofilm" was introduced into medical microbiology by Bill Costerton and has been used to describe microbial aggregation that adheres to a surface, ushering in a new era of microbiology research. Currently, it is estimated that less than 0.1% of the total microbial biomass is found as a planktonic

phenotype, so the concept of biofilm is widely accepted. Furthermore, the concept biofilm has acquired importance in the biomedical field since is connected to chronic infections caused by polymicrobial biofilms, so the studies and researches have increased exponentially over the past two decades. In Figure 1 the number of biomedical publications of polymicrobial biofilms is shown (Bahamondez-Canas *et al.*, 2019; Bjarnsholt, 2013; Metcalf *et al.*, 2016; Murray *et al.*, 2014; Vestby *et al.*, 2020; Wei *et al.*, 2019).

Researches have shown that these polymicrobial communities are responsible of pathogenesis of many chronic diseases and infections, being more aggressive than monomicrobial diseases, since biofilms present greater resistance and tolerance to antibiotics (Bahamondez-Canas *et al.*, 2019; Metcalf *et al.*, 2016; Vestby *et al.*, 2020). This section will give a more detailed understanding of formation, interaction, and properties studies of biofilms.

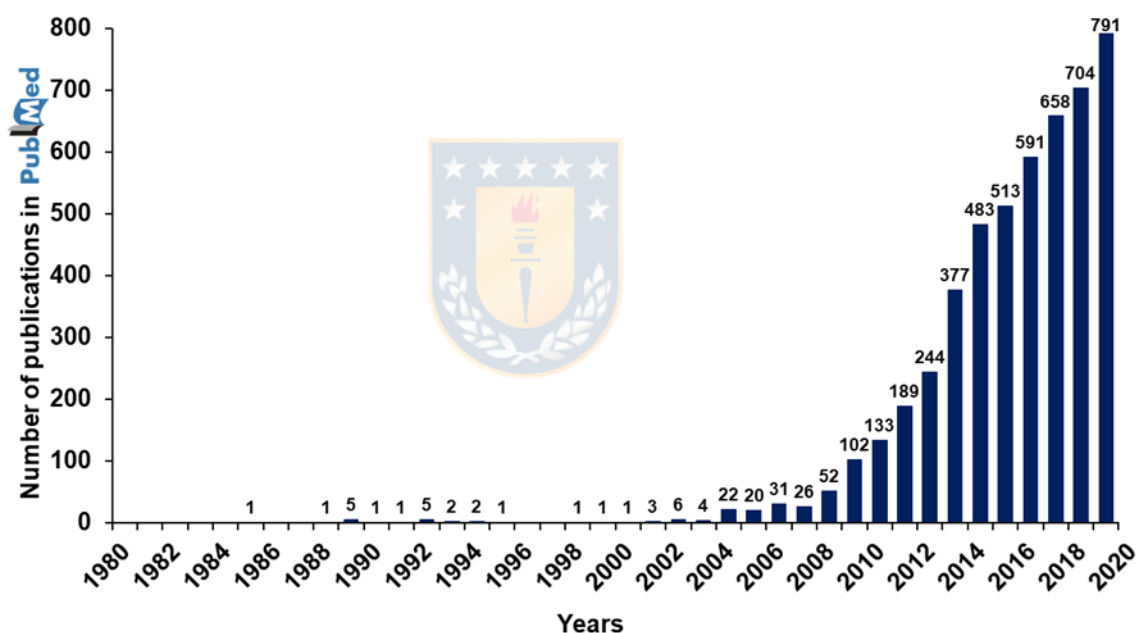


Figure 1. Number of biomedical publications per year of polymicrobial biofilms archived in PubMed central (PMC, 2020).

2.1 Biofilm formation

The biofilm development has been usually studied through in vitro systems. Figure 2 illustrates the main stages described for the formation of these communities. Microorganisms must be close to a surface (approximately 10-20 nm) to initiate the fixing process. Initially, it was established that this stage consists of the union by van der Waals forces, electrostatics, and hydrophobic interactions, however, these are not strong enough to avoid the elimination of species by fluid shear forces. Dunne (2002) described that, after the above-mentioned

process, an additional stage occurs involving an irreversible union of microorganisms through fixation appendages such as pili or fimbriae sited on the outer layer of the microbe, forming complexes with the surface. Flagella and pili are essential to provide mechanical support to the biofilm, which was demonstrated by O'Toole and Kolter in 1998, where *Pseudomonas aeruginosa* mutants with an amount deficient of flagella and pili type IV were unable to initiate biofilm formation. These two stages in the fixation process are widely accepted to describe the adherent strength observed by these microbial communities attached to a surface (Dunne, 2002; O'Toole and Kolter, 1998; Palmer *et al.*, 2007; Rabin *et al.*, 2015).

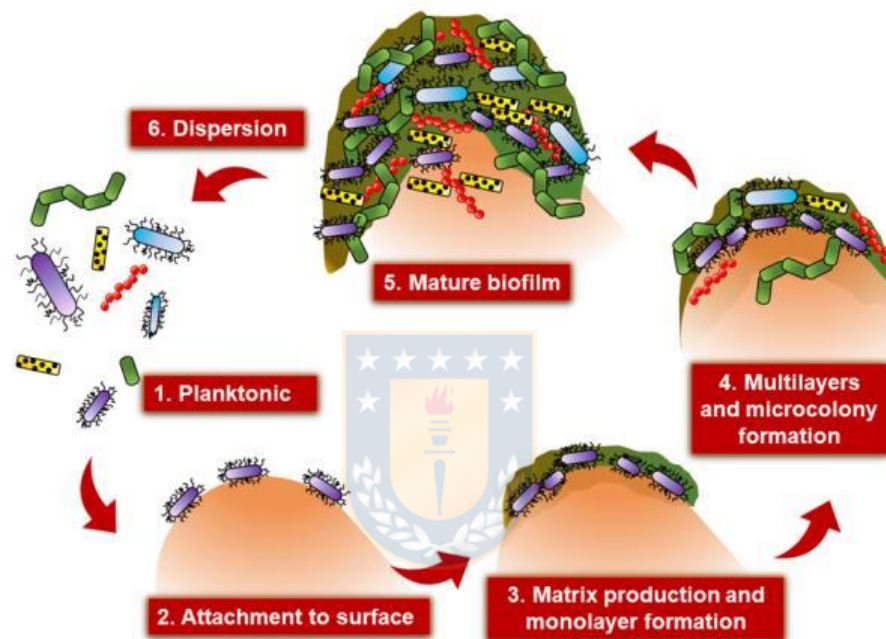


Figure 2. Schematic representation of polymicrobial biofilm formation. (1) Microbes are in their planktonic state. (2) The cells are reversibly joined to a surface. (3) Irreversible union by matrix production and subsequent formation of monolayers. (4) Formation of multilayers and initiation of microcolonies. (5) Maturation of the polymicrobial biofilm. (6) Some members of the biofilm detach, returning to their planktonic state to colonize new surfaces.

The first species colonizing a surface is called pioneering microorganisms or early colonizers, which begin to secrete extracellular polymeric substances (EPS), such as proteins, polysaccharides, glycoproteins, lipids, extracellular DNA, among others, with the aim of protecting and strengthening the binding to a surface. Subsequently, it begins a process called co-aggregation, which consists of the incorporation of other species through microbe-microbe interactions. In this way, microorganisms undergo a transition from their planktonic state and initiate the biofilm maturation process, implying a change in the expression of genes and the modification of their organization according to their metabolism and aerodynamic tolerance, for example, anaerobic microorganisms are found in the deepest

layers in order avoid exposure to oxygen (Bjarnsholt, 2013; Percival *et al.*, 2015a; Peters *et al.*, 2012; Rabin *et al.*, 2015; Willems *et al.*, 2016).

The final stage is dispersion, which is necessary for the biofilm to survive the nutrient shortage caused by high population and competition. This process involves the release of microorganisms in planktonic state, to colonize other surfaces and form new biofilms. The mechanism of this stage has not been fully understood. Costerton *et al* (1999) established that this was a process in which microbes are released by shear forces. Although planktonic bacteria reproduce rapidly and have a high growth rate, biofilm status is the predominant phenotype, since in this way they are resistant to shear forces, they avoid being dragged by water flows or the bloodstream, being a thousand times more resistant than individual cells. This stage is the one the most concern because, at this stage, microorganisms can spread in all regions of the body, generating serious complications in diseases or infections (Bjarnsholt, 2013; Costerton *et al.*, 1999; Rabin *et al.*, 2015).

2.2 Metagenomics

As previously discussed, chronic diseases and infections caused by polymicrobial biofilms have been studied extensively in recent decades. Scientists recognize two molecular processes that microorganisms with a biofilm growth phenotype develop to generate these pathologies. The first is based on damaging the host's tissues, producing necrosis and dead cells that are used by these species to feed. The other process involves the restructuring of the cellular cytoskeleton from effector proteins that are responsible for ordering the host's cellular pathways to prevent mitosis, migration, and apoptosis. Polymicrobial biofilms use other molecular mechanisms to aggregate and dominate other microorganisms, that is, biofilms are a consortium that exercises control over all the individual species that compose it. In this way, it can coordinate the actions necessary for the survival of the microbial community. Consequently, at first, the recognition of this coordination impacted their study because they motivated the study of microorganisms as individual species. At present, biofilms are evaluated as a single entity with a set of genes that need to be expressed to colonize the host, avoid being eliminated and obtain the necessary nutrients for their survival (Kim *et al.*, 2010; Kuramitsu *et al.*, 2007; Wolcott *et al.*, 2008, 2013).

The distributive genome hypothesis explains the organization of genes in biofilms and has been the most accepted theory in the scientific community. This establishes that each one of the microorganisms constituting the consortium, has only a proportion of the total genes, so that all members of the community share the supragenoma, which leads to a decrease in energy of the individual cells by only maintaining a fragment of all genes. It has been

recognized that species use horizontal gene transfer (HGT) to develop this genomic plurality, causing persistence of infection as new strains are continuously produced. The effectiveness of genome distribution is achieved through quorum detection systems, facilitating DNA transfer between members. The function of this system will be discussed with more detail in a subsequent section (Donati *et al.*, 2010; Ehrlich *et al.*, 2010; Seoane *et al.*, 2011; Wolcott *et al.*, 2013).

The supragenoma-formation mechanism explains two important properties of biofilms: tolerance and resistance. Although these characteristics are confused and even used as synonyms, their concepts are different. Tolerance consists in microorganisms surviving in the presence of antibiotics, while resistant biofilms can survive and continue the process of community growth despite the incidence of drugs. All bacteria, regardless of their phenotype, can adopt resistance, while only those grow with biofilm phenotype are tolerant to the multiple drugs developed to combat them. Biofilms achieve antibiotic tolerance when the consortium reaches a certain density of microorganisms, which is favored by the characteristic three-dimensional architecture helping to generate oxygen and nutrient gradients. *In vitro* transcriptome studies have revealed that these communities have places where these gradients are limited, causing the slow growth of members genetically identical to the rest, which are called latent cells or stationary phase. This differentiated growth explains the tolerance to antibiotics, since these are mainly directed to regions with biologic active processes, i.e., where biofilm grows exponentially, while the stationary phase remains intact, prepared to continue the maturation process (Bjarnsholt, 2013; Folsom *et al.*, 2010; Hentzer *et al.*, 2005; Mulcahy *et al.*, 2008).

Moreover, biofilm resistance has been shown to be generated by spontaneous mutations and HGT. The growth of biofilm phenotype promotes conjugation rates, due to the high density of species in an ordered structure, which favors HGT. The most popular classical and molecular tools for monitoring and quantifying HGT in biofilms are based on fluorescent detection of plasmids involved between donors and transconjugants. Ghigo (2001) demonstrated that *Escherichia coli* conjugative pili promoted the transfer of conjugative plasmids, favoring the biofilm formation. Tanner and colleagues illustrated that HGT could occur between species, when they observed that *E. coli* transferred a plasmid with resistance genes to *Acinetobacter baumannii* and *P. aeruginosa*. These studies are alarming, since only a conjugative event can generate resistance throughout the biofilm, aggravating infections. It is important to note that horizontal gene transfer is difficult in regions where there is a high accumulation of metabolic products, i.e. where the growth rate is low, compared with biofilm regions that are permissive

(Ghigo, 2001; Madsen *et al.*, 2012; Orazi and O'Toole, 2019; Tanner *et al.*, 2017; Wolcott *et al.*, 2013).

In particular, Gram-negative bacteria have been documented to generate resistance because they produce genetically encoded enzymes or chromosomes such as β -lactamases, whose function is based on hydrolyzing β -lactam antibiotics, that are directed to the cell wall. These enzymes have been found in clinical samples of otitis media and cystic fibrosis infections. In this context, the property produced in the biofilm is called passive resistance, because, unlike the previous ones, only one microorganism with the resistance factor protects other members that do not have this factor, being unnecessary the direct interaction between species to grant preserve the entire biofilm. Weimer and colleagues found that a nontypable strain of *Haemophilus influenzae* (NTHi 86-028NP) that produced β -lactamases protected *Streptococcus pneumoniae* from antibiotics. These two bacteria have been blamed for otitis media (Høiby *et al.*, 2010; Orazi and O'Toole, 2019; Weimer *et al.*, 2011; Wolcott *et al.*, 2013).

The recalcitrant characteristics of these communities represent a public health problem because, although their formation and growth are interrupted, the surviving cells retain these properties, which is why metagenomic studies are still used, since, in addition to allowing the development of clinical diagnoses, through its study is possible to analyze the distribution of genes in polymicrobial biofilms and achieve a better understanding of their ecology and functions in artificial and natural systems (Ribeiro *et al.*, 2017; Schmeisser *et al.*, 2017).

2.3. Polymicrobial interactions

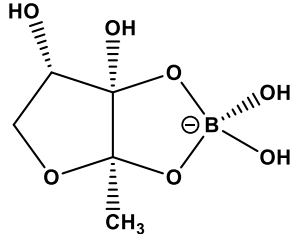
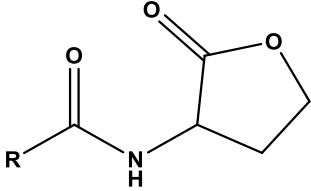
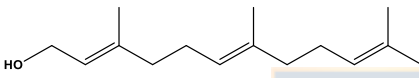
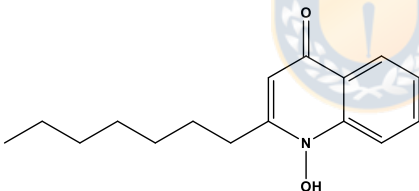
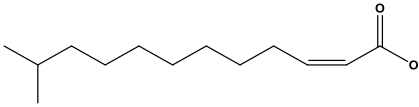
Polymicrobial biofilms have a large number and variety of species in a relatively small structure, so microorganisms must interact to establish the organization of the consortium. However, it should be kept in mind that polymicrobial communities can exhibit cooperative or antagonistic interactions, which makes their interaction mechanisms connected to differentiating biological characteristics. Therefore, the interactions are complex in nature and depend on the context of the analysis. One the most important mechanisms are known as Quorum Sensing Systems (QS), which are the molecules allowing communication between the members of the biofilm. This process involves the secretion of chemical signals that depend on the density of species present in the biofilm, with the aim of organizing phenotypic changes at the population level from regulated intracellular signaling. In this way, important functions in the biofilm are controlled, such as obtaining nutrients (Gabriliska and Rumbaugh, 2015; Peters *et al.*, 2012; Rickard *et al.*, 2003; Stewart and Franklin, 2008; Willems *et al.*, 2016). The study of the interaction of microorganisms with biofilm growth phenotype is a

relatively new area in microbiological analysis, since most investigations have been based on the behavior of planktonic cells, which, today, it is a completely different perspective to those based on biofilms as reference point (Gabriliska and Rumbaugh, 2015). In this section, the rationale for quorum detection systems will be exposed, along with synergistic and antagonistic interactions in polymicrobial communities.

2.3.1. Quorum detection systems (QS): Microorganisms communicate from the microbe-microbe crosstalk called quorum detection system. The term 'quorum' is used to refer to the minimum number of bacteria per biofilm volume that are necessary to activate a gene expression. Microorganisms are not aware of density of microbes in the biofilm, but QS allows them to distinguish the species present, because the behavior of each microorganisms that responds to the signal is different. QS allows the acquisition of nutrients, promotes colonization, increases virulence, and alters physiological factors such as bioluminescence. Autoinducer 2 (AI-2) is the most documented and studied QS molecule, as high concentrations of AI-2 have been found in chronic wounds. This molecule can be detected by Gram-negative, Gram-positive, and even, anaerobic bacteria. Another QS studied are systems controlled by N-Acyl-L-homoserine lactone (AHL), in Gram-negative bacteria. This molecule varies between species but has a basic structure of homoserine lactone with latera acyl chain, and its length varies from 4 to 16 carbons. The AHL-QS system controls conjugation of plasmids or virulence gene expressions. Haudecoeur and Faure reported that the bacterial pathogen, *Agrobacterium tumefaciens*, used the AHL-QS system for the transport of virulence genes in the host. It has described that AHL-deficient *P. aeruginosa* bacteria were more susceptible to antibiotics than AHL-competent (Bjarnsholt, 2013; Haudecoeur and Faure, 2010; Orazi and O'Toole, 2019; Peleg *et al.*, 2010; Peters *et al.*, 2012; Rabin *et al.*, 2015; Wolcott *et al.*, 2013). Although these two molecules are the most studied, there are other compounds, such as secondary metabolites and wastes from other microorganisms. Table 1 sets out some quorum detection systems which have been described.

It should be noted that these molecules may also exert negative effects on biofilms by adverse reactions. Orazi and O'Toole (2019) discovered in *in vitro* studies HQNO affected the cell membrane of *S. aureus* causing it to be more susceptible to antibiotics (Orazi and O'Toole, 2019; Orazi *et al.*, 2019), so QS is only effective when there is a synergistic interaction between species, which does not happen in all cases. When a species colonizes a surface, it uses these molecules to communicate with other microorganisms that, when it encounters early colonizers, initiates an interaction that can be cooperative or antagonistic.

Table 1. Quorum detector molecules.

Quorum detector	Structure	Fundamentals	References
AI-2		It is produced by Gram-negative and Gram-positive bacteria, through the LuxS enzyme. It is of importance in bacteria such as <i>E. coli</i> to regulate protein production and biofilm formation.	González Barrios <i>et al.</i> , 2006; Lu <i>et al.</i> 2017.
AHL	 <p>R - 4-18 carbon chain</p>	Homoserine lactone molecule and a lateral chain of fatty acyl, from 4 to 18 carbons. QS found mainly in Gram-negative bacteria.	Chan <i>et al.</i> , 2015; Ma <i>et al.</i> 2018.
Farnesol		Produced by the fungal organism <i>Candida albicans</i> . Its presence has been shown to protect bacteria such as <i>Staphylococcus aureus</i> , increasing the biofilm's resistance to antibiotics.	Kong <i>et al.</i> , 2017; Langfor <i>et al.</i> , 2009; Polke and Jacobsen, 2017
2-n-heptyl-4-hydroxyquinoline-N-oxide (HQNO)		Molecule excreted by <i>P. aeruginosa</i> . <i>In vitro</i> studies have shown that it influences the physiology of <i>Staphylococcus aureus</i> , giving it more resistant to antibiotics.	Hazan <i>et al.</i> , 2016; Orazi and O'Toole, 2019.
Diffuse Signal Factors (DSF)	 <p>cis-11-methyl-dodecanoic acid</p>	<i>Cis-2</i> unsaturated fatty acid molecules, responsible for regulating biological functions. Biofilms from bacteria excreting these compounds, such as <i>Stenotrophomonas maltophilia</i> , exhibited high resistance to antibiotics.	Ryan and Dow 2011; Zhou <i>et al.</i> , 2017.

2.3.2. Synergistic interactions: Synergy was defined by Bjornson in 1982 as the cooperative interaction of two or more bacterial species. Members in a biofilm prefer to develop synergy with the aim of achieving greater growth, tolerance, and virulence. The more cooperative interaction and the more genetic resources the community present, for example, with mixed members of bacterial and fungal organisms, the more benefits the biofilm will present. Metabolic cooperation, resistance, and tolerance, are benefits of synergy in biofilms,

presenting more possibilities to survive. Cooperation between microorganisms is worrying they worsen a disease, presenting a more aggressive behavior than infections caused by planktonic cells (Gabriliska and Rumbaugh, 2015; Murray *et al.*, 2014; Willems *et al.*, 2016; Wolcott *et al.*, 2013).

Aggregation of multiple species for the formation of consortium is an example of synergy, where they interact with the objective of protecting themselves and feeding on an extracellular matrix to initiate a growth process. This mechanism consists of reversible union of other species, and early colonizers, of different genetics, determine which microorganisms may be beneficial to the community. Another cooperative mechanism consists of cross-metabolic feeding, which is referred by other authors as syntrophic, which consists of a microorganism benefiting from the metabolic by-products of another present species in the biofilm. Ramsey *et al* (2011) found in a murine infection model that *Aggregatibacter actinomycetemcomitans*, a Gram-negative anaerobic bacterium, which has been proposed as responsible for periodontitis, took advantage of the L-lactate produced by *Streptococcus gordonii*, being a bacterium that is part from oral microbiota, to improve its survival and, consequently, pathogenesis in the host. This process is different from co-location, which is another synergistic mechanism that promotes the growth of another, giving it the necessary resources for its development. Waste products are also used by other microorganisms as a source of nutrients. Diaz *et al.* (2002) published a study in which *Fusobacterium nucleatum*, an anaerobic bacterium responsible for the maturation of dental plaque, generated CO₂ as a waste product, and this was used by *Porphyromonas gingivalis* to increase its pathogenesis in periodontal diseases (Diaz *et al.*, 2002; Ramsey *et al.*, 2011; Rickard *et al.*, 2003; Wolcott *et al.*, 2013).

2.3.3. Competitive interactions: Biofilms present a highly organized three-dimensional architecture, but of reduced extension, generating competition for space and nutrients. The co-aggregation process also promotes antagonistic interaction because, although the area of colonization increases, species prefer to approach the nutrients source. When microbial antagonism occurs, species begin to produce chemical inhibitors that can kill or disrupt the growth and physiology of other members. Kreth *et al* (2008) observed that *Streptococci* of oral microbiota generated H₂O₂ due to the aerobic environment, which generates an antagonistic interaction of *Streptococcus mutans*, the main pathogen of tooth decay, causing the production of antistreptococcal bacteriocins. It has also been observed that a microorganism may begin to occupy all surface-fixing sites, with the aim of preventing the union of new species (Elias and Banin, 2012; Gabriliska and Rumbaugh, 2015; Kreth *et al.*,

2008; Peters *et al.*, 2012). This interaction has been poorly studied because cooperation between species predominates over antagonistic due to benefits it gives to the biofilm. Competitive interaction is a desired effect for the host, as it increases the community's susceptibility (Elias and Banin, 2012).

2.4. Extracellular matrix

Bill Costerton introduced the biofilm term in 1987, defining it as a community of bacterial cells that are encapsulated in a polymer matrix attached to a surface. In the section 1.1 was shown that the first step for the formation of a polymicrobial biofilm involves physical and reversible adhesion on a surface. At this stage, early colonizers begin the production of an extracellular matrix, which contains various extracellular polymeric substances (EPS) such as proteins, lipids, polysaccharides, extracellular DNA, biosurfactants, flagella and pili. This matrix, like any other aggregate, requires physical forces to prevent its disintegration, providing protection to high doses of antibiotics to the polymicrobial community, which would be lethal if they had a planktonic phenotype. Furthermore, this matrix, or "matrixoma", as other authors call it, allows to catch antibiotics, eliminate oxygen-free radicals, and preserves the community of predators and phagocytes (Bjarnsholt, 2013; Karygianni *et al.*, 2020).

2.4.1. Composition of Extracellular matrix: EPS was defined by Flemming and collaborators in 2007 as the "dark matter" of the biofilm, due to the large number of biopolymers present in the matrix and the complexity of its analysis. It should be noted that its structure and composition depend on the members of the biofilm, as well as the availability of nutrients and environmental stress. Some authors decide to divide the matrix between components that are associated with the cell surface, such as pili type IV and flagella, responsible for promoting the adhesion of microbes, and those that are secreted extracellularly such as proteins, polysaccharides, lipids, DNA and extracellular RNA, which contribute to matrix aggregation. Figure 3 outlines the matrix components. Some environmental components can also be added and contribute to the strength of the biofilm. For example, Marsh and collaborators in a recent review described how proteins that are present in saliva are added to the matrix and are exploited by microorganisms to feed (Bowen *et al.*, 2018; Flemming *et al.*, 2007, 2016; Karygianni *et al.*, 2020; Marsh *et al.*, 2016).

Biofilms have also been shown to contain minerals that are products of the biomineralization of their constituent members. Oppenheimer-Shaanan *et al* (2016) studied the Gram-positive soil bacterium, *Bacillus subtilis*, which is characterized by developing architecturally strong and complex biofilms. They found that this bacterium is an active producer of calcite,

protecting community members from antibiotics and environmental aggressions, which has been used in the biotechnology area as a proposal for bioremediation of soil structure (Karygianni *et al.*, 2020; Li *et al.*, 2015; Oppenheimer-Shaanan *et al.*, 2016).

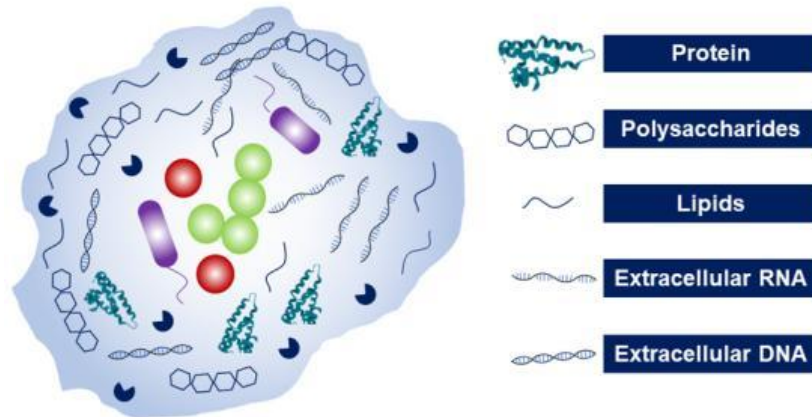


Figure 3. Schema of the basic components in matrix.

2.4.2. Physicochemical properties of extracellular matrix: The most important physical property of the matrix, apart from promoting the adhesion of other bacteria by flagella and pili, is to form stable aggregate networks. Sullan *et al* (2015) determined that Gram-positive *S. mutans* were bound to salivary agglutinins immobilized by P1 adhesions, which were added to the extracellular matrix. Taglialegna *et al* (2016) found a similar behavior with *S. aureus*, since they showed that it produced Bap proteins that formed amyloid-like fibers, giving it resistance to scaffolding. Strength is also attributed to matrix viscosity, due to extracellular DNA and exopolysaccharides. This was demonstrated by Hou *et al* (2017), using ATR-FTIR spectroscopy combined with tribometry, found that *S. aureus* was more resistant to shear when its production of polysaccharides is high in the initial adhesion stage (Hou *et al.*, 2017; Karygianni *et al.*, 2020; Sullan *et al.*, 2015; Taglialegna *et al.*, 2016). Moreover, the matrix also has chemical properties because it acts as reservoir and diffusion medium of various biomolecules, generating gradients of nutrients, oxygen, QS molecules, inorganic ions, metabolites, and pH. The morphology of the biofilm can be rough, smooth, and porous, generating what some authors call as heterogeneous "microenvironments" within the biofilm, influencing its properties. Arnaouteli *et al* (2017) studied biofilms formed by *Bacillus subtilis*, a Gram-positive bacterium present in the soil. The researchers found that this species produces BslA proteins, whose functionality depended on redox environments, since, in the anoxic regions, this protein was in its monomeric form, improving the structure of the biofilm, while in the rich region in oxygen, the protein appeared as a dimer, generating a hydrophobic

community (Arnaouteli *et al.*, 2017; Flemming and Wingender, 2010; Karygianni *et al.*, 2020).

2.4.3. Functions of extracellular matrix: The matrix is considered the most important component of polymicrobial biofilms, since, in its absence, the community would not exist. In fact, the main difference in planktonic and biofilm growth is the set of EPS. The matrix represents 90 % of the total dry mass of the biofilm, while only 10 % corresponds to the microorganisms that compose it. Antibiotic resistance and tolerance have been attributed to the EPS diffusion limits and associated degradative enzymes. Adam *et al* (2002) assessed the importance of the matrix when they cultivated the fungal species *C. albicans* with two species of *Staphylococcus epidermidis*: one specie that did not generate matrix and another that produced it. The results showed that *C. albicans* was more susceptible to fungicides with the species that did not develop the aggregate, so it was unable to produce compounds that protected *S. epidermidis*, while the biofilm was more resistant to matrix-producing bacteria, preserving *C. albicans* from fungicides and, in turn, protecting the microbe from the drug. On the other hand, Kong *et al* (2016) demonstrated that a mixed biofilm of the fungal species *C. albicans* with *S. aureus* bacteria exhibited high drug tolerance because *C. albicans* secreted β -1,3-glucan that was added in the matrix, promoting the strength of the biofilm. A more recent investigation of these two species was developed by Kean *et al* (2017), who highlighted the importance of extracellular DNA in the matrix, which promoted the adhesion of *S. aureus* and the development of the mixed biofilm (Adam *et al.*, 2002; Flemming and Wingender, 2010; Kean *et al.*, 2017; Kong *et al.*, 2016; Orazi and O'Toole, 2019).

Isolation for the EPS study represents a challenge because the matrix always remains attached to the bacteria, so the extraction process can damage cells and cause intracellular material to leak into the matrix. The functions and properties of polymicrobial scaffolding have led researches focused on treatments against these microbial communities to focus on blocking the vital functions of EPS, inhibiting adhesion, degrading EPS using enzymes or other agents that prevent consortium formation or even causing the mechanical disruption from energy and light-based methods. However, these researches have conducted their studies on single-bacterium models, and few have focused on analyzing polymicrobial biofilms (Karygianni *et al.*, 2020; Koo *et al.*, 2017; Flemming and Wingender, 2010).

2.5. Biofilm habitats

As previously indicated, biofilm formation is a highly efficient adaptive mechanism, and as a consequence, its presence is widely generalized. However, biofilm is not synonymous with

disease. These communities are also responsible for positive effects, for example, promoting the growth and development of plants, and even defending living hosts, increasing their immune resistance, the generation of biotechnological products, among others. However, when biofilms act as pathogens they become aggressive towards the host. This section will discuss the habitats of polymicrobial biofilms, both biotic and abiotic, and the impact of their presence.

2.5.1. Biotic habitats

In healthy individuals, polymicrobial biofilms found in the oral cavity and gastrointestinal tract have been identified and studied. The oral cavity is an environment that promotes the formation of microbial communities, since it is warm, humid, presents enough nutrients for its diet, and factors such as pH, the closeness between teeth and salivary flow generate optimal conditions for colonization of these species. Oral biofilms are better known as dental plaques, and it was the first location in the human body where biofilms were described. Associated diseases will be discussed in more detail in section 2.4. Studies have shown that bacteria have a favorable adaptation to this habitat, due to the multiple structures of teeth and tissues such as tongue, gums and palate, causing a rapid growth of microorganisms that are resistant to environmental stressors (Bjarnsholt, 2013; Duran-Pinedo and Frias-Lopez, 2015; Filoche *et al.*, 2010; Jakubovics and Kolenbrander, 2010; Willems *et al.*, 2016).

As mentioned in the previous section, the glycoproteins present in saliva, along with metabolic products produced by early colonizers, initiate matrix formation in the enamel on the tooth's surface. Initially, the microorganisms detected were commensal *Streptococci* such as *Streptococcus mitis* and *Streptococcus oralis*, which correspond to 60 to 90 % of the oral microbiota, along with other species of this genus. In addition, it was claimed that other microorganisms such as *Veillonella*, *Actinomyces*, *Gemella*, and *Neisseria*, were also present, however, with metagenomic techniques such as gene-based cloning 16S rRNA approximately 700 more species were identified. Today, it is considered that it is considered that around 1000 bacterial species have colonized, either temporarily or permanently the oral mucosa. Although it has been little studied, it has been shown that fungi, mainly of *Candida* species, are part of the oral microbiome. These biofilms remain intact, therefore, oral hygiene is important to remove these communities, because, if the necessary oral care is not presented, the consortium begins to accumulate and grow on the surface of the teeth and in gingival grooves, causing pathologies that will be discussed later (Bjarnsholt, 2013; Manson *et al.*, 2008; Peters *et al.*, 2012; Willems *et al.*, 2016).

After the oral cavity, the intestine is the second biotic habitat most colonized by biofilms. Bacterial species that interact symbiotically with the host have been estimated at 500 to 1,000. Metagenomic cloning techniques 16S rRNA have determined that this environment hosts species of *Bacteroides*, *Bifidobacterium*, *Streptococcus*, *Lactobacillus*, *Collinsella*, *Eubacterium* and *Clostridium*, which can produce biofilms. The gut microbiota is important for the health of humans. For example, studies have reported that these species protect the intestinal epithelium from pathogens through antagonistic interactions. Changes in diet, or the effect of antibiotics, causes the death of these microorganisms and triggers conditions such as chronic diarrhea, which is treated with probiotics that are bacteria with positive effects in the treatment of a pathology. Rosenfeldt *et al* (2002) found that probiotic treatment of lactic acid-producing species, *Lactobacillus*, produced positive effects in children with chronic diarrhea (Bjarnsholt, 2013; Rosenfeldt *et al.*, 2002; Zoetendal *et al.*, 2002).

Skin represents another region in the body where biofilms are generated, mainly in the epidermis, sweat ducts, and hair follicles. The host-biofilm interaction is also synergistic. Iwase and colleagues found that *Staphylococcus epidermidis*, a harmless commensal bacterium in human skin, inhibited the colonization of opportunistic microorganisms such as *S. aureus*. However, Büttner *et al* (2015) described in a recent review, that the implantation of medical devices can generate an opportunistic invasive activity of this microorganism, forming biofilms that generate pathologies in the host. Other non-sterile regions such as the urinary system and the female reproductive tract have been places where these polymicrobial communities live (Bjarnsholt, 2013; Büttner *et al.*, 2015; Iwase *et al.*, 2010; Ribeiro *et al.*, 2017).

2.5.2. Abiotic habitats: Polymicrobial biofilms can form anywhere, as they are resistant to even the extremes environments. Although the study of these communities is recent, they have existed since the earliest times, being found in deposits where life could not be considered. Rasmussen published the first fossil evidence of microbial life in 3235 million-year-old massive volcanic sulfide filament deposits, which is consistent with the thermophilic origin of life (Rasmussen, 2000; Yin *et al.*, 2019).

Surfaces in the midst of non-sterile water, whether sea or fresh, create an ideal environment for the immediate growth of a biofilm. This was observed since 1977, when Geesey *et al.*, observed sessile microorganisms in an alpine current. The growth of biofilms in these media has been a major problem, mainly in drinking water pipes, due to the infections that can be acquired by the population that consumes it. Since the last millennium *P. aeruginosa* has been reported in tap water pipes, being a direct source of infection. These observations have

served as an alternative for wastewater treatment. In these, the species are responsible for colonizing the flocs of wastewater to degrade organic matter, phosphorus, nitric oxides, among other non-toxic compounds. However, the colonization of microorganisms such as *Actinobacteria*, *Bacteroidetes*, *Firmicutes* and *Proteobacteria*, which act as sulfide oxidizers and sulfate reducers, are also responsible for the deterioration by corrosion of wastewater collection systems as demonstrated by Gomez-Alvarez and colleagues (Bjarnsholt, 2013; Gomez-Alvarez *et al.*, 2012; Schmeisser *et al.*, 2017; Wagner *et al.*, 2002).

Soil is another habitat where a wide variety of microorganisms with biofilm phenotype are found. In section 1.4.1 *Bacillus subtilis* was mentioned, which contributes to the soil structure, generating strong biofilms due to its high production of calcite. Bacteria of this same genus that are found in the rhizosphere are also responsible for the growth and acquisition of plant defenses, since the absence of these microbes, makes it more susceptible to soil pathogens (Bjarnsholt, 2013; Kloepper *et al.*, 2004; Oppenheimer-Shaanan *et al.*, 2016). Biofilms can be found in other extreme environments, whether high salinity, pressure, pH, among others. However, currently, the most studied abiotic habitat is the surface of medical devices, since it represents a direct means of infection, developing pathologies that will expanded later.

3. Study methods of biofilms

Before this new era of research in microbiology, infection study techniques were based on methods that were culture-dependent, so all diseases were attributed to species in planktonic status. However, the technology contracted techniques independent of cultivation, which allowed verifying that microorganisms were organized in communities, generating biofilms (Peters *et al.*, 2012). The biofilm study is carried out using *in vitro* or *in vivo* models, which will be studied in this section, as well as the measurement and identification techniques used to evaluate these polymicrobial consortia.

3.1 *In vitro* models

In vitro models are relevant and widely used because they allow the development of observations that answer questions that must be subsequently confirmed by *in vivo* models, since their simplicity does not reflect a real situation. The challenge currently is to develop *in vitro* models that generate a near-reality environment (Gabriliska and Rumbaugh, 2015). *In vitro* models are classified as static, when nutrients are limited, and dynamic, when there is a constant supply of these resources. Figure 4 illustrates the most used static and dynamic *in vitro* methods.

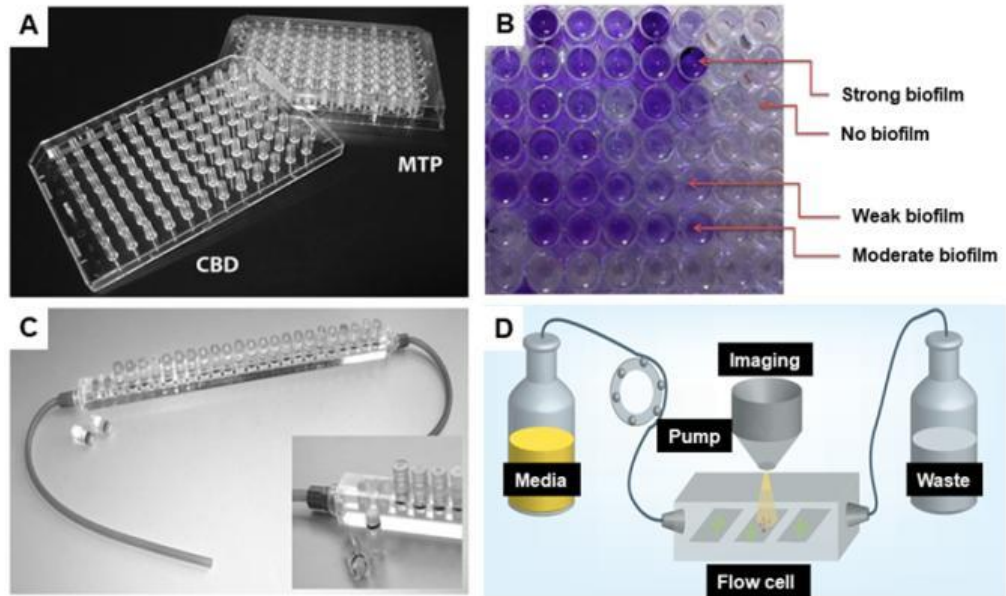


Figure 4. More used static and dynamic *in vitro* models. (A) Microtiter plate (CBD) and the Calgary biofilm device. (B) Interpretation of violet crystal staining. An intense color reflects effective biofilm. The decrease in this intensity shows a weaker biofilm formation, while if there is no staining, there was no biofilm formation. (C) Modified Robbins device, where the coupons are inserted into the liquid stream. (D) Flow cell system. Fresh media of a receptacle is pumped through a flow cell and into a waste receptacle. The rate at which media flows through the system will determine the amount of shear force at which biofilm cells are exposed. (Modified: (A) and (C) from Azeredo *et al.*, 2017, (B) from Vijayababu *et al.*, 2018, and (D) from Gabrielska and Rumbaugh, 2015).

3.1.1. Static models: These models are the most used and the least expensive, however, they present the most limitations, so the results obtained, generally, differ from the *in vivo* models. These are used to analyze the adhesion of a biofilm on a surface that is usually a plastic, however, it is difficult to evaluate its growth because nutrients are limited, and are rapidly depleted (Gabrielska and Rumbaugh, 2015).

Microtiter plate assay (Figure 4A) is the most widely used method of conducting biofilm research. This model, developed by Madilyn Fletcher, consists of the cultivation of bacteria in the wells of a polystyrene plate, with the aim of evaluating the adherence, maturation, metabolism and tolerance of a biofilm on a surface that can provide a total of 96 wells. To study the adhesion of the species to the surface, the wells are emptied and washed to remove planktonic cells, while the biomass that remains attached is controlled through crystal violet staining (Figure 4B). The advantages are its easy handling and economy; however, it presents the drawback of not allowing the distinction of free cells with respect to the settled at the bottom of the wells. Calgary's biofilm model (Figure 4A) emerged to solve the problems of microtiter plates. It has a cover with pins that fit the wells, which are analyzed, since, on these, the biofilm will be presented, and not the planktonic cell sediments. However, in these

two models, the availability of nutrients is limited, so the results are irrelevant considering the complexity of the habitats that colonize these microorganisms (Azeredo *et al.*, 2017; Bjarnsholt, 2013; Gabriliska and Rumbaugh, 2015).

Despite the above, relevant biofilm research has been developed using static models. Karched *et al* (2015) applied the culture wells to compare the temporal transitions of two phenotypes: a planktonic culture and another with biofilm growth. The investigated species were *Porphyromonas gingivalis*, *Aggregatibacter actinomycetemcomitans*, *Prevotella intermedia*, and *Parvimonas micra*, which are associated with periodontal pathologies. The result of crystalline violet staining was weaker for the biofilms of *P. intermedia*, *P. micra*, *F. nucleatum* and *C. rectus* than for *A. actinomycetemcomitans* and *P. gingivalis* (Gabriliska and Rumbaugh, 2015; Karched *et al.*, 2015).

3.1.2. Dynamic models: Dynamic models differ from static models, in that there is a constant supply of nutrients, which increases costs, in addition that their use and analysis is complex. However, it is possible to develop studies over a long period of time, in addition to modeling shear forces and making an approach to a situation close to reality (Gabriliska and Rumbaugh, 2015).

The Robbins device is an *in vitro* model consisting of removable plugs that are unilaterally exposed to flowing liquid (Figure 4C). In this technique, nutrient gradients are generated, and not a uniform flow of these, simulating a real situation where microorganisms must find a way to feed. Blanc and colleagues used a Robbins device modified with hydroxyapatite discs to evaluate the behavior and growth of *Streptococcus oralis*, *Actinomyces naeslundii*, *Veillonella parvula*, *Fusobacterium nucleatum*, *Aggregatibacter actinomycetemcomitans* and *Porphyromonas gingivalis*, obtaining results according to the oral biofilms observations as resistance to shear forces and antibiotics. Drip flow reactors are other dynamic models in which continuous fluid forces are generated, promoting a heterogeneous environment of nutrients and resources, so microorganisms must search for the maturation of the consortium. Woods *et al* (2012) achieved successful biofilm growth for *S. aureus* and *P. aeruginosa* species, the results of which were consistent with previous research on chronic wounds (Blanc *et al.*, 2014; Coenye and Nelis, 2010; Gabriliska and Rumbaugh, 2015; Woods *et al.*, 2012).

The flow cell system (Figure 4D) is the most widely used *in vitro* model to study biofilms, since this has allowed to develop hypotheses that were subsequently confirmed, such as the resistance of these communities to antibiotics and shear forces. In this technique, microorganisms grow on a glass surface, and present a continuous nutrient with the aim of

analyzing the growth of these communities. This model is non-invasive and has the advantage of being reproducible. It is assumed that, when these species generate three-dimensional structures, they are exhibiting wild behavior, so this model has been optimal for biofilm formation. Flow cells allow uninterrupted monitoring, being effective for relevant observations. Despite these advantages, it continues to be a model far from reality, since the habitat of a biofilm provides the conditions and nutrients that are used by microorganisms, depending on complex factors that cannot be modeled *in vitro*. For example, this technique cannot be used to study chronic wounds, since it is impossible to modulate the host's immune response, in addition to other factors such as inflammation and matter such as mucosa, pus, necrotic tissue, among others, obtaining results that are not consistent with what is observed in other researches (Bjarnsholt, 2013; Lee *et al.*, 2005).

3.1.3. Microcosm: For the results and observations in these techniques to be extrapolated to reality, the habitats in which biofilms grow must also be modeled. This is performed by mimicking environments *in situ* and even using *ex vivo* tissues. There have been a wide variety of studies that mimic the oral cavity, for example, the research by Blanc *et al* (2014), who arranged hydroxyapatite discs to model the dental structure. Lundstrom *et al* (2010) meanwhile, used 35 bovine incisors with excised pulps. The teeth were covered with mucin and were inoculated with standardized suspensions of *Streptococcus sanguinis*, *Actinomyces viscosus*, *Fusobacterium nucleatum*, *Peptostreptococcus micros* and *Prevotella nigrescens*, to evaluate the efficacy of various bactericides. It has also been tried to emulate chronic wounds, with components such as collagen, artificial skin, and addition of blood components. Bjarnsholt used growth models in a semi-solid collagen matrix, and observed that aggregates formed by *S. aureus* and *P. aeruginosa* were similar to those found in chronic wounds, exhibiting the same growth phenotypes, as well as their resistance and tolerance to antibiotics. Sun and colleagues developed the Lubbock's wound model, with red blood cells next to bovine plasma, and studied biofilm formation of *P. aeruginosa* and *S. aureus*. The morphological similarity between the model and a real chronic wound is evident (Figure 5A). Taking scanning electron micrographs (SEM) of biofilms in both models (Figure 5B) shows a similar growth. The urinary tract has also tried to be simulated by Samaranayake and collaborators, who developed models with Foley's catheter, artificial urine, and glucose, to evaluate the growth of *C. albicans* biofilms with *P. aeruginosa* and *E. coli*. Young *et al.* developed a dental microcosm with discs of bovine enamel, human saliva and sucrose and was monitored for 10 days by fluorescence images (Figure 5C), obtaining optimal biofilm

growth with this microcosm (Bjarnsholt 2013; Gabriliska and Rumbaugh, 2015; Blanc *et al* 2014; Kim *et al.*, 2014; Lundstrom *et al.*, 2010; Samaranayake *et al.*, 2014; Sun *et al.*, 2008).

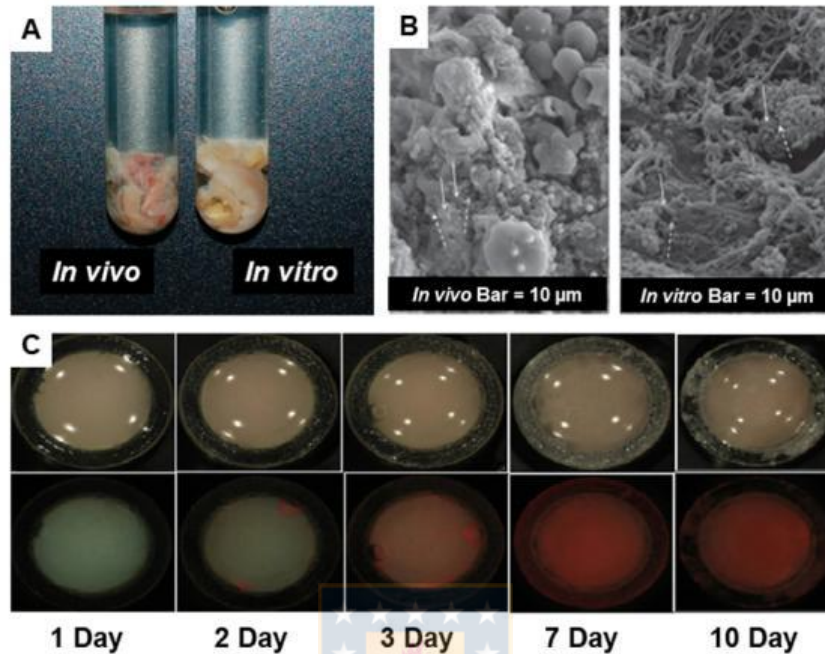


Figure 5. Examples of microcosm. (A) Visual comparison between Lubbock's chronic wound and a sample of real debridement, exhibiting a clear similarity. (B) Comparison of scanning electron micrographs (SEM) of biofilms *in vivo* and *in vitro* that highlight the similarity in the structure and community of the biofilm since both images show rod-shaped bacteria (solid arrows) and cocci-shaped bacteria (dotted arrows). (C) Biofilm growth in a dental microcosm of bovine enamel. Images in the top line are white light, while in the bottom line are images of red fluorescence. The increase in fluorescence intensity indicates strong biofilm growth (Modified from: (A) and (B) from Sun *et al.*, 2008 and (C) from Kim *et al.*, 2014).

3.2. *In vivo* models

In vivo models allow to analyze the interaction of polymicrobial biofilms with the host, as well as the immune response against to these communities, which is impossible with *in vitro* models. These study techniques are mainly carried out on invertebrates such as flies, nematodes, and moths. However, the challenge is that observations in these experiments are relevant to humans. Fly models, for example, are made with *Drosophila melanogaster dipterans*, which have served to analyze the immune response that is generated with the colonization of biofilms. Korgaonkar *et al* (2013) studied the virulence of *P. aeruginosa* with the *Drosophila* model, finding that *P. aeruginosa* generated synergy with the Gram-positive commensal bacteria of flies, causing their death. Other researchers prefer to use the *Caenorhabditis elegans nematode* model, since its transparent body allows constant monitoring of the biofilm infection process. Cruz and colleagues employed this model,

perceiving that the interaction of *E. faecalis* and *C. albicans* has a negative impact on the virulence which was attributed to inhibition of the hyphae morphogenesis of *C. albicans* by *E. faecalis*. The moth model, specifically with *Galleria mellonella* larvae, have been less used, but they represent an alternative study because they are large and easy to manipulate (Cruz *et al.*, 2013; Edwards and Kjellerup, 2012; Gabriliska and Rumbaugh, 2015; Korgaonkar *et al.*, 2013; Rendueles *et al.*, 2012; Vilela *et al.*, 2015).

The few investigations that can be developed in mammals are carried out in mice, rats, and rabbits. These murine models have presented an optimal predictive level of pathology in humans. Porcine models have also been widely used due to similarities in immune response. However, *in vivo* murine, or porcine models are restricted by ethical concerns. Gabriliska and Rumbaugh (2015) described in a review of biofilm study models, investigations where wound pathogens such as *S. aureus* and *P. aeruginosa* were grown *in vitro* for biofilm formation and transferred into mouse wounds, preserving structure and distribution, so these models are successful (Gabriliska and Rumbaugh, 2015; Lebeaux *et al.*, 2013; Rabin *et al.*, 2015; Roberts *et al.*, 2015).

3.3. Measurement and identification

Another challenge for biofilm research is the measurement of biomass, EPS, metabolic activity, and identification microorganisms. Although traditional techniques such as Gram staining are methods used for the detection of biofilms and infection hotspots, they only have a predictive value, so they must be accompanied by more elaborate processes (Azeredo *et al.*, 2017). Table 2 contains some techniques for measuring and quantifying some components in biofilms.

Table 2. Methods for measuring components in biofilms.

Component	Technical	Foundation	References
Biomass	Confocal Laser Scanning Microscopy (CLSM)	Represents the three-dimensional structure of the biofilm from the acquisition of planes at different depths.	Bridier et al., 2010 ; Daddi Oubekka et al., 2012 .
	Scanning Electron Microscopy (SEM)	Preferred method for biofilm visualization because it produces a three-dimensional appearance that allows understanding of the surface structure of the sample.	Hasan et al., 2015 ; Van Laar et al., 2015 .
	Atomic Force Microscopy (AFM)	It allows obtaining biological images at the micrometer and nanometer scale from the raster scan of a sharp tip on the surface, while the interaction between the sample and the probe tip is measured.	Azeredo et al., 2017 ; Lower, 2015 .
	Violet glass staining	The method consists of staining components of the matrix and cells, alive or dead in the biofilm.	Azeredo et al., 2017 .
	Electrochemical impedance spectroscopy	Detects changes in the diffusion coefficient of an added redox solute. The decrease in current is associated with an increase in the thickness of the biofilm.	Dominguez-Benetton et al., 2012 .
Identification of microorganisms	Fluorescent hybridization <i>in situ</i> (FISH)	It is the most used method for the identification of microorganisms. In this technique, oligonucleotides that were labeled with fluorescence-emitting probes hybridize with ribosomal RNA in previously fixed species. This procedure must be accompanied by a microscopy technique to understand the functions of biofilm members.	Azeredo et al., 2017 ; Musat et al., 2016 .
Metabolic activity	Visible spectroscopy	A tetrazolium is decomposed by dehydrogenase enzymes in formazan that emits in the visible region, which allows a control of metabolic activity in biofilms.	Ramage, 2016 .
	Alamar Blue Reduction	Alamar blue is reduced by the reabsorption effect of metabolically active species, allowing it to correlate with total metabolism in the biofilm.	Van den Driessche et al., 2014 .

4. Diseases associated with polymicrobial biofilms

Microorganisms are responsible for causing infections in the human body, whose immune system generates an immediate response, such as fever or inflammation, with the aim of eliminating these opportunistic species. When the immune system achieves its objective, it is considered that the human body experienced an acute infection, however, when it persists despite the immune response and treatment with antibiotics, it is understood that the infection is chronic, caused by polymicrobial biofilms (Bjarnsholt, 2013; Sekirov and Finlay, 2006).

Studying the growth of microorganisms with biofilm phenotypes, meant a change in the infection paradigm, because these were attributed to bacteria of a single species with virulence factors, acting as pathogens. Although this explains acute infections, it is unable to justify a chronic infection. Biofilms are estimated to be 1000 times more resistant and tolerant to antibiotics than planktonic cells, being responsible for chronic wounds and persistent infections in regions of the body such as the oral cavity, lung, middle ear, among others. These polymicrobial communities have been estimated to be responsible of 65 to 80 % of all infections (Macià *et al.*, 2018; Orazi and O'Toole, 2019; Roberts *et al.*, 2015; Wolcott *et al.*, 2013). This section will expose some diseases and infections caused by biofilms as well as their diagnosis and current treatments.

4.1. Diagnostics

Infections caused by polymicrobial biofilms are complex to diagnose, because it is important to identify all the species that cause virulence, however, current diagnostic methods can only detect organisms that are found in highest proportion in biofilm. The challenge is to develop diagnostic procedures that allow identification and subsequent quantification of each individual member (Macià *et al.*, 2018; Wolcott *et al.*, 2013).

The first part of the diagnosis consists of obtaining the sample which is evaluated by Gram staining and microscopy in order to establish growth parameters such as temperature, duration, aerobic or anaerobic medium, among others. The growing methods have been unsuccessful, because the difficult extraction of the biofilm that is attached to a surface. In fact, there is a risk that biopsies do not contain any bacteria, due to the heterogeneous distribution of these species in biofilms. Ultrasound surface treatment for consortium extraction has been a successfully employed alternative. Rohacek *et al* (2010) analyzed cardiac devices, cultivating the sonicated fluid obtained from the treatment of devices with ultrasound, identifying bacteria such as *Staphylococcus aureus*, *Streptococcus mitis* among

other Gram-positive anaerobic cocci (Bjarnsholt, 2013; Rohacek *et al.*, 2010; Thomsen *et al.*, 2010).

Molecular methods, such as 16S rRNA metagenomic cloning techniques, along with polymerase chain reaction (PCR) testing, are used for clinical diagnosis. PCR is responsible for reading the genomic fragment for the identification of species; however, it does not allow the distinction of living cells from dead ones. Furthermore, this technique presents the requirement for a specific primer, which is not practical considering that biofilms present multiple species, therefore, other study methods have been developed to improve clinical diagnosis. Costerton *et al.* (2011) described the novel IBIS strategy, developed by David Ecker's team, which involves weighting the genomic fragments produced by PCR employing mass spectrometry. The weight is used to calculate the initial composition, identifying all species, regardless of that are known, unknown, pathogenic, harmless, among others. The pharmaceutical company Abbot acquired Plex ID, which is a molecular diagnostic technique that provides a set of primers for the identification of a greater number of species by IBIS. In some cases, the identification of the microorganisms is not enough, so the presence of mRNA is evaluated to demonstrate polymicrobial activity (Bjarnsholt, 2013; Costerton *et al.*, 2011; Wolcott *et al.*, 2013).

All the aforementioned techniques are still far from providing an effective diagnosis of chronic infections causing by biofilms, since they do not provide information about the nature, commensal or pathogenic, of the members of the consortium, so the criterion used for diagnosis of biofilm infection is the persistence of the disease, despite antibiotic treatment. The development of a successful diagnosis still represents a clinical challenge at the present (Bjarnsholt, 2013; Macià *et al.*, 2018).

4.2. Chronic wounds

Patients with cardiovascular disease or diabetes are susceptible to developing chronic wounds, which are exploited by opportunistic microorganisms to develop biofilms. A wound is considered chronic when it does not heal, even with aggressive antibiotic treatment. Chronic wounds can last up to more than 12 weeks, while acute wounds heal by less than 4 weeks. This has represented a public health problem, generating great economic impact worldwide. In 2012-2013, the UK spent 4 % of total national health service, that is, approximately 5.3 billion pounds in chronic wound management, while, in the United States, US Medicare in 2014 reported that treatment costs of 8.2 million inhabitants with chronic wounds ranged from 28.1 million to 96.8 billion (Bahamondez-Canas *et al.*, 2019; Bjarnsholt, 2013; Klassen *et al.*, 2020).

Wound infection becomes complex to eradicate when opportunistic microorganisms optimally develop a biofilm, where EPS inhibits the immune response of neutrophils, which produce oxygen and proteinases around the biofilm, causing inflammation in the host. Schierle *et al* (2009) used a murine model of infection, finding that the host is unable to heal wounds colonized by *S. aureus* (Figure 6A and 6B). Bahamondez-Canas and colleagues stated in a recent review that, in the dispersion phase (Figure 2), planktonic cells caused recurrent acute infections, aggravating the patient's situation. Prolonged healing of these wounds can lead to sepsis, amputation and, in the worst case, death (Bahamondez-Canas *et al.*, 2019; Peters *et al.*, 2012; Sen *et al.*, 2009; Schierle *et al.*, 2009).

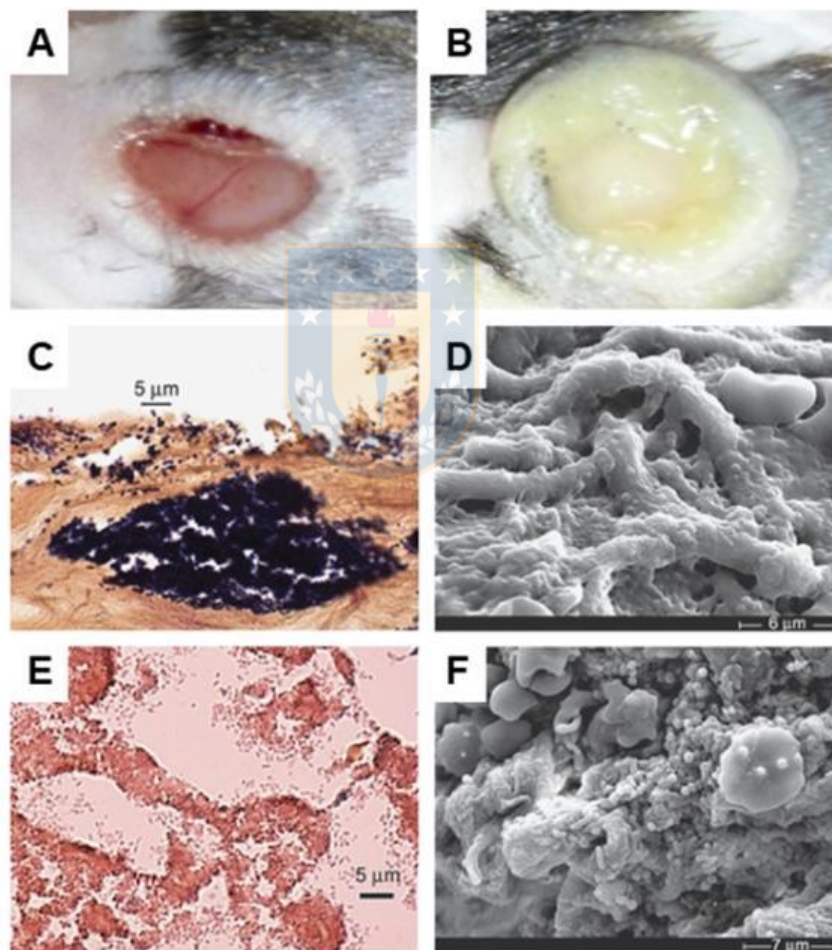


Figure 6. Chronic biofilm-mediated wounds. (A) Wound of a mouse not colonized by biofilms. (B) Chronic wound of a mouse colonized by biofilms of *S. aureus*. (C) Microphotograph of a Gram-stained pressure ulcer sample showing a biofilm formed by *Staphylococcus* and *Enterococcus*. (D) SEM images of the pressure ulcer sample illustrating a biofilm of cocci-bacteria cells that colonize collagen beams within the wound. (E) Gram-stained diabetic foot ulcer sample microphotograph showing a biofilm formed by Gram-negatives near the tissue surface. (F) SEM of a pressure ulcer sample showing cocci and rods bacteria (Modified: (A) and (B) from Schierle *et al.*, 2009. (C), (D), (E) and (F) from James *et al.*, 2008).

The species detected in most chronic wounds are Gram-positives bacteria as *Staphylococcus aureus*, *S. epidermis* and the Gram-negative species such as *Pseudomonas aeruginosa*. Other species such as *Morganella morganii*, *Streptococcus pyogenes* and *Enterococcus durans* have also been reported as aggravating species in chronic cutaneous leishmaniasis ulcers. James and colleagues were among the first researchers in 2008 to verify, using photomicrographs of Gram-stained wounds and SEM images, biofilm formation in chronic wounds caused by pressure ulcers and diabetic foot. Researchers found that pressure ulcer wounds were colonized by cocci biofilm-forming (Figure 6C and 6D), while diabetic foot wounds contained Gram-negative rod communities (Figure 6E and 6F) (Bahamondez-Canas *et al.*, 2019; Bjarnsholt, 2013; James *et al.*, 2008; Salgado *et al.*, 2016; Vestby *et al.*, 2020).

Therapies of this disease consist of the elimination of tissue fluid through the application of negative pressure by means of an electronic vacuum pump (VAC), with the aim of decreasing the microbial population and increasing vascularity for tissue repair. There are other treatments such as hyperbaric oxygen installation (HBO), which involves the application of pure oxygen at pressures above 1 atm, improving the function of neutrophils, host angiogenesis and inhibition of anaerobic organisms, increasing the biofilm susceptibility. Techniques used prior to the use of antibiotics, such as worm debridement therapy (MDT) consisting of releasing antimicrobial enzymes during feeding, have been successful in dealing with wound chronicity (Peters *et al.*, 2012; Rani *et al.*, 2007).

4.3 Lung infections in patients with cystic fibrosis

Lung infections caused by biofilms are mainly evident in cystic fibrosis (CF) patients. In 1989, it was determined to be a common autosomal recessive genetic disorder in the Caucasian population, generated by mutations in the cystic fibrosis transmembrane conductance regulator (CFTR), which is a chloride channel whose mutation in the phenylalanine 508 residue, causes an incorrect folding of this biomolecule, producing cell degradation. This mutation unbalances the secretion of chloride ions, generating excess cations, promoting an osmotic imbalance and eventual dehydration that directly affects the mucosa tissues. Cystic fibrosis produces an accumulation of mucosa, raising the appropriate conditions for polymicrobial colonization. These opportunistic species are inhaled and trapped in the respiratory tract, so they cannot be eliminated. The subsequent formation of polymicrobial biofilms is the cause of disease and mortality in cystic fibrosis patients (Gabriliska and Rumbaugh, 2015; Lebeaux *et al.*, 2013; Peters *et al.*, 2012).

The identified pathogenic bacteria species are *P. aeruginosa*, *S. aureus*, *Streptococcus milleri*, *Haemophilus influenzae*, *Streptococcus pneumoniae*, *Moraxella catarrhalis* and *Burkholderia cenocepacia*. Generally, *S. aureus* and *H. influenzae* colonize lungs of hosts in childhood. While the presence of *H. influenzae* decreases with age, *P. aeruginosa* begins to colonize the lungs. *P. aeruginosa* is the predominant bacterium in 40 % of patients, and initiates colonization in the paranasal sinuses, however, biofilms of this species have been found in the lung tissue and sputum of CF patients (Figure 7). The immune response is based on the migration of neutrophils to the biofilm, generating inflammation and obstruction of the airways (Figure 7C), consuming the available oxygen by the metabolic activity of the biofilm, favoring the biofilm of *P. aeruginosa* and the presence of anaerobic species such as *Actinomyce*, *Prevotella*, *Propionibacterium* and *Veillonella* (Filkins and O'Toole, 2015; Gabriliska and Rumbaugh, 2015; Macià *et al.*, 2018; McGuigan and Callaghan, 2015; Peters *et al.*, 2012; Vandeplassche *et al.*, 2019; Vestby *et al.*, 2020).

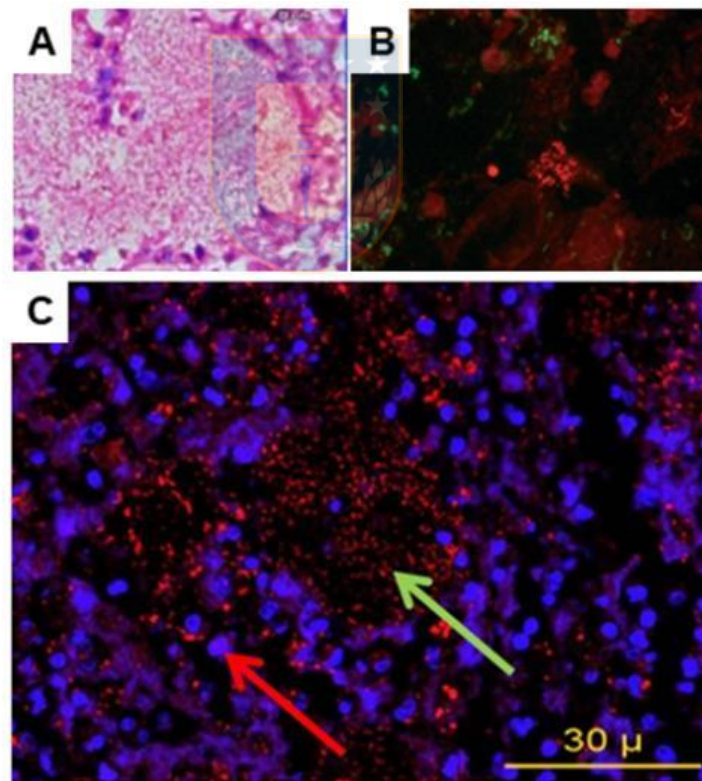


Figure 7. Biofilms of *P. aeruginosa*. (A) Detection of massive bacterial biofilms by Gram- staining in the respiratory zone. (B) PNA-FISH visualization of aggregates of *P. aeruginosa* (red) and other bacterial species (green). (C) PNA FISH visualization of *P. aeruginosa* in endobronchial mucus in an explanted lung from a patient with cystic fibrosis. The bacteria are displayed in red and aggregate in a biofilm (green arrow). Blue fluorescence shows inflammatory cells, mainly neutrophils, that surround the biofilm (Modified: (A) from Bjarnsholt, 2009, (B) from Rudkjøbing *et al.*, 2012, (C) from Crabbé *et al.*, 2019).

The quorum detection molecule, AI-2, is primarily responsible for the interaction in these infections, as a large amount of this has been found in the sputum of CF patients. Other studies have shown that *P. aeruginosa* and *S. aureus* present cooperative and antagonistic interactions in biofilm growth. *S. aureus* produces a QS molecule of HQNO, which inhibits the growth of *P. aeruginosa*. Hoffman and colleagues found that the QS molecule of HQNO, produced by *P. aeruginosa*, protected *S. aureus* from antibiotics. However, Peters and colleagues described, in a biofilm review, that compounds secreted by *S. aureus* inhibited the growth of *P. aeruginosa*. Bragonzi *et al.*, used a murine model and found that there was increased biofilm formation when *P. aeruginosa* was grown with *B. cenocepacia*, because it responds to AHL secreted by *P. aeruginosa* (Bragonzi *et al.*,2012; Hoffman *et al.*,2006; McGuigan and Callaghan, 2015; Peters *et al.*, 2012; Sibley *et al.*, 2006).

Chotirmall and collaborators found the dimorphic fungal species *Candida albicans* in the sputum of people with CF. As discussed in previous sections, this fungus forms resistant biofilms with polymicrobial species, causing pathogenesis in the host when it enters deep tissues in its elongated hyphal form, perforating epithelial tissues. The interaction of this fungal species with bacteria such as *P. aeruginosa* has been shown to be exclusively antagonistic. This microbe produces AHL-QS, which causes cell lysis of the hyphal surface, while studies of Cugini and colleagues showed that yeast produces farnesol, which is toxic to *P. aeruginosa* (Chotirmall *et al.*,2010; Cugini *et al.*, 2007; Peters *et al.*, 2012).

Antibiotic treatments, as is usual in biofilms, are ineffective. The choice of antibiotics is made by routine microbiology tests, and although this therapy has been shown to decrease diversity by 72 hours, biofilm recovers in less than 30 days, because it is impossible to modulate the micro-environmental factors of a lung with CF, differing the results obtained *in vitro* from those *in vivo* (Daniels *et al.*, 2013; Filkins and O'Toole, 2015; Vandeplassche *et al.*, 2019; Zhao *et al.*, 2012).

4.4. Oral diseases

Polymicrobial biofilms in the oral cavity have been the most studied because access for community extraction is elemental. Polymicrobial biofilms form rapidly in the oral cavity. Studies have shown that species take approximately 48 hours to transfer from individual cells to a complex biofilm. Through proper oral hygiene, oral flora presents synergy with the host, however, ecological changes develop pathologies such as periodontal diseases and dental caries, which affects 60 to 90 % of children and almost a large part of the adult population. In the early 1960s, Gram-positive anaerobic bacterium *Streptococcus mutans*, was identified as the species responsible for dental caries, however, it is currently known that this bacterium

adheres to the tooth surface through glucosyltransferases and initiates the aggregation of other bacteria, presenting all the growth characteristics of a polymicrobial biofilm. The polymicrobial biofilm stops the host signaling pathways, so the mucosa does not generate an immune response (Bjarnsholt, 2013; Peters *et al.*, 2012; Willems *et al.*, 2016).

Figure 8A shows the organization of some microbial species in dental plaque. The species that colonize this habitat are, generally, aciduric and acidogenic whose lactic acid, product of carbohydrates fermentation, dissolves the hydroxyapatite crystals of the teeth, causing a dental hole accompanied by gingivitis and subsequent loss of the tooth. When gingivitis persists, it causes periodontitis. *Aggregatibacter actinomycetemcomitans*, *Porphyromonas gingivalis*, *Treponema denticola*, and *Tannerella forsythia* species have been reported to be members of mature biofilms, or "red complex", as some authors define it. Although it was initially attributed to periodontal diseases, *P. gingivalis* is not the main generator of periodontal pathogenesis.

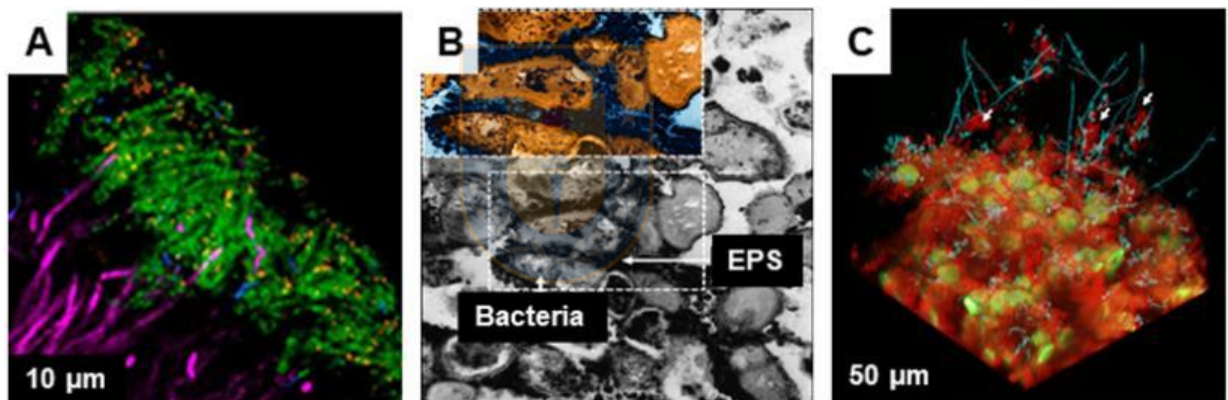


Figure 8. Oral biofilms. (A) Spatial organization of dental plaque biofilm using FISH of *Corynebacterium*, *Streptococcus*, *Porphyromonas* and *Haemophilus/Aggregatibacter* species. (B) Microscopic image of children plaque with active cavities. The selected area shows exopolysaccharides in blue and the bacteria were colored in orange. (C) Three-dimensional representation of biofilm architecture Bacterial and fungal species *C. albicans* are tangled and surrounded by an EPS-rich matrix (Modified: (A) from Mark Welch *et al.*, 2016, (B) from Hajishengallis *et al.*, 2017, (C) Falsetta *et al.*, 2014).

In fact, this species was found in only 50 % of patients with periodontitis, and even, the red complex has been detected in healthy people. Pathogenesis has been attributed to archaea species in biofilms that accumulate in the subgingival pocket (Peters *et al.*, 2012; Willems *et al.*, 2016).

EPS of oral biofilms are mainly glucan and fructan biomolecules, which are responsible for the virulence of tooth decay (Figure 8B). Glucan, is an insoluble polysaccharide, protecting members of the consortium from environmental stress as the shear forces caused by saliva.

In addition, saliva is employed by the host to neutralize acids generated by members of the community, due to its buffering capacity, however, when these biofilms accumulate on the surface of the tooth, saliva is unable to penetrate it because glucan in the matrix. The host's diet is essential in the matrix and, consequently, in the oral microbiota. Adler and colleagues determined, from the data of 34 early European skeletons, that the transition from hunter-gatherer to agriculture, changed the microbial community to a disease-associated configuration, since the appearance of *S. mutans* is observed due to a diet rich in sugar. Sucrose is fundamental to the growth of biofilms of this species, since it breaks it down into glucans, constituting the matrix and improving microbial adhesion-cohesion (Adler *et al.*, 2013; Bjarnsholt and Givskov, 2007; Bowen *et al.*, 2018; Lebeaux *et al.*, 2013; Sandt *et al.*, 2007; Willems *et al.*, 2016).

Streptococcal species produce glycosyltransferases B, C and D increase the virulence of the polymicrobial biofilm. In particular, glycosyltransferase B facilitates colonization of the fungal species *C. albicans*. Falsetta *et al* (2014) demonstrated, from *in vitro* models, that the biofilm biomass is higher when *C. albicans* grows with *S. mutans* due to the high production of EPS by these two species, generating a biofilm with a highly complex architecture (Figure 8C) that caused high virulence in murine models (Falsetta *et al.*, 2014; Gabriliska and Rumbaugh, 2015; Willems *et al.*, 2016). Although the main pathogens of oral infections are summarized in this section, it is still a challenge to evaluate the contribution of all species, because their behavior depends on environmental conditions, and the oral cavity is a constantly changing habitat, which has also hindered the development of effective therapy (Bowen *et al.*, 2018; Willems *et al.*, 2016).

4.5 Otitis media

Otitis media (OM) is an infection that involves the Eustachian tube between the tympanic membrane and the inner part, which people usually experience in childhood. The Eustachian tube has the function of protecting humans from opportunistic organisms and the elimination of secretions. Children have a less functional and smaller Eustachian tube than in adulthood. Otitis can be divided into acute OM, with effusion, or with chronic support. Annually, 709 million people suffer acute OM, and 51% of these are younger than 5 years of age. Symptoms include fever, otalgia, vomiting, pain, and an effusion in the middle ear, however, this resolves in a few weeks when the infection is acute. When the infection is chronic, it causes hearing loss in the patient. In the United States, annual costs to serve OM exceed \$5 billion due to prolonged antibiotic therapies because of constant infection (Bjarnsholt, 2013;

Gabrilska and Rumbaugh, 2015; Kyd *et al.*, 2016; Peters *et al.*, 2012; Silva and Sillankorva, 2019).

The first demonstration that these infections are caused by biofilms was carried out by Post in 2001, using a murine model, observed with SEM the growth of *H. influenzae* in a biofilm form in the middle ear mucosa. This was the first microbial species to be attributed the etiology of OM. Other commensal species that inhabit the upper respiratory tract such as *S. pneumoniae* and *Moraxella catarrhalis* also cause pathogenesis in the host (Figure 9B and 9C). These species have been shown to live synergistically with the host, however, they generate pathologies when epithelial wounds are caused by previous viral respiratory infections, such as infection with influenza A virus, which is responsible for predisposing the patient (Figure 9A). Wren *et al* (2014) employed a murine model demonstrating that co-infection with influenza A and *S. pneumoniae*, promoted colonization and inhibiting inflammatory responses within the nasopharynx and middle ear chamber (Gabriliska and Rumbaugh, 2015; Post, 2001; Silva and Sillankorva, 2019; Wren *et al.*, 2014).

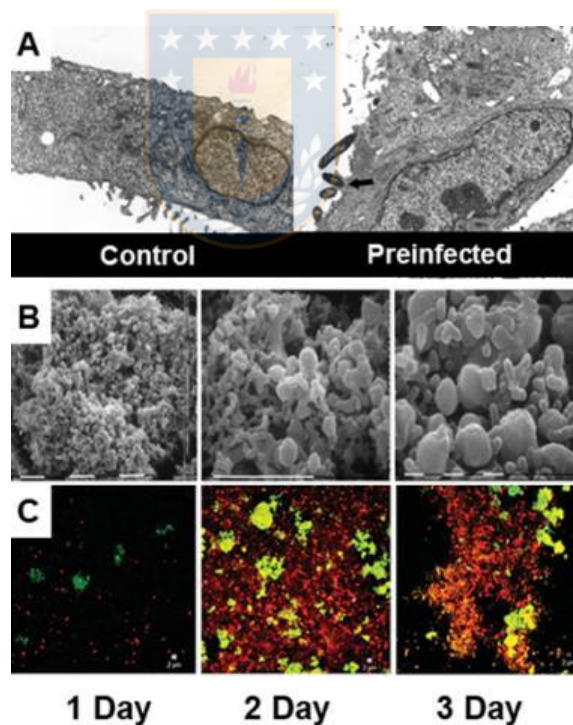


Figure 9. Infections that cause otitis media. (A) Comparison of the respiratory epithelial cell line without infection (Control) with the pre-infected, improving the adhesion of NTHi. (B) Polymicrobial biofilms of *H. influenzae* and *M. catarrhalis* monitored for 3 days by SEM. (C) monitored by CLSM (Modified: (A) from Jiang *et al.*, 1999, (B) and (C) from Armbruster *et al.*, 2010).

These biofilms employ AI-2 to resist antibiotic treatment. Perez *et al* (2014) developed *in vitro* and *in vivo* studies with murine models, to evaluate the biofilms of *Moraxella catarrhalis* and

Streptococcus pneumoniae, evidencing high resistance due to the interactions of these species mediated by AI-2. The interaction of *H. influenzae* and *S. pneumoniae* has not been completely understood. Kyd *et al* (2016), in a review of biofilms in the respiratory tract, stated that, although *S. pneumoniae* had competitive interactions with *H. influenzae* producing acidic by-products such as H₂O₂, there has also been evidence that the growth of a biofilm between these two species is extremely resistant due to *H. influenzae* protects *S. pneumoniae* with the production of β -lactamases (Gabriliska and Rumbaugh, 2015; Kyd *et al.*, 2016; Perez *et al.*, 2014).

Treatment for otitis media is based on pain relievers and antibiotics. Due to the resistance of these communities, other anti-biofilm alternatives have been sought. Cavaliere *et al* (2014) obtained successful results using EDTA as a chelating agent for matrix compounds of a biofilm developed by non-typeable *H. influenzae*, weakening the consortium, being more susceptible to antibiotics (Cavaliere *et al.*, 2014; Silva and Sillankorva, 2019; Vestby *et al.*, 2020).

4.6 Biofilm infections acquired by medical devices

Throughout this section were exposed polymicrobial biofilms that colonize tissues or host mucosa; however, another major clinical problem are infections that are spread by the insertion of devices into the body such as catheters, nutrition tubes and orthopedic devices. Since the last millennium, in 1982, *S. aureus* was detected in a patient's pacemaker, causing a persistent infection (Lebeaux *et al.*, 2013; Peters *et al.*, 2012; Percival *et al.*, 2015b).

Parental nutrition tubes are used for patients who are unable to chew, serving as a support for their feeding. However, it has been shown that this is a direct route for the colonization of species such as *staphylococci*, *pseudomonas*, and even fungal organisms of the genus *Candida*, which move to the stomach and intestine for development of biofilms, which manifests in conditions such as chronic diarrhea. Catheters are another of the most studied devices, since the presence of biofilms from *S. epidermidis*, has been identified, causing chronic infections. The probability of developing an infection to developing catheter-associated infections is estimated to increase by 10 % for each day that the device is in the body (Peters *et al.*, 2012; Percival *et al.*, 2015b).

The study methods used to evaluate this infection should be *in vivo*, to evaluate the host's response when an external object is inserted into a body. One of the most famous studies was developed at the beginning of this millennium by Rupp and collaborators called the model of central venous catheter infection (CVC) of rat, where the importance of intercellular adhesion of polysaccharide (PIA) and autolysin AtlE for the formation of biofilms of *S.*

epidermidis were evaluated. Chauhan *et al.* evaluated infection in venous-access ports with species of *Escherichia coli*, *Pseudomonas aeruginosa*, *Staphylococcus aureus* and *Staphylococcus epidermidis* surgically placed in adult rats using quantitative and noninvasive bioluminescence, observing effective biofilm growth and pathology development (Chauhan *et al.*, 2012; Lebeaux *et al.*, 2013).

Current treatments are based on developing biomaterials that prevent the adhesion of polymicrobial biofilms. Francolini and Donelli (2010) described in a biofilm prevention review, as hydrophilic polymers such as hyaluronic acid and poly-N-vinylpyrrolidone reduce the adhesion of *S. epidermidis* and, consequently biofilm growth. Palencia *et al* (2020) developed new antibacterial and non-hemolytic materials based on cationic polyurethanes with quaternary ammonium units from tricomponent synthesis with diisocyanate, a polyol of low molecular weight and N-carboxymethyl-N,N,N-triethylammonium chloride, which exhibited optimal antibacterial properties and low hemolytic activity. John *et al* (2007) evaluated ureteral hydrogels which, besides of their hydrophilic property, allow the controlled drug release (Francolini and Donelli, 2010; John *et al.*, 2007; Palencia *et al.*, 2020). These biomaterials serve as a prevention of polymicrobial biofilms, because when these communities have colonized a surface, their removal is problematic. In the next section the treatments investigated when the consortia grew and develop pathologies will be exposed.

5. Novel treatments

The resistance of polymicrobial biofilms is one of the greatest public health challenges. Traditional treatments such as antibiotic therapies are not recommended because they can promote resistance and tolerance of consortia. Currently, the effective method of eliminating infection caused by these communities is to eliminate the infected area, however, it involves the loss of a part of the patient's body (Bjarnsholt, 2013; Baptista *et al.*, 2018). This has generated new research to combat these infections. These will be discussed in this section.

5.1 Nanoparticle-based treatments

Nanomaterials, since their discovery in 1980, have been the focus of research for applications in medicine. Nanoparticles (NPs) are particles with dimensions between 1 and 100 nm, which have been a research focus due to their bioactivity and versatility. These have been used as a means of drug delivery or as agents directed to the biofilm to combat it. NPs are classified into metallic, non-metallic, polymeric, among others, according to the material used to synthesize it. Its mechanism of action is based on interrupting bacterial metabolism and

growth, either affecting its cell membranes, generating oxidative stress, modifying gene expression or producing enzymatic inhibition (Baptista *et al.*, 2018; Buch *et al.*, 2019; Kuang *et al.*, 2018; Wei *et al.*, 2019).

The most popular NPs are metallic, as ions and metal oxides have been shown to exhibit antimicrobial properties. Silver NPs (AgNPs) are the most popular because, besides of their antimicrobial activity, they also promote wound healing. Baptista and colleagues described in a recent review that AgNPs present various mechanisms of action, such as disruption to the cell membrane to generate oxidative stress that inhibits ATP production and subsequent DNA production, or the release of Ag⁺ ions that interact with thiol groups of cell membrane, affecting their functions. These various bactericidal mechanisms hardly cause resistant. Baptista *et al* (2018) analyzed the effectiveness of AgNPs against *S. mutans* biofilms by developing microtiter plate assays, obtaining better bactericidal activity than traditional mouthwashes. Acharya and collaborators employed AgNPs demonstrating high efficacy to combat *Klebsiella pneumoniae* (Figure 10).

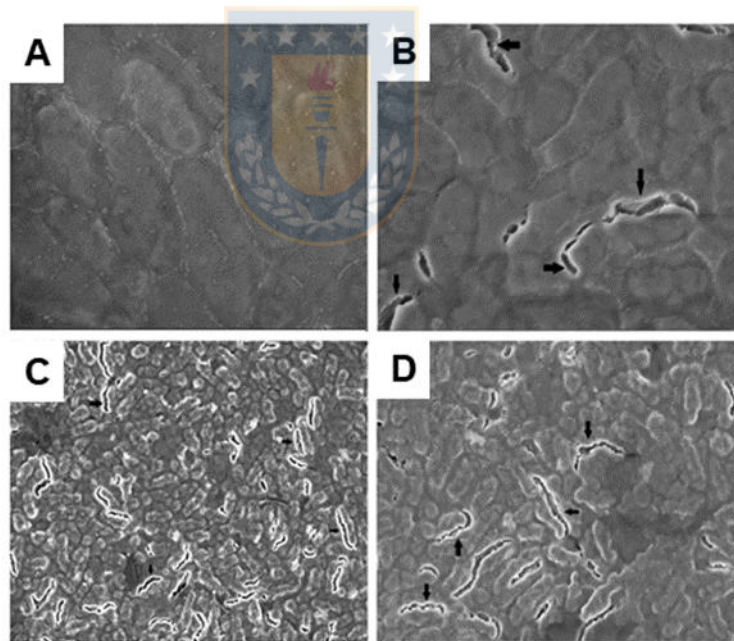


Figure 10. SEM images of *K. pneumoniae* biofilms. (A) Without treatment. (B) Post-treatment with AgNPs. (C) and (D) show biofilm disruption due to interaction with AgNPs (Modified from Acharya *et al.*, 2018).

Sanchez *et al.* recently synthesized AgNPs through chemical reduction with poly(vinylpyrrolidone), sodium citrate, N-methyl-D-glucamine and meglumine antimoniate, and evaluated their bactericidal power with strains of *E. coli* and *S. aureus*, obtaining increased antimicrobial activity with N-methyl-D-glucamine and meglumine antimoniate due to

the strong electrostatic interaction between the protonated amine and the phosphate groups of the bacterial membrane. The disadvantages of metallic nanoparticles are their high doses required to ensure their effectiveness, so they can become toxic to other host cells and to the possible appearance of polymicrobial biofilms with metal NP resistance. (Acharya *et al.*, 2018; Baptista *et al.*, 2018; Buch *et al.*, 2019; Kuang *et al.*, 2018; Mihai *et al.*, 2018; Sanchez *et al.*, 2019).

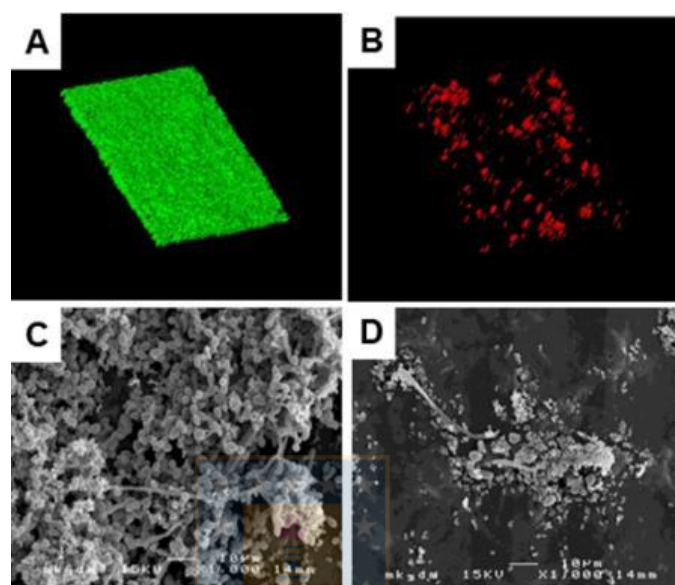


Figure 11. Polymicrobial biofilm images of *Candida albicans* and *Staphylococcus aureus*. (A) CLSM images before treatment and (B) after treatment with CNP loaded with curcumin. (C) SEM images before treatment and (D) after therapy (Modified from Ma *et al.*, 2020).

Polymer nanoparticles have also been of interest because they have advantages such as chemical stability and no toxicity to the host's biological membranes. NPs based on cationic polymers such as quaternary ammonium polyethyleneimine NPs have demonstrated their bactericidal activity. Esmaeili *et al* (2007) developed NPs from biodegradable and biocompatible polymers such as poly(lactic-co-glycolic acid) and were loaded with rifampicin antibiotics, evidencing bactericidal activity than the free drug. Hybrids with polymers and metallic NPs have been developed in recent years with the aim of achieving greater efficiency. Palencia *et al* (2017) synthesized nanostructured polymers from a polymerizable nanostructured crosslinker based on AgNPs and acrylic acid, used in polymerization via free radicals of sodium styrene sulfonate to produce nanostructures of polystyrene sulfonate, which exhibited antimicrobial activity for the *E. coli* and *S. aureus* (Beyth *et al.*, 2015; Buch *et al.*, 2019; Esmaeili *et al.*, 2007; Mihai *et al.*, 2018; Palencia *et al.*, 2017; Wei *et al.*, 2019). Biopolymer NPs have also been investigated. Qi *et al* (2004) were among the first researchers to employ chitosan nanoparticles (CNP), a natural cationic biopolymer, showing

that these NPs inhibited the growth of *E. coli*, *S. aureus*, *Salmonella typhimurium* and *Salmonella enterica*, since CNP interacts with the negative surface of bacterial cells, causing their cell death. Ma *et al* (2020) loaded curcumin into CNP and evaluated their antibiofilm activities against *Candida albicans* and *Staphylococcus aureus* from monitoring with SEM and CLSM to observe the biofilm architecture. Biopolymers have also been used to functionalize AgNPs. You *et al* (2017) built a hybrid metal collagen/chitosan scaffold with AgNPs, demonstrating, besides bactericidal activity, optimal wound healing employing *in vivo* models, acting as an ideal dermal substitute for wound restoration (Kuang *et al.*, 2018; Ma *et al.*, 2020; Mihai *et al.*, 2018; Qi *et al.*, 2004; You *et al.*, 2017).

Liposome NPs have also been used for the supply of antibiotics because it perfectly mimics a cell membrane, since it has a hydrophobic cover and an inner nucleus with hydrophilic polar heads, which are oriented to the outside when they are in water. These structures fuse with cell membranes and release the drug into cells. The smaller size these structures present, the more effective they will be. Dong *et al* (2015) investigated the distribution and anti-biofilm effect of *S. aureus* and *P. aeruginosa* of phospholipid liposomes of different sizes, finding that the inhibition of community growth was greater when the size of the liposome was smaller (Buch *et al.*, 2019; Dong *et al.*, 2015).

The effect of NPs can be improved by combining them with "smart" materials, the release of which is generated in response to a stimulus such as pH or bacterial products. Antibiotic-carrying nanoparticles were made from diblock copolymers composed of 2-(dimethylamino) ethyl methacrylate (DMAEMA), butyl methacrylate (BMA) and 2-propylacrylic acid (PAA) (p(DMAEMA)-bp-(DMAEMA-co-BMA-co-PAA) that were able to bind to hydroxyapatite (HA), saliva-coated HA (sHA) and exopolysaccharides with acid pH release, being more effective in combating *S. mutans* than the antibiotic free. Hydrogels have also been materials used as scaffolding to transport NP or antibiotics. Montaser *et al* (2016) prepared alginate and chitosan hydrogels with AgNPs, showing bactericidal activity against biofilms of *S. aureus* and *E. coli* using a murine model (Buch *et al.*, 2019; Demidova-Rice *et al.*, 2012; Kuang *et al.*, 2018; Montaser *et al.*, 2016).

Nanoparticle research still presents unresolved issues, such as the removal of NP from the body, or immunogenicity since a host immune response may render them unable to exert their antimicrobial activity. Unknowns arise because NP activity in cells is unknown, as SEM and even transmission electron microscopy (TEM) are exclusively functional with metallic NPs due to their high electronic density. However, it is currently one of the most innovative and promising strategies for the treatment of chronic infections produced by polymicrobial biofilms (Buch *et al.*, 2019; Şen Karaman *et al.*, 2018).

5.2 Treatment with natural products

Phytochemical-based treatments and plant-based natural products are gaining interest, as they have various mechanisms of action that prevent bacteria from developing resistance. Monte *et al* (2014) investigated phytochemicals such as coumarins, indole-3-carbinol, salicylic acid and saponin, which affected motility and quorum detection activity (QS), interfering in the polymicrobial interactions of *E. coli* and *S. aureus*, affecting the growth of biofilms. Flavonoids are the most evaluated secondary metabolites and phenolic compounds. Philip and colleagues (2014), in recent research, studied the effect of cranberry polyphenols, finding, from an *in vitro* model employing hydroxyapatite discs, that these altered factors such as bacterial adhesion, virulence, and structural architecture of biofilms, decreasing the biomass of *Streptococcus sobrinus* biofilms (Monte *et al.*, 2014; Philip *et al.*, 2019; Wei *et al.*, 2019).

Honey has also been employed because it presents bactericidal components such as hydrogen peroxide, flavonoids, phenolic compounds, organic acids, beeswax, among others. Its antibiofilm power is interfering with its QS, making it a structure susceptible to environmental stress. Voidarou and collaborators the efficacy of honey, showing bactericidal activity against pathogens and their respective reference strains at varying levels. Maddocks and colleagues, meanwhile, determined that Manuka honey disrupted bacterial adhesion to fibronectin, fibrinogen, and collagen, as well as causing death in biofilms of *S. aureus*, *P. aeruginosa* and *Streptococcus pyogenes* (Bertesteanu *et al.*, 2014; Maddocks *et al.*, 2013; Wei *et al.*, 2019; Voidarou *et al.*, 2011).

Other natural products, such as green tea, have been used for the development of mouthwashes decreasing the presence of *Lactobacilli* and *S. mutans*, attributed mainly to the presence of catechin polyphenols, which, according to studies by Taylor *et al* (2005), are interspersed in phospholipid bilayers, interrupting the processes associated with the bacterial cytoplasmic membrane, affecting virulence and resistance to antibiotics of *S. aureus* biofilms. Study of Xu and collaborators found that these polyphenols also decreased virulence of *S. mutans* strains (Kuang *et al.*, 2018; Taylor *et al.*, 2005; Xu *et al.*, 2011). Secondary metabolites, such as flavonoids, terpenoids, alkaloids, tannins, among others, also are involved in QS inhibition. Lahiri *et al* (2019) described, in a recent review, that alkaloids such as 1,3,4-oxadiazole, inhibited the QS HQNO signal in *P. aeruginosa*, affecting polymicrobial interaction, decreasing its resistance and tolerance (Bouyahya *et al.*, 2017; Lahiri *et al.*, 2019). The use of natural products as secondary metabolites of flavonoids, alkaloids, terpenoids, among others, are still unwell studied, however, they represent a novel strategy, since these bioactive compounds are not toxicity, and may give additional benefits to the biofilm removal.

5.3 Phage therapy

Bacteriophages are viruses that infect and generate cell lysis in members of the polymicrobial biofilm, so phage therapy has attracted attention as an alternative to combat these communities. Its mechanism of action basically consists of lysing the biofilm region where high metabolic activity occurs, so the growth of the members goes from exponential to null. Bacteriophages continue to replicate, so they can also infect the stationary phase of biofilm where antibiotics do not have any effect (Azeredo and Sutherland, 2008; Pires *et al.*, 2017a). Although phage therapy has been a novel treatment, these antimicrobial agents have been shown to be unable to completely remove biofilms, due to the EPS makes it difficult for bacteriophages to bind to cell surfaces of pathological agents. The effectiveness of bacteriophage therapy depends on biofilm conditions. Łoś *et al* (2007) demonstrated that the depletion of a carbon source in the culture, inhibits the lytic development of three *E. coli* phages. Furthermore, these communities have been reported to be capable of developing resistance to these agents. Pires *et al* (2017a, 2017b) evaluated the effectiveness of phages against the *P. aeruginosa* biofilm, finding that, although a significant reduction in consortium members was achieved, the appearance of phage resistant strains was observed. A similar phenomenon was reported by Fu *et al* (2010), who developed hydrogel-coated catheters with lithic phages of *P. aeruginosa*, finding a decrease in the biofilm in 24 hours, however, after 48 hours, there was a new growth with resistant species. Resistance is attributed to factors such as phage DNA exclusion or degradation, blocking of the replication, transcription and translation of these viruses, and modification of bacterial receptors. QS is essential for effectiveness of phage therapy increased when a QS inhibitor was added in a *P. aeruginosa* biofilm (Fu *et al.*, 2010; Łoś *et al.*, 2007; Pires *et al.*, 2017a, 2017b).

There are other factors that increase the effectiveness of phage therapy, such as debridement, which involves removing dead tissue to initiate therapy. Mendes *et al* (2013) assessed the feasibility of combating chronic bacterial infections caused by *S. aureus* and *P. aeruginosa* with topically administered bacteriophages in *in vivo* models with diabetes mellitus animals, being effective in fighting these communities, especially when applied together with wound debridement. Phage therapy has also been combined with treatment with antibiotics or enzymes, obtaining promising results. Rahman *et al* (2011) evaluated the treatment of *S. aureus* communities with a phage and antimicrobial agents, evidencing a strong biofilm removal effect, in addition to structural changes in the biofilm matrix and a substantial decrease in the number of bacteria. On the other hand, Gutierrez *et al* (2015) demonstrated that phage-encoded depolymerases are effective in preventing and dispersing *staphylococcal*

biofilms, making bacteria more susceptible to the action of antimicrobials (Gutiérrez *et al.*, 2015; Kadam *et al.*, 2019; Mendes *et al.*, 2013; Pires *et al.*, 2017a; Rahman *et al.*, 2011).

Natural products have also been researched to accompany phage therapy. Oliveira *et al.* (2018) evaluated, with an *ex vivo* model with porcine skin, treatment with phages and honey which, as mentioned above, has gained recognition due to its antibacterial, antioxidant and anti-inflammatory and healing properties, being effectiveness due to honey's ability to damage the bacterial cell membrane and also its ability to penetrate the biofilm matrix, promoting and improving subsequent phage infection (Kadam *et al.*, 2019; Oliveira *et al.*, 2018). Phage therapy is extremely attractive, but evidence shows that its treatment is not effective enough, so is used with other therapies. Its use in human diseases has shown that phage therapy is apparently safe and inexpensive, so it continues to be a research alternative, with the aim of improving its effectiveness.

5.4 Vaccines

The development of a vaccine against polymicrobial biofilms is a main challenge. A vaccine for these communities differs from Koch's molecular postulates, as the immune response against a single virulence factor will not solve a biofilm infection due to multiple virulence factors, species, and genes. Vaccine evaluation should be carried out *in vivo*, as the selection of antigenic targets should have the ability to ensure that immunogenic proteins are expressed during infection. This vaccine should be able to attack all present species in the biofilm, however, that may be dangerous because commensal species can be affected. The vaccine can only have a set of multiple antigenic proteins if it is verified that the infection is caused by polymicrobial biofilms, representing great problems due to the current drawbacks for diagnosis (Brady *et al.*, 2006; Hagan and Mobley, 2007; Peters *et al.*, 2012; Rollenhagen *et al.*, 2004).

Several vaccines have been developed to combat polymicrobial biofilms. Zhang *et al.* (2009) developed a vaccine based on the 40 kDa outer membrane protein of *P. gingivalis* administered sublingually with a plasmid vector of cDNA, a protective immune response, obtaining promising results in a murine model, however, there is still no approved vaccination against periodontitis. Peters *et al.* (2012) established in a review of polymicrobial interactions that a possible vaccine for this disease should contain antigens against *F. nucleatum* and *P. gingivalis*, since, if the population of these species is not decreased, they can continue with the growth of biofilm with other microorganisms, developing the same or other pathologies. The heptavalent pneumococcal conjugate vaccine (PCV7), composed of capsular oligosaccharides and polysaccharides of *S. pneumoniae* strains, arose to limit ear infections

such as OM, however, this is not effective for other species such as *H. influenzae*. Therefore, in the United States and other countries the use of PCV13, which protects humans against 13 *pneumococcal* serotypes, while PPSV23, another *pneumococcal* vaccine, protects against 23 *S. pneumoniae* serotypes. The main concern for the development of a vaccine against a polymicrobial biofilm is that, while some species can be eliminated, other microorganisms can colonize the niche and continue with the growth of the consortium. Therefore, current research has studied the development of vaccines that, instead of attacking the members, affect properties such as the microbial or matrix interaction that weakens the consortium and, in turn, allows the elimination of polymicrobial species. However, much research is still lacking to develop effective vaccines (Harro *et al.*, 2010; Peters *et al.*, 2012; Silva and Sillankorva, 2019; Zhang *et al.*, 2009).

6. Conclusions and perspectives

Microbes come together to form biofilms that are highly organized communities attached to a surface. The growth of biofilm phenotype allows them to survive environmental stress and gives them properties such as tolerance and resistance to antibiotics, which has represented a public health problem because they are responsible for various pathologies that are not treated efficiently. The dynamic interactions of these species, and the development of an EPS matrix, are also responsible for the chronicity of infections, with effective therapy prevailing against these properties of the consortium.

Although research about alternative treatments such as nanoparticles, natural products, phage therapy and vaccines have taken on relevance in the biomedical field, the area of "polymicrobial biofilms" can still be considered new, because there are mechanisms of their growth and interaction that are not yet understood. Biotechnological research should focus on the development of materials that prevent the colonization of these microorganisms, since, once the biofilm has been formed, its removal is a complex task that in most cases is solved by debriding the affected area. The focus of the therapies, on the other hand, should be to combat the matrix and inhibit microbe-microbe interactions, which are the factors responsible for the strength of these communities. This review aims to contribute with concepts and studies that promote these investigations, with the aim of being closer to an effective treatment that allows reducing the impact generated by polymicrobial biofilms on human health, food and biotechnology industries, among others.

Conflict interest. Authors declare that there is no conflict of interest regarding the publication of this paper.

Acknowledgements. A. Espinosa, M. Palencia and S. Palencia thank to University del Valle and Mindtech s.a.s. (AFICAT). S. Palencia and A. García thank Conicyt and Universidad de Concepción for the resources provided

References

- Acharya, D.; Singha, K. M.; Pandey, P.; Mohanta, B.; Rajkumari, J.; Singha, L. P. Shape Dependent Physical Mutilation and Lethal Effects of Silver Nanoparticles on Bacteria. *Sci. Rep.* 2018, 8 (1), 201. <https://doi.org/10.1038/s41598-017-18590-6>
- Adam, B.; Baillie, G. S.; Douglas, L. J. Mixed Species Biofilms of *Candida Albicans* and *Staphylococcus Epidermidis*. *J. Med. Microbiol.* 2002, 51 (4), 344-349. <https://doi.org/10.1099/0022-1317-51-4-344>
- Adler, C. J.; Dobney, K.; Weyrich, L. S.; *et al.* Sequencing Ancient Calcified Dental Plaque Shows Changes in Oral Microbiota with Dietary Shifts of the Neolithic and Industrial Revolutions. *Nat. Genet.* 2013, 45 (4), 450-455. <https://doi.org/10.1038/ng.2536>
- Armbruster, C. E.; Hong, W.; Pang, B.; *et al.* Indirect Pathogenicity of *Haemophilus Influenzae* and *Moraxella Catarrhalis* in Polymicrobial Otitis Media Occurs via Interspecies Quorum Signaling. *mBio* 2010, 1 (3), e00102-10. <https://doi.org/10.1128 / mBio.00102-10>
- Arnaouteli, S.; Ferreira, A. S.; Schor, M.; *et al.* Bifunctionality of a Biofilm Matrix Protein Controlled by Redox State. *Proc. Natl. Acad. Sci. U. S. A.* 2017, 114 (30), E6184-E6191. <https://doi.org/10.1073/pnas.1707687114>
- Azeredo, J.; Azevedo, N. F.; Briandet, R.; *et al.* Critical Review on Biofilm Methods. *Crit. Rev. Microbiol.* 2017, 43 (3), 313-351. <https://doi.org/10.1080 / 1040841X.2016.1208146>
- Azeredo, J.; Sutherland, I. W. The Use of Phages for the Removal of Infectious Biofilms. *Curr. Pharm. Biotechnol.* 2008, 9 (4), 261-266. <https://doi.org/10.2174/138920108785161604>
- Bahamondez-Canas, T. F.; Heersema, L. A.; Smyth, H. D. C. Current Status of *In Vitro* Models and Assays for Susceptibility Testing for Wound Biofilm Infections. *Biomedicines* 2019, 7 (2), 34. <https://doi.org/10.3390/biomedicines7020034>
- Baptista, P. V.; McCusker, M. P.; Carvalho, A.; *et al.* Nano-Strategies to Fight Multidrug Resistant Bacteria "A Battle of the Titans". *Front. Microbiol.* 2018, 9, 1441. <https://doi.org/10.3389/fmicb.2018.01441>
- Bertesteanu, S.; Triaridis, S.; Stankovic, M.; *et al.* Polymicrobial Wound Infections: Pathophysiology and Current Therapeutic Approaches. *Int. J. Pharm.* 2014, 463 (2), 119-126. <https://doi.org/10.1016/j.ijpharm.2013.12.012>
- Beyth, N.; Hourri-Haddad, Y.; Domb, A.; Khan, W.; Hazan, R. Alternative Antimicrobial Approach: Nano-Antimicrobial Materials. *Evid. Based Complement. Alternat. Med.* 2015, 2015, 246012. <https://doi.org/10.1155 / 2015/246012>
- Bjarnsholt, T. The Role of Bacterial Biofilms in Chronic Infections. *APMIS Suppl.* 2013, 121 (136), 1-51. <https://doi.org/10.1111/apm.12099>
- Bjarnsholt, T.; Givskov, M. The Role of Quorum Sensing in the Pathogenicity of the Cunning Aggressor *Pseudomonas Aeruginosa*. *Anal. Bioanal. Chem.* 2007, 387 (2), 409-414. <https://doi.org/10.1007/s00216-006-0774-x>
- Bjarnsholt, T.; Jensen, P. Ø.; Fiandaca, M. J.; Pedersen, J.; Hansen, C. R.; Andersen, C. B.; Høiby, N. *Pseudomonas aeruginosa* biofilms in the respiratory tract of cystic fibrosis patients. *Pediatr. Pulmonol.* 2009, 44 (6), 547-558 <https://doi.org/10.1002/ppul.21011>
- Blanc, V.; Isabal, S.; Sánchez, M. C.; *et al.* Characterization and Application of a Flow System for in Vitro Multispecies Oral Biofilm Formation. *J. Periodont. Res.* 2014, 49 (3), 323-332. <https://doi.org/10.1111/jre.12110>
- Bouyahya, A.; Dakka, N.; Et-Touys, A.; Abrini, J.; Bakri, Y. Medicinal Plant Products Targeting Quorum Sensing for Combating Bacterial Infections. *Asian Pac. J. Trop. Med.* 2017, 10 (8), 729-743. <https://doi.org/10.1016/j.apjtm.2017.07.021>

- Bowen, W. H.; Burne, R. A.; Wu, H.; Koo, H. Oral Biofilms: Pathogens, Matrix, and Polymicrobial Interactions in Microenvironments. *Trends Microbiol.* 2018, 26 (3), 229-242. <https://doi.org/10.1016/j.tim.2017.09.008>
- Brady, R. A.; Leid, J. G.; Camper, A. K.; Costerton, J. W.; Shirtliff, M. E. Identification of *Staphylococcus Aureus* Proteins Recognized by the Antibody-Mediated Immune Response to a Biofilm Infection. *Infect. Immun.* 2006, 74 (6), 3415-3426. <https://doi.org/10.1128/IAI.00392-06>
- Bragonzi, A.; Farulla, I.; Paroni, M.; et al. Modelling Co-Infection of the Cystic Fibrosis Lung by *Pseudomonas Aeruginosa* and *Burkholderia Cenocepacia* Reveals Influences on Biofilm Formation and Host Response. *PLoS One* 2012, 7 (12), e52330. <https://doi.org/10.1371/journal.pone.0052330>
- Bridier, A.; Dubois-Brissonnet, F.; Boubetra, A.; Thomas, V.; Briandet, R. The Biofilm Architecture of Sixty Opportunistic Pathogens Deciphered Using a High Throughput CLSM Method. *J. Microbiol. Methods* 2010, 82 (1), 64-70. <https://doi.org/10.1016/j.mimet.2010.04.006>
- Buch, P. J.; Chai, Y.; Goluch, E. D. Treating Polymicrobial Infections in Chronic Diabetic Wounds. *Clin. Microbiol. Rev.* 2019, 32 (2), e00091-18. <https://doi.org/10.1128/CMR.00091-18>
- Büttner, H.; Mack, D.; Rohde, H. Structural Basis of *Staphylococcus Epidermidis* Biofilm Formation: Mechanisms and Molecular Interactions. *Front. Cell. Infect. Microbiol.* 2015, 5 (14). <https://doi.org/10.3389/fcimb.2015.00014>
- Cavaliere, R.; Ball, J. L.; Turnbull, L.; Whitchurch, C. B. The Biofilm Matrix Destabilizers, EDTA and DNaseI, Enhance the Susceptibility of Nontypeable *Hemophilus Influenzae* Biofilms to Treatment with Ampicillin and Ciprofloxacin. *Microbiologyopen.* 2014, 3 (4), 557-567. <https://doi.org/10.1002/mbo3.187>
- Chan, K. G.; Liu, Y. C.; Chang, C. Y. Inhibiting N-acyl-homoserine lactone synthesis and quenching *Pseudomonas* quinolone quorum sensing to attenuate virulence. *Front. Microbiol.* 2015, 6, 1173. <https://doi.org/10.3389/fmicb.2015.01173>
- Chauhan, A.; Lebeaux, D.; Decante, B.; et al. A Rat Model of Central Venous Catheter to Study Establishment of Long-Term Bacterial Biofilm and Related Acute and Chronic Infections. *PLoS One* 2012, 7 (5), e37281. <https://doi.org/10.1371/journal.pone.0037281>
- Chotirmall, S. H.; O'Donoghue, E.; Bennett, K.; Gunaratnam, C.; O'Neill, S. J.; McElvaney, N. G. Sputum *Candida Albicans* Presages FEV₁ Decline and Hospital-Treated Exacerbations in Cystic Fibrosis. *Chest* 2010, 138 (5), 1186-1195. <https://doi.org/10.1378/cofre.09-2996>
- Coenye, T.; Nelis, H. J. *In Vitro* and *in Vivo* Model Systems to Study Microbial Biofilm Formation. *J. Microbiol. Methods* 2010, 83 (2), 89-105. <https://doi.org/10.1016/j.mimet.2010.08.018>
- Costerton, J. W. A short history of the development of the biofilm concept. In *Microbial Biofilms*; Ghannoum, M., O'Toole, G. A., Eds.; ASM Press: Washington, DC, 2004; pp 4-19. <https://doi.org/10.1111/apm.12686>
- Costerton, J. W.; Post, J. C.; Ehrlich, G. D.; et al. New Methods for the Detection of Orthopedic and Other Biofilm Infections. *FEMS Immunol. Med. Microbiol.* 2011, 61 (2), 133-140. <https://doi.org/10.1111/j.1574-695X.2010.00766.x>
- Costerton, J. W.; Stewart, P. S.; Greenberg, E. P. Bacterial Biofilms: A Common Cause of Persistent Infections. *Science* 1999, 284 (5418), 1318-1322. <https://doi.org/10.1126/science.284.5418.1318>
- Crabbé, A.; Jensen, P. Ø.; Bjarnsholt, T.; Coenye, T. Antimicrobial Tolerance and Metabolic Adaptations in Microbial Biofilms. *Trends Microbiol.* 2019, 27 (10), 850-863. <https://doi.org/10.1016/j.tim.2019.05.003>
- Cruz, M. R.; Graham, C. E.; Gagliano, B. C.; Lorenz, M. C.; Garsin, D. A. *Enterococcus faecalis* inhibits hyphal morphogenesis and virulence of *Candida albicans*. *Infect. Immun.* 2013, 81 (1), 189-200. <https://doi.org/10.1128/IAI.00914-12>
- Cugini, C.; Calfee, M. W.; Farrow, J. M. 3rd.; Morales, D. K.; Pesci, E. C.; Hogan, D. A. Farnesol, a Common Sesquiterpene, Inhibits PQS Production in *Pseudomonas Aeruginosa*. *Mol. Microbiol.* 2007, 65 (4), 896-906. <https://doi.org/10.1111/j.1365-2958.2007.05840.x>
- Daddi Oubekka, S.; Briandet, R.; Fontaine-Aupart, M. P.; Steenkeste, K. Correlative Time-Resolved Fluorescence Microscopy to Assess Antibiotic Diffusion-Reaction in Biofilms. *Antimicrob. Agents Chemother.* 2012, 56 (6), 3349-3358. <https://doi.org/10.1128/AAC.00216-12>
- Daniels, T. W.; Rogers, G. B.; Stressmann, F. A.; et al. Impact of Antibiotic Treatment for Pulmonary Exacerbations on Bacterial Diversity in Cystic Fibrosis. *J. Cyst. Fibros.* 2013, 12 (1), 22-28. <https://doi.org/10.1016/j.jcf.2012.05.008>

- Demidova-Rice, T. N.; Hamblin, M. R.; Herman, I. M. Acute and Impaired Wound Healing: Pathophysiology and Current Methods for Drug Delivery, Part 2: Role of Growth Factors in Normal and Pathological Wound Healing: Therapeutic Potential and Methods of Delivery. *Adv. Skin Wound Care* 2012, 25 (8), 349-370. <https://doi.org/10.1097/01.ASW.0000418541.31366.a3>
- Diaz, P. I.; Zilm, P. S.; Rogers, A. H. *Fusobacterium Nucleatum* Supports the Growth of *Porphyromonas Gingivalis* in Oxygenated and Carbon-Dioxide-Depleted Environments. *Microbiology* 2002, 148 (2), 467-472. <https://doi.org/10.1099 / 00221287-148-2-467>
- Dominguez-Benetton, X.; Seveda, S.; Vanbroekhoven, K.; Pant, D. The Accurate Use of Impedance Analysis for the Study of Microbial Electrochemical Systems. *Chem. Soc. Rev.* 2012, 41 (21), 7228-7246. <https://doi.org/10.1039/c2cs35026b>
- Donati, C.; Hiller, N. L.; Tettelin, H.; *et al.* Structure and Dynamics of the Pan-Genome of *Streptococcus Pneumoniae* and Closely Related Species. *Genome Biol.* 2010, 11 (10), R107-R126. <https://doi.org/10.1186/gb-2010-11-10-r107>
- Dong, D.; Thomas, N.; Thierry, B.; Vreugde, S.; Prestidge, C. A.; Wormald, P. J. Distribution and Inhibition of Liposomes on *Staphylococcus Aureus* and *Pseudomonas Aeruginosa* Biofilm. *PLoS One* 2015, 10 (6), e0131806. <https://doi.org/10.1371/journal.pone.0131806>
- Dunne, W. M. Jr. Bacterial Adhesion: Seen Any Good Biofilms Lately?. *Clin. Microbiol. Rev.* 2002, 15 (2), 155-166. <https://doi.org/10.1128 / CMR.15.2.155-166.2002>
- Duran-Pinedo, A. E.; Frias-Lopez, J. Beyond Microbial Community Composition: Functional Activities of the Oral Microbiome in Health and Disease. *Microbes Infect.* 2015, 17 (7), 505-516. <https://doi.org/10.1016 / j.micinf.2015.03.014>
- Edwards, S.; Kjellerup, B. V. Exploring the Applications of Invertebrate Host-Pathogen Models for *in Vivo* Biofilm Infections. *FEMS Immunol. Med. Microbiol.* 2012, 65 (2), 205-214. <https://doi.org/10.1111 / j.1574-695X.2012.00975.x>
- Ehrlich, G. D.; Ahmed, A.; Earl, J.; *et al.* The Distributed Genome Hypothesis as a Rubric for Understanding Evolution *in Situ* During Chronic Bacterial Biofilm Infectious Processes. *FEMS Immunol. Med. Microbiol.* 2010, 59 (3), 269-279. <https://doi.org/10.1111 / j.1574-695X.2010.00704.x>
- Elias, S.; Banin, E. Multi-species Biofilms: Living with Friendly Neighbors. *FEMS Microbiol. Rev.* 2012, 36 (5), 990-1004. <https://doi.org/10.1111 / j.1574-6976.2012.00325.x>
- Esmaili, F.; Hosseini-Nasr, M.; Rad-Malekshahi, M.; Samadi, N.; Atyabi, F.; Dinarvand, R. Preparation and Antibacterial Activity Evaluation of Rifampicin-Loaded Poly Lactide-Co-Glycolide Nanoparticles. *Nanomedicine* 2007, 3 (2), 161-167. <https://doi.org/10.1016 / j.nano.2007.03.003>
- Falsetta, M. L.; Klein, M. I.; Colonne, P. M.; *et al.* Symbiotic Relationship Between *Streptococcus Mutans* and *Candida Albicans* Synergizes Virulence of Plaque Biofilms *in Vivo*. *Infect. Immun.* 2014, 82 (5), 1968-1981. <https://doi.org/10.1128 / IAI.00087-14>
- Filkins, L. M.; O'Toole, G. A. Cystic Fibrosis Lung Infections: Polymicrobial, Complex, and Hard to Treat. *PLoS Pathog.* 2015, 11 (12), e1005258. <https://doi.org/10.1371/journal.ppat.1005258>
- Filоче, S.; Wong, L.; Sissons, C. H. Oral Biofilms: Emerging Concepts in Microbial Ecology. *J. Dent. Res.* 2010, 89 (1), 8-18. <https://doi.org/10.1177/0022034509351812>
- Flemming, H. C.; Neu, T. R.; Wozniak, D. J. The EPS Matrix: The "House of Biofilm Cells". *J. Bacteriol.* 2007, 189 (22), 7945-7947. <https://doi.org/10.1128 / JB.00858-07>
- Flemming, H. C.; Wingender, J. The Biofilm Matrix. *Nat. Rev. Microbiol.* 2010, 8 (9), 623-633. <https://doi.org/10.1038/nrmicro2415>
- Flemming, H. C.; Wingender, J.; Szewzyk, U.; *et al.* Biofilms: An Emergent Form of Bacterial Life. *Nat. Rev. Microbiol.* 2016, 14 (9), 563-575. <https://doi.org/10.1038 / nrmicro.2016.94>
- Folsom, J. P.; Richards, L.; Pitts, B.; *et al.* Physiology of *Pseudomonas Aeruginosa* in Biofilms as Revealed by Transcriptome Analysis. *BMC Microbiol.* 2010, 10, 294. <https://doi.org/10.1186 / 1471-2180-10-294>
- Francolini, I.; Donelli, G. Prevention and Control of Biofilm-Based Medical-Device-Related Infections. *FEMS Immunol. Med. Microbiol.* 2010, 59 (3), 227-238. <https://doi.org/10.1111 / j.1574-695X.2010.00665.x>
- Fu, W.; Forster, T.; Mayer, O.; Curtin, J. J.; Lehman, S. M.; Donlan, R. M. Bacteriophage Cocktail for the Prevention of Biofilm Formation by *Pseudomonas Aeruginosa* on Catheters in an *in Vitro* Model System. *Antimicrob. Agents Chemother.* 2010, 54 (1), 397-404. <https://doi.org/10.1128 / AAC.00669-09>

- Gabrilska, R. A.; Rumbaugh, K. P. Biofilm Models of Polymicrobial Infection. *Future Microbiol.* 2015, 10 (12), 1997-2015. <https://doi.org/10.2217/fmb.15.109>
- Ghigo, J. M. Natural Conjugative Plasmids Induce Bacterial Biofilm Development. *Nature* 2001, 412 (6845), 442-445. <https://doi.org/10.1038/35086581>
- Gomez-Alvarez, V.; Revetta, R. P.; Santo Domingo, J. W. Metagenome analyses of corroded concrete wastewater pipe biofilms reveal a complex microbial system. *BMC Microbiol.* 2012, 12 (1), 122. <https://doi.org/10.1186/1471-2180-12-122>
- González Barrios, A. F.; Zuo, R.; Hashimoto, Y.; Yang, L.; Bentley, W. E.; Wood, T. K. Autoinducer 2 Controls Biofilm Formation in *Escherichia Coli* Through a Novel Motility Quorum-Sensing Regulator (MqsR, B3022). *J. Bacteriol.* 2006, 188 (1), 305-316. <https://doi.org/10.1128/JB.188.1.305-316.2006>
- Gutiérrez, D.; Briers, Y.; Rodríguez-Rubio, L.; *et al.* Role of the Pre-neck Appendage Protein (Dpo7) from Phage vB_SepiS-philPLA7 as an Anti-biofilm Agent in *Staphylococcal* Species. *Front. Microbiol.* 2015, 6, 1315. <https://doi.org/10.3389/fmicb.2015.01315>
- Hagan, E. C.; Mobley, H. L. Uropathogenic *Escherichia Coli* Outer Membrane Antigens Expressed During Urinary Tract Infection. *Infect. Immun.* 2007, 75 (8), 3941-3949. <https://doi.org/10.1128/IAI.00337-07>
- Hajishengallis, E.; Parsaei, Y.; Klein, M. I.; Koo, H. Advances in the Microbial Etiology and Pathogenesis of Early Childhood Caries. *Mol. Oral Microbiol.* 2017, 32 (1), 24-34. <https://doi.org/10.1111/omi.12152>
- Harro, J. M.; Peters, B. M.; O'May, G. A.; *et al.* Vaccine Development in *Staphylococcus Aureus*: Taking the Biofilm Phenotype into Consideration. *FEMS Immunol. Med. Microbiol.* 2010, 59 (3), 306-323. <https://doi.org/10.1111/j.1574-695X.2010.00708.x>
- Hasan, S.; Danishuddin, M.; Khan, A. U. Inhibitory Effect of Zingiber Officinale Towards *Streptococcus Mutans* Virulence and Caries Development: *In Vitro* and *in Vivo* Studies. *BMC Microbiol.* 2015, 15 (1), 1. <https://doi.org/10.1186/s12866-014-0320-5>
- Haudecoeur, E.; Faure, D. A Fine Control of Quorum-Sensing Communication in *Agrobacterium Tumefaciens*. *Commun. Integr. Biol.* 2010, 3 (2), 84-88. <https://doi.org/10.4161/cib.3.2.10429>
- Hazan, R.; Que, Y. A.; Maura, D.; *et al.* Auto Poisoning of the Respiratory Chain by a Quorum-Sensing-Regulated Molecule Favors Biofilm Formation and Antibiotic Tolerance. *Curr. Biol.* 2016, 26 (2), 195-206. <https://doi.org/10.1016/j.cub.2015.11.056>
- Hentzer, M.; Eberl, L.; Givskov, M. Transcriptome analysis of *Pseudomonas aeruginosa* biofilm development: Anaerobic respiration and iron limitation. *Biofilms* 2005, 2 (1), 37-61. <https://doi.org/10.1017/S1479050505001699>
- Hoffman, L. R.; Déziel, E.; D'Argenio, D. A.; *et al.* Selection for *Staphylococcus Aureus* Small-Colony Variants Due to Growth in the Presence of *Pseudomonas Aeruginosa*. *Proc. Natl. Acad. Sci. U. S. A.* 2006, 103 (52), 19890-19895. <https://doi.org/10.1073/pnas.0606756104>
- Høiby, N.; Bjarnsholt, T.; Givskov, M.; Molin, S.; Ciofu, O. Antibiotic Resistance of Bacterial Biofilms. *Int. J. Antimicrob. Agents* 2010, 35 (4), 322-332. <https://doi.org/10.1016/j.ijantimicag.2009.12.011>
- Hou, J.; Veeregowda, D. H.; van de Belt-Gritter, B.; Busscher, H. J.; van der Mei, H. C. Extracellular Polymeric Matrix Production and Relaxation under Fluid Shear and Mechanical Pressure in *Staphylococcus aureus* Biofilms. *Appl. Environ. Microbiol.* 2017, 84 (1), e01516- e01517. <https://doi.org/10.1128/aem.01516-17>
- Iwase, T.; Uehara, Y.; Shinji, H.; *et al.* *Staphylococcus Epidermidis* Esp Inhibits *Staphylococcus Aureus* Biofilm Formation and Nasal Colonization. *Nature* 2010, 465 (7296), 346-349. <https://doi.org/10.1038/nature09074>
- James, G. A.; Swogger, E.; Wolcott, R.; *et al.* Biofilms in Chronic Wounds. *Wound Repair Regen.* 2008, 16 (1), 37-44. <https://doi.org/10.1038/nature09074>
- Jakubovics, N. S.; Kolenbrander, P. E. The Road to Ruin: The Formation of Disease-Associated Oral Biofilms. *Oral Dis.* 2010, 16 (8), 729-739. <https://doi.org/10.1111/j.1601-0825.2010.01701.x>
- Jiang, Z.; Nagata, N.; Molina, E.; Bakaletz, L. O.; Hawkins, H.; Patel J. A. Fimbria-mediated Enhanced Attachment of Nontypeable *Haemophilus Influenzae* to Respiratory Syncytial Virus-Infected Respiratory Epithelial Cells. *Infect. Immun.* 1999, 67 (1), 187-192. <https://doi.org/10.1128/IAI.67.1.187-192.1999>
- John, T.; Rajpurkar, A.; Smith, G.; Fairfax, M.; Triest, J. Antibiotic Pretreatment of Hydrogel Ureteral Stent. *J. Endourol.* 2007, 21 (10), 1211-1216. <https://doi.org/10.1089/end.2007.9904>

- Kadam, S.; Shai, S.; Shahane, A.; Kaushik K. S. Recent Advances in Non-Conventional Antimicrobial Approaches for Chronic Wound Biofilms: Have We Found the 'Chink in the Armor'?. *Biomedicines* 2019, 7 (2), 35. <https://doi.org/10.3390/biomedicines7020035>
- Karched, M.; Bhardwaj, R. G.; Inbamani, A.; Asikainen, S. Quantitation of Biofilm and Planktonic Life Forms of Coexisting Periodontal Species. *Anaerobe* 2015, 35 (Pt A), 13-20. <https://doi.org/10.1016/j.anaerobe.2015.04.013>
- Karygianni, L.; Ren, Z.; Koo, H.; Thurnheer, T. Biofilm Matrixome: Extracellular Components in Structured Microbial Communities. *Trends Microbiol.* 2020. <https://doi.org/10.1016/j.tim.2020.03.016>
- Kean, R.; Rajendran, R.; Haggarty, J.; *et al.* *Candida albicans* Mycofilms Support *Staphylococcus aureus* Colonization and Enhances Miconazole Resistance in Dual-Species Interactions. *Front. Microbiol.* 2017, 8, 258. <https://doi.org/10.3389/fmicb.2017.00258>
- Kim, M.; Ashida, H.; Ogawa, M.; Yoshikawa, Y.; Mimuro, H.; Sasakawa, C. Bacterial Interactions with the Host Epithelium. *Cell Host Microbe* 2010, 8 (1), 20-35. <https://doi.org/10.1016/j.chom.2010.06.006>
- Kim, Y. S.; Lee, E. S.; Kwon, H. K.; Kim, B. I. Monitoring the Maturation Process of a Dental Microcosm Biofilm Using the Quantitative Light-induced Fluorescence-Digital (QLF-D). *J. Dent.* 2014, 42 (6), 691-696. <https://doi.org/10.1016/j.jdent.2014.03.006>
- Klassen, A.; van Haren, E. L.; Cross, K.; *et al.* International Mixed Methods Study Protocol to Develop a Patient-Reported Outcome Measure for All Types of Chronic Wounds (The WOUND-Q). *BMJ Open* 2020, 10 (3), e032332. <https://doi.org/10.1136/bmjopen-2019-032332>
- Kloepper, J. W.; Ryu, C. M.; Zhang, S. Induced Systemic Resistance and Promotion of Plant Growth by *Bacillus* spp. *Phytopathology* 2004, 94 (11), 1259-1266. <https://doi.org/10.1094 / PHYTO.2004.94.11.1259>
- Kong, E. F.; Tsui, C.; Kucharíková, S.; Andes, D.; Van Dijck, P.; Jabra-Rizk, M. A. Commensal Protection of *Staphylococcus aureus* against Antimicrobials by *Candida albicans* Biofilm Matrix. *mBio.* 2016, 7 (5), e01365-16 <https://doi.org/10.1128 / mBio.01365-16>
- Kong, E. F.; Tsui, C.; Kucharíková, S.; Van Dijck, P.; Jabra-Rizk, M. A. Modulation of *Staphylococcus Aureus* Response to Antimicrobials by the *Candida Albicans* Quorum Sensing Molecule Farnesol. *Antimicrob. Agents Chemother.* 2017, 61 (12), e01573-17. <https://doi.org/10.1128 / AAC.01573-17>
- Koo, H.; Allan, R. N.; Howlin, R. P.; Stoodley, P.; Hall-Stoodley, L. Targeting Microbial Biofilms: Current and Prospective Therapeutic Strategies. *Nat. Rev. Microbiol.* 2017, 15 (12), 740-755. <https://doi.org/10.1038/nrmicro.2017.99>
- Korgaonkar, A.; Trivedi, U.; Rumbaugh, K. P.; Whiteley, M. Community Surveillance Enhances *Pseudomonas Aeruginosa* Virulence During Polymicrobial Infection. *Proc. Natl. Acad. Sci. U. S. A.* 2013, 110 (3), 1059-1064. <https://doi.org/10.1073/pnas.1214550110>
- Kreth, J.; Zhang, Y.; Herzberg, M. C. *Streptococcal* Antagonism in Oral Biofilms: *Streptococcus Sanguinis* and *Streptococcus Gordonii* Interference with *Streptococcus Mutans*. *J. Bacteriol.* 2008, 190 (13), 4632-4640. <https://doi.org/10.1128/JB.00276-08>
- Kuang, X.; Chen, V.; Xu, X. Novel Approaches to the Control of Oral Microbial Biofilms. *BioMed Res. Int.* 2018, 2018, 1–13. <https://doi.org/10.1155/2018/6498932>
- Kuramitsu, H. K.; He, X.; Lux, R.; Anderson, M. H.; Shi, W. Interspecies Interactions Within Oral Microbial Communities. *Microbiol. Mol. Biol. Rev.* 2007, 71 (4), 653-670. <https://doi.org/10.1128 / MMBR.00024-07>
- Kyd, J.M.; Krishnamurthy, A.; Kidd, S.P. Interactions and mechanisms of respiratory tract biofilms involving *Streptococcus pneumoniae* and nontypeable *Haemophilus influenzae*. *Microbial Biofilms - Importance and Applications*; Dharumadurai, D., Thajuddin, N., Eds.; IntechOpen: London, 2016; pp 299-327. <https://doi.org/10.5772/63500>
- Lahiri, D.; Dash, S.; Dutta, R.; Nag, M. Elucidating the Effect of Anti-Biofilm Activity of Bioactive Compounds Extracted from Plants. *J. Biosci.* 2019, 44 (2), 52. <https://doi.org/10.1007/s12038-019-9868-4>
- Langford, M. L.; Atkin, A. L.; Nickerson, K. W. Cellular Interactions of Farnesol, a Quorum-Sensing Molecule Produced by *Candida Albicans*. *Future Microbiol.* 2009, 4 (10), 1353–1362. <https://doi.org/10.2217/fmb.09.98>
- Lebeaux, D.; Chauhan, A.; Rendueles, O.; Beloin, C. From *in vitro* to *in vivo* Models of Bacterial Biofilm-Related Infections. *Pathogens* 2013, 2 (2), 288-356. <https://doi.org/10.3390/patogenos2020288>

- Lee, B.; Haagensen, J. A.; Ciofu, O.; Andersen, J. B.; Høiby, N.; Molin, S. Heterogeneity of Biofilms Formed by Nonmucoid *Pseudomonas Aeruginosa* Isolates from Patients with Cystic Fibrosis. *J. Clin. Microbiol.* 2005, 43 (10), 5247-5255. <https://doi.org/10.1128/JCM.43.10.5247-5255.2005>
- Lower, S. K. Atomic Force Microscopy to Study Intermolecular Forces and Bonds Associated with Bacteria. *Adv. Exp. Med. Biol.* 2011, 715, 285-299. https://doi.org/10.1007/978-94-007-0940-9_18
- Li, X.; Chopp, D. L.; Russin, W. A.; Brannon, P. T.; Parsek, M. R.; Packman, A. I. Spatial Patterns of Carbonate Biomineralization in Biofilms. *Appl. Environ. Microbiol.* 2015, 81 (21), 7403-7410. <https://doi.org/10.1128/AEM.01585-15>
- Łoś, M.; Golec, P.; Łoś, J. M.; *et al.* Effective Inhibition of Lytic Development of Bacteriophages Lambda, P1 and T4 by Starvation of Their Host, *Escherichia Coli*. *BMC Biotechnol.* 2007, 7, 13. <https://doi.org/10.1186/1472-6750-7-13>
- Lu, S. Y.; Zhao, Z.; Avillan, J. J.; Liu, J.; Call, D. R. Autoinducer-2 Quorum Sensing Contributes to Regulation of Microcin PDI in *Escherichia coli*. *Front. Microbiol.* 2017, 8, 2570. <https://doi.org/10.3389/fmicb.2017.02570>
- Lundstrom, J. R.; Williamson, A. E.; Villhauer, A. L.; Dawson, D. V.; Drake, D. R. Bactericidal Activity of Stabilized Chlorine Dioxide as an Endodontic Irrigant in a Polymicrobial Biofilm Tooth Model System. *J. Endod.* 2010, 36 (11), 1874-1878. <https://doi.org/10.1016/j.joen.2010.08.032>
- Ma, H.; Ma, S.; Hu, H.; *et al.* The biological role of N-acyl-homoserine lactone-based quorum sensing (QS) in EPS production and microbial community assembly during anaerobic granulation process. *Sci. Rep.* 2018, 8 (15793), 15793. <https://doi.org/10.1038/s41598-018-34183-3>
- Ma, S.; Moser, D.; Han, F.; Leonhard, M.; Schneider-Stickler, B. Tan, Y. Preparation and antibiofilm studies of curcumin loaded chitosan nanoparticles against polymicrobial biofilms of *Candida albicans* and *Staphylococcus aureus*. *Carbohydr. Polym.* 2020, 241, 116254. <https://doi.org/10.1016/j.carbpol.2020.116254>
- Macià, M. D.; Del Pozo, J. L.; Díez-Aguilar, M.; Guinea, J. Microbiological Diagnosis of Biofilm-Related Infections. *Enferm. Infecc. Microbiol. Clin.* 2018, 36 (6), 375-381. <https://doi.org/10.1016/j.eimce.2017.04.015>
- Maddocks, S. E.; Jenkins, R. E.; Rowlands, R. S.; Purdy, K. J.; Cooper, R. A. Manuka Honey Inhibits Adhesion and Invasion of Medically Important Wound Bacteria *in Vitro*. *Future Microbiol.* 2013, 8 (12), 1523-1536. <https://doi.org/10.2217/fmb.13.126>
- Madsen, J. S.; Burmølle, M.; Hansen, L. H.; Sørensen, S. J. The Interconnection Between Biofilm Formation and Horizontal Gene Transfer. *FEMS Immunol. Med. Microbiol.* 2012, 65 (2), 183-195. <https://doi.org/10.1111/j.1574-695X.2012.00960.x>
- Manson, J. M.; Rauch, M.; Gilmore, M. S. The Commensal Microbiology of the Gastrointestinal Tract. *Adv. Exp. Med. Biol.* 2008, 635, 15-28. https://doi.org/10.1007/978-0-387-09550-9_2
- Mark Welch, J. L.; Rossetti, B. J.; Rieken, C. W.; Dewhirst, F. E.; Borisy, G. G. Biogeography of a Human Oral Microbiome at the Micron Scale. *Proc. Natl. Acad. Sci. U. S. A.* 2016, 113 (6), E791-E800. <https://doi.org/10.1073/pnas.1522149113>
- Marsh, P. D.; Do, T.; Beighton, D.; Devine, D. A. Influence of Saliva on the Oral Microbiota. *Periodontol.* 2000 2016, 70 (1), 80-92. <https://doi.org/10.1111/prd.12098>
- McGuigan, L.; Callaghan, M. The Evolving Dynamics of the Microbial Community in the Cystic Fibrosis Lung. *Environ. Microbiol.* 2015, 17 (1), 16-28. <https://doi.org/10.1111/1462-2920.12504>
- Mendes, J. J.; Leandro, C.; Corte-Real, S.; *et al.* Wound Healing Potential of Topical Bacteriophage Therapy on Diabetic Cutaneous Wounds. *Wound Repair Regen.* 2013, 21 (4), 595-603. <https://doi.org/10.1111/wrr.12056>
- Metcalf, D.; Bowler, P.; Parsons, D. Wound Biofilm and Therapeutic Strategies. In *Microbial Biofilms - Importance and Applications*; Dharumadurai, D., Thajuddin, N., Eds.; IntechOpen: London, 2016; pp 271-298. <https://doi.org/10.5772/63238>
- Mihai, M. M.; Preda, M.; Lungu, I.; Gestal, M. C.; Popa, M. I.; Holban, A. M. Nanocoatings for Chronic Wound Repair-Modulation of Microbial Colonization and Biofilm Formation. *Int. J. Mol. Sci.* 2018, 19 (4), 1179. <https://doi.org/10.3390/ijms19041179>
- Monte, J.; Abreu, A. C.; Borges, A.; Simões, L. C.; Simões, M. Antimicrobial Activity of Selected Phytochemicals against *Escherichia coli* and *Staphylococcus aureus* and Their Biofilms. *Pathogens* 2014, 3 (2), 473-498. <https://doi.org/10.3390/pathogens3020473>
- Montaser, A. S.; Abdel-Mohsen, A. M.; Ramadan, M. A.; *et al.* Preparation and Characterization of Alginate/Silver/Nicotinamide Nanocomposites for Treating Diabetic Wounds. *Int. J. Biol. Macromol.* 2016, 92, 739-747. <https://doi.org/10.1016/j.ijbiomac.2016.07.050>

- Mulcahy, H.; Charron-Mazenod, L.; Lewenza, S. Extracellular DNA Chelates Cations and Induces Antibiotic Resistance in *Pseudomonas Aeruginosa* Biofilms. *PLoS Pathog.* 2008, 4 (11), e1000213. <https://doi.org/10.1371/journal.ppat.1000213>
- Murray, J. L.; Connell, J. L.; Stacy, A.; Turner, K. H.; Whiteley, M. Mechanisms of synergy in polymicrobial infections. *J. Microbiol.* 2014, 52 (3), 188-199. <https://doi.org/10.1007/s12275-014-4067-3>
- Musat, N.; Foster, R.; Vagner, T.; Adam, B.; Kuypers, M. M. Detecting Metabolic Activities in Single Cells, With Emphasis on nanoSIMS. *FEMS Microbiol. Rev.* 2012, 36 (2), 486-511. <https://doi.org/10.1111/j.1574-6976.2011.00303.x>
- Neu, T. R.; Lawrence, J. R. Innovative Techniques, Sensors, and Approaches for Imaging Biofilms at Different Scales. *Trends Microbiol.* 2015, 23 (4), 233-242. <https://doi.org/10.1016/j.tim.2014.12.010>
- Oliveira, A.; Sousa J. C.; Silva A. C.; Melo L. D. R.; Sillankorva, S. Chestnut Honey and Bacteriophage Application to Control *Pseudomonas aeruginosa* and *Escherichia coli* Biofilms: Evaluation in an *ex vivo* Wound Model. *Front. Microbiol.* 2018, 9, 1725. <https://doi.org/10.3389/fmicb.2018.01725>
- Oppenheimer-Shaanan, Y.; Sibony-Nevo, O.; Bloom-Ackermann, Z.; *et al.* Spatio-temporal assembly of functional mineral scaffolds within microbial biofilms. *NPJ Biofilms Microbiomes* 2016, 2, 15031. <https://doi.org/10.1038/npjbiofilms.2015.31>
- Orazi, G.; O'Toole, G. A. "It Takes a Village": Mechanisms Underlying Antimicrobial Recalcitrance of Polymicrobial Biofilms. *J. Bacteriol.* 2019, 202 (1), e00530-19. <https://doi.org/10.1128/JB.00530-19>
- Orazi, G.; Ruoff, K. L.; O'Toole, G. A. *Pseudomonas Aeruginosa* Increases the Sensitivity of Biofilm-Grown *Staphylococcus Aureus* to Membrane-Targeting Antiseptics and Antibiotics. *mBio* 2019, 10 (4), e01501-19 <https://doi.org/10.1128/mBio.01501-19>
- O'Toole, G. A.; Kolter, R. Flagellar and Twitching Motility Are Necessary for *Pseudomonas Aeruginosa* Biofilm Development. *Mol. Microbiol.* 1998, 30 (2), 295-304. <https://doi.org/10.1046/j.1365-2958.1998.01062.x>
- Palencia, M.; Córdoba, A.; Arrieta, Á. Stimuli-sensitive nanostructured poly(sodium 4-styrene sulfonate): Synthesis, characterization, and study of metal ion retention properties. *J. Appl. Polym. Sci.* 2017, 135 (11), 46001. <https://doi.org/10.1002/app.46001>
- Palencia, M.; Lerma, T. A.; Arrieta, Á. Antibacterial and non-hemolytic cationic polyurethanes with N-carboxymethyl-N,N,N-triethylammonium groups for bacteremia-control in biomedical-using materials. *Mater. Today Commun.* 2020, 22, 100708. <https://doi.org/10.1016/j.mtcomm.2019.100708>
- Palmer, J.; Flint, S.; Brooks, J. Bacterial Cell Attachment, the Beginning of a Biofilm. *J. Ind. Microbiol. Biotechnol.* 2007, 34 (9), 577–588. <https://doi.org/10.1007/s10295-007-0234-4>
- Peleg, A. Y.; Hogan, D. A.; Mylonakis, E. Medically Important Bacterial-Fungal Interactions. *Nat. Rev. Microbiol.* 2010, 8 (5), 340-349. <https://doi.org/10.1038/nrmicro2313>
- Percival, S. L. Importance of Biofilm Formation in Surgical Infection. *Br. J. Surg.* 2017, 104 (2), e85-e94. <https://doi.org/10.1002/bjs.10433>
- Percival, S.L.; McCarty, S. M.; Lipsky, B. Biofilms and Wounds: An Overview of the Evidence. *Adv. Wound Care (New Rochelle)* 2015a, 4 (7), 373-381. <https://doi.org/10.1089/herida.2014.0557>
- Percival, S. L.; Suleman, L.; Vuotto, C.; Donelli, G. Healthcare-associated Infections, Medical Devices and Biofilms: Risk, Tolerance and Control. *J. Med. Microbiol.* 2015b, 64 (Pt 4), 323-334. <https://doi.org/10.1099/jmm.0.000032>
- Perez, A. C.; Pang, B.; King, L. B.; *et al.* Residence of *Streptococcus Pneumoniae* and *Moraxella Catarrhalis* Within Polymicrobial Biofilm Promotes Antibiotic Resistance and Bacterial Persistence in Vivo. *Pathog. Dis.* 2014, 70 (3), 280-288. <https://doi.org/10.1111/2049-632X.12129>
- Peters, B. M.; Jabra-Rizk, M. A.; O'May, G. A.; Costerton, J. W.; Shirliff, M. E. Polymicrobial Interactions: Impact on Pathogenesis and Human Disease. *Clin. Microbiol. Rev.* 2012, 25 (1), 193-213. <https://doi.org/10.1128/CMR.00013-11>
- Philip, N.; Bandara, H. M. H. N.; Leishman, S. J.; Walsh, L. J. Effect of Polyphenol-Rich Cranberry Extracts on Cariogenic Biofilm Properties and Microbial Composition of Polymicrobial Biofilms. *Arch. Oral Biol.* 2019, 102, 1-6. <https://doi.org/10.1016/j.archoralbio.2019.03.026>
- Pires D. P.; Dötsch, A.; Anderson, E. M.; *et al.* A Genotypic Analysis of Five *P. aeruginosa* Strains after Biofilm Infection by Phages Targeting Different Cell Surface Receptors. *Front. Microbiol.* 2017a, 8, 1229. <https://doi.org/10.3389/fmicb.2017.01229>

- Pires, D. P.; Melo, L.; Vilas Boas, D.; Sillankorva, S.; Azeredo, J. Phage Therapy as an Alternative or Complementary Strategy to Prevent and Control Biofilm-Related Infections. *Curr. Opin. Microbiol.* 2017b, 39, 48-56 <https://doi.org/10.1016/j.mib.2017.09.004>
- Polke, M.; Jacobsen, I. D. Quorum Sensing by Farnesol Revisited. *Curr. Genet.* 2017, 63 (5), 791-797. <https://doi.org/10.1007/s00294-017-0683-x>
- Post, J. C. Direct Evidence of Bacterial Biofilms in Otitis Media. *Laryngoscope* 2001, 111 (12), 2083-2094. <https://doi.org/10.1097/00005537-200112000-00001>
- Qi, L.; Xu, Z.; Jiang, X.; Hu, C.; Zou, X. Preparation and antibacterial activity of chitosan nanoparticles. *Carbohydr. Res.* 2004, 339 (16), 2693–2700. <https://doi.org/10.1016/j.carres.2004.09.007>
- Rabin, N.; Zheng, Y.; Opoku-Temeng, C.; Du, Y.; Bonsu, E.; Sintim, HO. Biofilm Formation Mechanisms and Targets for Developing Antibiofilm Agents. *Future Med. Chem.* 2015, 7 (4), 493-512. <https://doi.org/10.4155/fmc.15.6>
- Rahman, M.; Kim, S.; Kim, S. M.; Seol, S. Y.; Kim, J. Characterization of Induced *Staphylococcus Aureus* Bacteriophage SAP-26 and Its Anti-Biofilm Activity with Rifampicin. *Biofouling* 2011, 27 (10), 1087-1093. <https://doi.org/10.1080/08927014.2011.631169>
- Ramage, G. Comparing Apples and Oranges: Considerations for Quantifying Candidal Biofilms with XTT [2,3-bis(2-methoxy-4-nitro-5-sulfo-phenyl)-2H-tetrazolium-5-carboxanilide] and the Need for Standardized Testing. *J. Med. Microbiol.* 2016, 65 (4), 259-260. <https://doi.org/10.1099/jmm.0.000237>
- Ramsey, M. M., Rumbaugh, K. P., Whiteley, M. Metabolite Cross-Feeding Enhances Virulence in a Model Polymicrobial Infection. *PLoS Pathog.* 2011, 7 (3), e1002012. <https://doi.org/10.1371/journal.ppat.1002012>
- Rani, S. A.; Pitts, B.; Beyenal, H.; *et al.* Spatial Patterns of DNA Replication, Protein Synthesis, and Oxygen Concentration Within Bacterial Biofilms Reveal Diverse Physiological States. *J. Bacteriol.* 2007, 189 (11), 4223-4233. <https://doi.org/10.1128/JB.00107-07>
- Rasmussen, B. Filamentous Microfossils in a 3,235-million-year-old Volcanogenic Massive Sulphide Deposit. *Nature* 2000, 405 (6787), 676-679. <https://doi.org/10.1038/35015063>
- Rendueles, O.; Ferrières, L.; Frétaud, M.; *et al.* A New Zebrafish Model of Oro-Intestinal Pathogen Colonization Reveals a Key Role for Adhesion in Protection by Probiotic Bacteria. *PLoS Pathog.* 2012, 8 (7), e1002815. <https://doi.org/10.1371/journal.ppat.1002815>
- Rickard, A. H.; Gilbert, P.; High, N. J.; Kolenbrander, P. E.; Handley, P. S Bacterial Coaggregation: An Integral Process in the Development of Multi-Species Biofilms. *Trends Microbiol.* 2003, 11 (2), 94-100. [https://doi.org/10.1016/S0966-842X\(02\)00034-3](https://doi.org/10.1016/S0966-842X(02)00034-3)
- Ribeiro, S. M.; de Castro, A. P.; Franco, O. L. Metagenomic approach to study biofilm in medical context. *Med. Res. Arch.* 2017, 5 (5).
- Rohacek, M.; Weisser, M.; Kobza, R.; *et al.* Bacterial Colonization and Infection of Electrophysiological Cardiac Devices Detected With Sonication and Swab Culture. *Circulation* 2010, 121 (15), 1691-1697. <https://doi.org/10.1161/CIRCULATIONAHA.109.906461>
- Roberts, A. E.; Kragh, K. N.; Bjarnsholt, T.; Diggle, S. P. The Limitations of *In Vitro* Experimentation in Understanding Biofilms and Chronic Infection. *J. Mol. Biol.* 2015, 427 (23), 3646-3661. <https://doi.org/10.1016/j.jmb.2015.09.002>
- Rollenhagen, C.; Sörensen, M.; Rizos, K.; Hurvitz, R.; Bumann, D. Antigen Selection Based on Expression Levels During Infection Facilitates Vaccine Development for an Intracellular Pathogen. *Proc. Natl. Acad. Sci. U. S. A.* 2004, 101 (23), 8739-8744. <https://doi.org/10.1073/pnas.0401283101>
- Rosenfeldt, V.; Michaelsen, K. F.; Jakobsen, M.; *et al.* Effect of Probiotic *Lactobacillus* Strains in Young Children Hospitalized with Acute Diarrhea. *Pediatr. Infect. Dis. J.* 2002, 21 (5), 411-416. <https://doi.org/10.1097/00006454-200205000-00012>
- Rudkjøbing, V. B.; Thomsen, T. R.; Alhede, M.; *et al.* The Microorganisms in Chronically Infected End-Stage and Non-End-Stage Cystic Fibrosis Patients. *FEMS Immunol. Med. Microbiol.* 2012, 65 (2), 236-244. <https://doi.org/10.1111/j.1574-695X.2011.00925.x>
- Samaranayake, Y. H.; Bandara, H. M.; Cheung, B. P.; Yau, J. Y.; Yeung, S. K.; Samaranayake, L. P. Enteric Gram-negative Bacilli Suppress Candida Biofilms on Foley Urinary Catheters. *APMIS* 2014, 122 (1), 47-58. <https://doi.org/10.1111/apm.12098>
- Sanchez, Y.; Palencia, M.; Mora, M. A first approach to the development of new drugs with leishmanicidal activity via control of surface properties of silver nanoparticle. *J. Sci. Tech. Appl.* 2019, 6, 1-16. <https://doi.org/10.34294/jjsta.19.6.46>

- Sandt, C.; Smith-Palmer, T.; Pink, J.; Brennan, L.; Pink, D. Confocal Raman Microspectroscopy as a Tool for Studying the Chemical Heterogeneities of Biofilms in Situ. *J. Appl. Microbiol.* 2007, 103 (5), 1808-1820. <https://doi.org/j.1365-2672.2007.03413.x>
- Schierle, C. F.; De la Garza, M.; Mustoe, T. A.; Galiano, R. D. Staphylococcal Biofilms Impair Wound Healing by Delaying Reepithelialization in a Murine Cutaneous Wound Model. *Wound Repair Regen.* 2009, 17 (3), 354-359. <https://doi.org/10.1111/j.1524-475X.2009.00489.x>
- Schmeisser, C.; Krohn-Molt, I.; Streit, W. R. Metagenome Analyses of Multispecies Microbial Biofilms: First Steps Toward Understanding Diverse Microbial Systems on Surfaces. In *Functional Metagenomics: Tools and Applications*; Charles, T., Liles, M., Sessitsch, A., Eds.; Springer: Cham, 2017; pp 201-215. https://doi.org/10.1007/978-3-319-61510-3_12
- Sekirov, I.; Finlay, B. B. Human and Microbe: United We Stand. *Nat. Med.* 2006, 12 (7), 736-737. <https://doi.org/10.1038/nm0706-736>
- Şen Karaman, D.; Manner, S.; Rosenholm, J. M. Mesoporous Silica Nanoparticles as Diagnostic and Therapeutic Tools: How Can They Combat Bacterial Infection?. *Ther. Deliv.* 2018, 9 (4), 241-244. <https://doi.org/10.4155/tde-2017-0111>
- Silva M. D.; Sillankorva, S. Otitis Media Pathogens - A Life Entrapped in Biofilm Communities. *Crit. Rev. Microbiol.* 2019, 45 (5-6), 595-612. <https://doi.org/10.1080/1040841X.2019.1660616>
- Sen, C. K.; Gordillo, G. M.; Roy, S.; *et al.* Human Skin Wounds: A Major and Snowballing Threat to Public Health and the Economy. *Wound Repair Regen.* 2009, 17 (6), 763-771. <https://doi.org/10.1111/j.1524-475X.2009.00543.x>
- Seoane, J.; Yankelevich, T.; Dechesne, A.; Merkey, B.; Sternberg, C.; Smets, B. F. An Individual-Based Approach to Explain Plasmid Invasion in Bacterial Populations. *FEMS Microbiol. Ecol.* 2011, 75 (1), 17-27. <https://doi.org/10.1111/j.1574-6941.2010.00994.x>
- Short, F. L.; Murdoch, S. L.; Ryan, R. P. Polybacterial human disease: the ills of social networking. *Trends Microbiol.* 2014, 22 (9), 508-516. <https://doi.org/10.1016/j.tim.2014.05.007>
- Sibley, C. D.; Rabin, H.; Surette, M. G. Cystic Fibrosis: A Polymicrobial Infectious Disease. *Future Microbiol.* 2006, 1 (1), 53-61. <https://doi.org/10.2217/17460913.1.1.53>
- Stewart, P. S.; Franklin, M. J. Physiological Heterogeneity in Biofilms. *Nat. Rev. Microbiol.* 2008, 6 (3), 199-210. <https://doi.org/10.1038/nrmicro1838>
- Sullan, R. M.; Li, J. K.; Crowley, P. J.; Brady, L. J.; Dufrêne, Y. F. Binding Forces of *Streptococcus Mutans* P1 Adhesin. *ACS Nano* 2015, 9 (2), 1448-1460. <https://doi.org/10.1021/nn5058886>
- Sun, Y.; Dowd, S. E.; Smith, E.; Rhoads, D. D.; Wolcott, R. D. *In Vitro* Multispecies Lubbock Chronic Wound Biofilm Model. *Wound Repair Regen.* 2008, 16 (6), 805-813. <https://doi.org/10.1111/j.1524-475X.2008.00434.x>
- Taglialegna, A.; Navarro, S.; Ventura, S.; *et al.* *Staphylococcal* Bap Proteins Build Amyloid Scaffold Biofilm Matrices in Response to Environmental Signals. *PLoS Pathog.* 2016, 12 (6), e1005711. <https://doi.org/10.1371/journal.ppat.1005711>
- Tanner, W. D.; Atkinson, R. M.; Goel, R. K.; *et al.* Horizontal Transfer of the bla_{NDM-1} Gene to *Pseudomonas Aeruginosa* and *Acinetobacter Baumannii* in Biofilms. *FEMS Microbiol. Lett.* 2017, 364, 8. <https://doi.org/10.1093/femsle/fnx048>
- Taylor, P. W.; Hamilton-Miller, J. M.; Stapleton, P. D. Antimicrobial Properties of Green Tea Catechins. *Food Sci. Technol. Bull.* 2005, 2, 71-81. <https://doi.org/10.1616/1476-2137.14184>
- Thomsen, T. R.; Aasholm, M. S.; Rudkjøbing, V. B.; *et al.* The Bacteriology of Chronic Venous Leg Ulcer Examined by Culture-Independent Molecular Methods. *Wound Repair Regen.* 2010, 18 (1), 38-49. <https://doi.org/10.1111/j.1524-475X.2009.00561.x>
- Turonova, H.; Neu, T. R.; Ulbrich, P.; *et al.* The Biofilm Matrix of *Campylobacter Jejuni* Determined by Fluorescence Lectin-Binding Analysis. *Biofouling* 2016, 32, 597-608. <https://doi.org/10.1080/08927014.2016.1169402>
- Van den Driessche, F.; Rigole, P.; Brackman, G.; Coenye, T. Optimization of Resazurin-Based Viability Staining for Quantification of Microbial Biofilms. *J. Microbiol. Methods* 2014, 98, 31-34. <https://doi.org/10.1016/j.mimet.2013.12.011>
- Van Laar, T. A.; Chen, T.; You, T.; Leung, K. P. Sublethal Concentrations of Carbapenems Alter Cell Morphology and Genomic Expression of *Klebsiella Pneumoniae* Biofilms. *Antimicrob. Agents Chemother.* 2015, 59 (3), 1707-1717. <https://doi.org/10.1128/AAC.04581-14>

CAPÍTULO III: HIPÓTESIS, OBJETIVO GENERAL Y OBJETIVOS ESPECÍFICOS

Hipótesis

Candida albicans y *H. pylori* establecen una interacción simbiótica, este tipo de interacción se ve afectado impactando directamente en la viabilidad de la bacteria.

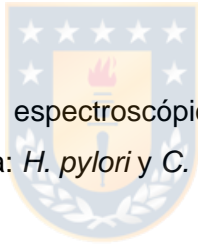
La hipótesis anterior parte del hecho de la existencia de estas interacciones, y, en consecuencia, no sólo hay que describirlas sino diseñar cómo medirla, lo que, a nivel científico fue un reto metodológico y con gran impacto a nivel de las ciencias microbiológicas.

Objetivo general

Describir los diferentes tipos de interacción entre *H. pylori* y *C. albicans*, así como su efecto sobre la viabilidad de la bacteria.

Objetivos específicos

1. Desarrollar una metodología espectroscópica para el estudio de las interacciones superficiales bacteria- levadura: *H. pylori* y *C. albicans*.
2. Determinar los tipos de interacción entre *H. pylori* y *C. albicans*.
3. Establecer el efecto de la coexistencia entre *H. pylori* y *C. albicans* sobre la viabilidad bacteriana.



Capítulo IV: Mid-infrared vibrational spectrum characterization of outer surface of *Candida albicans* by Functionally-Enhanced Derivative Spectroscopy (FEDS)

Paper 3:

Mid-infrared vibrational spectrum characterization of outer surface of *Candida albicans* by Functionally-Enhanced Derivative Spectroscopy (FEDS)

Sixta Palencia^{1,2*}, Apolinaria García¹, Manuel Palencia^{2,3}

¹ *Laboratory of Bacterial Pathogenicity, Department of Microbiology, Faculty of Biological Sciences, Universidad de Concepción, Concepción – Chile*

² *Microbiology and Bioengineering Division, Mindtech Research Group (Mindtech-RG), Mindtech s.a.s., Cali – Colombia*

³ *Research Group in Science with Technological Applications (GI-CAT), Department of Chemistry, Faculty of Natural and Exact Sciences, Universidad del Valle, Cali – Colombia*

Corresponding author: sixta.palencia3004@gmail.com

Accepted for publication in Russian version ZhPS Vol. 88, No.1 (January-February) 2021.

Journal of Applied Spectroscopy

Paper reg. No. 14-20 | ISSN 1573-8647 | www.springer.com/journal/10812

Mid-infrared vibrational spectrum characterization of outer surface of *Candida albicans* by Functionally-Enhanced Derivative Spectroscopy (FEDS)

Sixta Palencia^{1,2*}, Apolinaria García¹, Manuel Palencia^{2,3}

¹ Laboratory of Bacterial Pathogenicity, Department of Microbiology, Faculty of Biological Sciences, Universidad de Concepción, Concepción – Chile

² Microbiology and Bioengineering Division, Mindtech Research Group (Mindtech-RG), Mindtech s.a.s., Cali – Colombia

³ Research Group in Science with Technological Applications (GI-CAT), Department of Chemistry, Faculty of Natural and Exact Sciences, Universidad del Valle, Cali – Colombia

Corresponding author: sixta.palencia3004@gmail.com

Abstract

The objective of this work was to evaluate the ability of FEDS algorithm for the characterization of surface of microorganisms, exactly *Candida albicans*, by mid-IR spectroscopy, and using the technique of cellulose sensing surface. This work is a key stage in the study of cell-cell and cell-surface interactions between microorganisms including the study of polymicrobial biofilms. By the above, *C. albicans* was selected as microorganism model due to its importance for medical science and human health. Spectra were recording in triplicate, from 4000 to 500 cm^{-1} by ATR technique. It was concluded that FEDS transform of mid-IR spectrum is a powerful analytical tool for the improving of spectral analysis by IR spectroscopy. In the particular case of *C. albicans* biofilms, it was observed that by FEDS is possible to perform the deconvolution of signals and achieve a better differentiation of them. For interpretation, serine, threonine, glycine, alanine, glutamic acid, proline and N-Acetyl-D-glucosamine units were taken as molecular models since these molecules have been described as main components in the cell wall of *C. albicans*. In this way, it was found that vibrational spectrum of *C. albicans* biofilms can be understood considering only the main components of cell wall.

Keywords: *Candida albicans*, Mid-IR spectrum, Biofilm, FEDS transform, Sensing surface

Introduction

A biofilm is understood to be an assemblage of microbial cells that is irreversibly associated with a surface, and which is enclosed in a matrix of primarily polysaccharide material, but that

also, it can be constituted by non-cellular materials such as mineral crystals, corrosion particles, clay or silt particles, or blood component -ts, among other [1-4]. In addition, biofilms can colonize abiotic and biotic surfaces and proceed through distinct stages which can be broadly categorized into reversible adhesion stage and irreversible cohesion stage [3, 4]. But also, it is widely recognized that biofilms are an important problem for human health contributing to ~80 % of the hospital infections [4].

On the other hand, adhesion between bacteria and surfaces can be studied by a variety of methods as scanning electron microscopy (SEM), transmission electron microscopy (TEM), fluorescence microscopy, among other [2, 5]. The main limitations in the case of SEM and TEM is the high cost of equipment, high perturbation of samples and limited molecular information. Fluorescence techniques are based on 'the making' of systems which are different to those that are being studied.

It is proposed that, by the correct characterization of surface, important information of microorganism surface can be obtained and directed toward multiple objectives. In particular, the study of interactions between microorganisms is an important aspect in the study of pathogenicity and prevalence mechanisms. In consequence, in this study the analysis of microorganism surface was visualized to be satisfactorily carried out by spectroscopic techniques, since they permit to obtain molecular-level surface information, in particular, it is proposed the use of infrared spectroscopy in the mid-infrared (mid-IR) by the Attenuate Total Reflectance (ATR) technique.

Mid-IR spectroscopy is based on the use of IR radiation to produce changes of vibrational states at molecular level. In addition, it is characterized by being a non-destructive, fast, easy to use and highly sensitive method for microbial analysis, but also, it requires a small sample size without complex pre-treatment procedures. In addition, it is a very useful method for the determination of the presence or absence of functional groups, the analysis of new or changes of molecular interactions by monitoring and examination of the position, displacements and intensity of the different IR signals [6-8], monitoring of bioprocess as bio-fermentation, microbial biodegradation pathways and bacterial biofilms on implantable devices [9-12]. However, for microbiological analysis, the main limitations of mid-IR spectroscopy are: high spectral similitude between spectra of different microorganisms, the high overlap of signals and widening of adjacent signals [6-8]. For the resolving of these problems usually mathematical and computerized methods are used, being the most common the Fourier deconvolution [13-15]. However, though from a conceptual approach the Fourier self-deconvolution is simple, its application is limited by the relatively-high complexity of computation, the appearing of negative intensities from calculations, the highly sensitive to

the noise and the appearing of 'false' signals resulting of mathematical arguments without physical meaning [13]. In contrast, a simple method for the deconvolution and the increase of spectral resolution of signals have been recently developed, this method is based on the transformation of spectrum by the use of derivative algorithm enhanced by functional transformations and has been named Functionally-Enhanced Derivative Spectroscopy (FEDS) [15].

The objective of this work was to evaluate the ability of FEDS algorithm for the characterization of surface of microorganisms, exactly *Candida albicans*, through the analysis by mid-IR spectroscopy of artificial biofilm deposited on spectrally-marked cellulose surface. This work is a key stage in the study, by IR spectroscopy, of cell-cell and cell-surface interactions between microorganisms including the study of polymicrobial biofilms.

Materials and methods

Yeast strains and growing conditions.

ATCC strains of *Candida albicans* were used as model of microorganism, this was supplied by Laboratory of Bacterial Pathogenicity of Universidad de Concepción. This yeast was selected due to importance for researches in human health.

Candida albicans strain was grown by inoculating in tryptic soy broth (TSB) (Invitrogen, Carlsbad, CA, USA) and standardized to 0.5 in the Mc-Farland scale by absorbance measurements at 625 nm using turbidity standards prepared from BaCl₂ solution (0.048 molL⁻¹) and H₂SO₄ (0.18 molL⁻¹). Later, sub-samples of yeast were separately inoculated in agar Müller-Hinton incubating for 24 hours at 37 °C. Gram stain was performed when the yeast growth was evidenced.

Preparation of samples and recording of spectra.

Artificial yeast biofilms, or biolayers, were deposited on ultrafiltration cellulose membranes which were previously modified using a spectral marker (CISM®, Mindtech s.a.s., Colombia). CISM® is a spectral marker producing a characteristic mid-IR signal at ~2268 cm⁻¹; this signal is absent in the mid-IR spectrum of yeast and, in consequence, it can be used for the monitoring of background signals associated with cellulose support.

In order to eliminate residual composition of growth medium on the surface, after forming the biolayer on the support, samples were successively washed with deionized water and dried using a laminar flow oven with temperature control at 40 °C per 12 hours. To warrant this stage, spectra of support and blank experiments, i.e., growth medium without bacterium, were

compared with the respective spectra of biofilm samples. Finally, bilayers were analyzed using an infrared spectrophotometer with ATR using a ZnSe crystal (ATR, IR-Affinity, Shimadzu Co). Bilayers were performed in triplicate, and average spectra for each replicate were recorded by 20 scans from 500 to 4000 cm^{-1} . Data were extracted in file format .txt in order to carry out the analysis using a spreadsheet.

Pre-treatment of data.

For each region of spectrum being analyzed, data were auto-scaled with respect to the values of minimum and maximum absorbances (a_{\min} and a_{\max} , respectively).

$$b_j = \frac{a_j - a_{\min}}{a_{\max} - a_{\min}} \quad (1)$$

where a_j and b_j are the experimental absorbance in the j -position and the corresponding auto-scaled absorbance, respectively. Note that j -position can be directly correlated with the wavenumber. In order to avoid calculation mistakes resulting to scaling from 0 to 1 during the application of FEDS algorithm, the zero absorbance was approximated by the calculation of average value between two adjacent values of absorbance satisfying that $b_{j-1} < b_j < b_{j+1}$ with $b_j = 0$. Since derivative spectrum is strongly sensitive to the noise in the original signal, the smoothing of spectral noise was decreased by the use of average-based spectral filter (ABSF) [15]. ABSF is given by

$$ABSF(b_i; N = 20) = \frac{1}{3} \sum_j^{j+2} (b_j) \left| \begin{array}{l} N=20 \\ N=1 \end{array} \right. \quad (2)$$

ABSF is the moving average with a data window of 3 and 20 cycles ($N = 20$). Thus, for each b_j , b_{j+1} and b_{j+2} , the corresponding average value is calculated, and subsequently, this procedure is repeated N times. However, as the spectrum line function in the absorbance domain is modified by the use of Equation 2, the same transformation of data is performed on values of wavenumbers (ν) in order to correct the displacements respect to original spectrum (*i.e.*, maximum points in original spectrum should be the same in the original and smoothed spectra) [15].

Fundamentals and calculations.

For the application of FEDS transform to the mid-IR spectrum, the spectrum is considered to be a function \mathbf{z} with $\mathbf{z}:(\nu_j, b_j)$. By FEDS, a new spectrum with sharper signals is obtained, but also, since the intensities of signals with a higher SNR are increased, the deconvolution of overlapped signals is produced. Thus, for the obtaining of FEDS intensities, the first step is

the calculation of the first-order derivative of the inverse of normalized spectrum, therefore, FEDS transform is a method of derivative spectroscopy applied on the inverse function of IR spectrum. This first stage can be easily calculated by:

$$\frac{dz}{dv} = \frac{\frac{1}{b_j} - \frac{1}{b_{j-1}}}{v_j - v_{j-1}} \quad (3)$$

Assuming that $v_j - v_i$ is always a constant (this assumption is valid for almost all instrumental equipment), Equation 3 is rewritten to be

$$p = \frac{1}{b_j} - \frac{1}{b_{j-1}} \quad (4)$$

where p denotes an auxiliary function p in order to simplify the notation (the notation p comes from the Spanish word '*primera*' alluding to the use of the first derivative). Since Equation 4 defines positive and negative values, the mathematical operator $1/(|x|)^{0.5}$ is applied, where x denotes any mathematical arguments. This operator is equal to scale factor defined under the wavelet concept which is used to define the general expression of 'mother wavelet' [15]. Thus, for each b_i , a new function called Function P transforms the values of function p by

$$P_j = \frac{1 + b_j}{\sqrt{|p_j|}} \quad (5)$$

where $(1 + b_j)$ is an amplification factor for the assignation of a weight congruent with absorbance intensity and P defines a new magnitude called FEDS intensity.

At the present, FEDS transform only has been used for quantification of water contents in mixture with organic acids, determination by spectral analysis of dimerization constant, deconvolution of mid-infrared spectrum of quaternized poly(vinyl chloride) for assignation of signals, and the recognition of specific signal in polymers [15, 16].

Result and Discussion

Mid IR spectrum of *C. albicans* biofilms.

In the Figure 1 are shown the main signals identified in the IR spectrum of *C. albicans*. These signals have been described widely in several works [7-8, 17-24]. However, they do not permit to obtain specific information about the biofilm since these are commons for all microorganisms. A summary of the signals and their chemical nature is shown in Table 1. By the above, the use of FEDS appears as an interesting analytical tool for the increasing of spectral resolution of IR spectra. In order to ease the analysis FEDS of spectrum, different analysis windows were defined: 4000-3000 cm^{-1} , 3000-2500 cm^{-1} , 2500-2000 cm^{-1} , 2000-

1300 cm^{-1} and 1300-600 cm^{-1} . FEDS spectrum of *C. albicans* biofilm (4000-3000 cm^{-1} and 3000-2500 cm^{-1}).

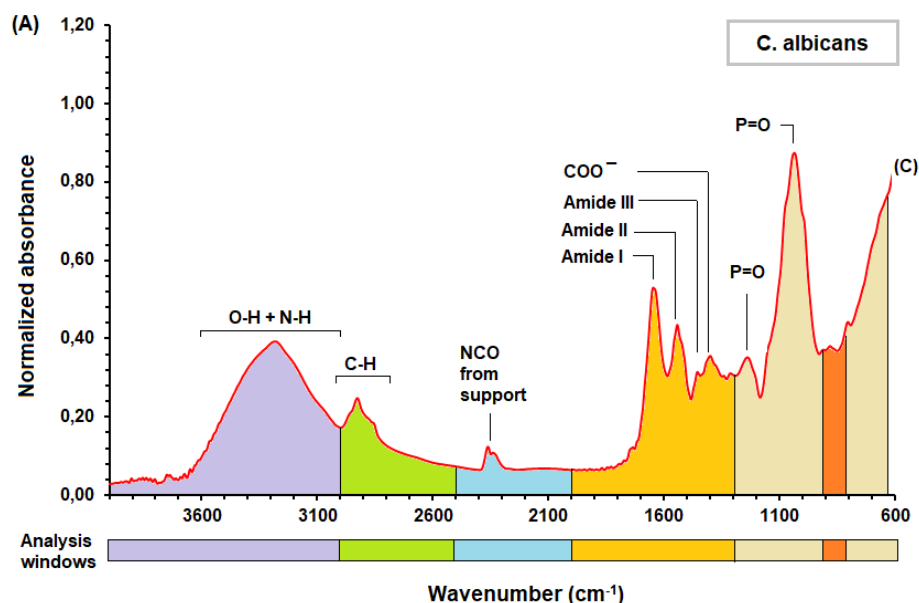


Fig 1. Averaged IR spectrum of *C. albicans* obtained by ATR technique.

Table 1. Assignment of main signals observed in the mid-IR spectrum of *C. albicans* biofilms.

Analysis window (cm^{-1})	Wavenumber (cm^{-1})	Description
3000 – 4000	No specified	Vibrations associated with O-H and N-H groups. It is not possible to indicate a specific signal due to the overlap. This band is affected by the presence of water, alcohols, amines, etc. [8, 15]
2500 – 3000	2800 – 3000	Vibrations associated with C-H. These vibrations can be C-H of methyl groups, methylene groups or C-H in a ring or cyclic structure [8].
	< 2800	Though S-H vibrations are not identified these are expected in this region (usually these are very weak signals) [21]. In addition, some vibrations modes of N-H are expected in this region [21].
2000 – 2500	2240 – 2350	Vibration of NCO. This signal is not associated with the bacterial biofilm but that is associated with spectral marker onto support surface [22-24].
1300 – 2000	1650	Amide I corresponding to C=O stretching vibration with minor contributions from out-of-phase CN stretching vibration, the CCN deformation and the NH in-plane bending [20].
	1550	Amide II corresponding to out-of-plane combination of the NH in plane bending and the CN stretching vibration with smaller contributions from the CO in plane bending and the CC and NC stretching vibrations [20].
	1450	Amide III corresponding to the in-phase combination of NH bending and the CN stretching vibration with small contributions from the CO in plane bending and the C-C stretching vibration [20].
	1400	Symmetric stretching of carboxylate group observed in several bacteria [7, 19].
600 – 1300	1240	Vibration of P=O (γ_1). The assignment was based on models for DNA phosphodiester group [17-18] and by comparison with results of other researchers with different bacteria [19].
	1050	P=O (γ_2). The assignment was based on models for DNA phosphodiester group [17-18] and by comparison with results of other researchers with different bacteria [19].

In the Figure 2, the analysis windows of FEDS spectrum of *C. albicans* corresponding to 4000-3000 cm^{-1} and 3000-2500 cm^{-1} are shown. Between 4000 and 3000 cm^{-1} are observed two signals, since in this region signals associated with vibrations of O–H and N–H are expected, the first one, at 3560 cm^{-1} , was associated with O–H groups whereas the second one, at 3281 cm^{-1} , was associated with N–H groups due to larger electronegativity of oxygen atom compared with electronegativity of nitrogen atom. Both signals can be explained by the presence of peptidoglycan on the surface of the *C. albicans* which is constituted by disaccharides and peptides with O–H groups and N–H units on their structures [25].

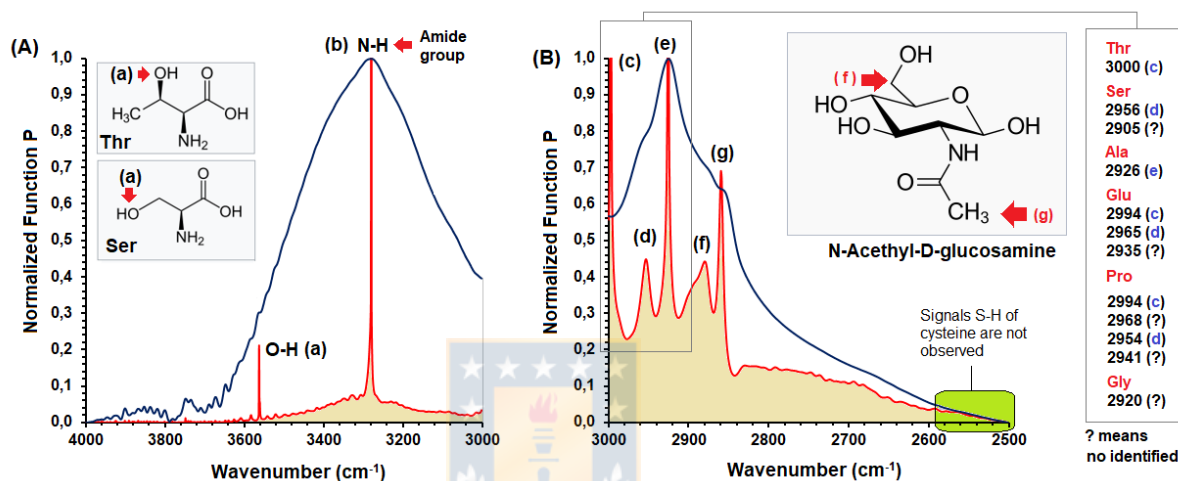


Fig 2. FEDS transform of IR spectrum of *C. albicans* obtained by ATR technique: (A) 3000-4000 cm^{-1} and (B) 2500-3000 cm^{-1} .

Signal associated with O–H is expected result because about 80 to 90 % of the cell wall of *C. albicans* is constituted by carbohydrate, being described by three types of polysaccharides: (i) branched polymers of glucose containing β -1,3 and β -1,6 linkages (β -glucans), corresponding to 20-40 % of dry weight of the cell wall, (ii) unbranched polymers of N-acetyl-D-glucosamine (NAcGlc) containing β -1,4 bonds (chitin), corresponding to 1-2 % of dry weight of the cell wall, and (iii) polymers of mannose (mannan) covalently associated with proteins (glyco[manno]proteins) [25-27].

It is important to indicate that the outer layer of the cell wall of *C. albicans* is mainly composed by mannoproteins [27], which would explain the signal associated with N–H and O–H vibrations since the amount of chitin is very small. Whereas chitin is 1-2 % of cell wall, the mannoproteins correspond to approximately 40 % of the cell wall of *C. albicans* [26-27], and given that these are localized in the external layer of yeasts, these are expected to show a better interaction with IR ray during ATR analysis. By the above, and considering the main amino acid composition of cell wall of *C. albicans* [28], where three fractions of amino acids

are described, it is concluded that O–H signals could be mainly associated with side segments of threonine and serine, whereas the signal N–H is mainly associated with N–H vibrations of amide groups of peptide chains formed by threonine, serine, glutamic acid, proline, glycine and alanine (see Table 2; in addition, respective structures are shown in the Figure 3).

Note that, by computational calculations based on Density Functional Theory, or DFT, O–H signal for serine in aqueous solution is expected at 3500 cm⁻¹, but it is observed at 3529 cm⁻¹; however, by the formation of hydrogen bonds this signal is displaced to 3556 cm⁻¹ [29]. On the other hand, O–H signal for threonine in aqueous solution is expected, by DFT, at 3560 cm⁻¹ by the formation of hydrogen bonds [29].

Table 2. Main amino acids constituting the cell wall of *Candida albicans*. Fraction A, B and C corresponding to 24, 10 and 70-80 % of wall cell, respectively [28].

Fraction	Protein content (%)	Main amino acids	Content of amino acid (%)	Main no-peptide structural units on the chains of amino acids			
A	> 50	Threonine (Thr)	21.1	-CH ₂	-CH ₃	-OH	-
		Serine (Ser)	13.3	-CH ₂	-OH	-	-
		Glutamic acid (Glu)	12.3	-CH ₂	-OH	C=O	COO-
		Proline (Pro)	12.2	-CH	-CH ₂	-	-
		Glycine (Gly)	6.7	-CH ₂	-	-	-
B	> 90	Serine (Ser)	20.6	-CH ₂	-OH	-	-
		Threonine (Thr)	15.5	-CH ₂	-CH ₃	-OH	-
		Alanine (Ala)	12.4	-CH ₃	-	-	-
		Glutamic acid (Glu)	9.8	-CH ₂	-OH	C=O	COO-
		Proline (Pro)	7.6	-CH	-CH ₂	-	-
C	~ 25	Serine (Ser)	15.2	-CH ₂	-OH	-	-
		Alanine (Ala)	13.9	-CH ₃	-	-	-
		Glycine (Gly)	11.7	-CH ₂	-	-	-
		Glutamic acid (Glu)	9.2	-CH ₂	-OH	C=O	COO-
		Threonine (Thr)	8.1	-CH ₂	-CH ₃	-OH	-

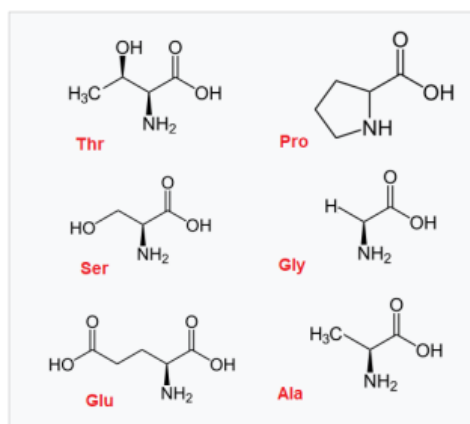


Fig 3. Structure of main amino acids forming the cell wall of *C. albicans*.

The above is coherent with the results obtained by FEDS transform which situates the signal at 3560 cm^{-1} . Note that this signal is not observed into IR spectra of *C. albicans*, and only it can be identified by FEDS, demonstrating the FEDS ability to produce the deconvolution of IR spectrum and visualize overlapped signals. In addition, the analytical power of FEDS, as tool for data analysis, is also evidenced in the ability to associate, in conjunction with theoretical and computational calculations, this specific signal with O–H of side chain of amino acids on the peptide chain, suggesting that the same could be performed with analysis of theoretical spectra of monomers of the respective polysaccharides. Thus, the basic structural units identified in the cell wall of *C. albicans*, i.e., glucose (glucans), N-Acetyl-D-glucosamine (chitin) and mannose (mannan) can be used in conjunction with DFT to ease the assignation of signals obtained by FEDS [26-28], for example, for sucrose, which is a disaccharide constituted by glucose and fructose units, the O–H signal on fructose are expected at 3559 cm^{-1} whereas for glucose are expected at 3382 cm^{-1} [30]. Note that peptidoglycans of *C. albicans* are not formed by fructose units but by glucose units and, in consequence, the important signal for our analysis is at 3382 cm^{-1} . For mannose, the experimental spectrum shows the vibration signal of O–H between 3000 and 3500 cm^{-1} [31], and from computational data at 3742 , 3740 , 3736 , 3603 , 3305 and 3249 cm^{-1} [32]. Other authors describe three vibrations associated with O–H stretching of Mannan I or poly- β -D-(1-4) mannose: 3497 , 3462 and 3365 cm^{-1} [33]. Finally, for N-Acetyl-D-glucosamine, the signals associated with the O–H stretching are expected at 3458 , 3391 , 3376 , 3326 and 3197 cm^{-1} [34]. The above suggests that, by the use of FEDS, signals of O–H vibration produced by peptides can be differentiate of signals of O–H vibration produced by polysaccharides forming the peptidoglycans.

The signal at 2280 cm^{-1} , identified by FEDS and easily visualized in the IR spectrum, it is associated with N–H stretching. This signal is directly related with amide groups (–CONH–) resulting of the linking of amino acids to form polypeptides in the outer layer of wall cell.

On the other hand, signals observed in the analysis window among 3000 - 2500 cm^{-1} are not important because these are present in many organic molecules. Considering that the main signals are associated with the outer layer of cell wall, from vibrational analysis by computational techniques, signals associated with side units of main amino acids described in the Table 2 were used in order to achieve a coherent assignation of signals.

Thus, for threonine, one signal at 3000 cm^{-1} have been described and associated with C–H in the CH_3 , whereas, for serine three signals have been described at 3004 cm^{-1} (stretching), 2956 cm^{-1} (asymmetric stretching) and 2905 cm^{-1} (symmetric stretching) associated with C–H in CH_2 [29]. For alanine, asymmetric stretching of CH in CH_3 have been experimentally

observed at 2926 cm^{-1} and for glutamic acid, vibration associated with CH stretching in CH_2 is observed at 2994 cm^{-1} , CH_2 asymmetric stretching is observed at 2965 cm^{-1} and CH_2 symmetric stretching at 2935 cm^{-1} [35]. For proline, antisymmetric stretches associated with CH_2 are observed at 2994 and 2968 whereas symmetric stretches are observed at 2954 and 2941 cm^{-1} [36]. For glycine, two signals associated with asymmetric stretching at 3084 cm^{-1} and symmetric stretching at 2920 cm^{-1} have been observed in IR spectrum [4]. In consequence, in the analysis window between 2500 and 3000 cm^{-1} are expected about eleven signals associated with C–H vibrations in CH_2 and CH_3 groups. In this way, signals described in the Figure 2 as c, d and e can be associated with vibrational modes of C–H in CH_2 and CH_3 of main amino acids forming the outer layer of cell wall of *C. albicans*.

On the other hand, during the study of FTIR spectroscopy as a potential tool for the study of structural modifications of *C. albicans*, signals associated with vibrations of CH_2 from lipids have been described at 2851 , 2873 , 2924 and 2960 cm^{-1} , whereas one signal associated with C–H from methyl groups is assigned at 2893 cm^{-1} [37]. During the study of FTIR spectroscopy as a potential tool for the study of structural modifications of *C. albicans*, signals associated with vibrations of CH_2 from lipids at 2851 , 2873 , 2924 and 2960 cm^{-1} , whereas one signal associated with C–H from methyl groups was assigned at 2893 cm^{-1} [37]; however, this assignation was not considered due to low content of lipids in the cell wall of *C. albicans* (1-7 %) [26].

By the analysis of FT-IR spectra of N-Acetyl-D-glucosamine (NAcGlc), two signals have been described at 2829 and 2893 cm^{-1} for solid state and 2895 cm^{-1} in aqueous solution; however, by theoretical calculations, these signals are expected to 2889 cm^{-1} for C–H and 2859 cm^{-1} for CH_2 [34]. Since: (i) 80-90 % of the cell wall of *C. albicans* is formed by carbohydrates including NAcGlc, (ii) mannose polymers (mannan), which do not exist as such but these are found in covalent association with proteins (mannoproteins), represent about 40 % of the total cell wall polysaccharide corresponding to the main material of the cell wall matrix of *C. albicans* and (iii) mannose polymers are linked to the protein moiety through asparagine by N-glycosidic bonds through two NAcGlc units [26], it is concluded that the signals f and g can be associated with signals from NAcGlc; thus: signal at 2880 cm^{-1} is assigned to C–H in CH_3 of NAcGlc (f) whereas signal at 2860 cm^{-1} is assigned to C–H in CH_2 (g) of NAcGlc.

In addition, important conclusions can be directed considering the signals that no appearing in the spectrum. For example, stretching associated with C–H bond in phenyl ring of phenylalanine are expected to appears at 2918 cm^{-1} [35], and for cysteine three signals are expected at 2543 , 2545 and 2552 cm^{-1} associated with vibrational modes of S–H bond [21]. The above is coherent with the low content of phenylalanine (fraction A, B and C: between

3.5 and 4.6 %) and cysteine (fraction A: 0.3 %; fractions B and C: no identified) described in previous publications [28].

FEDS spectrum of *C. albicans* biofilm (2500-2000 cm^{-1}).

In the Figure 4 is shown the FEDS transform of IR spectrum of *C. albicans* in the region between 2000-2500 cm^{-1} . In this region is not usual found signals in samples of living organism, in addition, it is characterized because very few functional groups have infrared signals in this region. The main and more characteristic signal corresponds to isocyanate group ($-\text{NCO}$) which was used as spectral marker of the surface of cellulose support. Note that, for methyl isocyanate, the stretching signal associated with $-\text{NCO}$ has been identified at 2288 cm^{-1} [38] whereas for phenyl isocyanate the same signal is described at 2285 cm^{-1} (asymmetric stretching), but with two additional signals with lower intensity at 2340 and 2370 cm^{-1} corresponding to non-fundamental signals [39]. Results obtained by FEDS are coherent with the signals from phenyl isocyanate since the marker used was based on MDI. Signals identified were at 2365 cm^{-1} (**h**), 2340 cm^{-1} (**i**) and 2278 cm^{-1} (**j**).

Other non-fundamental signals associated with symmetric stretching of $-\text{NCO}$ (it is expected at 1448 cm^{-1}) have been reported at 2207 and 2090 cm^{-1} (these signals were identified as **k₁** and **k₂**, respectively) [39]. But also, in this region appears one signal of combination at 2128 cm^{-1} (**k₃**) which can change depending of molecular ordering of water molecules [40].

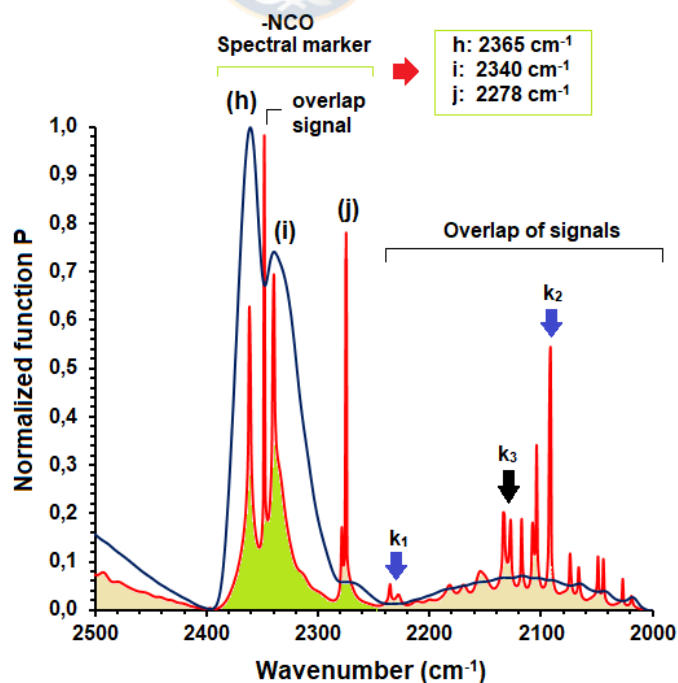


Fig 4. FEDS spectrum of *C. albicans* biofilms between 2500-2000 cm^{-1} .

FEDS spectrum of *C. albicans* biofilm (1300-2000 cm^{-1}).

In the Figure 5 is shown the FEDS transform of IR spectrum of *C. albicans* in the region between 2000-1300 cm^{-1} . As it is expected, the complexity of FEDS spectrum is increased in comparison with IR spectrum, being the above a typical observation in derivative spectroscopy. For its interpretation, the direct comparison with IR spectrum was performed and, as a result of this procedure, four signals were identified: Am⁻¹, Am-2, Am-3 and -COO⁻ which were previously explained in the Table 1. But also, by analysis of relative-minimum point in the line function of spectrum is possible to identify eight overlap signals, which it is seen to be reasonable because the number of signals in this region is significantly increased.

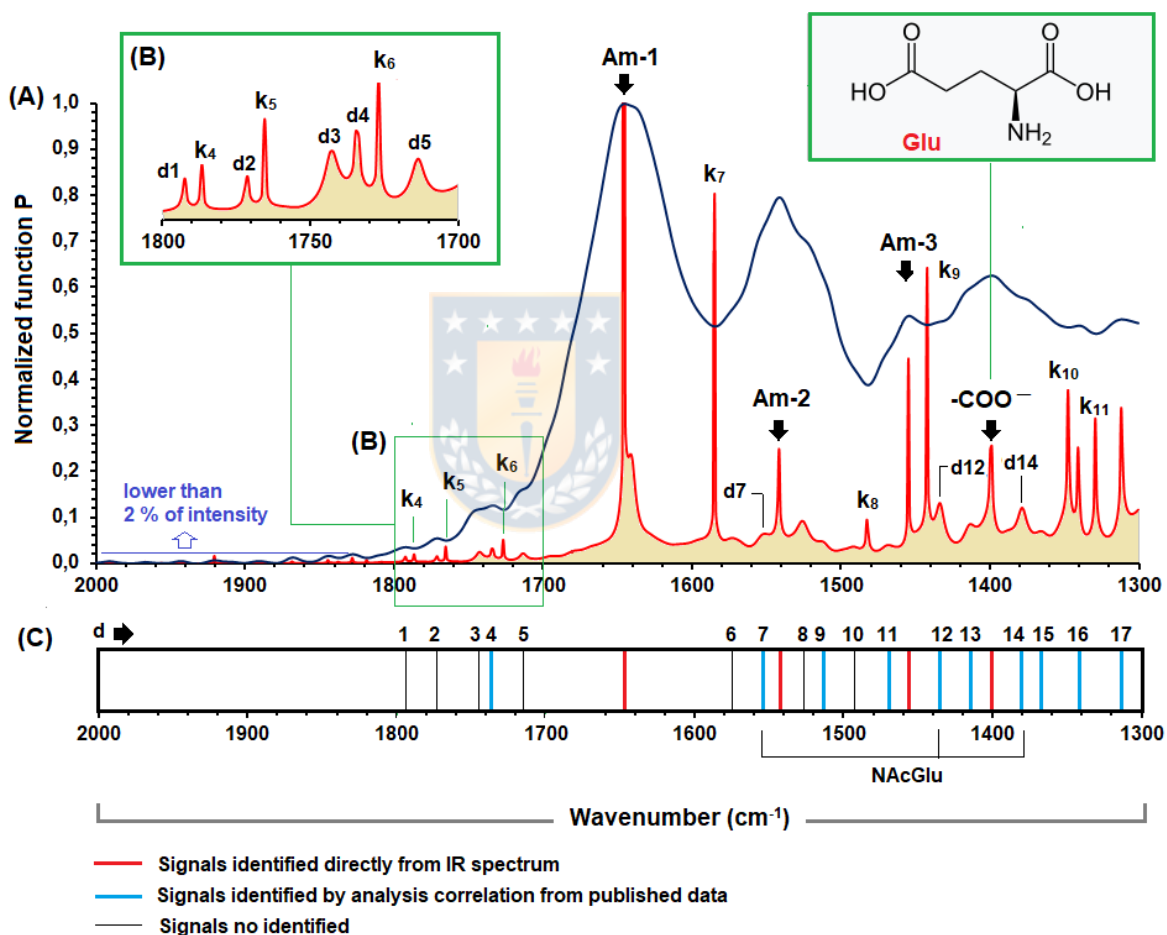


Fig 5. (A) FEDS spectrum of *C. albicans* biofilms between 2000-1300 cm^{-1} (B) magnification of region between 1800 and 1700 cm^{-1} , and (C) signal discontinuous patterns for range under study.

These signals were named from **k4** to **k11** in order to continue with the numbering of overlap signals previously identified. In addition, signals with FEDS intensity lower than 2 % were not taken in consideration since its contribution is very small (signals between 1800 and 2000 cm^{-1}

1). Thus, 17 new signals are obtained from FEDS transform for this analysis window, these were named from **d1** to **d13**.

Note that assignment of signals is very difficult due to nature of the sample, the appearing of new signals that previously were not identified in the IR spectrum, and the lack available information about FEDS transform and IR spectra of *C. albicans*. Therefore, to carry out the assignment the signals, the signals of main components previously identified constituting the cell wall of *C. albicans* were used to perform a correlation analysis. Thus, the set of signals described for individual molecules in the analysis windows were grouped with a variation of ± 5 cm^{-1} and compared with signals observed from FEDS spectrum (see Table 3).

Table 3. Analysis of correlation of signals described for main components of cell wall of *C. albicans* [4, 29, 34-36]. Correlation of signals was performed with a tolerance of ± 5 . Analysis window between 1300 and 2000 cm^{-1} . Shaded rows correspond to signals with adequate correlation.

Signal	Wavenumber for main components of <i>C. albicans</i> (cm^{-1})						FEDS	Id. Code	
	Ala	Gly	Ser	Thr	Glu	Pro			NacGlu
No identified							1794	d1	
C=O (st)					1781				
No identified							1772	d2	
No identified							1743	d3	
NH (b)		1730					1735	d4	
No identified							1715	d5	
C=O (st) + others		1703							
C=O (st)						1687			
COO (v)				1640	1635				
CH (b) + CH ₂ (b)									
C=O (v)							1627		
NH ₂ (sc)		1610	1610						
NH ₂ (b)	1595			1596					
No identified							1570	d6	
NH (v)							1550	d7	
NH ₂ (b)						1542			
No identified							1525	d8	
CH ₂ (b)		1504	1509				1510	d9	
CH ₂ (b) + OH (b)									
No identified							1490	d10	
C-O-H (v)				1481			1483	k₈	
CH ₂ (r), CH ₂ (b)			1468			1472	1473	d11	
CN (st), OH (v)						1465			
CH ₂ (b)				1452		1457	1452		
CH ₃ (v)						1448			
CH (v), OH (v)							1430	1435	d12
OH (b), C-O-H		1412	1411	1415	1405			1415	d13
N-C-H (v)		1410							
CH ₂ (sc)									
CH (b-in-p)									
CO (st) + CH ₂ (t)					1386		1388		

CH (v), OH (v)				
CH (v), OH (v)			1377	1380
CH ₂ (w)	1354		1361	1365
C-OH (st)			1357	
NH ₂ (sc)				
CH (v)			1348	
NH (b) + CN (b)	1341	1340		1342
C-C-H (v)				
N-C-H (v)				
H-C-O (v)				
CO (st) + CO (st)	1334	1337		
CH (st) + C-C (v)				
CH ₂ (d-in-p)			1325	1328
CH (v), CH ₂ (v)				
C-O-H (v)	1312		1314	1312
CH ₂ (w)				
CH ₂ (t)		1301	1302	
CH ₂ (d-out-p)				

Symbols: stretching (st), bending (b), scissoring (sc), bending in-plane (b-in-p), torsion (t), no-specified vibration (v), rocking (r), wagging (w), deformation (d), deformation in-plane (d-in-p), deformation (d-out-p).

Grey row shows the signals obtained by FEDS which can be correlated with at least one signal described in previous publications.

Red letter indicates the signals which was not possible identify by this procedure.

By correlation analysis, signals **d1**, **d2**, **d3**, **d5**, **d6**, **d8** and **d10** were not identified. On the other hand, many of these signals are common for many organic compounds and, from analytical point of view, these are not important. In particular, the signal k_8 that is identified as an overlap signal is seen to show an adequate correlation with the vibration of C–O–H, and therefore, it is not completely clear if there is some hidden signal since this signal is coherent with the presence of –OH group on the side chain of threonine which is an important component of cell wall of *C. albicans*. On the other hand, three signals are identified to be very important since these are associated only with NAcGlu units: **d7** (1550 cm⁻¹), **d12** (1435 cm⁻¹) and **d14** (1380 cm⁻¹).

FEDS spectrum of *C. albicans* biofilm (1300-600 cm⁻¹).

In the Figure 6 is shown the FEDS transform of IR spectrum of *C. albicans* in the region between 1300-600 cm⁻¹. It can be seen that complexity of FEDS spectrum in this region increases compared with IR spectrum. By a procedure analogous to that applied for the region between 2000-1300 cm⁻¹, the assignation of signal was based on available information of IR vibrations of main components of cell wall of *C. albicans* and by direct comparison with IR spectrum. Thus, by direct comparison were identified two signals associated with P=O links (named to be y_1 and y_2 , respectively). On the other hand, from correlation analysis (see Table 4), some signals were not identified (**E10**, **E11**, **E16**, **E20**, **E23** and **E24**) and other were correlated with multiples vibrations associated with different groups of amino acids and

NAcGlu, therefore, an exact assignment was not possible. However, four signals correlated only with NAcGlu permitting that these can be associated with this specific component, thus, signals **E7** (1000 cm^{-1}), **E15** (830 cm^{-1}), **E17** (780 cm^{-1}) and **E25** (630 cm^{-1}) could be used for the monitoring of cell wall of *C. albicans*. But also, the signal **E12** correlated only with one amino acid, Glu, and, in consequence, this signal emerges as important candidate for the monitoring of glutamic acid in this type of biofilms, however, specific studies should be directed in this way.

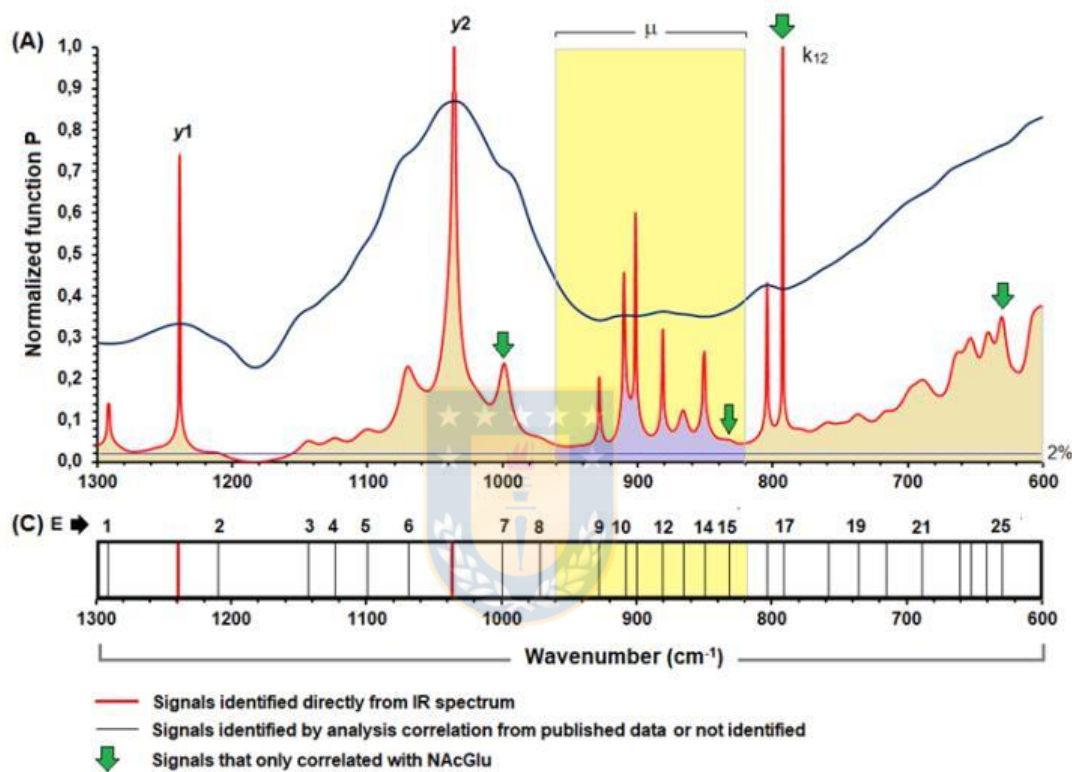


Fig 6. (A) FEDS spectrum of *C. albicans* biofilms between $1300\text{-}600\text{ cm}^{-1}$ and (B) signal discontinuous patterns for range under study.

Table 4. Analysis of correlation of signals described for main components of cell wall of *C. albicans* [4, 29, 34-36]. Correlation of signals was performed with a tolerance of ± 5 to ± 8 . Analysis window between 600 and 1300 cm^{-1} . Shaded rows correspond to signals with adequate correlation.

Signal	Wavenumber for main components of <i>C. albicans</i> (cm^{-1})							FEDS	Id. code
	Ala	Gly	Ser	Thr	Glu	Pro	NAcGlu		
CH (v), OH (v), CH ₂ (d)		1296					1290	1292	E1
CH ₂ (t), CH ₂ (t) + NH (b-in-p)					1279	1274			
CH (v), CN (v), NH (v)							1261		

CH (v), OH (v) C-N (st) ring, H- C-C (v)	1250		1244	1248			
CH (v), CH (d)			1201	1206	1210	E2	
C-C-H (v)		1193					
NH ₂ (r)			1164				
CH ₂ (t), CH ₂ (b) + CH (b) + NH ₂ (b)	1149		1147		1143	E3	
CO (v), CC (v), OH (b) + CH ₂ (t) + CN (st), NH (v), H-C-C (v)	1134		1139		1136		
CC (v), CH ₂ (v), CO (v), CN (v), OH (b-in-p)			1124		1127	1123	E4
CC (st) + CH (b) + NH (b)	1114						
CC (v), CO (v), CN (st) + OH (b- in-p)		1111	1108		1106	1112	
CH ₂ (r), C-C (st)			1092	1093		1099	E5
CC (v), CO (v), NH (v), H-C-C (v)	1086				1088		
N-C (st)				1079		1070	E6
CO (v), C-C (st) ring, CC (v), CN (v)	1057		1048	1053			
CH ₃ (v), CO (v), CC (v)					999	1000	E7
C-C (st) ring			983				
CH ₃ (v), C=O (v), CC (v)	976				973	970	E8
N-C-C (b)	936						
CN (v), CO (v), CC (v), CH (v), C-C (st) ring	924		924	927	929		E9
C-C (r), CNH (b)	918		917				
					908		E10
					900		E11
NH ₂ (t) + CH ₂ (t)	893						
CC (st) + CO (st)		886			882		E12
C-N (st) ring, CH ₂ (r)			874				
CN (v), CO (v), CC (v), CH (v)	865			862	866		E13
N-C (v), CN (st) + CC (st)	850	852			850		E14
C-C (st)				824	830		E15
HOCC (b-out-p) + CH ₂ (r)		814					
					803		E16
CO (v), CC (v)				787	780		E17
C=O (r) out-of- plane, N-C-C (v), C-C (v), HNC (b) + CCH (b)	769	772	771				

C=O (r) for carboxyl, CH ₂ (r)		754	757	759	E18
O-C-O (v)		743		738	E19
CO (v)				727	
				715	E20
CO (v), NH ₂ (b)	698			704	
CN (v), C=O (v), NH (v), COOH (b)			687	687	690
C=O (r) ureide, HOCC (b-out-p)		668	666		
C=O... H ₂ O		661		660	E22
				655	E23
NH ₂ (b-out- plane), CCC (b) + COO (b)	646		646		
				640	E24
CO (v), C=O (v), CC (v)				625	630
COOH (b-in-p)			612		E25
OH (d-out-p), COOH (b) + NCCO (b)	607			608	

Symbols: stretching (st), bending (b), scissoring (sc), bending in-plane (b-in-p), torsion (t), no-specified vibration (v), rocking (r), wagging (w), deformation (d), deformation in-plane (d-in-p), deformation (d-out-p).

Grey row shows the signals obtained by FEDS which can be correlated with at least one signal described in previous publications.

Red letter indicates the signals which was not possible identify by this procedure.

Finally, a summary of characterization by FEDS of *C. albicans* biofilm from mid-IR spectrum (4000-600 cm⁻¹) is shown in the Table 5.

Table 5. Summary of characterization by FEDS of *C. albicans* biofilm (Signals associated with overlap, and those signals were not identified, are omitted).

Analysis window (cm ⁻¹)	Wavenumber (cm ⁻¹)	Signal ID	Description
3000 – 4000	3560	a	Stretching of O–H. It is assigned to correspond to hydroxyls on amino acid structure (Thr and Ser)
	3280	b	Stretching of N–H. It is assigned to correspond to link in the peptide bond of polypeptides in the outer layer of cell wall
2500-4000	3000	c	C–H in CH ₂ and CH ₃ on the side chains of amino acids
	2950	d	C–H in CH ₂ and CH ₃ on the side chains of amino acids
	2925	e	C–H in CH ₂ and CH ₃ on the side chains of amino acids
	2880	f	C–H in CH ₃ on the side chains of NAcGlc
	2860	g	C–H in CH ₂ on the side chains of NAcGlc
2000-2500	2365	h	Asymmetric stretching of -NCO
	2340	i	Non-fundamental vibration of asymmetric stretching of -NCO
	2278	j	Non-fundamental vibration of asymmetric stretching of -NCO
	2207	k ₁	Non-fundamental vibration of symmetric stretching of -NCO
	2090	k ₂	Non-fundamental vibration of symmetric stretching of -NCO
	2128	k ₃	Combination signal of liquid water (high overlap of signals)
1300-2000	1735	d4	NH bending from Gly
	1550	d7	Vibration of N-H
	1510	d9	CH ₂ bending and combination of CH ₂ bending + OH bending

	1483	k ₈	Overlap signal. Also, it could be associated with -OH on Thr
	1470	d11	Multiple vibrations CH ₂ , CN and OH
	1435	d12	CH and OH on NAcGlu
	1415	d13	Multiple vibrations CH ₂ , CH and N-C-H
	1380	d14	CH and OH vibrations associated with NAcGlu
	1365	d15	CH ₂ vibration in some amino acids (Ala and Pro)
	1342	d16	NH + CN bending, vibrations of C-C-H, N-C-H and H-C-O
	1312	d17	vibrations of C-O-H and CH ₂
600-1300	1292	E1	Many structural contributions from amino acids and NAcGlu
	1238	y1	Vibration associated with P=O
	1210	E2	Many structural contributions from amino acids and NAcGlu
	1143	E3	Many structural contributions from amino acids and NAcGlu
	1123	E4	Many structural contributions from amino acids and NAcGlu
	1099	E5	Many structural contributions from amino acids and NAcGlu
	1070	E6	Many structural contributions from amino acids and NAcGlu
	1035	y2	Vibration associated with P=O
	1000	E7	Signal correlating only with NAcGlu associated with CH ₃ , CO and CC
	970	E8	Many structural contributions from amino acids and NAcGlu
	929	E9	Many structural contributions from amino acids and NAcGlu
	882	E12	Many structural contributions from amino acids and NAcGlu
	866	E13	Many structural contributions from amino acids and NAcGlu
	850	E14	Many structural contributions from amino acids and NAcGlu
	830	E15	Signal correlating only with NAcGlu associated with CC
	780	E17	Signal correlating only with NAcGlu associated with CO and CC
	759	E18	Many structural contributions from amino acids and NAcGlu
	738	E19	Many structural contributions from amino acids and NAcGlu
	690	E21	Many structural contributions from amino acids and NAcGlu
	660	E22	Many structural contributions from amino acids and NAcGlu
	630	E25	Signal correlating only with NAcGlu associated with C=O, CO and CC

Conclusions

FEDS transform of mid-IR spectrum is a powerful analytical tool for the improving of analysis of IR spectra. For correct application of technique is required a minimum amount of noise in the working spectra; in addition, reproducibility should be warrant by the implementation of standardized protocols and the use of an appropriate number of samples.

On the other hand, results obtained by FEDS demonstrate the capacity of FEDS for the improving of analysis of mid-IR spectra of microorganisms. In the particular case of *C. albicans* biofilms, it was observed that, by FEDS, is possible the deconvolution of signals, permitting to obtain a better differentiation of them. In this way, it was evidenced that vibrational spectrum of *C. albicans* biofilms can be understood taking in consideration only the main components of yeast cell wall, and therefore, it is concluded that good results in the signal assignation during the spectral characterization of *C. albicans* surface can be obtained from IR spectra of individual components of cell wall (Ser, Thr, Gly, Ala, Glu, Pro, and NAcGlu units could be taken as molecular models for the signal analyses).

Acknowledgments. Sixta Palencia thanks to Conicyt-Chile, Universidad de Concepción (Chile) and Universidad del Valle (Colombia) by the funds for the performing of the project and doctoral scholarship. Authors thanks to Mindtech s.a.s. by the support into acquisition of spectral marker.

Conflicts of interest. The authors declare that they have no conflict of interest.

References

- [1] J.M. Hornby, E.C. Jensen, A.D. Lisec, J.J. Tasto, B. Jahnke, R. Shoemaker, P. Dussault and K.W. Nickerson. *Appl. Environ. Microbiol.* 67, 2982–2992 (2001).
- [2] H.H. Tuson and D.B. Weibel. *Soft Matter.* 9, 4368–4380 (2013).
- [3] C.R. Arciola, D. Campoccia, G.D. Ehrlich and L. Montanaro. *Adv. Exper. Med. Biol.* 830, 29–46 (2015).
- [4] A. Kumar, A. Alam, M. Rani, N.Z. Ehtesham and S.E. Hasnain. *Inter. J. Med. Microbiol.* 307, 481-489 (2017).
- [5] A. Elbourne, J. Chapman, A. Gelmi, D. Cozzolino, R.J. Crawford and V.K. Truong. *J. Colloid Interf. Sci.* 546, 192-210 (2019).
- [6] A. Alvarez-Ordoñez, D. Mouwen, M. Lopez and M. Prieto. *J. Microbiol. Met.* 84, 369-378 (2006).
- [7] J. Ojeda, M. Dittrich. *Microbial systems biology: Methods and Protocols, Methods in Molecular Biology.* Springer Science (2012).
- [8] J. Prakash, S. Kar, C. Lin, C.Y. Chen, C.F. Chang, J.S. Jean and T.R. Kulp. *Spectrochim. Acta Part A: Mol. Biomol. Spectr.* 116, 478-484 (2013).
- [9] M. Dadd, D. Sharp, A. Pettman and C. Knowles. *J. Microbiol. Met.* 41, 69-75 (2000).
- [10] W. Huang, D. Hopper, R. Goodacre, M. Beckmann, A. Singer and J. Draper. *J. Microbiol. Met.* 67, 273-280 (2006).
- [11] Z. Khatoon, C. McTiernan, E. Suuronen, T.F. Mah and E. Alarcon. *Heliyon* 4, e01067 (2018).
- [12] D. Singhalage, G. Seneviratne, S. Madawala and I. Manawasinghe. *Ceylon J. Sci.* 47, 77-83 (2018).
- [13] W. Friesen and K. Michaelian. *Appl. Spectr.* 45, 50-56 (1991).
- [14] T. Vazhnova and D. Lukyanov. *Anal. Chem.* 85, 11291-11296 (2013).
- [15] M. Palencia. *J. Adv. Res.* 14, 53-62 (2018).
- [16] M. Palencia, T. Lerma and N. Afanasjeva. *Eur. Polym. J.* 115, 212-220 (2019).
- [17] Y. Guan, C.J. Wurrey and G.J. Thomas. *Biophys. J.* 66, 225-235 (1994).
- [18] Y. Guan and G.J. Thomas. *Biopol.* 39, 813-835 (1996).
- [19] W. Jiang, A. Saxena, B. Song, B.B. Ward, T.J. Beveridge and S. Myneni. *Langmuir* 20, 11433-11442 (2004).
- [20] A. Barth. *Biochim. Biophys. Acta* 1767, 1073-1101 (2007).
- [21] S. Parker. *Chem. Phys.* 424, 75-79 (2013).
- [22] T.A. Lerma, S. Collazos and A. Cordoba. *J. Sci. Technol. Appl.* 1, 30-38, (2016).
- [23] M. Palencia, T.A. Lerma and A. Cordoba. *J. Sci. Technol. Appl.* 1, 39-52 (2016).
- [24] N. Arbelaez, T.A. Lerma and A. Cordoba. *J. Sci. Technol. Appl.* 2, 75-83 (2017).
- [25] W. Volmer, D. Blanot, M.A. De Pedro. *FEMS Microbiol. Rev.* 32, 149-167 (2008).
- [26] W. Lajeau, J.L. López-Ribot, M. Casanova, D. Gozalbo and J.P. Martínez. *Microbiol. Mol. Biol. Rev.* 62, 130–180 (1998).
- [27] E. Reyna-Beltran, C.I. Bazan, M. Iranzo, S. Mormeneo, J.P. Luna-Arias. *The Cell Wall of Candida albicans: A Proteomics View.* doi:10.5772/intechopen.82348 (2019).
- [28] J. Ruiz-Herrera, S. Mormeneo, P. Vanaclocha, J. Font-de-Mora, M. Iranzo, I. Puertes and R. Sentandreu. *Microbiol.* 140, 1513-1523 (1994).
- [29] W. Nsangou. *Comput. Theoret. Chem.* 966, 364-374 (2011).
- [30] E. Wiercigroch, E. Szafraniec, K. Czamara, M.Z. Pacia, K. Majzner, K. Kochan, A. Kaczor, K. Baranska and K. Malek. *Spectrochim. Acta Part A: Mol. Biomol. Spectr.* 185, 317-335 (2017).

- [31] H.A. Wells and R.H. Atalla. *J. Mol. Struct.* 224, 385-424 (1990).
- [32] M.W. Ellzy. Computational and experimental studies using absorption spectroscopy and vibrational circular dichroism. Thesis. Drexel University. 1-333 (2006).
- [33] I. Nieduszynsky and R.H. Marchessault. *Canadian J. Chem.* 50, 2130-2138 (1972).
- [34] A. Kovacs, B. Nyerges and V. Izvekov. *J. Phys. Chem.* 112, 5728-5735 (2008).
- [35] M.E. Mohamed and A.M.A. Mohammed. *Inter. Lett. Chem., Phys. Astron.* 10, 1-17 (2013).
- [36] L.E. Fernández, G.E. Delgado, L.V. Maturano, R.M. Tótaró and E.L. Varetti. *J. Mol. Struct.* 1168, 84–91 (2018).
- [37] I. Adt, D. Toubas, J.M. Pinon, M. Manfait and G.D. Sockalingum. *Arch. Microbiol.* 185, 277-285 (2006).
- [38] R.P. Hirschmann, R.N. Kniseley and A. Fassel. *Spectrochim. Acta* 21, 2125-2133 (1965).
- [39] C.V. Stephenson, W.C. Coburn and W.S. Wilcox. *Spectrochim. Acta* 17, 933-946 (1961).
- [40] F.O. Libnau, O.M. Kvalheim, A.A. Christy and J. Toft. *Vibrational Spectr.* 7, 243–254 (1994).



Capítulo V: Vibrational spectrum characterization of outer surface of *Helicobacter pylori* biofilms by Functionally-Enhanced Derivative Spectroscopy (FEDS)

Paper 4:

Vibrational spectrum characterization of outer surface of *Helicobacter pylori* biofilms by Functionally-Enhanced Derivative Spectroscopy (FEDS)

Sixta L. Palencia^{a, b}, Apolinaria García^a, Manuel Palencia^{c*}

^a *Laboratory of Bacterial Pathogenicity, Department of Microbiology, Faculty of Biological Sciences, Universidad de Concepción, Concepción – Chile*

^b *Mindtech Research Group (Mindtech-RG), Mindtech s.a.s., Cali – Colombia*

^c *Research Group in Science with Technological Applications (GI-CAT), Department of Chemistry, Faculty of Natural and Exact Sciences, Universidad del Valle, Cali – Colombia*

Corresponding author: manuel.palencia@correounivalle.edu.co

Journal of the Chilean Chemical Society

65, N°4, 5015-5022, 2020/0717-9707/<https://www.jcchems.com/index.php/JCCHEMS>

Vibrational spectrum characterization of outer surface of *Helicobacter pylori* biofilms by Functionally-Enhanced Derivative Spectroscopy (FEDS)

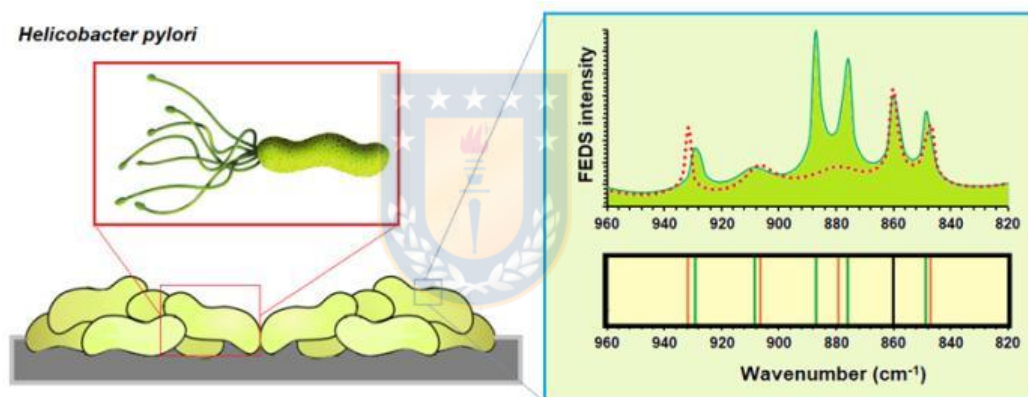
Sixta L. Palencia^{a, b}, Apolinaria García^c, Manuel Palencia^{c*}

^a Laboratory of Bacterial Pathogenicity, Department of Microbiology, Faculty of Biological Sciences, Universidad de Concepción, Concepción – Chile

^b Mindtech Research Group (Mindtech-RG), Mindtech s.a.s., Cali – Colombia

^c Research Group in Science with Technological Applications (GI-CAT), Department of Chemistry, Faculty of Natural and Exact Sciences, Universidad del Valle, Cali – Colombia

Graphical abstract



Abstract

Mid-infrared spectroscopy in conjunction with Functionally-Enhanced Derivative Spectroscopy (IR+FEDS) is a powerful analytical tool for the improving of analysis of microorganism IR spectra. The objective of this work is to characterize the outer surface of two *H. pylori* strains by IR+FEDS. This work is a key stage for the study of cell-cell and cell-surface interactions between microorganisms, as well as, for polymicrobial biofilm characterizations where *H. pylori* species are involved. For that, artificial bacterial biofilms, or bacterial bilayers, were deposited on ultrafiltration cellulose membranes which were previously modified by covalent insertion of a spectral marker and used as sensing surface for analysis of bacterium bilayers. Bilayers were analyzed using an infrared spectrophotometer with ATR and data were analyzed by classic procedures and by deconvolution based on FEDS transform. It is concluded that, for correct application of technique is required a minimum amount of noise in

the working spectra which can be achieved by simple smoothing algorithms; in addition, reproducibility must be warranted by the implementation of standardized protocols and the use of an appropriate number of samples. It is concluded that in addition to typical signals associated with IR spectrum of microorganisms, by FEDS, a better and more detailed description of outer membrane of *H. pylori* biofilms can be performed. In particular, the detecting and monitoring of cysteine-rich proteins can be satisfactorily performed by IR+FEDS.

Keywords. *Helicobacter pylori*; infrared spectrum; biofilm; FEDS transform; surface sensing

1. Introduction

Helicobacter pylori is a micro-aerophilic Gram-negative bacterium; since it is able to colonize the gastric mucosa *H. pylori* is considered an etiologic agent in a variety of gastroduodenal diseases and peptic ulcers; in addition, its study is particularly important because it is a biological risk factor for the development of gastric cancer [1-7]. It has been reported that about of half the adult population in all world is infected with this microorganism [6-7].

The surface of *H. pylori*, in addition to usual biological function that it fulfills in every microorganism, provides a vital interface for pathogen-host interactions and interaction with other microorganisms [4, 5-11]. Surface proteins of *H. pylori*, including the outer membrane proteins, can be experimentally identified by selective solubilization and sucrose gradient centrifugation for enrichment of outer membrane fractions [3, 12-13]. In *H. pylori*, these techniques produce an enriched outer membrane fractions, and many surface proteins have been assumed and described. However, these preparations are severely contaminated by inner membrane components and not necessarily corresponds to true surface composition of the bacterium [3, 13]. But also, it is well-known that different levels of molecular organization are required for the correct functioning of proteins, in consequence, destructive methods of cellular integrity produce the loss of information on the real state of surface.

On the other hand, microbial surface can be studied by several methods including Scanning Electron Microscopy (SEM), Transmission Electron Microscopy (TEM), Fluorescence Microscopy (FM), Infrared Spectroscopy (IR spectroscopy), Raman Spectroscopy, among others [14, 15]. The main limitations in the case of SEM and TEM is the high cost of equipment, the relatively high complexity of analysis, the high perturbation of samples and the obtaining of limited molecular information. On the other hand, the FM is a more economic and simpler alternative, but it requires a high perturbation of the samples to produce the

fluorescence which is not inherent to many microorganisms [16-17]. IR and Raman spectroscopies are based on the use of IR radiation to produce changes of vibrational states at molecular level. In particular, IR spectroscopy is a non-destructive, fast, easy to use and highly sensitive method [18-20]. However, for microbiological analysis, the main limitations of IR spectroscopy are the high spectral similitude between spectra of different microorganisms, and the overlap and widening of adjacent signals [18-20]. For the resolving of these problems usually the Fourier self-deconvolution is used [21-23]; however, its application is limited by the complexity of computation, the appearing of negative intensities from calculations, the highly sensitive to the noise, and the appearing of 'false' signals resulting of mathematical arguments without physical meaning [21]. In contrast, Functionally-Enhanced Derivative Spectroscopy (FEDS) is a simple method to obtain the spectral deconvolution and increase of spectral resolution of signals [24]. FEDS is based on the transformation of spectrum by the first-order derivative calculated from inverse of data constituting the IR spectrum, in combination with a set of simple working functions. In addition, it has the advantage that its interpretation is completely coherent with IR analysis. A complete description of principles has been previously published [24].

Given the importance to know the surface composition of outer membrane in real conditions of growth, technique in situ operating under controlled conditions and producing a minimal perturbation of biological system are highly desired. In this way, here it is proposed the study of bacterial surface by the building of artificial bilayers, or biofilms, followed by the subsequent direct analysis using some spectroscopic technique, in specific, mid-IR infrared spectroscopy (IR spectroscopy) by attenuated total reflectance (ATR) in conjunction with FEDS. Thus, the objective of this work was to characterize the outer surface of two *H. pylori* strains by IR+FEDS. At the present, there are not previous publications about *H. pylori* outer membrane characterization, by this technique, and with the high degree of resolution of signals achieved.

2. Experimental Section

2.1 Bacterial strains and growing conditions of microorganisms

As bacterial models were used two *H. pylori* strains: *H. pylori* ATCC J99 (American Type Culture Collection, USA) and *H. pylori* ATCC 43504 (American Type Culture Collection, USA). *H. pylori* strains were grown by inoculating in Columbia agar plates (Oxoid, England) supplemented with 7 % horse blood and incubated under microaerobic conditions in the

presence of 5 % O₂, 10 % CO₂ and 85 % N₂ at 37 °C for 4 days. Bacterial growth was verified by Gram stain and urease test and SEM.

2.2 Preparation of cellulose sensing surface

Ultrafiltration cellulose membranes modified using a spectral marker based on methylene diphenyl isocyanate (MDI, Aldrich, USA) were used as sensing surface. MDI is considered a spectral marker producing a characteristic IR signal at ~2268 cm⁻¹; this signal is absent in the IR spectra of bacteria and, in consequence, it can be used for the monitoring of background signals associated with cellulose support, and the analysis of biolayer thickness. Sensing surface were prepared by immersion of membranes (1 cm²) in dissolution of MDI (MDI/dioxane 1:1 v/v ratio) per 5 days. Catalysts were not used in order to avoid the introduction of residual signals into experimental spectra. Cellulose sensing surface were characterized by SEM to visualize the porous morphology and by Atomic Force Microscopy coupled to Raman Spectroscopy (AFM-Raman, INTEGRA Spectra, model NT-MDT) for the determination of the presence of C=O groups associated to isocyanate units.

2.3 Preparation of samples and recording of spectra

In order to eliminate residual composition of growth medium on the surface, after forming the biolayer on the support, samples were successively washed with deionized water and dried using a laminar flow oven with temperature control at 40 °C per 12 hours. To warrant this stage, spectra of support and blank experiments, i.e., growth medium without bacterium, were compared with the respective spectra of biofilm samples. Finally, biolayers were analyzed using an infrared spectrophotometer with ATR using a ZnSe crystal (ATR, IR-Affinity, Shimadzu Co). Biolayer were performed in triplicate, and average spectra for each replicate were recorded by 20 scans from 500 to 4000 cm⁻¹. Data were extracted in file format .txt in order to carry out the analysis using a spreadsheet.

2.4 Calculations

Experimental IR spectrum is a set of data defined by two columns, where the first one contains the wavenumbers whereas the second one contains the respective absorbances. Thus, each row has a position in the wavenumber scale defined according the target spectrum region. The number of points, in the working spectrum region, is defined by experimental parameters and by instrumental characteristics. Since FEDS is sensitive to residual noise in the spectrum, it is necessary to carry out a smoothing of data previous to application of FEDS transform. Details are given below.

2.5 Pre-treatment of data

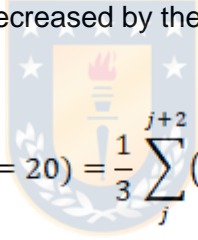
For each region of spectrum being analyzed, data are auto-scaled with respect to the values of minimum and maximum absorbances (a_{\min} and a_{\max} , respectively).

$$b_j = \frac{a_j - a_{\min}}{a_{\max} - a_{\min}} \quad (1)$$

where a_j and b_j are the experimental and auto-scaled absorbances in the j -th wavenumber position. In order to avoid calculation mistakes resulting to scaling from 0 to 1 during the application of FEDS algorithm, the zero absorbance was approximated by the calculation of average value between two adjacent values of absorbance satisfying that $b_{j-1} < b_j < b_{j+1}$ with $b_j = 0$ (deterministic approximation). Note that, other approximations can be performed depending of analyst; in addition, this approximation is seen to not affect significantly the spectrum due to that it is the minimum value of absorbance detected.

2.6 Smoothing of spectrum

Since derivative spectrum is strongly sensitive to the noise in the original signal, the smoothing of spectral noise was decreased by the use of average-based spectral filter (ABSF) [24]. ABSF is given by


$$ABSF(b_i; N = 20) = \frac{1}{3} \sum_j^{j+2} (b_j) \Bigg|_{N=1}^{N=20} \quad (2)$$

ABSF is the moving average with a data window of 3 and 20 cycles ($N = 20$). For the above, for each b_j , b_{j+1} and b_{j+2} is calculated the corresponding average value, and subsequently, this procedure is repeated N times. However, as the spectrum line function in the absorbance domain is modified by the use of Equation 2, the same transformation of data is performed on values of wavenumber (ν) in order to correct the displacements respect to original spectrum (i.e., maximum points in original spectrum should be the same in the original and smoothed spectra) [24]. Therefore, for ν ABSF is

$$ABSF(\nu_i; N = 20) = \frac{1}{3} \sum_j^{j+2} (\nu_j) \Bigg|_{N=1}^{N=20} \quad (3)$$

Note that, depending of N value used in the equations 1 and 2 a loss of data is produced, therefore, it is recommended consider this effect during the definition of working range.

4. Theoretical Background

For the application of FEDS transform to the mid-IR spectrum, the spectrum is considered to be a function z with $\mathbf{z}:(v_j, b_j)$. By FEDS, a new spectrum with sharper signals is obtained, but also, since the intensities of signals with a higher SNR are increased, the deconvolution of overlapped signals is produced.

For the obtaining of FEDS intensities, the first step is the calculation of the first-order derivative of the inverse of normalized spectrum, therefore, FEDS transform is a method of derivative spectroscopy applied on the inverse function of IR spectrum. This first stage can be easily calculated by:

$$\frac{dz}{dv} = \frac{\frac{1}{b_j} - \frac{1}{b_{j-1}}}{v_j - v_{j-1}} \quad (4)$$

Assuming that $v_j - v_{j-1}$ is always a constant (this assumption is valid for almost all instrumental equipment), Equation 4 is rewritten to be

$$p_j = \frac{1}{b_j} - \frac{1}{b_{j-1}} \quad (5)$$

where p denotes an auxiliary function formed by all values of p_j obtained by the equation 5. Therefore, p is used in order to simplify the notation (the notation p comes from the Spanish word '*primera*' alluding to the use of the first derivative). Since function p defines positive and negative values, the mathematical operator $\phi = 1/(|x|)^{0.5}$ is applied, where x denotes any mathematical arguments, and ϕ is the 'key point' of data transformation. This operator is equal to scale factor defined under the wavelet concept which is used to define the general expression of 'mother wavelet' [24]. Thus, for each b_j , a new function called Function P transforms the values of function p by

$$P_j = \frac{1 + b_j}{\sqrt{|p_j|}} = \phi(1 + b_j) \quad (6)$$

where $(1 + b_j)$ is an amplification factor for the assignment of a weight congruent with experimental absorbance intensities and P defines a new magnitude usually called FEDS intensity. It is important to note that P is not directly related with the absorbances, and therefore it is not directly related with the concentration; however, by auxiliary-fitting functions is possible to produce the re-scaling of FEDS spectrum in order to obtain a new spectrum where the main FEDS signals are equals to those obtained in the IR spectrum.

At the present, FEDS transform only has been used for quantification of water contents in mixture with organic acids, determination by spectral analysis the dimerization constant of

acetic acid, deconvolution of mid-infrared spectrum of quaternized poly(vinyl chloride), analysis of binary mixtures and the characterization of biological tissue of fish [24-27].

5. Result and Discussion

4.1 Characterization of cellulose sensing surface

In the Figure 1A the AFM-Raman spectra of cellulose membrane and cellulose sensing surface are shown where it can be identified the C=O signals at 1600 cm^{-1} , this signal is explained by the insertion of molecules of MDI on the surface of cellulose. A representation of chemical nature of surface is shown in the Figure 1B. Thus, surface of modified cellulose is basically formed by isocyanate groups anchored to cellulose surface by urethane bonds. As it is expected, membrane surface is not affected and cellulose sensing surface corresponds with some porosity degree (Figure 1C).

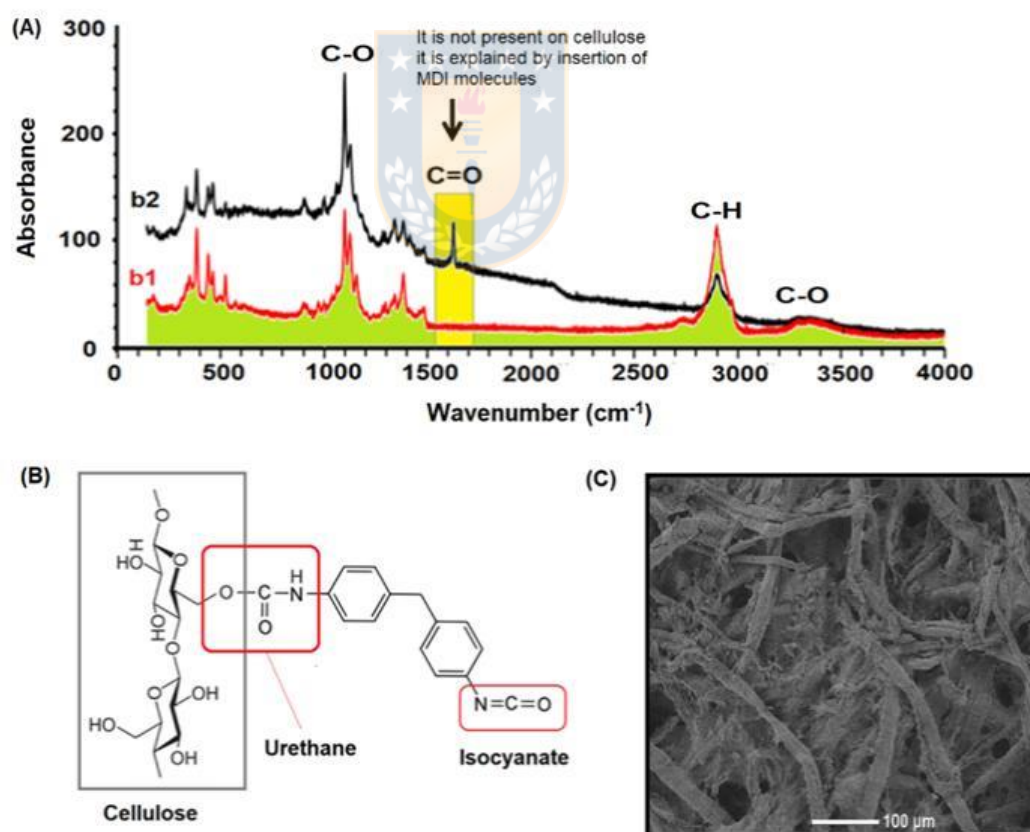


Figure 1. (A) AFM-Raman spectra of cellulose membrane and cellulose sensing surface (b1 and b2, respectively), (B) illustration of chemical structure of cellulose sensing surface and (C) SEM image of surface.

4.2 Verification of *H. pylori* biolayers

The verification of *H. pylori* strains was verified by Gram staining (see Figure 2A) and the forming of biolayer by SEM (Figure 2B). It can be seen that bacterium cells have a bacillar form instead of coccoid shape. In consequence, it was verified that the pathogenic morphology of bacterium was analyzed in the next experiments. The above is relevant due to molecular composition of coccoid and bacillar states is not the same, and in consequence, the coccoid shape is not useful for the aim proposed.

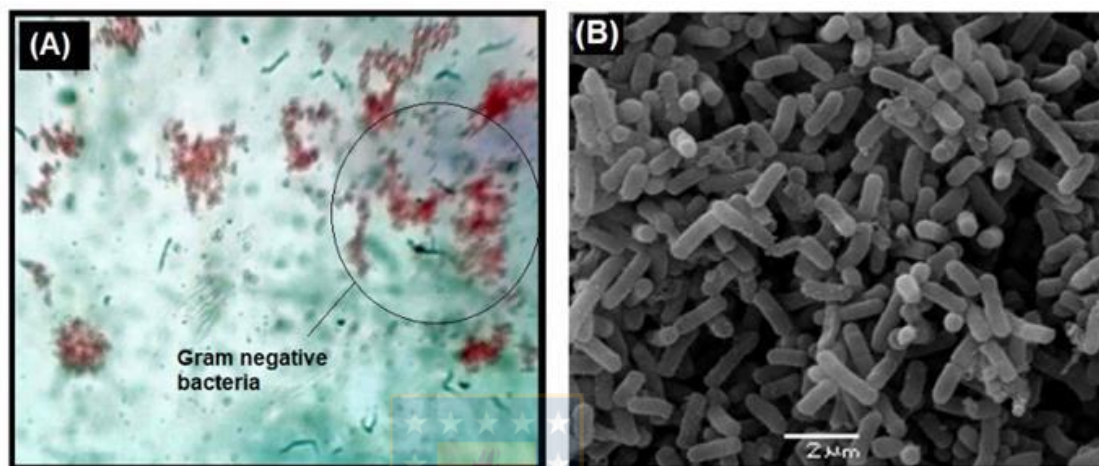


Figure 2. (A) photo of Gram staining of *H. pylori* strains and (B) SEM image of *H. pylori* on the cellulose sensing surface.

4.3 Reproducibility of IR spectra and effect of the noise

During FEDS analysis the first step is the verification of quality of spectra in term of reproducibility followed of elimination of end spectrum noise. Since there is not previous experiments of FEDS transform which can used as reference parameters, the reproducibility analysis of spectra is very important stage. In this way, in the Figures 3A and 3B are shown the IR spectra for the target strains of *H. pylori*. It can be observed that spectra are very similar for both *H. pylori* strains. In addition, regions with relatively high residual noise is evidenced (see Figure 3C). As example, a comparison of FEDS transformation applied to mean working spectra with and without smoothing, for *H. pylori* J99, is shown in the Figure 4. It can be concluded that, when FEDS transform is applied without the use of smoothing tool ABSF the results are not satisfactory due to many signals are observed; by contrast, when ABSF with $N = 20$ was performed, the main signals remaining in the spectrum in a manner consistent with the IR spectrum.

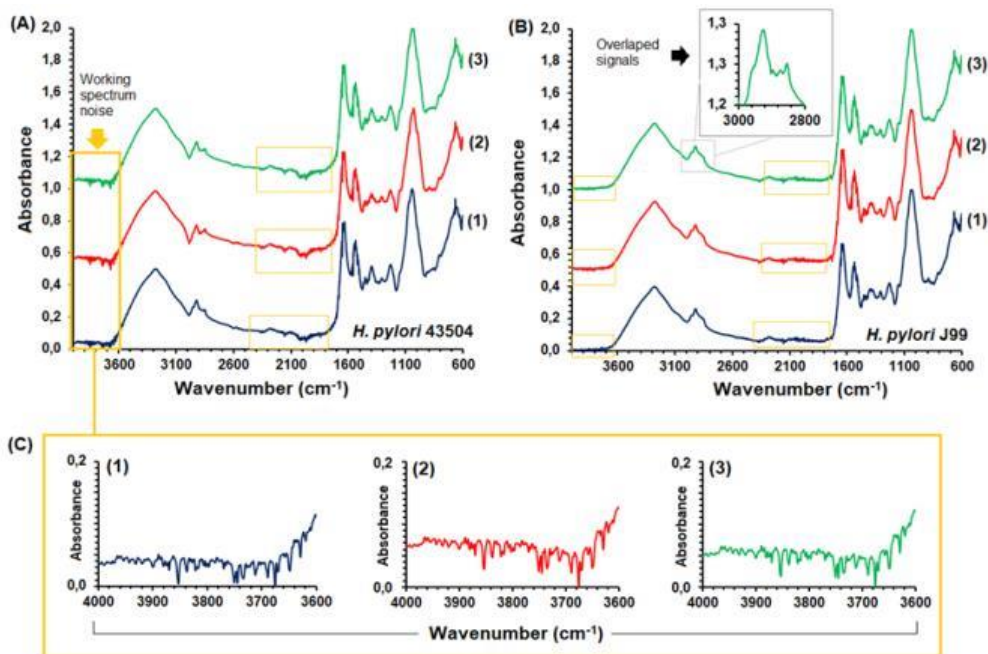


Figure 3. Mid-IR spectra of *H. pylori* strains: 43504 (A) and J99 (B), and illustration of end spectrum noise (C) for region between 3600 and 400' cm^{-1} (1, 2 and 3 indicates the respective replicates).

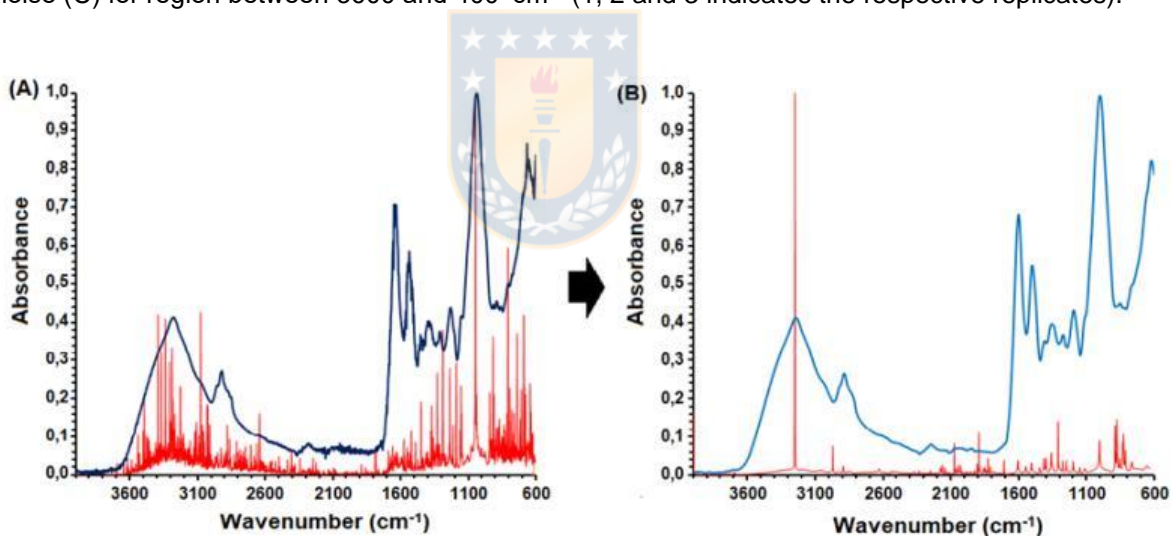


Figure 4. Illustration of effect of the use of FEDS transform without to perform the minimization of residual noise.

But also, after to apply the ABSF algorithm, an adequate reproducibility of FEDS spectra was obtained in all cases. An illustration of excellent correlation obtained between the replicates of *H. pylori* J99 is shown in the Figure 5A. However, though reproducibility is adequate, it is recommended the obtaining of corresponding mean spectrum in order to obtain conclusions with greater statistical significance. Also, it is observed that some signals are strongly decreased in intensity hindering its direct observation.

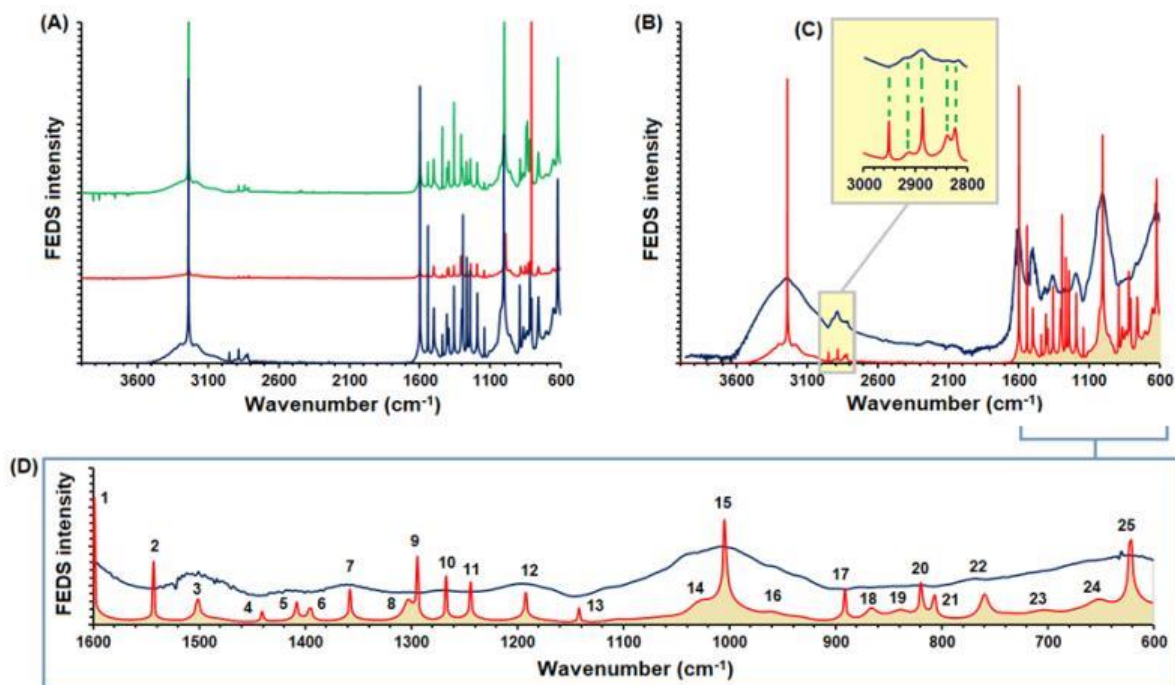


Figure 5. (A) Illustration of reproducibility of FEDS transform applied to mid-IR spectra of *H. pylori* J99 after to application of ABSF algorithm with $N = 20$, (B) comparison of FEDS transform of averaged spectrum of *H. pylori* J99 and its respective averaged IR spectrum, (C) correlation of FEDS and IR signals in the range from 3000 to 2800 cm^{-1} and (D) identification of signals obtained by FEDS transform in the range from 1600 to 600 cm^{-1} compared with the respective mid-IR spectrum.

Since FEDS intensity is not directly related with absorbance or with concentration, a high FEDS intensity should not be interpreted as greater or lesser number of functional groups on the surface. In addition, it is evidenced that a correct application of FEDS should produce a FEDS spectrum with one or more coincident signals, in consequence, it is suggested that, as first step during analysis of FEDS spectrum, direct comparison with its corresponding IR spectrum should be performed (see Figures 5B and 5C). Finally, in the Figure 5D an expansion of region among 1600 and 600 cm^{-1} is shown. Note that, with $N = 20$, FEDS spectra, between 1600 and 600 cm^{-1} , 25 signals are identified whereas from IR spectrum 9 signals strongly overlapped are observed.

4.4 Generalized description of signals

An important aspect determining the effectivity of analysis it is the correct differentiation of signals. Therefore, these have been classified in two main types: (i) 'true' signals associated with relative maximum values (signals-d) and (ii) 'apparent' signals associated with relative minimum values (signals-k). Here, it is suggested the use of **d** and **k** in order to avoid confusions, however, there is not no formal reason for this designation. Note that, between

1600 and 600 cm^{-1} , in this specific case, 25 signals were identified, where $d + k = 25$ being d and k the number of **d** and **k** signals, respectively. By direct observation of spectra, this question can be easily resolved (see Figure 6). Thus, it can be concluded that values for this example are $d = 17$ and $k = 8$.

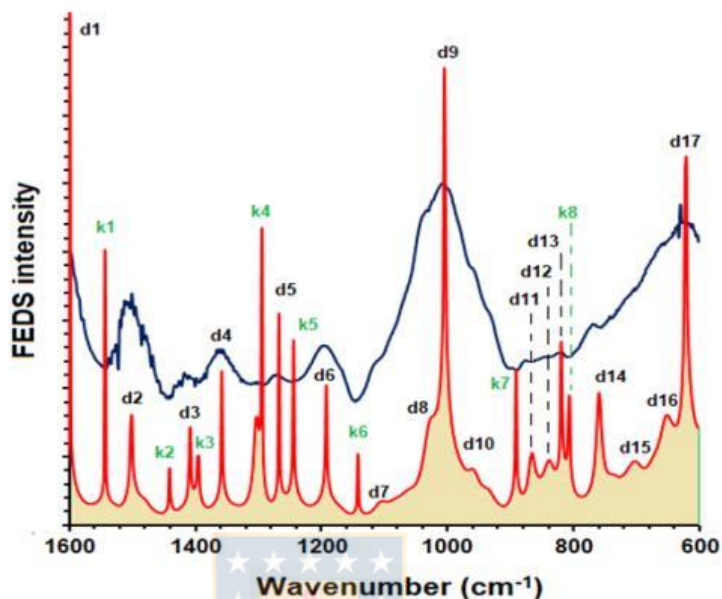


Figure 6. Assignment of signals **d** and **k** for *H. pylori* 43504 spectrum.

An important aspect related with the signal-**d** and signal-**k** is that a better correlation of different spectra could be performed because the spectral comparison is based on two types of signals. In addition, displacements can be analyzed respect to signals-**k** and not only respect to wavenumber associated with each signal being an alternative to ease the spectral analysis. Another characteristic aspect of signal-**k** is that these signals are overlap signals, and therefore, when two signals are located on each side of the same signal-**k**, it is an evidence of adjacent signals are true signals.

4.5 Analysis of IR spectra of *H. pylori* biofilms

Main signals identified in the IR spectra of *H. pylori* are shown in the Figure 7. In order to ease the analysis FDS of spectra, different analysis windows or spectral ranges, were defined: (A) 4000-3000 cm^{-1} , (B) 3000-2500 cm^{-1} , (C) 2500-2000 cm^{-1} , (D) 2000-1300 cm^{-1} and (E) 1300-600 cm^{-1} . In addition, a summary of the main signals and their chemical nature is shown in the Table 1.

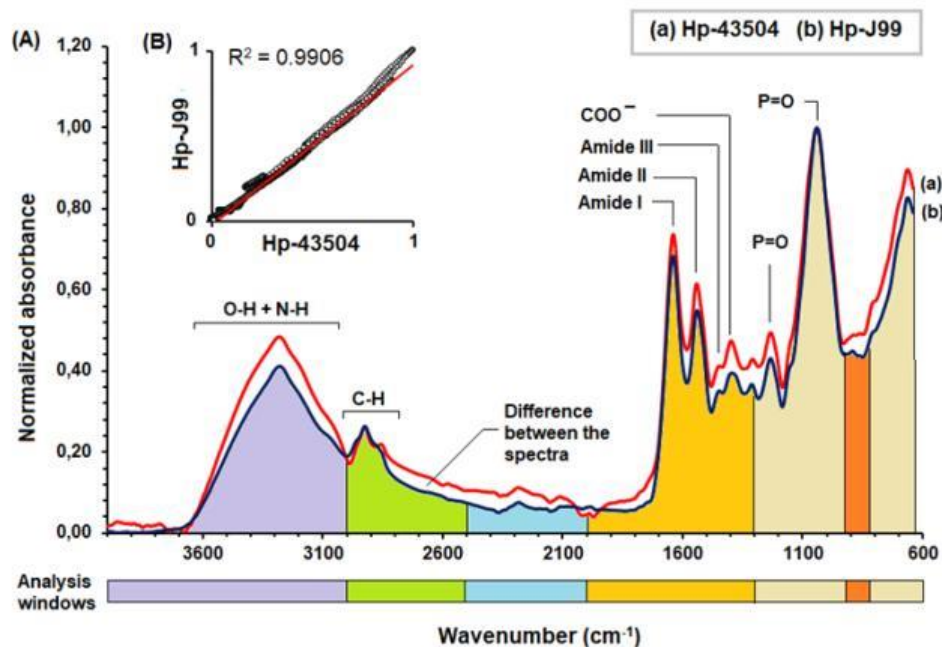


Figure 7. Averaged mid-IR spectra of *H. pylori* strains obtained by ATR technique. (a) *H. pylori* 43504 and (b) *H. pylori* J99.

Table 1. Assignment of main signals observed in the average mid-IR spectrum of *H. pylori* biofilms: ATCC J99 and ATCC 43504

Analysis range (cm ⁻¹)	Wavenumber (cm ⁻¹)	Description
3000 – 4000	No specified	Vibrations associated with O-H and N-H groups. It is not possible to indicate a specific signal due to the overlap. This band is affected by the presence of water, alcohols, amines, etc.
2500 – 3000	2800 – 3000	Vibrations associated with C-H. These vibrations can be C-H of methyl groups, methylene groups or C-H in a ring or cyclic structure.
2000 – 2500	2240 – 2350	Vibration of NCO. This signal is not associated with the bacterial biofilm but that is associated with spectral marker onto support surface.
1300 – 2000	1650	Amide I corresponding to C=O stretching vibration with minor contributions from out-of-phase CN stretching vibration, the CCN deformation and the NH in-plane bending.
	1550	Amide II corresponding to out-of-plane combination of the NH in plane bending and the CN stretching vibration with smaller contributions from the CO in plane bending and the CC and NC stretching vibrations.
	1450	Amide III corresponding to the in-phase combination of NH bending and the CN stretching vibration with small contributions from the CO in plane bending and the C-C stretching vibration.
	1400	Symmetric stretching of carboxylate group observed in several bacteria.
600 – 1300	1240	Vibration of P=O (ν_1). The assignment was based on models for DNA phosphodiester group and by comparison with results of other researchers with different bacteria.
	1050	P=O (ν_2). The assignment was based on models for DNA phosphodiester group and by comparison with results of other researchers with different bacteria.

These signals are similar to those described for diverse microorganisms in several works [20-21, 28-30] and, though important information can be obtained from them, for specific analysis of outer surface of *H. pylori* are not very useful. In addition, it can be seen that for both strains the IR spectra are very similar, being the correlation coefficient (R^2) calculated about 0.9906, in consequence, the differentiating information contained in the spectra is lower than 10 %. By a classic analysis of IR spectra could be concluded that the two strains under study are the same. In consequence, this first analysis permits to establish that it is not possible differentiate the target strains of *H. pylori* using the classic method used for the interpretation of IR spectra. However, it is clear that some signals can be used for the monitoring of the surface changes since these are easy and correctly identified.

4.6 FEDS analysis of *H. pylori* biofilms

In the region from 4000 cm^{-1} to 1300 cm^{-1} , 39 signals-d and 13 signals-k were observed for both bacteria (see Figures 8 and 9). In the region from 4000 to 3000 cm^{-1} is observed the signal associated with N-H vibrations, which is explained by the peptides, proteins or aminoglycosides on the surface of the bacterium.

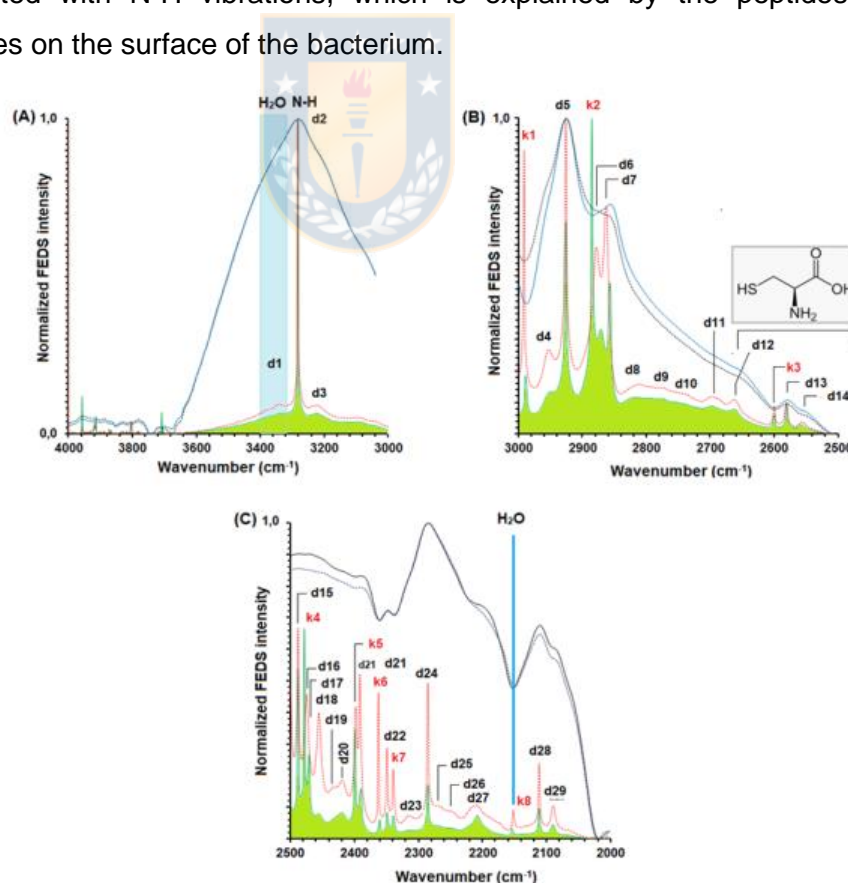


Figure 8. FEDS spectra for averaged mid-IR spectra of *H. pylori* 43504 (Dotted red and black lines) and *H. pylori* J99 (green and black lines, respectively): (A) 4000 - 3000 cm^{-1} , (B) 3000 - 2500 cm^{-1} and (C) 2500 - 2000 cm^{-1} .

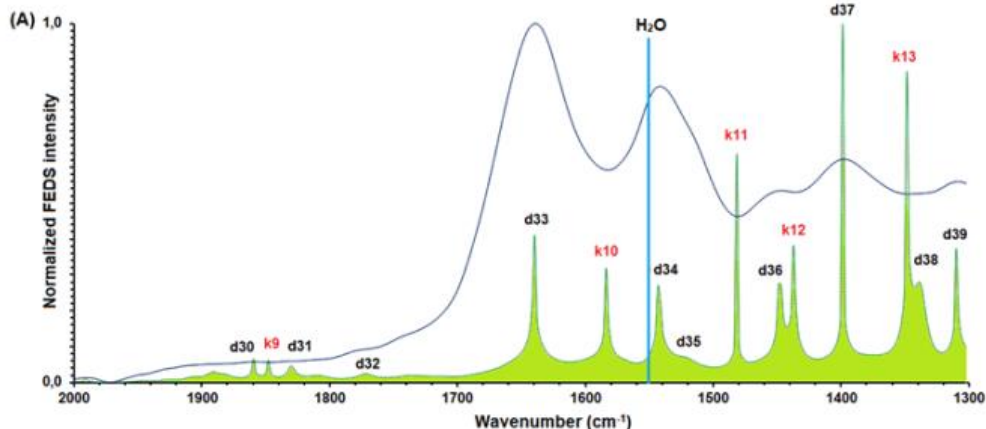


Figure 9. FEDS spectra for averaged mid-IR spectra of *H. pylori* 43504 (Dotted red and black lines) and *H. pylori* J99 (green and black lines, respectively): (A) 2000-1300 cm^{-1} .

Two signals-d are identified as **d1** and **d2** which are associated with similar vibrations of N-H or O-H but with a weaker intensity. The first strategy of analysis is to check the presence of water since it is part of living cell and the dried procedure not necessarily warrants the total elimination of water; for the above, previously-published IR and FEDS spectra of water were used [24, 31-32]; in consequence, by comparison with them, it is suggested that **d1** could be associated with water molecules remains in the external layer.

In order to verify the previous hypothesis, in the spectrum should exist more information related with the presence of water molecules. Thus, for water molecule in liquid phase, in the respective FEDS spectrum, scissor bending at 1550 cm^{-1} and a combination signal at 2150 cm^{-1} has been described; however, it can be seen that, in both spectra, a weak signal at 2150 cm^{-1} is identified to be **k8**, and therefore, since it is defined to be an overlap signal, the presence of this signal cannot be unequivocally associated with water molecules. On the other hand, signal at 1550 cm^{-1} was not evidenced, in consequence, signals **d1** and **d3** were assigned to be OH of alcohols (e.g., glycosides contained in the surface); the above is coherent with the signals FEDS described for low-molecular weight alcohols [24], and with vibrations of O-H groups described for pentoses (ribose, 2-deoxy-D-ribose, arabinose and xylose) [33], for N-acetyl-D-glucosamine [34], and for D-glucuronic acid [34], which are components usually identified in Gram negative bacterium biofilms [33-36]. A summary of main signals is shown in the Table 2.

Table 2. Main signals associate for water [24, 31-32].

Technique	Wavenumber (cm ⁻¹)	Description
IR-spectroscopy	3700-3800	Multiples signals associated with H ₂ O (g) and CO ₂ (g)
	3600 - 3700	Small amount of H ₂ O (l)
	2300 - 2350	Multiples small signals associated with H ₂ O (g) and CO ₂ (g)
	1620 - 1550	Multiples small signals associated with H ₂ O (g) and CO ₂ (g)
	650	Small signal associated with H ₂ O (g) and CO ₂ (g)
FEDS	3060	Asymmetric stretching of H-O-H
	3020	Symmetric stretching of H-O-H
	2150	Combination signal (weak intensity)
	1660	Scissor bending
	1200	No identified and no verified by other sources
	700	No identified

Signals in the region between 3000 and 2500 cm⁻¹ are associated mainly with CH₂ and CH₃ vibrations (from **d4** to **d7**), since these signals are commons for many organic compounds these were considered as no important. However, in IR spectrum, S-H vibrations are difficultly identified, usually one single signal with weak intensity is described. However, in amino acids, and in particular, for cysteine, three signals associated with the S-H group are expected from computational analysis by Density Functional Theory or DFT: ~2560, ~2580 and ~2600 cm⁻¹ [37]. These signals were identified for *H. pylori* 43504 and *H. pylori* J99 at 2550 cm⁻¹ (**d13**), 2580 cm⁻¹ (**d14**) and 2600 cm⁻¹ (**d15**). In addition, for cysteine, a signal associated with N-H vibrations is also identified at 2660 cm⁻¹ corresponding to **d12** [37]; the importance of this signal is that it can be used as a marking signal to facilitate the location of S-H signals during the analysis of spectra. However, it is important to look for more characteristic signals of this amino acid in order to evaluate the coherence in the analysis. Thus, S-H in-plane bending is expected at 1064 cm⁻¹ and C-S stretching at 692 cm⁻¹ [37]. Both signals were identified and named as **d43** and **d52**, respectively (see Figure 10).

The above is coherent with the analysis of outer membrane protein families where have been identified cysteine residues [38], in particular, they worked, among other, with the strain *H. pylori* J99 that is the same strains used by us. In addition, the protein designed HpcA (*H. pylori* cysteine-rich protein A) have been identified to be produced by *H. pylori* gene HP0211, and it is characterized by a molecular weight of 27.3 kDa containing 250 amino acids, of which 14 (5.6 %) are cysteines [39-40]. Other outer membrane proteins characterized by high content of cysteine are HpcC (gene HP1098) and cysteine-rich protein X (HP1117) among other [41-42].

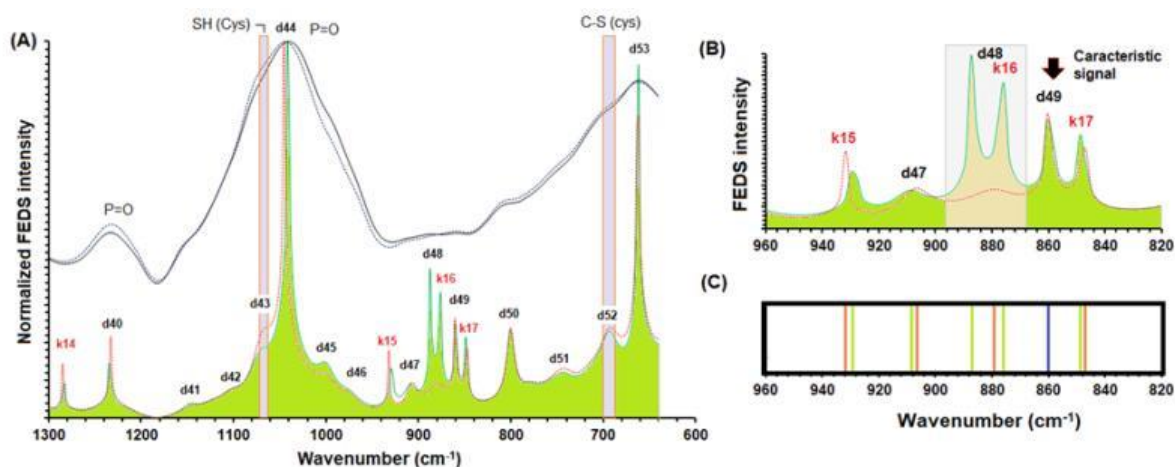


Figure 10. FEDS spectra for averaged mid-IR spectra of *H. pylori* 43504 (Dotted red and black lines) and *H. pylori* J99 (green and black lines, respectively) between 1300 and 600 cm⁻¹ (A) and 960 and 820 cm⁻¹ (B). Comparison of FEDS spectra for bacteria by discontinuous pattern of signals (C).

In the range between 2500 and 2000 cm⁻¹ is expected the signal associated with spectral marker (signal α) (see Table 3). Spectral marker used has units of phenyl isocyanate on its structure, therefore, the analysis was directed toward the identification of signals associated with the group -NCO; thus, signals identified were the vibration of N=C=O at 2285 cm⁻¹ (**d24**) and 2265 cm⁻¹ (**d25**). These signals have been described in the range of 2280-2230 cm⁻¹ [43], and exactly at 2285 cm⁻¹ [44]. One additional vibration of NCO was identified at 2210 cm⁻¹ (**d27**) which have been described in the range 2260-2130 cm⁻¹ [43]. Other four non-fundamental signals are associated with the marker and were satisfactorily identified: 2345 cm⁻¹ (**d22**), 2390 cm⁻¹ (**d21**), 2700 cm⁻¹ (**d11**) and 2870 cm⁻¹ (**d6**) which have been previously described at 2340, 2370, 2700 and 2870 cm⁻¹ [44].

Signals associated with PO₂⁻ groups have been described from the study of ribose-phosphate links at 1230-1244 cm⁻¹ and 1084-1089 cm⁻¹ [45], however, according to the first IR spectrum analysis, these signals were assigned at 1240 cm⁻¹ (**d40**) and 1050 cm⁻¹ (**d44**) which were previously identified in the IR-spectrum (P=O). However, the assignment of signal **d44** should be revised. Note that, from analysis computational of dimethylphosphate, four signals have been described: 1205 cm⁻¹ (P=O asymmetric stretching), 1083 cm⁻¹ (P=O symmetric stretching), 824 cm⁻¹ (P-O asymmetric bending) and 760 cm⁻¹ (P-O symmetric bending), in addition, the same four signals have been obtained for ethylmethylphosphate but with significant displacements [46]. The above suggests that it should not be expected the obtaining of the same positions since the nature of groups linked to phosphate units are very different. In consequence, the results published by Heidari (2016) are expected to be a better comparison with the systems under study. Other researchers have described four signals with

positions very similar to those described by Heidari, these are 1241 cm^{-1} (PO_2^-), 1110 cm^{-1} (PO_2^-), 801 cm^{-1} (OPO) and 751 cm^{-1} (OPO) [28]. In addition, Hidari (2016) also describes two signals at 970 cm^{-1} and 916 cm^{-1} . In consequence, signals assigned were 1235 cm^{-1} (**d40**), 1045 cm^{-1} (**d44**) (taking in consideration that other signals possibly can be associated with **d42**, these are: 970 cm^{-1} (**d46**), 916 cm^{-1} (**d47**), 801 cm^{-1} (**d50**) and 745 cm^{-1} (**d51**).

Signals associated with amine I, amine II, amine III and COO were identified by direct comparison of IR spectra: 1640 cm^{-1} (**d33**), 1540 cm^{-1} (**d34**), 1445 cm^{-1} (**d36**) and 1400 cm^{-1} (**d37**). Finally, it can be seen that a sub-range defined between 820 cm^{-1} and 960 cm^{-1} appears as a characteristic pattern in the spectra. The above is based on: (i) signal **d49** is completely the same in both strains, but at the same time, signals **d47**, **k15** and **k17** appear to be slightly displaced and (ii) two signals in the spectrum of *H. pylori* J99 (**d48** and **k16**) are not identified in the spectrum of *H. pylori* 43504 which shows only one signal (see figure 10B and 10C). The above suggests that it is possible to define a comparison patten in order to discriminate between these microorganisms, however, the above hypothesis should be experimentally evaluated.

Table 3. Main signals associate with group isocyanate on the phenyl isocyanate [43-44].

Technique	Wavenumber (cm^{-1})	Description
IR- spectroscopy	2285	Asymmetric stretching of -NCO
	2210	Stretching of $\text{OC}\equiv\text{N}$
	1448	-NCO
	632	-NCO
	589	-NCO
FEDS ⁽¹⁾	2870	No-fundamental vibration
	2700	No-fundamental vibration
	2390	No-fundamental vibration
	2345	No-fundamental vibration
	2285	Fundamental vibration of -NCO (Asymmetric stretching)
	2265	Fundamental vibration of -NCO (Asymmetric stretching)
	2210	Stretching of $\text{OC}\equiv\text{N}$
1448	Fundamental vibration of -NCO	

(1) FEDS signals described in the table were determined from experimental results and compared satisfactorily with previous publications

5. Conclusions

FEDS transform of IR spectrum is a powerful analytical tool for the improving of analysis of microorganism IR spectra. For correct application of technique, a minimum amount of noise in

the working spectra is required; in addition, reproducibility should be warranted by the implementation of standardized protocols and the use of an appropriate number of samples. On the other hand, results obtained by FEDS demonstrate the capacity of FEDS for the improving of analysis of IR spectra of microorganisms. In the particular case of *H. pylori* strains, it was observed that, by FEDS, is possible the deconvolution of signals, permitting to obtain a better differentiation of them. In this way, it was evidenced that vibrational spectrum of *H. pylori* can be understood considering the main components of outer membrane cell, and therefore, it is concluded that good results in the spectral characterization of *H. pylori* surface can be obtained from IR spectra of individual bacterial components.

Acknowledgments. Sixta Palencia thanks to Conicyt-Chile, Universidad de Concepción (Chile) and Universidad del Valle (Colombia) by the funds for the performing of the project and doctoral scholarship. Authors thanks to Mindtech s.a.s. by the support into acquisition of spectral marker.

Conflicts of interest. The authors declare that they have no conflict of interest.

References

1. S. Phandis, M. Parlow, M. Levy, D. Ilver, C. Caulkins, J. Connors, B. Dunn, *Infect. Immun.*, 64, 905 (1996).
2. M. Chmiela, E. Czkwianianc, T. Wadstrom, W. Rudnicka, *Gut* 40, (1997).
3. A.M. Alkout, C.C. Blackwell, D.M. Weir, I.R. Poxton, R.A. Elton, W. Luman, K. Palmer, *Gastroenterol.*, 112, 1179 (1997).
4. G. Sachs, D. Scott, D. Weeks, K. Melchers, *Trends Microbiol.*, 9, 532 (2001).
5. S.L. Palencia, G. Lagos, A. García, *J. Sci. Technol. Appl.*, 1, 53 (2016).
6. V. Marqués, B. Cunha, A. Couto, P. Sampaio, LP. Fonseca, S. Aleixo, CRC. Calado, *Spectrochim. Acta A: Mol. Biomol. Spectr.*, 210, 193 (2018).
7. H. Zhao, Y. Wu, Z. Xu, R. Ma, Y. Ding, X. Bai, Q. Rong, Y. Zhang, B. Li, X. Ji, *Front. Microbiol.*, 10, 1 (2019).
8. G. Bode, F. Mauch, H. Ditschuneit, P. Malfertheiner, *J. General Microbiol.*, 139, 3029 (1993).
9. B.E. Dunn, N.B. Vakil, B.G. Schneider, M.M. Miller, J.B. Zitzer, T. Peutz. *Infection and Immunology.*, 65, 1181 (1997).
10. M.R. Amievalow, E.M. El-Omar, *Gastroenterol.*, 134, 306 (2008).
11. H. Shimomura, K. Hosoda, S. Hayashi, K. Yokota, Y. Hirai, *J. Bacteriol.*, 194, 2658 (2012).
12. A. Moran. *FEMS Immunol. Medical Microbiol.*, 10, 271 (1995).
13. N. Sabarth, S. Lamer, U.Zimny-Amdt, P.R. Jungblut, T.F. Meyer, D. Bumann. *J. Biol. Chem.*, 277, 27896 (2002).
14. H.H. Tuson, D.B. weibel. *Soft Matter.* 9, 4368 (2013).
15. S. Kumar, A.K. Rai, V.B. Singh, S.B. Rai. *Spectrochim. Act Part A: Mol. Biomol. Spectr.* 61, 2741 (2005).
16. M. Fischer, G.J. Triggs, T.F. Krauss. *Appl Environ. Microbiol.* 82, 1362 (2016).
17. A. Elbourne, J. Chapman, A. Gelmi, D. Cozzolino, R.J. Crawford, V.K. Truong. *J. Colloid Interf. Sci.* 546, 192-210 (2019).
18. F. Abbasian, E. Ghafar, S. Magierowsky. *Bioengineering (Basel).* 5, 1 (2018).
19. A. Alvarez-Ordoñez, D. Mouwen, M. López, M. Prieto, *J. Microbiol. Met.* 84, 369 (2011).

20. J. Ojeda, M. Dittrich in: *Microbial systems biology: Methods and Protocols*, Methods in Molecular Biology, Navid A. Springer Science, 2012, pp. 187-211.
21. J. Prakash, S. Kar, C. Lin, C.Y. Chen, C.F. Chang, J.S. Jean, T.R. Kulp. *Spectrochim. Act Part A: Mol. Biomol. Spectr.* 116, 478-484 (2013).
22. W. Friesen, K. Michaelian, *Appl. Spectr.* 45, 50-56 (1991).
23. T. Vazhnova, D. Lukyanov. *Anal. Chem.* 85, 11291-11296 (2013).
24. M. Palencia, *J. Adv. Res.* 14, 53 (2018).
25. M. Palencia, T. Lerma, N. Afanasjeva. *Eur. Polym. J.* 115, 212 (2019).
26. A. Otalora, M. Palencia, *J. Sci. Technol. Appl.* 6, 96 (2019).
27. L.R. Anaya, K.H. Libreros, V.J. Palencia, V.J. Atencio, M. Palencia. *J. Sci. Technol. Appl.* 6, 96 (2019).
28. Y. Guan, C.J. Wurrey, G.J. Thomas. *Biophys. J.*, 66, 225 (1994).
29. Y. Guan, G.J. Thomas. *Biopolym.* 39, 813 (1996).
30. W. Jiang, A. Saxena, B. Song, B.B. Ward, T.J. Beveridge, S. Myneni. *Langmuir.* 20, 11433 (2004).
31. E. Pretsch, C. Bühlmann, C. Affolter, C. Herrera, R. Martínez, *Determinación estructural de compuestos orgánicos*, Barcelona, Ed. Masson., 2005, 481 p.
32. F.O. Libnau, O.M. Kvalheim, A.A. Christy, J. Toft. *Vibr. Spectr.* 7, 243 (1994).
33. E. Wiercigroch, E. Szafraniec, K. Czamara, M.Z. Pacia, K. Majzner, K. Kochan, A. Kaczor, M. Baranska, K. Malek. *Spectrochim Acta Part A: Molec Biomol Spectr.* 185, 317 (2017).
34. A. Kovacs, B. Nyerges, V. Izvekov. *J Phys Chem.*, 112, 5728 (2008).
35. A. Moran. *FEMS Immunol. Medical Microbiol.*, 10, 271 (1995).
36. A. Moran, In: *Helicobacter pylori: Physiology and Genetics*. Mobley HLT, Mendz GL, Hazell SL (Eds). ASM Press. Washington DC, USA, 2001.
37. S. Parker. *Chem. Phys.* 424, 75-79 (2013).
38. C. Dumrese, L. Slomianla, U. Ziegler, S.S. Choi, A. Kalia, A. Fulujira, W. Lu, D. Berg, M. Benghezal, B. Marshall, P. Mittl. *FEBS. Lett.* 583, 1637 (2009).
39. R.A. Alm, J. Bina, B. Andrews, P. Doig, R. Hanckck, T. Trust, *Infect Immun.*, 68, 4155 (2000).
40. P. Cao, M.S. McClain, M.H. Forsyth, T. Cover. *Infect. Immun.*, 66, 2984 (1998).
41. P.R. Mittl, L. Luthy, P. Hunziker, M. Grutter. *The J. Biol. Chem.*, 275, 17693 (2000).
42. G. Zanottu, L. Cendron. *World J. Gastroenterol.*, 20, 1402 (2014).
43. E. Pretsch, C. Bühlmann, C. Affolter, C. Herrera, R. Martínez, "Determinación estructural de compuestos orgánicos", Barcelona, Ed. Masson., 2005.
44. C.V. Stephenson, W.C. Coburn, W.S. Wilcox. *Spectrochim. Acta.*, 17, 933-946 (1961).
45. A. Heidari, Austin J. *Analyt. Pharm. Chem.*, 3, 1058 (2016)
46. V. Andrushchenko, L. Benda, O. Pav, M. Dracinsky, P. Bour. *The J. Phys. Chem B.* 119, 10682 (2015).

Capítulo VI: Multiple surface interaction mechanisms direct the anchoring, co-aggregation and formation of polymicrobial biofilm between *Candida albicans* and *Helicobacter pylori*

Paper 5:

Multiple surface interaction mechanisms direct the anchoring, co-aggregation and formation of polymicrobial biofilm between *Candida albicans* and *Helicobacter pylori*

Sixta L. Palencia ^a, Apolinaria García ^a, Manuel Palencia ^{b, c*}

^a *Laboratory of Bacterial Pathogenicity, Department of Microbiology, Faculty of Biological Sciences, Universidad de Concepción, Concepción – Chile*

^b *Mindtech Research Group (Mindtech-RG), Mindtech s.a.s., Cali – Colombia*

^c *Research Group in Science with Technological Applications (GI-CAT), Department of Chemistry, Faculty of Natural and Exact Sciences, Universidad del Valle, Cali – Colombia*

Corresponding author: manuel.palencia@correounivalle.edu.co

Journal of Advanced Research

Submitted | ISSN 2090-1232 | www.journals.elsevier.com/journal-of-advanced-research

Multiple surface interaction mechanisms direct the anchoring, co-aggregation and formation of polymicrobial biofilm between *Candida albicans* and *Helicobacter pylori*

Sixta L. Palencia ^a, Apolinaria García ^a, Manuel Palencia ^{b, c*}

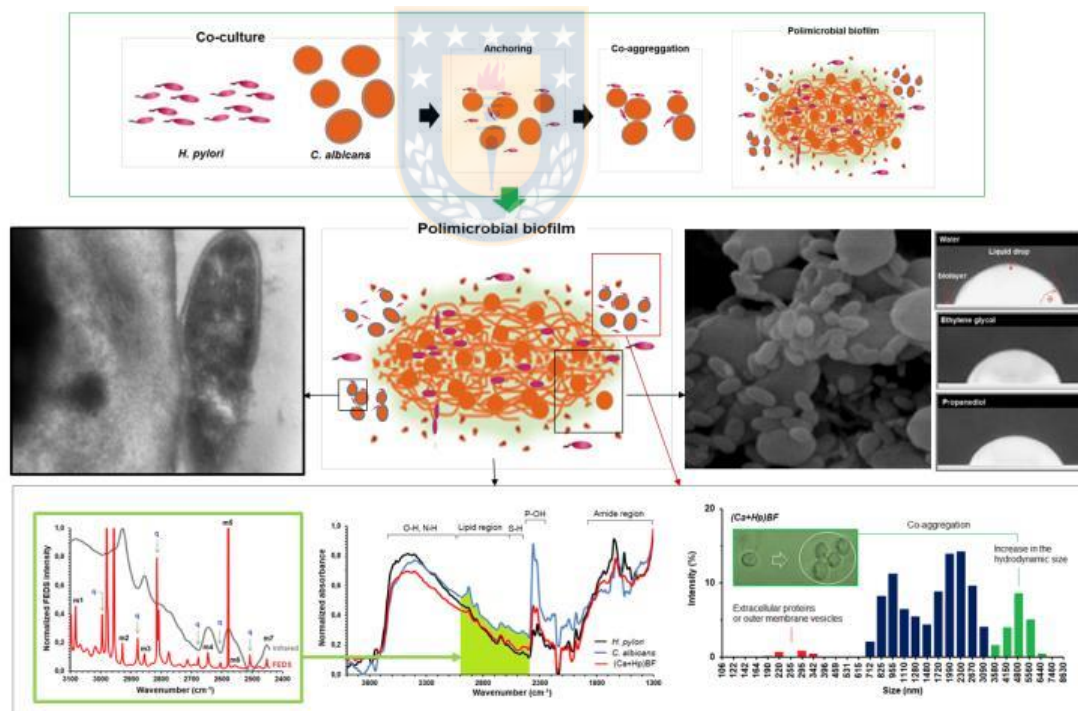
^a Laboratory of Bacterial Pathogenicity, Department of Microbiology, Faculty of Biological Sciences, Universidad de Concepción, Concepción – Chile

^b Mindtech Research Group (Mindtech-RG), Mindtech s.a.s., Cali – Colombia

^c Research Group in Science with Technological Applications (GI-CAT), Department of Chemistry, Faculty of Natural and Exact Sciences, Universidad del Valle, Cali – Colombia

Corresponding author: manuel.palencia@correounivalle.edu.co

Graphical abstract



Abstract

Polymicrobial biofilms have a significant impact on pathogenesis of infectious microorganisms. Many human diseases are affected by colonization of multi-species communities affecting negatively the treatments and increase the risks for the health. In

particular, co-existence between *C. albicans* and *H. pylori* has been described from stomach, a synergistic effect on ulcer pathogenesis has been proposed for several researchers. The objective of this work was to advance in the understanding of surface interaction between *H. pylori* and *C. albicans* for the formation of polymicrobial biofilms. Studies of microbial surfaces both bacterium, yeast and mixtures of them were carried out by infrared spectroscopy, deconvolution analysis, transmission and scanning electron microscopies and optic microscopy. Additional methods were used to contrast the results as dynamic light scattering, contact angle, agarose gel electrophoresis and gene amplification. Results evidenced that multiple surface interaction mechanisms direct the anchoring, co-aggregation and formation of polymicrobial biofilm between *C. albicans* and *H. pylori*: (i) hydrophobic interactions between non-polar peptide chains and lipid structures, (ii) hydrogen bonds between surface components of yeast and bacterium and (iii) thiol-mediated surface interactions. Evidence of internalization and electrostatic interactions were not evidenced. In addition, it is concluded that mixed system is forming from co-aggregation stage later to anchoring of *H. pylori* on the surface of *C. albicans*.

Keywords: *C. albicans*, *H. pylori*, co-aggregation, polymicrobial biofilm, Functionally-Enhanced derivative spectroscopy, surface properties

INTRODUCTION

Bacteria and fungi often are found in the same microhabitats forming dynamic communities known as polymicrobial biofilms. Thus, physical, chemical and biological interactions between these microorganisms can occur and play a key role in the functioning of numerous ecosystems, including bio-geo-chemical cycles in the soils, rhizospheric microhabitats of plants or impacting the health and diseases of plants and animals (Brogden and Guthmiller 2005; Deveau *et al* 2018). In humans, in the absence of disease, bacteria and fungi are usually found on cutaneous and mucosal surfaces as skin, oral cavity, gastrointestinal tract and reproductive tract (Peleg *et al* 2010; Peters *et al* 2012; Krüger *et al* 2019). In addition, several studies indicate that secreted molecules control many types of interactions between bacteria and fungi depending on the population density (Peleg *et al* 2010), but also, besides biochemical relations, physical interactions between bacteria and fungi have been described to be the beginning point for the forming of polymicrobial biofilms, in this way, the contact and aggregation between bacterial cells and yeast cells are the initial stages for this type of symbiotic association (Peleg *et al* 2010). In order to achieve a conceptual description, it has

been suggested to divide bacterium-fungi interactions in four classes: (i) antibiosis involving metabolite exchange, (ii) signaling and chemotaxis involving metabolite sensing and conversion, (iii) physicochemical changes followed by adhesion and (iv) protein secretion (Arvanitis *et al* 2015; Allison *et al* 2016; Deveau *et al* 2018). However, independently of classification used, the understanding of nature and mechanism of interactions is an important tool for the design of new strategies of treatment in the case of diseases produced by pathogens.

Candida albicans (*C. albicans*) is an opportunistic pathogenic yeast forming part of the human gut flora; however, it becomes a pathogenic microorganism in immunocompromised individuals under a variety of conditions, but also, from medical and economic overviews, it is a serious public health challenge due to its negative impact as consequence the high mortality rates and significant increase of care and hospitalization costs (Romeo and Crisen, 2009; Sardi *et al* 2013). It has been described that the *Candida* pathogenicity is eased by a number of virulence factors, being the adherence to tissues and medical devices the most important factors. In concordance with the above, *C. albicans* produces physical and chemical changes on the environment by formation and secretion of hydrolytic enzymes, as proteases, phospholipases and hemolysins, but also, by the presence of surface adhesins, *C. albicans* is able to bind amino acids and sugars on other surface, including the forming of polymicrobial biofilms (Pfaller and Diekema 2007; Lai *et al* 2012; Sardi *et al* 2013). Studies performed have evidenced that enhanced-bacterial virulence of *C. albicans* is resulting of interaction with *S. aureus* and *E. coli* (Peleg *et al* 2010). In addition, interactions between *C. albicans* and *Pseudomonas* spp, *Acinetobacter baumannii*, *Lactobacillus rhamnosus*, and *Staphylococcus epidermidis* are well-known and have been extensively described (Adam *et al* 2002; Gaddy *et al* 2009; Peleg *et al* 2010; Allison *et al* 2016; Ribeiro *et al* 2017).

On the other hand, *H. pylori* is a Gram-negative pathogenic bacteria colonizing the stomach and is estimated that ~ 50% of the human population is affected by it (Mahnaz *et al* 2015). *H. pylori* is adhered mainly to the gastric mucosa by various efficiently specialized mechanisms and is able to survive the adverse conditions in the stomach, such as acidity, peristalsis, nutrient availability, innate and adaptive immunity of the host and competing microorganisms, among others (Cover and Blaser 2009; Graham and Miftahussurur 2018). In addition, *H. pylori* can be considered as part of the transient human gastric microbiome since it is able to stay decades interacting with the gastric mucosa without causing harm to the host (asymptomatic carriers) (Nardone and Compare 2015). However, the presence of *H. pylori* is associated as a predisposing factor for the development of gastric pathologies such as gastritis, peptic ulcers, non-cardiac gastric adenocarcinoma and gastric MALT lymphoma

(Atherton 2006). Since 1994 it was recognized by the International Agency for Research on Cancer and the World Health Organization (WHO) as a category I carcinogen (Hsu *et al* 2007), therefore, the understanding of factors affecting its virulence and prevalence is an important goal to advance in the control and treatment.

Though *C. albicans* is present in some parts of the gastrointestinal tract, e.g., mouth, pharynx, and colon, it is not usually found in the esophagus, stomach, and small intestine though these are a way of passage for the yeast (Karczewska *et al* 2009; Allison *et al* 2016). However, *in vitro* studies has evidenced the ability of *C. albicans* to grow in an environment of pH = 2.0 and colonize *H. pylori*-associated gastric ulcers (Karczewska *et al* 2009; Allison *et al* 2016 *et al* 2016; Massarat *et al* 2016; Sánchez *et al* 2020). In consequence, it is evident that some type of efficient mechanism coexistence and adapting of *C. albicans* to survive at the low pH of stomach should be acting (Karczewska *et al* 2009) (see Figure 1). Recently, it has been proposed that *C. albicans* and *H. pylori* could interact by internalization of bacterium inside of yeast which acts as vehicle in bacterial transferring. However, the understanding how this interaction occurs is still a matter of debate since the specific information is very scarce, in fact, this internalization mechanism between *H. pylori* and *C. albicans* is not accepted by some researchers (N. Alipour 2017) and supported by others (Siavoshi and Saniee 2014; Siavoshi and Parastoo 2018)

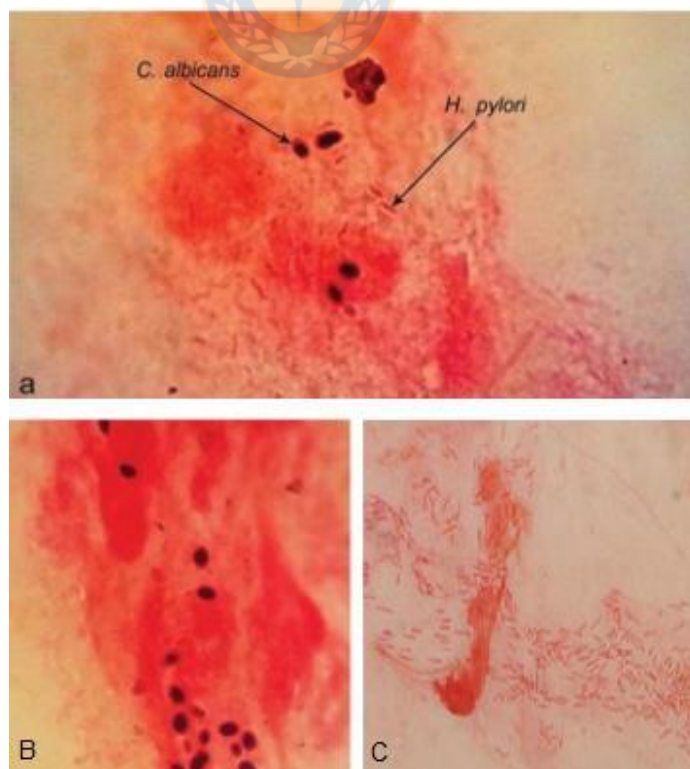


Figure 1. Microscopic observation of *H. pylori* and *C. albicans* in gastric biopsies from patients with gastritis: (a) simultaneous concurrence from *H. pylori* and *C. albicans*, (b) cell of *C. albicans* and (c) *H. pylori*.

bacillar form *H. pylori* (Image adapted from S. Massarat, P. Saniee, F. Siavoshi, R. Mokhtari, F. Mansour-Ghanaei, S. Khalili-Samani, Front Microbiol 2016, 7, 801; Copyright © 2016 CCBY).

It is well-known that *H. pylori* to colonize the stomach by urease-mediated biochemical processes through which creating alkaline micro-domains in the affected zones (Garcia *et al* 2014; Yonezawa *et al* 2015; Hathroubi *et al* 2018). Thus, in presence of *H. pylori*, some part of stomach should be better places for the growth of *C. albicans*, in consequence, *C. albicans* has a new proliferation niche as result of bacterial infection, which inevitably negatively impacts the success of treatment of bacterial gastric ulcers, but also, this coexistence could have implications for the adaptability of *H. pylori* in exgastric environment, their prevalence and pathogenicity. Additionally, *in vitro* and *in vivo* evidence of *H. pylori* biofilm formation in gastric and exgastric environments and the subsequent increase of resistance to antimicrobial agents have been described (Garcia *et al* 2014; Yonezawa *et al* 2015; Hathroubi *et al* 2018). However, studies of polymicrobial biofilms between *C. albicans* and *H. pylori* have not been previously published. The objective of this work was to advance in the understanding of surface interaction between *H. pylori* and *C. albicans* for the formation of polymicrobial biofilms.



EXPERIMENTAL SECTION

Microorganisms strain and growing conditions

***C. albicans* strain: ATCC 90028:** *C. albicans* ATCC 90028 was used as a yeast model. *C. albicans* strain was grown by inoculating in tryptic soy broth (TSB) (Invitrogen, Carlsbad, CA, USA) and standardized to 0.5 in the Mc-Farland scale by absorbance measurements at 625 nm using turbidity standards prepared from BaCl₂ solution (0.048 molL⁻¹) and H₂SO₄ (0.18 molL⁻¹). Later, sub-samples of yeast were separately inoculated in agar Müller-Hinton incubating for 24 hours at 37 °C. Gram stain was performed when the yeast growth was evidenced.

***H. pylori* strain: ATCC 43504:** *H. pylori* ATCC 43504 (American Type Culture Collection, USA) was used as bacterial model. *H. pylori* strain was grown by inoculating in Columbia agar plates (Oxoid, England) supplemented with 7 % horse blood and incubated under microaerobic conditions in the presence of 5 % O₂, 10 % CO₂ and 85 % N₂ at 37 °C for 4 days. Bacterial growth was standardized to 0.5 in the Mc-Farland by analogous procedure to that described for *C. albicans*, and verified by Gram stain, urease test and SEM (Phenom PRO X, ThermoFisher Scientific).

***C. albicans* and *H. pylori* mixtures:** Microbial mixtures, (Ca+Hp) BF, were made from the suspensions of bacteria and yeasts previously standardized. For the preparation of yeast and bacterial suspensions, colonies of *C. albicans* and *H. pylori* were dispensed separately in 50 ml of sterile physiological serum, until to obtain a homogeneous suspension. Afterward, the dispersions were standardized to correspond to 1×10^8 CFU/ml by the quantification of scattered-light intensity at 600 nm, using UV-vis spectrophotometry; then, a mixture of suspensions was performed using a 1:1 volume ratio.

Preparation of microorganism suspensions: For the preparation of yeast and bacterial suspensions, colonies of *C. albicans* and *H. pylori* were dispensed separately in 50 ml of sterile physiological serum, until to obtain a homogeneous suspension. Afterward, the dispersions were standardized to correspond to 1×10^8 CFU/ml by the quantification of scattered-light intensity at 600 nm, using UV-vis spectrophotometry; then, a mixture of suspensions was performed using a 1:1 volume ratio. After, aliquots of suspension mix were prepared in Eppendorf tubes (10 μ l) and were inoculated in BHI broth, incubating at 25, 30 and 37 °C for 48 hours under aerobic conditions. These tests were performed in triplicate. Microscopic observations of suspension mixes were performed and captured in digital format for its posterior analysis.

DNA extraction, gene amplification and electrophoresis

DNA extraction was performed using the UltraClean® Microbial DNA Isolation kit (M.O. BIO, USA), according to the manufacturer's instructions. Microbial cells are re-suspended in MicroBead solution (microspheres dispersion), followed by lysis solution. Thus, the cellular components that are lysed by centrifugation are separated. From the lysed cells, the released DNA is bound to a silica Spin Filter. Finally, the filter is washed, and the DNA is recovered in a certified DNA-free Tris buffer. Later, an amplification of the 16s rRNA gene was performed using the Sapphire Amp® Fast PCR Master Mix kit (TAKARA BIO INC, Japan). To each sample into working temperatures, as well as for their respective controls (Samples at temperature 25, 30 and 37 °C, positive control of *H. pylori* was *H. pylori* ATCC 43504 suspension and *Lactobacillus* sp and water were used as negative control, 6.25 μ l of Master Mix, 0.5 μ l of Forward Primer, 0.5 μ l of Reverse Primer, 3 μ l of each DNA sample and 2.25 μ l of PCR grade water were added. Finally, agarose gel electrophoresis was performed (Lonza, USA). Once the gel solidified, 2 μ l of 100 bp run marker (MASTROGEN, USA) in the range between 100 bp to 3,000 bp was added to the last well, then 5 μ l of the amplified samples was added to each well, and it was run the gel at 90 volts for 50 minutes.

Biofilm formation

Microbial biofilms were performed by deposition of individual colonies on ultrafiltration cellulose membranes (1 cm², MWCO: 10 kDa, Millipore, Merck). In order to eliminate residual composition of growth medium on the surface, after forming the biolayer on the support, samples were successively washed with deionized water and dried using a laminar flow oven with temperature control at 40 °C per 12 hours. To warrant this stage, spectra of support and blank experiments, i.e., growth medium without bacterium, were compared with the respective spectra of biofilm samples. Similar procedure was used for mixtures of *C. albicans* and *H. pylori*. In all cases, four replicates were prepared.

Biofilm study by infrared spectroscopy

Recording of spectra: By the use infrared (IR) spectroscopy, average spectra were obtained for biofilms of strains of *H. pylori*, *C. albicans* and (Ca+Hp) BF. Infrared spectra of four replicates were obtained using a spectrophotometer with Attenuated Total Reflectance (ATR) using a ZnSe crystal (IR-Affinity, Shimadzu Co). Each spectrum is recorded by 20 scans from 4000-500 cm⁻¹, with a maximum resolution of 0.5 cm⁻¹. In addition, Michelson interferometer (30° incident angle) equipped with Dynamic Alignment System Sealed interferometer with Automatic Dehumidifier and DLATGS detector equipped with temperature control mechanism were used. Data were extracted in file format .txt in order to carry out the analysis using a spreadsheet.

Selecting of region for spectral analysis: A strong overlap of the signals is expected due to the compositional complexity of the biofilms (Palencia *et al* 2020; Palencia *et al* 2021). A first comparison of differentiation capacity of IR spectra was performed by chemometric analysis using Principal Component Analysis (PCA). To study the biofilms, the region between 3100 and 2400 cm⁻¹ was selected, in this region, signals associated with cysteine units have been previously described for *H. pylori* by FEDS (Palencia *et al* 2020). In particular, *H. pylori* contains cysteine-rich proteins on its external membrane which are associated to disulfide bonds (-S-S-) which can be monitored from infrared spectra in conjunction with deconvolution techniques. Disulfide bonds are important in this research because they have been related with the anchoring of *H. pylori* to surfaces (Moonens *et al* 2017; Hamway *et al* 2020; Palencia *et al* 2020). In addition, in this spectral range, signals associated with invariant structural units can be easily identified, such as CH, CH₂ and CH₃, which can be used as internal markers for the analysis of signal displacements since they are weakly affected by neighboring electronegative groups. However, in multicomponent systems with a strong overlap of

signals, the vibration associated with -SH is often difficult to identify due to the overlap and the weak signal related with the stretching of -SH. In order to achieve an adequate comparative analysis of the biofilms, the deconvolution of the spectra was carried out to achieve a better resolution of signals.

FEDS deconvolution of IR Spectra: To carry out the deconvolution, Functionally Enhanced Derivative Spectroscopy (FEDS) was used. By the use of FEDS is possible to carry out the transformation of the spectrum of the biofilms allowing the construction of “spectral fingerprints” with higher resolution of signals in comparison with IR spectra. Details of this procedure have recently been published previously for *H. pylori* and *C. albicans* using artificial biofilms (Palencia *et al* 2020; Palencia *et al* 2021). Here, the analysis is focused in the building spectral fingerprints of biofilms and polymicrobial biofilms promoted from aqueous environments. Spectral data, both wavenumber (ν) and absorbance (a), were smoothed using Average-Based Spectral Filter (ABSF) with a data window of 3 and 20 cycles; later, self-scaling of data of absorbance was carried out and, finally, self-scaled data are used as in-put data for the deconvolution function permitting to obtain the corresponding FEDS spectra. Details of this procedure have been previously published (Palencia 2018; Garcia-Quintero *et al* 2018; Ojalora and Palencia 2019; Anaya *et al* 2019).

In order to define one standard criterion to identify the occurrence of shifts, considering that small differences are usual in the infrared spectra, spectral resolution defined by two consecutive wavenumbers was $\Delta\nu = 1.93 \text{ cm}^{-1}$, but also, and by FEDS transform a variability around $\Delta\nu \text{ cm}^{-1}$ is unavoidably produced due to differentiation procedure, in consequence, intrinsic variability of signals in FEDS is $\pm 2\Delta\nu \text{ cm}^{-1} = \pm 3.86 \text{ cm}^{-1} \approx \pm 4.0 \text{ cm}^{-1}$. By the above, $\Delta\nu$ lower than $\pm 4.0 \text{ cm}^{-1}$ were assumed to be not significant.

Biofilm study by microscopy: SEM, TEM and optic microscopy

Samples obtained from *C. albicans*, *H. pylori* and (Ca+Hp)BF were analyzed by Scanning Electron Microscopy (SEM) (JEOL 6380LV with resolution of 3.0 nm), Transmission Electron Microscopy (TEM) (JEOL-JEM 1200EXII with resolution of 0.15 nm) and optic microscopy (Nikon Eclipse E600 microscope). Samples were pretreated according to previously published methods: For SEM, chemical fixation was performed with paraformaldehyde, followed of dehydration with acetone, dried at 40 °C in temperature-controlled oven and coated with an ultrathin layer of gold; whereas for TEM, chemical fixation was performed using paraformaldehyde and osmium tetroxide, followed of dehydration with acetone and embedding in EMbed-812.

Size, cell wall thickness and cell volume of microorganisms were obtained from images of SEM and TEM using several size descriptors: Equivalent Sphere Radius (ESR) defined to be the radius of sphere with the same projected area than the object in the image (one-dimensional descriptor), Equivalent Circle Area (ECA) defined to be the area of circle with the same area than object in the image (two-dimensional descriptor) and Equivalent Sphere Volume (ESV) defined as the sphere with the same volume defined by the ECA (three-dimensional descriptor) (Mustard and Anderson 2005).

From optic microscopy videos were recorded using a digital camera DSC-H300 (Sony, 100x of digital zoom and 20.1 megapixels). From video, image sequences were extracted and analyzed. In all cases, image digital analysis was performed using Digital Micrograph 3.7.0 (Gatan Software Team; Gatan Inc., USA).

Study by Dynamic Light Scattering

Size and size distribution of particles in suspension for *H. pylori*, *C. albicans* and (Ca+Hp) BF were obtained using a 90 plus/BI-MAS equipped with Nano-hpp v330 software and detecting of particles from 1 nm to 6 μm . In all cases, measurements were performed in quadruplicate.

Study of surface hydrophilic-hydrophobic properties

To study the hydrophobic or hydrophilic nature of the surface of biofilms, the sessile drop method was used. For this, three testing liquids were deposited, separately, on the surface of the biofilms. The procedure was recorded in video format using a digital camera DSC-H300 (Sony, 100x of digital zoom and 20.1 megapixels). Subsequently, the pictures were extracted for the analysis of the contact angle of the liquid-air-biofilm interface. As working liquids, water, ethylene glycol and propane-1,3-diol were used since they have different polarity. In all cases, measurements were performed in quadruplicate. From contact angles, surface free energy and its components of working liquids, total surface free energy of biofilm was calculated using the van Oss-Chaudhury-Good theory (Palencia 2017; Cavitt *et al* 2020). For calculations software Surface-Q was (Mindtech s.a.s., Colombia).

RESULTS AND DISCUSSION

Study by IR spectroscopy and FEDS

H. pylori DNA mixed with *C. albicans* DNA have been detected from mixed growth between the bacterium and the yeast. This observation has been interpreted as evidence of internalization of *H. pylori* in the inner of the yeast (see Figure 2A and 2C). However, a

mixture of genetic material also is expected if *H. pylori* and *C. albicans* experience a strong surface interaction preventing the complete elimination of *H. pylori* from the growth medium because cell lysis for extraction of DNA is not a selective procedure (see Figure 2B). By experiments of (Ca+Hp) BF samples analyzed by agarose gel electrophoresis was verified the obtaining of mixtures of DNA. However, other hypothesis is related with the release of extracellular DNA from *H. pylori* during the formation of biofilms.

By IR spectroscopy, IR spectra of *H. pylori*, *C. albicans* and (Ca+Hp) BF were obtained (see Figure 2D). A complete analysis was previously published from artificial biolayers (Palencia *et al* 2020; Palencia *et al* 2021); however, in these new experiments from main signals are the same, however, a strong overlap and increase of absorbances was observed below 1300 cm^{-1} . By analysis of principal components was determined that 95 % of variability of *H. pylori*, *C. albicans* and (Ca+Hp) BF spectra can be described by two components. Results evidence that *H. pylori* and *C. albicans* spectra cannot be differentiated whereas (Ca+Hp) BF spectrum showed a great variability in comparison with the spectra of individual organisms (see Figure 2E). The above suggests that derivative deconvolution techniques are an alternative to increase the spectral differentiation without loss information from IR spectra (Palencia 2018).

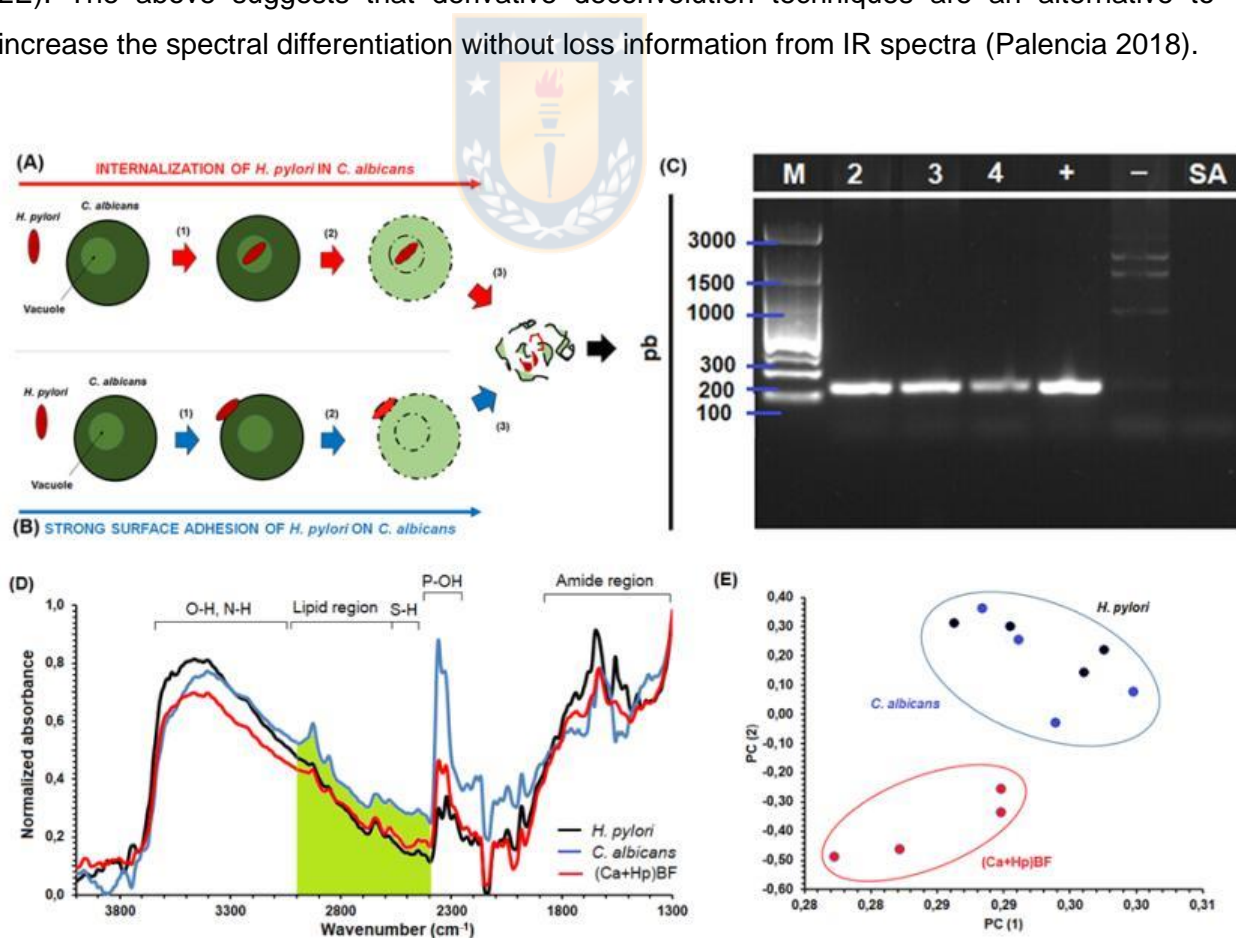


Figure 2. Hypotheses explaining the observation of mixed DNA from mixtures of *C. albicans* and *H. pylori*: (A) hypothesis of internalization and (B) hypothesis of surface anchoring (release of extracellular

DNA has not illustrated). (C) comparison of variability of spectra by analysis of principal component. and (D) IR spectra of *H. pylori*, *C. albicans* and (Ca+Hp) BF

Analysis of IR spectra were performed by three stages: (i) assignment of signals easily identified in the IR spectra from previously published information, (ii) comparison of FEDS spectra of *H. pylori* and *C. albicans* to identify characteristic signals, which can be: signals appearing in each IR and FEDS spectra (c, h and m for *C. albicans*, *H. pylori* and (Ca+Hp)BF, respectively), signals observed at the same wavenumbers from FEDS spectra of individual microorganisms (k), signals observed in only one from FEDS spectra (d), in particular, any shift of signals can be used to identify possible types of interactions associated with functional groups appearing in the spectrum.

Normalized infrared and FEDS spectra, between 3100-2400 cm^{-1} , obtained from biofilms of *H. pylori* and *C. albicans* are shown in Figure 3A and 3B. As it is expected, a strong overlap of signals is evidenced in the infrared spectra. However, seven signals can be identified and easily correlated with their respective FEDS spectra. For *C. albicans* spectrum the signals observed were c1 (3086 cm^{-1}), c2 (2930 cm^{-1}), c3 (2858 cm^{-1}), c4 (2652 cm^{-1}), c5 (2577 cm^{-1}), c6 (2555 cm^{-1}) and c7 (2445 cm^{-1}), whereas for *H. pylori* spectrum the signals observed were h1 (3084 cm^{-1}), h2 (2934 cm^{-1}), h3 (2868 cm^{-1}), h4 (2649 cm^{-1}), h5 (2585 cm^{-1}), h6 (2563 cm^{-1}) and h7 (2450 cm^{-1}). In general, with exception of c1 and h1 significant differences in the wavenumbers were observed. Spectral assignment of signals is summarized in Table 1.

Table 1. Summarize of signals identified in infrared and FEDS spectra of *C. albicans* and *H. pylori*.

<i>C. albicans</i>		<i>H. pylori</i>		Assignment
Signal	ν (cm^{-1})	Signal	ν (cm^{-1})	
c1	3086	h1	3084	Amide B (Fermi resonance between the first overtone of Amide II and N-H stretching)
c2	2930	h2	2934	Asymmetric stretching of C-H in CH_2 and CH_3
c3	2858	h3	2868	Symmetric stretching of C-H in CH_2 and CH_3
c4	2652	h4	2649	NH stretching vibrations of amino acids
c5	2577	h5	2585	SH stretching vibrations
c6	2555	h6	2563	SH stretching vibrations forming hydrogen bonds ($\text{S-H}\cdots\text{NH}_2$)
c7	2445	h7	2450	It could be associated to P-H bonds as result of stress or some metabolic process

Signals **c1** and **h1** were associated to Amide B vibration which is the result of Fermi resonance between the first overtone of Amide II and the N-H stretching vibration; this signal

is expected to be identified in all microorganisms since they contain peptides on their surface (Arrondo *et al* 1992; Arrondo *et al* 1993; Kong and Yu 2007). Signals **c2** and **h2** are associated with asymmetric stretches whereas **c3** and **h3** are associated to symmetric stretches from C-H in CH₂ and CH₃ on the side chains of amino acids such as alanine, aspartic acid or glycine (Barth 2000; Kumar *et al* 2005; Mohamed and Mohammed 2013), fatty acids (Adt *et al* 2006) and metabolites like to N-Acetyl-D-glucosamine (GlcNAc) which is a structural fragment constituting glycosylated proteins and chitin of *C. albicans* (Konopka 2012), but also, lipopolysaccharides in form of phosphorylated glucosamine of *H. pylori* (Leker *et al* 2017). In consequence, **c2**, **c3**, **h2** and **h3** do not provide important information, in term of nature of structural units, for the differentiation of *H. pylori* and *C. albicans* biofilms formed from individually cultures or from mixture of them, however, it is small shifts of signals could be used for the recognition of microorganisms on the surface.

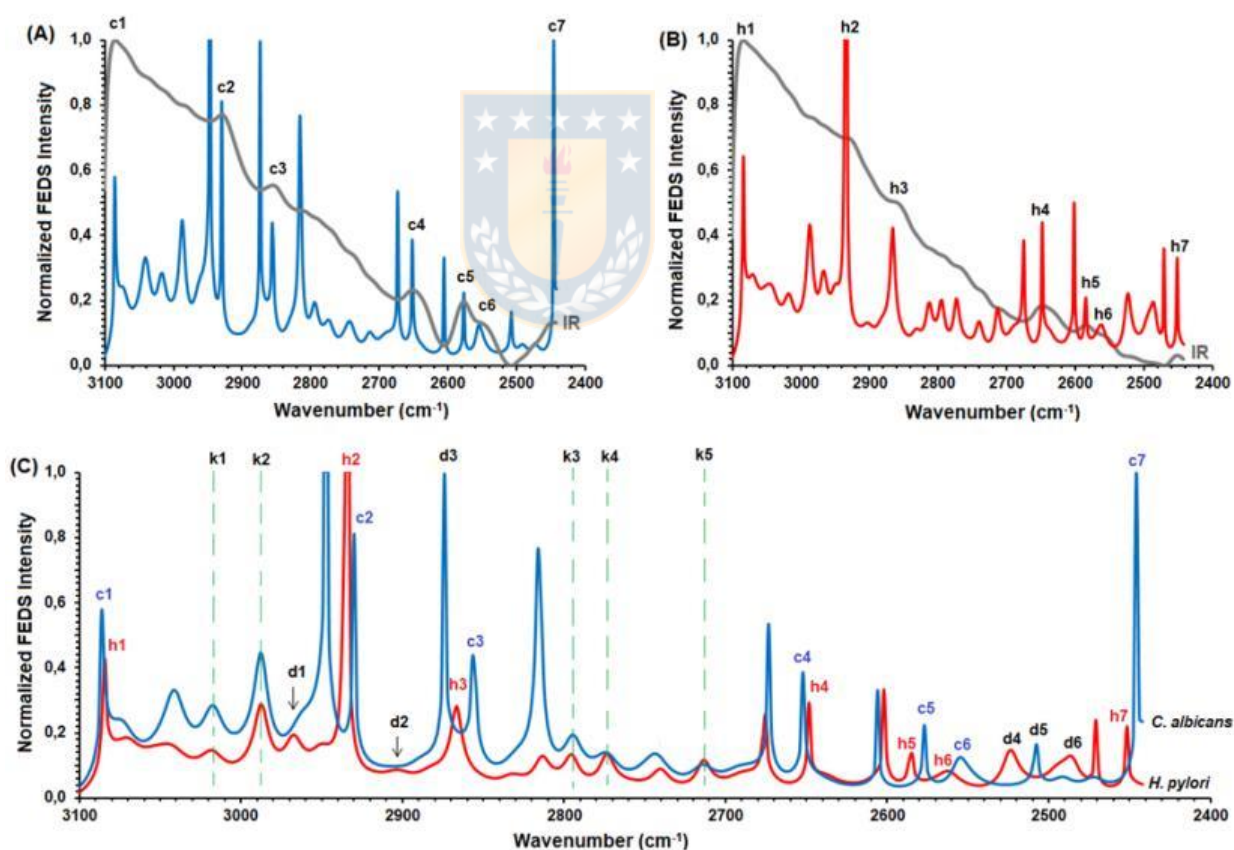


Figure 3. Normalized FEDS spectra of *C. albicans* and *H. pylori* biofilms between 3100 and 2450 cm⁻¹ overlapping with their respective normalized IR spectra, A and B, respectively. Comparison of FEDS spectra is shown in C. Signals **c**, **h**, **k** and **d** denote *Candida*, *Helicobacter*, 'no-shift signal' and 'characteristic signal', respectively.

On the other hand, by density Functional theory or DFT have been predicted for cysteine four signals: five signals associated with SH stretching vibrations (2543, 2545 and 2552 cm^{-1}) and two signals associated to NH stretching vibrations at 2639 cm^{-1} and 2960 cm^{-1} (Parker 2013; Wohlmeister *et al* 2017). Nevertheless, signal at 2960 cm^{-1} was not identified by the strong overlap; **c4** and **h4** were associated to NH stretching whereas **c5**, **c6**, **h5** and **h6** were associated to SH stretching since due to formation of hydrogen bonds these signals can appear between 2600 and 2550 cm^{-1} (Nyquist 2001a). Finally, **c7** and **h7** are not completely explained. However, it is suggested that could be associated with P-H bonds which appear in the range 2410-2442 cm^{-1} (Nyquist 2001b). Some authors have described vibrations of P-OH around 2400 cm^{-1} (Rungrodmitchai 2014). The above can be explained by the surface structures like polyphosphates, phospholipomannan of *C. albicans*, Lipid A 1-Phosphatase of *H. pylori* or others (Bode *et al* 1993; McGrath and Quinn 2000; Tran *et al* 2006; Gannedi *et al* 2020).

On the other hand, when FEDS spectra of *C. albicans* and *H. pylori* are compared several type of signals can be identified. The first set of signals is inherited from IR spectra; these are easily identified by overlaying of FEDS spectra and corresponding IR spectra. An advantage of the FEDS analysis is that, although the FEDS spectra are more complex in terms of the number of signals compared with IR spectra, the main signals of the IR spectra are contained in FEDS spectra and therefore their meaning and interpretation are maintained (see Figure 3C).

A second group of signals, named as **k1-k5**, are situated at exactly the same wavelengths in both spectra. By these signals was possible to corroborate that there is no systematic error in the transformation of the spectra and, consequently, the differences in the wavelengths between equivalent signals allowed to identify the occurrence of shifts of *C. albicans* and *H. pylori* respect to the spectrum of (Ca+Hp) BF. According to their origin, two types of signals are obtained by FEDS deconvolution: (i) signals associated with relative maxima, or primary signals, which are signals from the infrared spectrum directly correlated with the different vibrational modes of the sample components and (ii) signals associated with relative minima, or overlap signals, which do not have a direct relationship with vibrational modes of bonds or structural groups, but they do have a direct relationship with the position of two adjacent primary signals and the degree of overlap between them, therefore, the combination of the primary signals and the overlapping signals allows to define a more specific signal pattern and easier to compare due to the sharp shape of the different signals. It is important to note that overlap signals are not always visible, since for two strongly-overlapping adjacent signals, the signal is hidden below a critical separation distance; in consequence, for correct

separation of overlap signals is necessary the identification of primary signals from respective IR spectra (Otalora and Palencia, 2019).

An important observation from FEDS spectra of *C. albicans* and *H. pylori* is the enormous similarity in the spectral range analyzed. Nevertheless, the greatest differentiation of them is observed between 3000 cm^{-1} and 2840 cm^{-1} , and between 2660 cm^{-1} and 2450 cm^{-1} . Signals associated with these differences have been named to be **d1** (2968 cm^{-1} in *H. pylori*), **d2** (2903 cm^{-1} in *H. pylori*), **d3** (2875 cm^{-1} in *C. albicans*), **d4** (2524 cm^{-1} in *H. pylori*), **d5** (2509 cm^{-1} in *C. albicans*), and **d6** (2487 cm^{-1} in *H. pylori*).

On the other hand, IR and FEDS spectra of (Ca+Hp) BF are shown in Figure 4. It can be seen that the same primary signals identified for *C. albicans* and *H. pylori* can be assigned. Besides, IR and FEDS spectra of (Ca+Hp) BF showed the same signal patterns observed in IR and FEDS spectra for *C. albicans* and *H. pylori*.

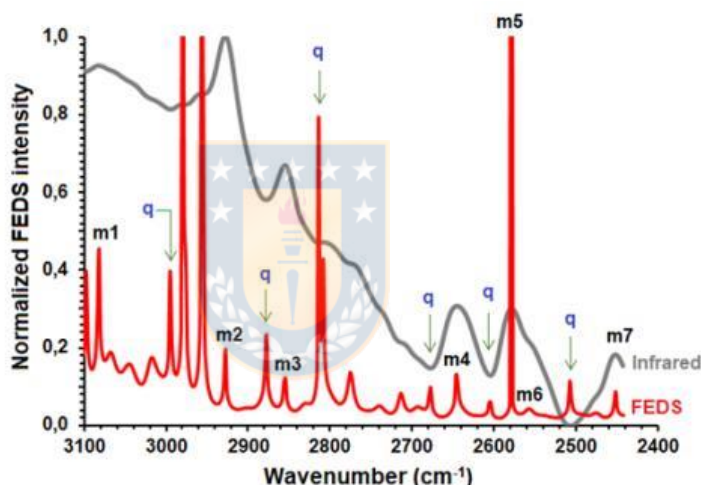


Figure 4. Normalized infrared and FEDS spectra of (Ca+Hp) BF. Signals FEDS associated with relative-minimum absorbance values showing the same patten observed for *C. albicans* and *H. pylori* spectra (q).

Comparison of the FEDS spectra of individual microorganisms and (Ca+Hp) BF is shown in Figure 5. A detailed comparison shows that the (Ca+Hp) BF spectrum is different from that obtained for *C. albicans* (see Figure 5A, 5B and 5C) and *H. pylori* (see Figure 5D, 5E and 5F).

From Figure 5A is observed that $\Delta\nu$ between **c1** and **m1** and between **c2** and **m2** is 2 cm^{-1} , therefore, it is concluded that there is no significant difference between signals. The same was observed between **h1** and **m1** but not between **h2** and **m2** ($\Delta\nu = 7 \text{ cm}^{-1}$) (Figure 5D). Since **c1** and **c2** are associated with C-H bonds of $-\text{CH}_2-$ and $-\text{CH}_3$, which do not form hydrogen bonds due to the relatively low electronegativity of the carbon atom compared with N or O atoms, it is expected that any perturbation of these signals is related with hydrophobic

interactions. However, while **k1** does not change, **k2** is shifted to lower wavenumbers, from 2988 cm^{-1} to 2980 cm^{-1} ($\Delta\nu = 8 \text{ cm}^{-1}$), giving rise to an overlap signal (**q1**). By this line of analysis, the presence of **k2** in the spectra of *C. albicans* and *H. pylori* suggests that **q1** is important to understand the molecular mechanisms promoting the co-aggregation stage for the formation of the (Ca+Hp)BF. One drawback is that this signal is not normally described in infrared studies of complex systems in which the usual practice is to include a set of signals, all associated to C-H stretches, in a wavenumber range. However, it is proposed that the C-H bonds associated with **k2** are not part of aliphatic fatty acid chains characteristic of biological membrane systems but they should be associated with polar structures from proteins or peptide structures. Therefore, bonds associated with O-C-H and N-C-H are candidates for this hypothesis because, in addition to amino acids forming proteins, glycosylphosphatidylinositol proteins (Gpi-P) of *C. albicans* contains units of terminal ethanolamine phosphate (EtAm-P) linked to sugars (Moreno-Ruiz *et al* 2009; Klis *et al* 2009).

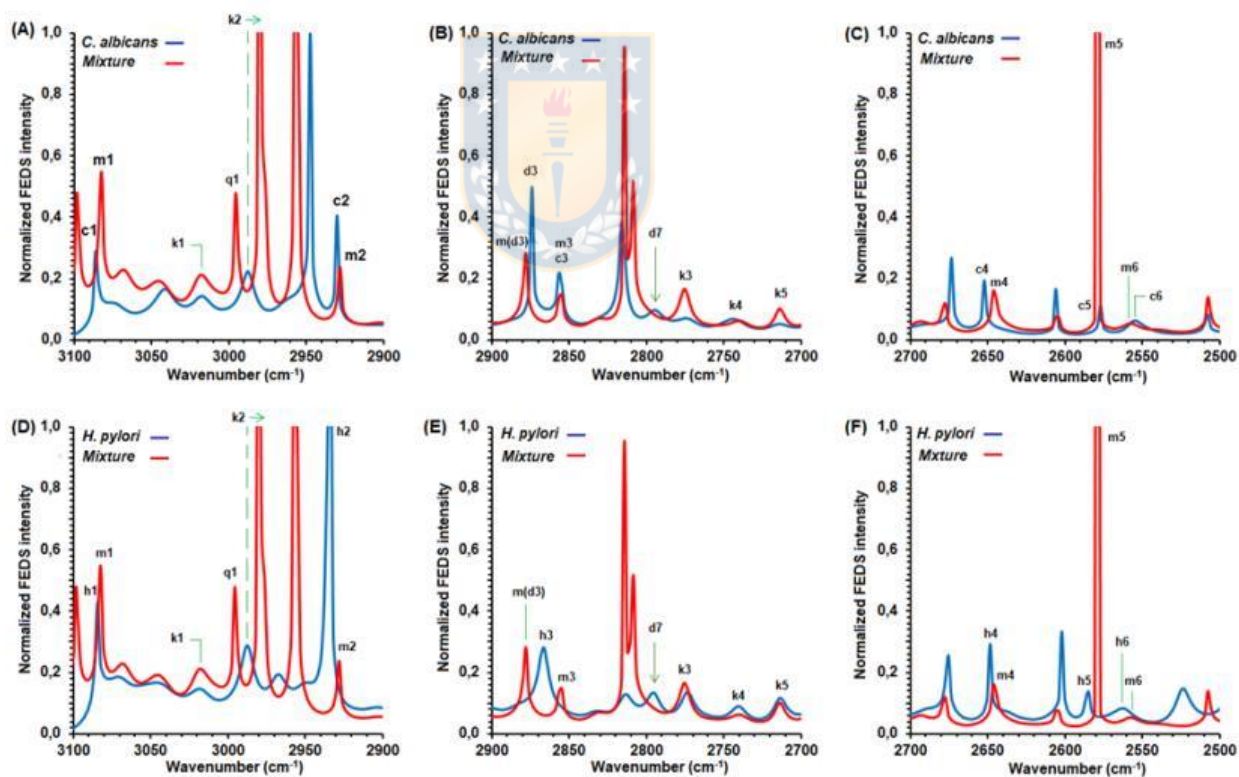


Figure 5. Normalized FEDS spectra of *C. albicans* and (Ca+Hp) BF (A, B and C) and *H. pylori* and (Ca+Hp) BF (D, E, F).

The above is consistent with the composition of cell wall of *C. albicans*, that is constituted by threonine (18.1 %), serine (13.3 %), glutamic acid (10.4 %) and proline (10.1 %), i.e., 51.9 %

of polar amino acids (Ruiz-Herrera *et al.* 1994). However, it is important to note that approximately 33 % of the cell wall of *C. albicans* is made up of non-polar amino acids: leucine (4.2 %), proline (10.1 %), isoleucine (6.1 %), glycine (6.7 %), valine (5.7 %) and alanine (~ 0.5 %) (Ruiz-Herrera *et al.* 1994), but also, it is consistent with the affinity of *C. albicans* to effectively adsorb non-polar aliphatic amino acids (alanine, leucine, and proline) (Hawser and Islam 1998). In consequence, the **k2** shift suggests that a potential route for the co-aggregation of *C. albicans* and *H. pylori* for the formation of polymicrobial biofilms is through hydrophobic interactions between non-polar peptide chains. Similar results are observed in the comparison between the *H. pylori* biofilm and (Ca+Hp) BF (see Figure 5D). Furthermore, the signal associated with C-H vibrations denoted by **h2** is shifted from 2934 cm^{-1} to 2927 cm^{-1} , reaffirming the hypothesis of co-aggregation mediated by hydrophobic interactions. However, it is suggested that these interactions should be through peptide segments of outer non-polar proteins since hydrophilic surface is expected for *H. pylori* from structural analysis of lipopolysaccharides (LPSs). It is well-known that LPSs are the main component of the bacterial cell wall of gram-negative bacteria and the presence of multiple outer membrane proteins described for *H. pylori* (Oleastro and Menard, 2013). Evidence experimental demonstrating an intimate contact at level surface between *C. albicans* and *H. pylori* is obtained from contact angle data, TEM and SEM and is shown and discussed in later sections.

The previous analysis agrees with observations from Figures 5B and 5C. Since the C-H bonds show symmetric and antisymmetric vibrations, if the previous approach is correct, it is expected that the **c3** signal in the *C. albicans* spectrum does not show a significant difference with the **m3** signal of the (Ca+Hp)BF, and at the same time, the **h3** signal should differ significantly of **m3**. From the spectra FEDS, a signal denoted **d3** is identified to the left of **c3**, which for (Ca+Hp) BF was denoted as **m(d3)** to indicate that it is the same signal **d3** but identified in the spectrum obtained from microorganism mixture. This signal corresponds to a relative minimum in the IR spectra, though their identification is easy from the IR spectra of yeast and (Ca+Hp) BF, from spectrum of *H. pylori* is not evident. The small displacement of **d3** to **m(d3)**, $\Delta\nu = 4.3 \text{ cm}^{-1}$, suggests that some type of disturbance occurred producing the modification of IR spectrum, or if preferred, the function of line that describes the spectrum was modified for the perturbation of surface *C. albicans*. This disturbance can be explained by the presence of the bacteria, since the signal associated with the respective vibration, **h3**, is observed at 2867 cm^{-1} ($\Delta\nu = 9 \text{ cm}^{-1}$). Thus, the superposition of the contributions in the spectrum of (Ca+Hp) BF produces a small displacement of the signal due to the widening of **m3** in its respective IR spectrum. A result of great importance is the disappearance of **h3**,

which reaffirms the hypothesis non-polar peptide-mediated hydrophobic interactions. Likewise, signals ranged between 2820 cm^{-1} and 2795 cm^{-1} are associated with N-CH_2 in aliphatic secondary and tertiary amines which are typical of peptides on the surface of microorganisms. In particular, for *C. albicans* spectra, units of EtAm-P should be shows this signal, however, the fact that signal is present in *H. pylori* spectra suggests that it is related strongly with amino acids like Arginine, Lisine, Asparagine or Glutamine.

In consequence, the disappearing of signal at 2795 cm^{-1} (**d7**), both for *C. albicans* and *H. pylori* spectra, is interpreted to be an evidence of a second type of interaction mediated by polar domains associated with C-N-H bonds, in addition to multiples hydrogen bonds resulting of polar domains on surface of microorganisms.

In the Figures 5C and 5F are shown the FEDS spectra of *C. albicans*, *H. pylori* and (Ca+Hp) BF between 2700 cm^{-1} and 2500 cm^{-1} . This spectral region is important because permits explore the possibility of covalent interactions between *C. albicans* and *H. pylori* via formation of disulfide bonds. It can be seen that signal **c4** which is associated with N-H vibrations is displaced to lower wavenumbers ($\Delta\nu = 5\text{ cm}^{-1}$). In addition, $\Delta\nu = 2\text{ cm}^{-1}$ when **h4** is compared with **m4**. This suggests the possibility of peptide-mediated interaction between *C. albicans* and *H. pylori*. Though this signal can be assumed to be a direct contribution of *H. pylori*, it should be noted that whereas spectra of *C. albicans* and (Ca+Hp)BF show the same signals for wavenumber lower than 2610 cm^{-1} , spectra of *H. pylori* and (Ca+Hp)BF are very different with multiple displacements. In consequence, a third interaction is possible by the hydrogen bonds (e.g., -S-H, NH_2 - or -S-H, O=CO-) and disulfide bonds which can be formed spontaneously under alkaline conditions ($-\text{SH} + -\text{SH} \rightarrow -\text{S-S-}$). The previous interaction mechanisms are possible due to the presence of cysteine-rich outer membrane proteins and extracellular urease on the surface of *H. pylori* (Krajewska 2009; Kao *et al* 2016) and the presence of cysteine on the surface of *C. albicans* (2.7 %) (Oleastro and Menard 2013).

From infrared analysis is shown that at least three possible interactions routes are possible between *H. pylori* and *C. albicans* to form polymicrobial biofilm: (i) hydrophobic interaction between peptide components from cell wall of *C. albicans* and *H. pylori* (mechanism 1); (ii) interaction by hydrogen bonds between polar amino acids from cell wall of *C. albicans* and outer-membrane proteins of *H. pylori*, and between polar domains associated with Gpi-P and LPSs (mechanism 2), and (iii) covalent interaction between thiol groups on the surface of microorganisms (mechanism 3).

In relation with the mechanism 1, it has been reported that the union of alkyl groups to polar groups, e.g., carbonyl, is affected in their vibratory movements as a function of the length of the alkyl chain (Nelson 2016). In this way, for shorter chain length is greater the effect of polar

groups, and conversely, as the chain length increases, the vibratory movements become independent of the influence of polar groups. Therefore, vibration wavelengths will be different for C-H bonds from CH₂ or CH₃ groups depending if they are part of amino acids or EtAm-P; for fatty acids the effect is lower for fatty acids the effect is less and consequently, through the spectroscopic analysis carried out, evidence of disturbance at the level of the lipid bilayer cannot be obtained. Likewise, for amino acids, shifts of wavenumbers would be expected since they have non-polar short chains. Similarly, it has been reported that the displacements of the signals associated with CH bonds are related to molecular packaging (Rommel *et al* 2012; Nelson 2016); thus, a decrease in packing will be associated with greater freedom of movement and consequently greater vibrational energy (displacement of signals at higher wavenumbers) (Rommel *et al* 2012). The above is important because a weakening of the yeast cell envelope of *C. albicans* due to the presence of *H. pylori* could manifest itself in a shift to larger wavenumbers; likewise, a restriction of freedom of movement would be associated with shifts to lower wavenumbers. However, an effect of this nature between microorganisms would only be appreciable if it occurs in a significant proportion of the sample, because the IR technique obtains information and builds the spectrum from the population of microorganisms that constitute it. Since the technique allows the monitoring of microorganisms without practically any disturbance, beyond the drying of the sample, these can have secreted substances for the conditioning of their immediate environment and, consequently, metabolic processes could mask any changes in terms of cell integrity when the concentration of extracellularly-secreted substance is significant. The biofilm matrix of *C. albicans* has been described to be composed of carbohydrates, such as β -glucans and mannan, as well as proteins, lipids, and extracellular DNA, and hexosamines, uronic acid, and phosphorus (Pierce *et al* 2017). But also, protein-protein interaction between *C. albicans* surface and foreign proteins have been described to occur through outer GPI proteins (Moreno-Ruiz *et al* 2009), in consequence, the main contribution is the fact to identify the contribution of non-polar amino acids in the interaction between *C. albicans* and *H. pylori*.

In relation with mechanism 2, formation of hydrogen bonds is the most evident interaction from a molecular point of view due to numerous polar groups on the surface associated with LPSs, outer membrane proteins and Gpi-P. In particular, LPSs of *H. pylori* are composed of three domains: a hydrophobic domain termed lipid A (or endotoxin), non-repeating core oligosaccharide formed by short chain of sugars, which connects the lipid A anchor to O-antigen and can be divided into inner and outer core regions, and a variable outermost polysaccharide (or O-antigen) constituting hydrophilic domain of the LPSs (Leker *et al* 2017). Composition of monosaccharides is very variate, however, different *H. pylori* strains contain

xylose (Xyl), mannose (Man), galactose (Gal), glucose (Glc), heptose (Hep), inositol, and N-Acetylglucosamine (GlcNAc) (Leker *et al* 2017). All component contains hydrogen atoms linked to highly electronegative oxygen, and therefore, multiples hydrogen bonds can be formed. In addition, it has been described that outer membrane of *H. pylori* is composed of LPSs contributing to colonization and persistence in the stomach, it is recognized that LPSs mediate several interactions between the bacterium and its surrounding environment (Li *et al* 2016; Leker *et al* 2017). On the other hand, the cell wall of *C. albicans* is a bilayer structure with an external protein coat consisting mainly of Gpi-Ps; which are often strongly mannosylated and phosphorylated, and are covalently linked to highly-branched β -1,6-glucan molecules linked to internal network of β -1,3-glucan molecules (Moreno-Ruiz *et al* 2009; Klis *et al* 2009; Pierce *et al* 2017). In addition, polypeptide content of the wall is estimated at 2.4–3.3 % (Moreno-Ruiz *et al* 2009).

In relation with mechanism 3, the formation of disulfide links and hydrogen bonds mediated by thiols (-SH) requires the presence of thiolated amino acid chains. It has been suggested that abundant cell wall proteins are interconnected by disulfide bridges, e.g., protein Pga59 and Pga62 which are GPI cell wall protein with cysteine residues, in addition, Pga59 and Pga62 are expressed to much higher levels in biofilms than in planktonic cultures (Klis *et al* 2009) and are required for cell wall integrity (Moreno-Ruiz *et al* 2009). The above is consistent with the observations about effect of N-acetylcysteine on *C. albicans* biofilms (El-Baky *et al* 2014; Santos *et al* 2020). In general, anti-biofilm activity of N-acetylcysteine is based on the breaking of disulfide (El-Baky *et al* 2014; Santos *et al* 2020). But in term of amino acid composition, it has been determined that the content of thiolated amino acids, i.e., cysteine and tyrosine, forming the wall cell are 2.7 and 3.4 %, respectively (Ruiz-Herrera *et al* 1994). In consequence, formation of specific disulfide bonds is low probably though possible. However, results suggest that surface interactions by the interpenetration of outer cell structures implies interactions of hydrogen on S-H with a rich surface in polar atoms. Finally, evidence of electrostatic interaction was not observed because analyzed range not offers information about charged groups.

On the other hand, IR and FEDS analysis by themselves do not allow to establish with total certainty the occurrence of these interactions. One of the main limitations that FEDS is a very recent tool for the analysis of complex biological systems, and therefore, like other deconvolution techniques, additional information is required in order to achieve an adequate interpretation, however, usually the information is not available or has been established through different conditions. In addition, systems studied in this research are characterized to be dynamic with high-variability in function of growth stage or adaptation; in consequence,

differences between planktonic cells and biofilms are expected. For example, whereas for *C. albicans* in planktonic state is characterized by Gpi-Ps and phosphodiester bridges in N-linked carbohydrate side-chains of cell wall proteins, the biofilm matrix of *C. albicans* is composed of carbohydrates, such as β -glucans and mannan, as well as proteins, lipids, and extracellular DNA, and hexosamines, uronic acid, and phosphorus (Pierce *et al* 2017).

The fact that the analysis by FEDS is carried out with practically zero disturbance of the sample allows to contrast between them with high precision suggest that is a promissory alternative to the *in situ* study of microorganisms and biofilms. Therefore, by IR and FEDS analyses can be concluded that the samples described as (Ca+Hp) BF correspond to the polymicrobial biofilm formed by *C. albicans* and *H. pylori*. But also, it is evidenced that in the formation of polymicrobial biofilms between *C. albicans* and *H. pylori*, the yeast domains the extension of biofilm because biofilm of *C. albicans* has a higher similarity with (Ca+Hp) BF, besides, in concordantly with microscopy observations, *C. albicans* acts as surface of anchoring of *H. pylori*. In order to contrast the results obtained in this first part, different experiments are analyzed and discussed in the next sections.

Study by microscopy: SEM, TEM and optic microscopy

Three different microscopy studies were performed: SEM, TEM and optic microscopy. Images of SEM of *C. albicans*, *H. pylori* and (Ca+Hp) BF are shown in Figure 6.

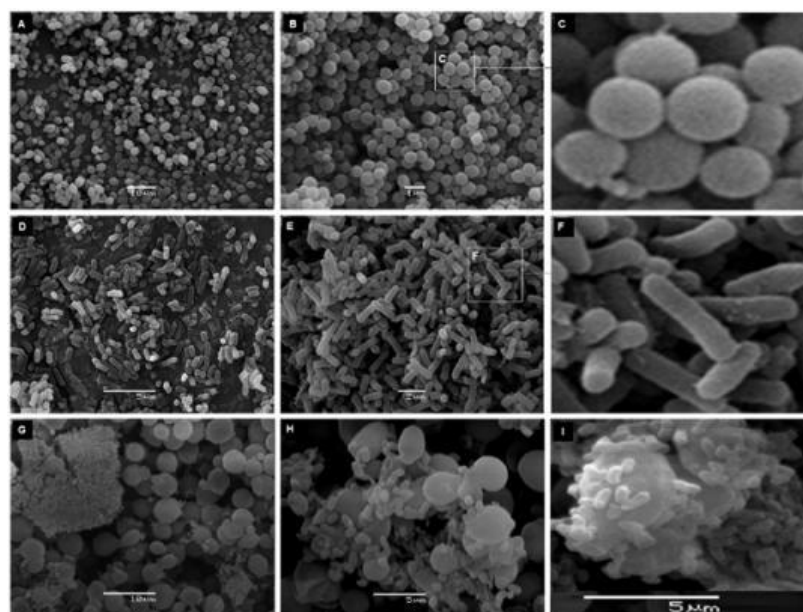


Figure 6. SEM images of *C. albicans* (A, B and C), *H. pylori* (D, E and F) and (Ca+Hp) BF (G, H and I).

In the images 6A, 6B and 6C show the *C. albicans* cells with a quasi-spherical shape and a smooth surface are observed, whereas in the images 6D, 6E and 6F are shown the *H. pylori* cells with bacillar morphology. From images different size descriptors were calculated (see Table 2).

Table 2. Size descriptors for *C. albicans* and *H. pylori* from individual cultures and mixtures.

Culture	Size descriptor	ESR (μm)	ECA (μm^2)	ESV (μm^3)
<i>C. albicans</i>	Mean cell size (S_{Ca})	0.31 ± 0.03	0.30 ± 0.05	0.13 ± 0.03
<i>H. pylori</i>	Mean cell size (S_{Ca})	0.50 ± 0.03	0.79 ± 0.09	0.53 ± 0.09
	$\sigma_1 = S_{Ca} / S_{Hp}$	0.62	0.38	0.24
(Ca+Hp)BF	Mean cell size (S_{Ca})	1.59 ± 0.39	8.38 ± 3.69	19.39 ± 11.82
	Mean cell size (S_{Hp})	0.60 ± 0.10	1.16 ± 0.38	0.97 ± 0.47
	$\sigma_2 = S_{Ca} / S_{Hp}$	2.7	7.2	20.0

An interesting observation is shown in the Figure 7 corresponding to a detailed analysis of image shown in the Figure 6G. For the formation of *H. pylori* biofilm in the mixture, different stages can be identified: (i) anchoring of *H. pylori* on the surface of *C. albicans*, (ii) co-aggregation of cells forming clusters, (iii) growth of *H. pylori* biofilm and (iv) total colonization of surface where *H. pylori* cells are the single identified. By size analysis of objects observed in Figure 7a is obtained that σ_2 is 3.6, 12.8 and 43.2 for ESR, ECA and ESV, respectively. Two important aspects are concluded by SEM: (i) it is verified the formation of biofilms of *H. pylori* in unfavorable conditions and in presence of *C. albicans*, and (ii) it was possible to identify the anchoring of bacterium cell on the surface of the yeast.

It can be seen that though in its bacillar morphology the bacterium is a very large entity to achieve adequate internalization within the yeast without causing significant damage to the yeast wall. However, these results should be taken with caution and at least three aspects must be considered: (i) the size obtained by SEM is a geometric projection in two dimensions of a three-dimensional body; (ii) hypothesis of *H. pylori* internalization in *C. albicans*, without a comprehensive explaining about internalization mechanism for this fact could be associated with a different morphology, i.e., coccoid (Siavoshi and Saniee 2014; Allison *et al* 2016), but also, extracellular DNA or outer membrane vesicle could be masking the results of Fluorescence Microscopy. Extracellular DNA has been identified as part of biofilm matrix of *H. pylori* and outer membrane vesicle with 20 to 500 nm in diameter containing phospholipids, proteins, LPSs, and DNA; these outer membrane vesicles are produced from both biofilm and planktonic systems (Hathroubi *et al* 2018); and (iii) the bacteria and yeast can be found in different growth stages with which the difference in size becomes more significant compared with size data obtained from individual cultures (see Figure 6H).

In Table 2 it can be seen that, for the system (Ca+Hp) BF, the size difference varies significantly with respect to the first estimate. These differences are explained due to the differences in the growth conditions since, for the mixture of microorganisms, the incubation conditions are favorable for the yeast and unfavorable for the bacteria. It can be observed that, consistently with the images of SEM, it is possible in term of size the internalization of bacteria; however, information or clues as to how such a process could occur were not identified.

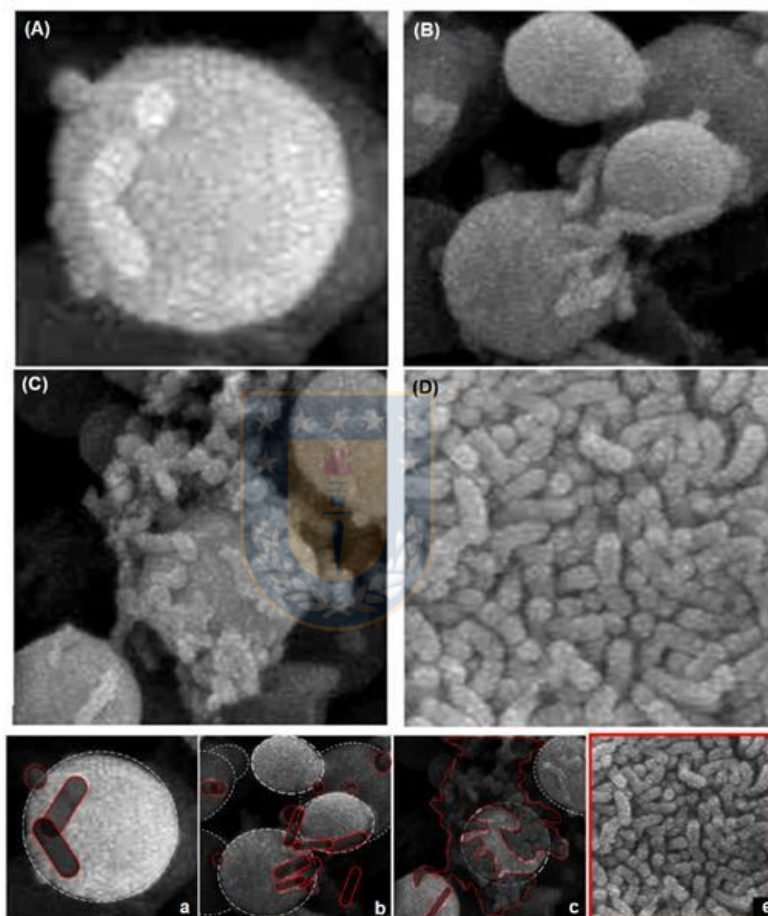


Figure 7. SEM images from Figure 5G illustrating different stage of *H. pylori* biofilm formation: (i) anchoring on the surface of *C. albicans*, (ii) co-aggregation of cells forming clusters, (iii) growth of *H. pylori* biofilm and (iv) total colonization of surface. Figures a-e highlights the particles in the image to ease the comparison.

In Figure 8 is shown images of TEM, from individual cultures, of *C. albicans* (Figure 8A, 8B and 8C) and *H. pylori* (Figure 8D); images of TEM for (Ca+Hp)BF are shown in Figure 8E, 8F and 8G. By TEM morphological aspects were calculated in order to try to elucidate the possible mechanisms of interaction between *H. pylori* and *C. albicans*. In particular, as it was explored the viability of internalization of *H. pylori* in the yeast, which is a hypothesis proposed from experiments of fluorescence microscopy where bacterium-like objects have

been described in the inner of yeast vacuoles (Siavoshi and Saniee 2014; Allison *et al* 2016). Previously by SEM was evidenced that is physically possible the internalization in term of size (see value of σ_2 in Table 2 and Figure 7). However, it is well- known that the cell wall is the first physical barrier that bacteria must cross to achieve the inner yeast. Cell wall of *C. albicans* represents a challenge for the bacteria due to its enormous relative size constituting 16 % of the yeast cell volume and which was calculated from TEM images to be $16.04 \pm 9.27 \mu\text{m}^3$ (see Figure 8). From TEM analysis was determined that thickness of cell wall of *C. albicans* is $0.20 \pm 0.02 \mu\text{m}$ ($\sim 200 \text{ nm}$); whereas the size *H. pylori*, in term of ESV, is $0.97 \pm 0.47 \mu\text{m}^3$ with a cell wall thickness of $34.1 \pm 4.4 \text{ nm}$, in consequence, the cell wall of *C. albicans* is ~ 7 times larger than cell wall of *H. pylori* (see Figure 8E and 8G). In addition, no significant change in the thickness of the wall cell of *C. albicans* was evidenced during cellular division (see Figure 8C and Table 3).

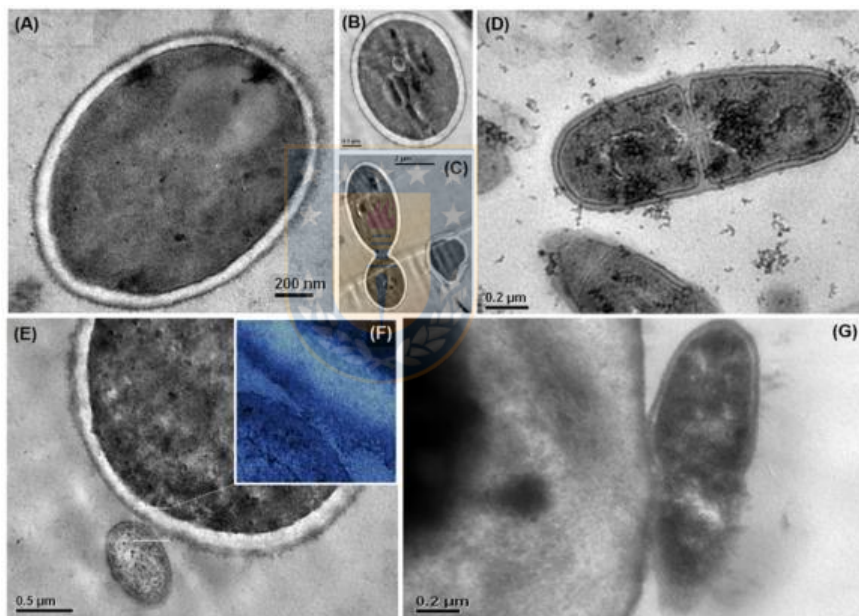


Figure 8. TEM images of *C. albicans* (A, B and C), *H. pylori* (D) from individual cultures and from mixtures (E, F and G).

Table 3. Cell dimensions for *C. albicans* and *H. pylori* determined by TEM (MCWT = Mean cell wall thickness)

Microorganism	Parameter evaluated	Size descriptor		
		ESR (μm)	ECA (μm^2)	ESV (μm^3)
<i>C. albicans</i>	Mean cell size (S_{Ca})	1.55 ± 0.23	7.61 ± 2.21	16.04 ± 6.88
	MCWT	0.20 ± 0.02	-	-
	MCWT during cell division	0.25 ± 0.06	-	-
	Mean inner volume	-	-	$13.54 \pm$

	Mean cell wall volume	-	-	6.88 2.5 ± 2.39
<i>H. pylori</i>	Mean cell size (S_{Ca})	0.42 ± 0.38	0.55 ± 0.45	0.31 ± 6.88
	MCWT	0.03 ± 0.01	-	-
	Mean inner volume	-	-	0.25 ± 0.13
	Mean cell wall volume	-	-	0.06 ± 0.01

On the other hand, from the TEM images, two important aspects related to the formation of polymicrobial biofilms between *C. albicans* and *H. pylori* were verified: (i) The anchoring of *H. pylori* on the surface of *C. albicans* takes place by direct contact interfacial suggesting a control of this first stage at surface level (see Figure 8F), in consequence, the multiple interactions could promote this stage; and (ii) after surface contact, *H. pylori* adheres to the surface (see Figure 8G). These two observations imply that some anchoring mechanism should be occurring in conjunction with a high affinity between the surfaces in contact; however, the surface affinity could be the result of the molecular nature of the cell interface or it may be due to surface conditioning subsequent to the attachment of *H. pylori*. Nevertheless, both SEM and TEM are fix observation of system latter to pre-treatment of samples, consequently, information on how the system reaches the observed state must be obtained through other types of techniques.

By optic microscopy, cultures corresponding to (Ca+Hp) BF were directly observed. Water flux was applied in order to evaluate the strong of anchoring of *H. pylori* on *C. albicans*. However, dispersion of cell was not possible. In Figure 9A can be seen the cell-like objects associated with *H. pylori* anchored on *C. albicans* cells. In Figure 9B, it is shown the co-aggregation over time of *C. albicans* and *H. pylori*.

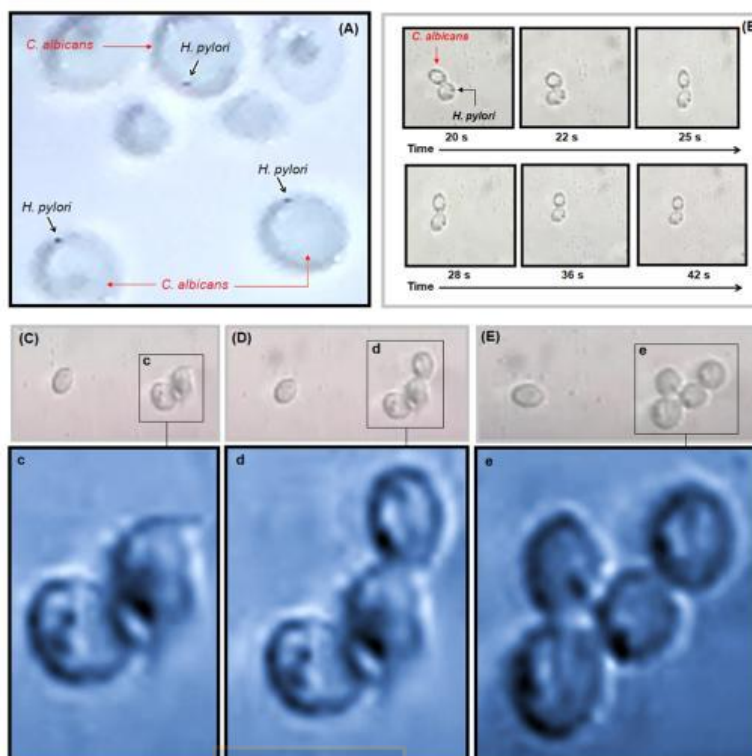


Figure 9. Image of optic microscopy of (Ca+Hp) BF (A), time-sequence of anchoring of *C. albicans* and *H. pylori* (B), time-sequence of co-aggregation of *C. albicans* and *H. pylori* (C, D, and E). Magnification of images is shown in c, d and e, respectively.

Changes of spatial orientation evidences the fix positions of *H. pylori* and its anchoring on the surface. However, recording in video format for longer times permitted to obtain evidence of simultaneous co-aggregation of cells (Figures 9C-9E). Thus, it is concluded that anchoring of *H. pylori* occurs in aqueous water previous to formation of biofilms by *C. albicans*, in consequence, co-aggregation of *C. albicans* can be defined as a mixed process of cellular aggregation that would lead to the formation of polymicrobial biofilms completely integrated by the two microorganisms instead of a process direct to the formation of yeast biofilm acting as a surface or substrate for the formation of a second biofilm.

Study by DLS

Size and size distribution by DLS is shown in Figure 10. It can be seen that alike to results obtained by SEM and TEM, the mean size of *C. albicans* is higher than mean size of *H. pylori*. By DLS, sizes changes from 1.7 to 4.8 μm for *C. albicans* and from 0.71 to 4.1 μm for *H. pylori* were obtained. For *H. pylori* is observed that substances with lower size are detected. These show a size from 122 nm to 459 nm and are associated probably with extracellular proteins, extracellular DNA or outer membrane vesicles (Hathroubi *et al* 2018).

For (Ca+Hp)BF the size distribution was characterized to be multimodal. Several aspects must be highlighted: (i) displacement of distribution to higher size is observed, which can be explained by aggregation of cells, (ii) planktonic cells of *C. albicans* (from 0.71 to 1.48 μm) and *H. pylori* (from 1.48 to 3.1 μm) apparently are presents and (iii) amount of extracellular lipoproteins, extracellular DNA and outer membrane vesicles were strongly decreased. Two situations could explain the above observation, the first is that concentration of extracellular substances decreased in the mixture due to reduction of some metabolic processes, and the second, that decrease of extracellular substances is associated with the interaction between microorganisms, e.g., absorption by *C. albicans* of extracellular substances. It has been demonstrated that ATCC 43504 biofilm contain proteomannans consisting of β -1,3- and β -1,6-glucan structures linked to proteoglycans (Hathroubi *et al* 2018), since these are analogous substances to that forming the inner layer of the *C. albicans* cell envelope is suggested that high degree of affinity between these substances and *C. albicans* cells is expected (Raa 2015; Hathroubi *et al* 2018).



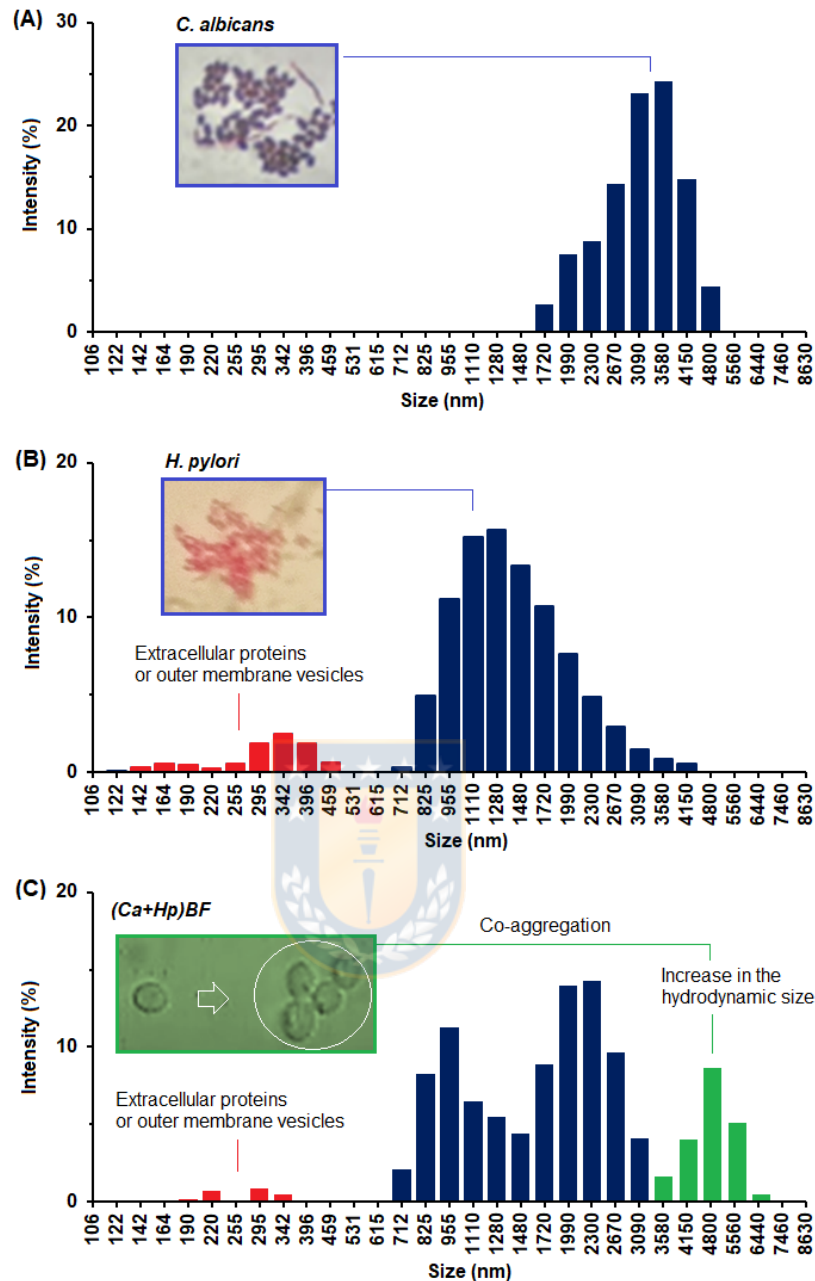


Figure 10. Size and size distribution by DLS of *C. albicans* (A), *H. pylori* (B) and (Ca+Hp) BF (C).

Study of hydrophilic-lipophilic properties of the surface

Measurements of contact angle for *C. albicans* and *H. pylori* biofilms are shown in the Table 4. Illustration of sessile drop method for the determination of contact angle for each working liquid is shown in the Figure 11. It can be seen from water contact angle that biofilm surface can be described in both cases to be with low hydrophilic surfaces ($45 < \theta < 90$) (Law 2014). However, definition of hydrophilic or hydrophilic surface is not a physical definition, therefore,

a better interpretation of contact angle is obtained by comparison with known surfaces (see Table 5).

Table 4. Measurements of contact angle (θ) of biolayer of *C. albicans* and *H. pylori* using three solvents with different polarities. Coefficient of variation appears in parenthesis followed of measured of contact angle, ϵ is dielectric constant of solvent at 25 °C (Sengwa *et al* 2003; Jazi *et al* 2010).

Microorganism	Water ($\epsilon = 78.3$)	Ethylene glycol ($\epsilon = 41.2$)	1,3-Propanediol ($\epsilon = 30.2$)
<i>C. albicans</i>	84.9 \pm 1.6 (1.9 %)	77.5 \pm 3.6 (4.6 %)	74.0 \pm 4.3 (5.8 %)
<i>H. pylori</i>	76.6 \pm 3.8 (4.9 %)	79.7 \pm 3.9 (4.9 %)	77.2 \pm 2.7 (3.5 %)

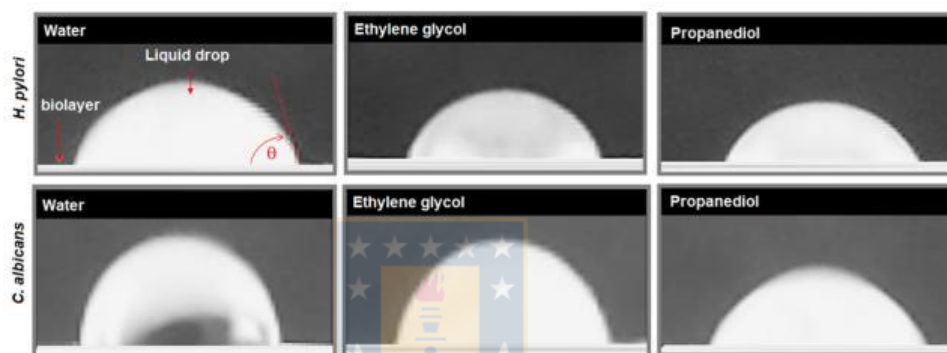


Figure 11. Contact angle measurements for *H. pylori* and *C. albicans* using water, ethylene glycol and 1,3-propanediol.

A comparison with non-polar polymeric surfaces permits conclude that in term of wettability with water both *C. albicans* and *H. pylori* surfaces are alike to poly(ethylene terephthalate) (PET) and poly(styrene) (PS), which are surface characterized to show a very low wettability. In consequence, results suggest that *C. albicans* and *H. pylori* surfaces have a high hydrophobic character. The above is even an aspect that differentiates *H. pylori* from other gram-negative bacteria such as *E. coli*, and *C. albicans* from other yeasts of the same genus such as *C. tropicalis*. But at the same time, the surface affinity between *C. albicans* and *H. pylori* towards hydrophobic surfaces, and between them, is higher. These results are consistent with description of lipid profiles of *H. pylori*, from which has been evidenced a high relative content of lysophospholipids which have been associated with a better adherence to epithelial cells *in vitro* (Tannaes *et al* 2006), but also, with the fact that *H. pylori* strains produce several characteristic lipids, e.g., steryl glycosides and cholesteryl glucosides (Huang *et al* 2019). For the case of *C. albicans*, its surface hydrophobicity is well-known and has been associated to the promotion of adhesion process on surfaces; however, for *C. albicans*, the presence of negative charges on its surface also have been documented

(Hobden *et al* 1995; Hawser and Islam 1998). In addition, these results are consistent with those obtained from IR spectroscopy and FEDS. It can be observed that, while in *E. coli*, *C. tropicalis* and *H. pylori* the contribution of the dispersive and polar components is very similar, in *C. albicans* the dispersive contribution is much more significant. In comparison with polymeric surface, dispersive component is similar to observed for polypropylene (PP), PS and poly (vinyl alcohol), which are associated with London dispersion and hydrogen bonds. These results evidence that co-aggregation surface between *H. pylori* and *C. albicans* in aqueous environments is mainly promoted by dispersive forces, though a small electrostatic contribution could be present, which is expected to be small compared with *S. aureus*, *P. aeruginosa*, *E. coli* and *C. tropicalis* (see Table 5). The above is consistent with electrostatic adsorption of arginine by *C. albicans* (Hawser and Islam 1998), and the small amount of arginine and lysine in *H. pylori* biofilm (3.5 % and 7.9 %, respectively) (Stark *et al* 1999).

Table 5. Total surface free energy (γ_{total}) and their components according to van Oss-Chaudhury-Good theory: dispersive component (γ^{LW}), acid-base component (γ^{AB}), acidic component (γ_s^-), basic component (γ_s^+). All values are in mJ/m². Percentages of contribution of γ^{LW} and γ^{AB} to γ_{total} are shown in parenthesis. Contact angle with water (θ_w).

	θ_w	γ_{total}	γ^{LW}	γ^{AB}	γ_s^-	γ_s^+
<i>C. albicans</i>	84.9 ± 1.6	22.78	21.72 (95.3 %)	1.06 (4.7 %)	13.62	0.02
<i>H. pylori</i>	76.6 ± 3.8	17.34	6.97 (40.2 %)	10.37 (59.8 %)	30.25	0.89
PVA	51	42	42.0 (100 %)	0.0 (0.0 %)	-	-
PVAc	60.6	37.7 ± 2.9	24.8 ± 1.6 (65.7 %)	13.0 ± 1.5 (34.3 %)	-	-
PEG	63	43.9 ± 1.9	37.7 ± 8.1 (86.0 %)	6.9 ± 6.4 (14.0 %)	-	-
PET	69.8 ± 14	43.2 ± 2.5	37.6 ± 5.8 (86.8 %)	5.0 ± 4.2 (13.2 %)	-	-
PS	89.0 ± 10	41.8 ± 1.2	37.6 ± 3.8 (90.0 %)	4.2 ± 3.3 (10.0 %)	-	-
PP	101.5 ± 9	31.0 ± 3.9	28.9 ± 3.7 (93.2 %)	2.1 ± 2.5 (6.8 %)	-	-
<i>S. aureus</i>	-	43.9 ± 0.5	39.6 ± 0.4 (90.2 %)	4.3 ± 0.5 (9.8 %)	73.5	0.07
<i>P. aeruginosa</i>	-	39.3 ± 0.8	34.8 ± 0.5 (88.5 %)	4.4 ± 0.8 (11.5 %)	69.1	0.09
<i>E. coli</i>	19.1 ± 0.9	47.9	25.7 (53.7 %)	22.2 (46.3 %)	123.2	0.0
<i>C. tropicalis</i>	48.4 ± 0.7	40.4	20.5 ± 0.2 (50.8 %)	19.8 (49.2 %)	39.5	2.5

PVA: Poly(vinyl alcohol); PEG: Poly(ethylene glycol); PVAc: Poly(vinyl acetate); PET: Poly(ethylene terephthalate); PS: Poly(styrene); PP: Polypropylene (ADT 2020). Information about *S. aureus* and *P. aeruginosa* (Cavitt 2020); *E. coli* (Moreira *et al* 2015); *C. tropicalis* (Asri *et al* 2017).

CONCLUSIONS

Results evidence that hydrophobic or van der Waals interactions between non-polar peptide chains of cell wall of *C. albicans* and lipid substance or non-polar peptide chains from membrane of *H. pylori* influence the co-aggregation for the formation of polymicrobial biofilm between these microorganisms. It is suggested that this interaction occurs simultaneously with the formation of hydrogen bonds, and therefore, a strong cell-cell contact should be observed. After to co-aggregation stage, stronger interactions could take place as a result of the interaction of cysteine residues present in the outer proteins of both microorganisms. In consequence, anchoring of *H. pylori* is promoted previous to the formation of growth and consolidation of biofilm. Our results show that biofilm formed corresponds to polymicrobial biofilm, which though it is similar to biofilm of individual microorganisms by IR spectroscopy and FEDS was demonstrated that (Ca+Hp) BF corresponds to different system. It is concluded that the formation of *C. albicans* and *H. pylori* polymicrobial biofilm occurs through the combination of different mechanisms at the surface level: hydrophobic interactions between non-polar amino acids chains and lipid structures, formation of hydrogen bonds and covalent anchoring through the formation of disulfide bonds. No significant effect of electrostatic interaction or internalization were evidenced from our experiments.

Acknowledgments. Sixta Palencia thanks to Conicyt-Chile, Universidad de Concepción (Chile) and Universidad del Valle (Colombia) by the funds for the performing of the project and doctoral scholarship. Authors thanks to Mindtech s.a.s. by the support into acquisition of spectral marker.

Conflicts of interest. The authors declare that they have no conflict of interest.

REFERENCES

- Adam B, Baillie GS, Douglas LJ (2002) Mixed species biofilms of *Candida albicans* and *Staphylococcus epidermidis*. J Med Microbiol 51, 344-349. DOI: 10.1099/0022-1317-51-4-344
- ADT (2020) Base data: Accu Dyne Test (available in: <http://www.accudynetest.com/>)
- Adt I, Toubas D, Pinon JM, Manfait M, Sockalingum GD (2006) FTIR spectroscopy as a potential tool to analyse structural modifications during morphogenesis of *Candida albicans*. Arch Microbiol 185, 277-285. DOI: 10.1007/s00203-006-0094-8
- Alipour N, Gaeini N (2017) *Helicobacter* is preserved in yeast vacuoles! Does Koch's postulates confirm it?. World J Gastroenterol 28:2266-2268. DOI:10.3748/wjg.v23.i12.2266
- Allison D, Willems H, Jayatilake J, Bruno V, Peters BM, Shirliff M (2016) *Candida*-Bacteria Interactions: Their Impact on Human Disease. Microbiology Spectrum 4, VMBF-0030-2016. DOI: 10.1128/microbiolspec.VMBF-0030-2016.
- Anaya L, Libreros K, Palencia VJ, Atencio VJ, Palencia M (2019) Mid-infrared spectral characterization of fish scales: "Bocachico" (*Prochilodus magdalenae*) by functionally-enhanced derivative

- spectroscopy (FEDS) - A methodological approach. *Journal of Science with Technological Applications* 6, 28-39. DOI: 10.34294/j.jsta.19.6.39
- Arrondo JL, Goñi FM (1992) Structure and dynamics of membrane proteins as studied by infrared spectroscopy. *Prog. Biophys. Mol. Biol.* 72, 367-405. DOI: 10.1016/s0079-6107(99)00007-3
- Arrondo JL, Muga A, Castresana J, Goñi FM (1993) Quantitative studies of the structure of proteins in solution by Fourier-transform infrared spectroscopy. *Prog. Biophys. Mol. Biol.* 59, 23-56. DOI: 10.1016/0079-6107(93)90006-6
- Arvanitis A, Mylonakis E (2015) Fungal–bacterial interactions and their relevance in health, *Cellular Microbiol* 17:1442-1446. DOI: 10.1111/cmi.12493
- Asri M, Elabed A, Ghachtouli NE, Koraichi SI, Bahafid W, Elabed S (2017) Theoretical and Experimental Adhesion of Yeast Strains with High Chromium Removal Potential. *Environmental Engineering Science* 34,693-702. DOI: 10.1089/ees.2016.0515
- Atherton JC (2006) The pathogenesis of *Helicobacter pylori*-induced gastro-duodenal diseases. *Annual Rev Pathol: Mechanisms of Disease* 1, 63-96. DOI: 10.1146/annurev.pathol.1.110304.100125
- Barth A (2000) The infrared absorption of amino acid side chains. *Progress in Biophysics & Molecular Biology* 74, 141-173.
- Brogden KA, Guthmiller JM, Taylor CE (2005) Human polymicrobial infections. *Lancet.* 365:253–255. DOI: 10.1016/S0140-6736(05)70155-0
- Bode G, Mauch F, Ditschuneit H, Malfertheiner P (1993) Identification of structures containing polyphosphate in *Helicobacter pylori*. *Journal of General Microbiology* 139, 3029-3033.
- Cavitt TB, Carlisle JG, Dodds AR, Faulkner RA, Garfiel TC, et al (2020) Thermodynamic Surface Analyses to Inform Biofilm Resistance. *IScience* 23, 101702 (1-38). DOI: 10.1016/j.isci.2020.101702
- Cover TL, Blaser MJ (2009) *Helicobacter pylori* in health and disease. *Gastroenterol.* 136,1863-1873. DOI:10.1053/j.gastro.2009.01.073
- Deveau A, Bonito G, Uehling J, Paoletti M, Becker M, et al (2018) Bacterial-fungal interactions: ecology, mechanisms and challenges. *FEMS Microbial Review* 42:335-352. DOI: 10.1093/femsre/fuy008
- El-Baky RM, Dalia MM, Gamal F (2014) N-acetylcysteine inhibits and eradicates *Candida albicans* biofilms. *Am. J. Infect. Dis. Microbiol.* 2014, 2, 122–130. DOI: 10.12691/AJIDM-2-5-5
- Gaddy JA, Tomaras AP, Actis LA (2009) The *Acinetobacter baumannii* 19606 OmpA protein plays a role in biofilm formation on abiotic surfaces and in the interaction of this pathogen with eukaryotic cells. *Infect Immun* 77:3150–3160. DOI: 10.1128/IAI.00096-09
- Gannedi V, Ali A, Singh PP, Vishwakarma R (2020). Total synthesis of phospholipomannan of the *Candida albicans*. *The Journal of Organic Chemistry.* DOI: 10.1021/acs.joc.0c00402
- Garcia-Quintero A, Combatt E, Palencia M (2018) Structural study of humin and its interaction with humic acids by Fourier-transform mid-infrared spectroscopy. *Journal of Science with Technological Applications* 4, 28-39. DOI:10.34294/j.jsta.18.4.28
- Garcia A, Salas-Jara MJ, Herrera C, González C (2014) Biofilm and *Helicobacter pylori*: From environment to human host. *World Journal of Gastroenterology* 20, 5632-5638. DOI: 10.3748/wjg.v20.i19.5632
- Graham D, Miftahussurur M (2018) *Helicobacter pylori* urease for diagnosis of *Helicobacter pylori* infection: A mini review. *J. Adv. Res.* 13, 51-57, 2018. DOI: 10.1016/j.jare.2018.01.006
- Hawser Sp, Islam K (1998) Binding of *Candida albicans* to Immobilized Amino Acids and Bovine Serum Albumin. *Infection and immunity* 66, 140-144. DOI:10.1128/IAI.66.1.140-144.1998
- Hamway Y, Taxauer K, Neumeyer V, Fischer W, et al (2020) Cysteine Residues in *Helicobacter pylori* Adhesin HopQ are Required for CEACAM-HopQ Interaction and Subsequent CagA Translocation." *Microorganisms* 8, 465. DOI:10.3390/microorganisms8040465
- Hathroubi S, Servetas SL, Windham I, Merrell DS, Ottemann (2018) *Helicobacter pylori* Biofilm Formation and Its Potential Role in Pathogenesis. *Microbiology and Molecular Biology Review* 82, e1-18. DOI: 10.1128/MMBR.00001-18
- Hobden C, Teevan C, Jones L, O'shea P (1005) Hydrophobic properties of the cell surface of *Candida albicans*: a role in aggregation. *Microbiology* 141, 1875-1881.
- Hsu PI, Lai KH, Hsu PN, Lo GH, Yu HC, Chen WC, Tsay FW, Lin HC, Tseng HH, Ger LP, Chen HC (2007) *Helicobacter pylori* infection and the risk of gastric malignancy. *Am J Gastroenterol* 102:725-730. DOI:10.1111/j.1572-0241.2006.01109.x

- Huang Z, Zhang XS, Blaser M, London E (2019) *Helicobacter pylori* lipids can form ordered membrane domains (rafts). *Biochim Biophys Acta Biomembr* 1861, 183050. DOI:10.1016/j.bbamem.2019.183050
- Jazi B, Amiri H, Mohsen-Nia M (2010) Dielectric Constants of Water, Methanol, Ethanol, Butanol and Acetone: Measurement and Computational Study. *Journal of Solution Chemistry* 39, 701-708. DOI:10.1007/s10953-010-9538-5
- Kao CY, Sheu BS, Wu JJ (2016) *Helicobacter pylori* infection: An overview of bacterial virulence factors and pathogenesis. *Biomedical Journal* 39, 14-23. DOI: 10.1016/j.bj.2015.06.002
- Klis FM, Sosinska GJ, De Groot PWJ, Brul S (2009) Covalentlylinked cellwall proteins of *Candida albicans* and their role in virulence. *FEMS Yeast Resource*, 1013–1028. DOI: 10.1111/j.1567-1364.2009.00541.x
- Kong J, Yu S (2007) Fourier Transform Infrared Spectroscopic Analysis of Protein Secondary Structures. *Acta Biochimica et Biophysica Sinica* 39, 549-559. DOI: 10.1111/j.1745-7270.2007.00320.x
- Konopka JB (1997) N-Acetylglucosamine Functions in Cell Signaling. *Scientica* ID 489208. DOI: 10.6064/2012/489208
- Kovacs A, Nyerges B, Izvekov V (2008) Vibrational Analysis of N-Acetyl-r-D-glucosamine and α -D-Glucuronic Acid. *J. Phys. Chem. B* 2008, 112, 5728-5735. DOI: 10.1021/jp710432d
- Krajewska B (2009) Ureases I. Functional, catalytic and kinetic properties: A review. *Journal of Molecular Catalysis B: Enzymatic* 59, 9–21. DOI: 10.1016/j.molcatb.2009.01.003
- Krüger W, Vielreicher S, Kapitan M, Jacobsen ID, Niemiec MJ (2019) Fungal-bacterial interactions in health and disease, 8:1-45. DOI: 10.3390/pathogens8020070
- Kumar S, Rai AK, Singh VB, Rai SB (2005) Vibrational spectrum of glycine molecule. *Spectrochimica Acta A* 61, 2741-2746. DOI: 10.1016/j.saa.2004.09.029
- Lai CC, Wang CY, Liu WL, Huang YT, Hsueh PR (2012) Time to positivity of blood cultures of different *Candida* species causing fungaemia. *J Med Microbiol* 61, 701–704. DOI: 10.1099/jmm.0.038166-0
- Law KY (2014) Definitions for Hydrophilicity, Hydrophobicity, and Superhydrophobicity: Getting the Basics Right. *The Journal of Physical Chemistry Letters* 5, 686-688. DOI: 10.1021/jz402762h
- Leker K, Lozano-Pope I, Bandyopadhyay K, Choudhury BP, Obonyo M (2017) Comparison of lipopolysaccharides composition of two different strains of *Helicobacter pylori*. *BMC Microbiology* 17, 226. DOI: 10.1186/s12866-017-1135-y
- Li H, Liao T, Debowski A, Tang H, Nilsson HO, Stubbs K, Marshall BJ, Benhezal M (2016). Lipopolysaccharide Structure and Biosynthesis in *Helicobacter pylori*. *Helicobacter*, 1-17. DOI: 10.1111/hel.12301
- Mahnaz AM, Chamanrokh P, Whitehouse CA, Huq A (2015) Methods for detecting the environmental coccoid form of *Helicobacter pylori*. *Front. Public Health* 3:147. DOI: 10.3389/fpubh.2015.00147
- Massarat S, Saniee P, Siavoshi F, Mokhtari R, Mansour-Ghanaei F, Khalili-Samani S (2016) The Effect of *Helicobacter pylori* Infection, Aging, and Consumption of Proton Pump Inhibitor on Fungal Colonization in the Stomach of Dyspeptic Patients. *Front Microbiol* 7, 801. DOI: 10.3389/fmicb.2016.00801
- McGrath JW, Quinn JP (2000) Intracellular Accumulation of Polyphosphate by the Yeast *Candida humicola* G-1 in Response to Acid pH. *Applied and Environmental Microbiology* 66, 4068-4073. DOI: 10.1128/AEM.66.9.4068-4073.2000
- Mohamed ME, Mohammed A (2013) Experimental and Computational Vibration Study of Amino Acids. *International Letter of Chemistry, Physics and Astronomy* 10, 1-17. DOI: 10.18052/www.scipress.com/ILCPA.15.1
- Moonens K, Gideonsson P, Subedi S *et al* (2017) Structural insights into polymorphic ABO glycan binding by *Helicobacter pylori*. *Cell Host Microbe* 19, 55–66. DOI: 10.1016/j.chom.2015.12.004
- Moreira J, Simoes M, Melo LF, Mergulhao F (2015) *Escherichia coli* adhesion to surfaces—a thermodynamic assessment. *Colloid and Polymer Science* 293, 177–185. DOI: 10.1007/s00396-014-3390-x
- Moreno-Ruiz E, Ortu G, De Groot PW, et al (2009) The GPI-modified proteins Pga59 and Pga62 of *Candida albicans* are required for cell wall integrity. *Microbiology* 155,2004-2020. DOI: 10.1099/mic.0.028902-0
- Mustard AT, Anderson T (2005) Use of spherical and spheroidal models to calculate zooplankton biovolume from particle equivalent spherical diameter as measured by an optical plankton counter. *Limnology and Oceanography: Methods* 3, 183-189.

- Nardone G, Compare D (2015) The human gastric microbiota: Is it time to rethink the pathogenesis of stomach diseases?. *United Eur Gastroenterol J* 3, 255–260. DOI:10.1177/2050640614566846
- Nelson PN (2016) Chain Length and Thermal Sensitivity of the Infrared Spectra of a Homologous Series of Anhydrous Silver(I) n-Alkanoates. *International Journal of Spectroscopy*. 3068430, 1-9. DOI: 10.1155/2016/3068430
- Nyquist RA (2001a) Chapter 4 - Thiols, Sulfides and Disulfides, Alkanethiols, and Alkanedithiols (S-H stretching). *Interpreting Infrared, Raman, and Nuclear Magnetic Resonance Spectra Interpreting Infrared, Raman, and Nuclear Magnetic Resonance Spectra*, 65-83. DOI: 10.1016/B978-012523475-7/50184-4
- Nyquist RA (2001b) Chapter 8 - Phosphorus Compounds. *Interpreting Infrared, Raman, and Nuclear Magnetic Resonance Spectra Interpreting Infrared, Raman, and Nuclear Magnetic Resonance Spectra*, 231-350. DOI: 10.1016/B978-012523475-7/50188-1
- Oleastro M, Menard A (2013) The Role of *Helicobacter pylori* Outer Membrane Proteins in Adherence and Pathogenesis. *Biology* 2, 1110-1134. DOI: 10.3390/biology2031110
- Otalora A, Palencia M (2019) Application of functionally-enhanced derivative spectroscopy (FEDS) to the problem of the overlap of spectral signals in binary mixtures: Triethylamine-acetone. *Journal of Science with Technological Applications* 6, 96-107. DOI: 10.34294/j.jsta.19.6.44
- Palencia M (2017) Surface free energy of solids by contact angle measurements. *Journal of Science with Technological Applications* 2, 84-93. DOI: 10.34294/j.jsta.17.2.17
- Palencia M (2018) Functional transformation of Fourier-transform mid-infrared spectrum for improving spectral specificity by simple algorithm based on wavelet-like functions. *Journal of Advanced Research* 14, 53-62. DOI: 10.1016/j.jare.2018.05.009
- Palencia S, García A, Palencia M (2020) Vibrational spectrum characterization of outer surface of *Helicobacter pylori* biofilms by Functionally-Enhanced Derivative Spectroscopy (FEDS). *Journal of Chilean Chemical Society* (Accepted).
- Palencia S, García A, Palencia M (2021) Mid-infrared vibrational spectrum characterization of outer surface of *Candida albicans* by Functionally-Enhanced Derivative Spectroscopy (FEDS). *Journal of Applied Spectroscopy* (Accepted).
- Parker SF (2013) Assignment of the vibrational spectrum of L-cysteine. *Chemical Physics* 424, 75-79. DOI: 10.1016/j.chemphys.2013.04.020
- Peleg AY, Hogan DA, Mylonakis E (2010) Medically important bacterial-fungal interactions. *Nature Rev microbiol* 8:340-349. DOI:10.1038/nrmicro2313
- Peters BM, Jabra-Rizk MA, O'May GA, Costerton JW, Shirtliff ME (2012) Polymicrobial interactions: Impact on pathogenesis and human disease. *Clin. Microbiol Rev* 25:193–213. DOI: 10.1128/CMR.00013-11
- Pfaller MA, Diekema DJ (2007) Epidemiology of invasive candidiasis: a persistent public health problem. *Clin Microbiol Rev* 20:133-163. DOI: 10.1128/CMR.00029-06
- Pierce CG, Vila T, Romo JA, Montelongo-Jauregui D, Wall G, Ramasubramanian A, Lopez-Ribot JL (2017) The *Candida albicans* biofilm matrix: Composition, structure and function. *Journal of Fungi (Basel)* 3:14. DOI: 10.3390/jof3010014
- Raa J (2015) Immune modulation by non-digestible and non-absorbable beta-1,3/1,6-glucan. *Microbial Ecology in Health and Disease* 26:27824. DOI:10.3402/mehd.v26.27824
- Ribeiro FC, de Barros PP, Rossoni RD, Junqueira JC, Jorge AOC (2017) *Lactobacillus rhamnosus* inhibits *Candida albicans* virulence factors in vitro and modulates immune system in *Galleria mellonella*. *J Appl Microbiol* 122:201–211. DOI: 10.1111/jam.13324
- Romeo O, Crisen G (2009) Molecular Epidemiology of *Candida albicans* and Its Closely Related Yeasts *Candida dubliniensis* and *Candida africana*, *J Clin Microbiol* 47:212-214. DOI: 10.1128/JCM.01540-08
- Rommel V, Da Silva A, Pimentel A (2012) Infrared Spectroscopy of Anionic, Cationic, and Zwitterionic Surfactants. *Advances in Physical Chemistry*, 903272, 1-14. DOI: 10.1155/2012/903272
- Ruiz-Herrera J, Mormeneo S, Vanaclocha P, Font-de-Mora J, Iranzo M, Puertes I, Sentandreu R (1994) Structural organization of the components of the cell wall from *Candida albicans*. *Microbiology* 140, 1513-1523
- Rungrodmitchai S (2014) Rapid Preparation of Biosorbents with High Ion Exchange Capacity from Rice Straw and Bagasse for Removal of Heavy Metals. *The Scientific World Journal* 634837, 1-9. DOI: 10.1155/2014/634837

- Sanchez A, Parra S, Vega S, Bernasconi H, Campos V, Smith C, Sáez K, García A (2020) In Vitro incorporation of *Helicobacter pylori* into *Candida albicans* cause by acidic pH stress. *Pathogens*, 9. DOI: 10.3390/pathogens9060489
- Santos TS, Matheus L, Vega-Chacon Y, Garcia de Oliveira W (2020) Fungistatic Action of N-Acetylcysteine on *Candida albicans* Biofilms and Its Interaction with Antifungal Agents. *Microorganisms*, 8. DOI: 10.3390/microorganisms8070980
- Sardi JCO, Scorzoni L, Bernardi T, Fusco-Almeida AM, Mendes MJS (2013) *Candida* species: current epidemiology, pathogenicity, biofilm formation, natural antifungal products and new therapeutic options. *J Med Microbiol* 62:10-24. DOI: 10.1099/jmm.0.045054-0
- Sengwa RJ (2003) A comparative dielectric study of ethylene glycol and propylene glycol at different temperatures. *Journal of Molecular Liquids* 108, 47-60. DOI: 10.1016/S0167-7322(03)00173-9
- Siavoshi F, Saniee P (2014). Vacuoles of *Candida* yeast as a specialized niche for *Helicobacter pylori*. *World J Gastroenterol* 20:5263–5273. DOI: 10.3748/wjg.v20.i18.5263
- Siavoshi F, Parastoo S (2018) *Candida* accommodates non-culturable *Helicobacter pylori* in its vacuole - Koch's postulates aren't applicable. *World J Gastroenterol* 24:310-314. DOI:10.3748/wjg.v24.i2.310
- Stark RM, Gerwig GJ, Pitman RS, Potts LF, Williams NA, Greenman J, Weinzweig IP, Hirst TR, Millar MR (1999) Biofilm formation by *Helicobacter pylori*. Letter in *Applied Microbiology* 28, 121-126.
- Tannaes T, Bukholm IK, Bukholm G (2006) High relative content of lysophospholipids of *Helicobacter pylori* mediates increased risk for ulcer disease. *FEMS Immunology & Medical Microbiology* 44, 17-23. DOI: 10.1016/j.femsim.2004.10.003
- Tran A, Whittimore JD, Wyrick PB, McGrath SC, Cotter RJ, Trent MS (2006) The Lipid A 1-Phosphatase of *Helicobacter pylori* Is Required for Resistance to the Antimicrobial Peptide Polymyxin. *Journal of Bacteriology*. 188, 4531-4541. DOI: 10.1128/JB.00146-06
- Wohlmeister D, Barreto DR, Helfer VE, Calil LN, Buffon A, Fuentesfria AM, Corbellini VA, Pilger DA (2017) Differentiation of *Candida albicans*, *Candida glabrata*, and *Candida krusei* by FT-IR and chemometrics by CHROMagar™ *Candida*. *J Microbiol Met* 141, 121-125. DOI: 10.1016/j.mimet.2017.08.013
- Yonezawa H, Osaki T, Kamiya S (2015) Biofilm Formation by *Helicobacter pylori* and Its Involvement for Antibiotic Resistance. *Biomed Research International* 914791. DOI: 10.1155/2015/914791

Capítulo VII: Study of the promotion of the interconversion between coccoid and bacillary forms resulting of *Helicobacter pylori* and *Candida albicans* interaction

Paper 6

Capítulo VII: Study of the promotion of the interconversion between coccoid and bacillary forms resulting of *Helicobacter pylori* and *Candida albicans* interaction

Sixta L. Palencia¹, Homero Urrutia², Manuel Palencia³, Apolinaria García^{1*}

¹ *Laboratory of Bacterial Pathogenicity, Department of Microbiology, Faculty of Biological Sciences, Universidad de Concepción, Concepción – Chile*

² *Laboratory of Biofilms, Department of Microbiology, Faculty of Biological Sciences, Universidad de Concepción, Concepción – Chile*

³ *Research Group in Science with Technological Applications, Department of Chemistry, Faculty of Natural and Exact Sciences, Universidad del Valle, Cali - Colombia*

Corresponding author: apgarcia@udec.cl

Documento enviado a Microbial Pathogenesis

<https://www.sciencedirect.com/journal/microbial-pathogenesis>

Study of the promotion of the interconversion between coccoid and bacillary forms resulting of *Helicobacter pylori* and *Candida albicans* interaction

Sixta L. Palencia¹, Homero Urrutia², Manuel Palencia³, Apolinaria García^{1*}

¹ Laboratory of Bacterial Pathogenicity, Department of Microbiology, Faculty of Biological Sciences, Universidad de Concepción, Concepción – Chile

² Laboratory of Biofilms, Department of Microbiology, Faculty of Biological Sciences, Universidad de Concepción, Concepción – Chile

³ Research Group in Science with Technological Applications, Department of Chemistry, Faculty of Natural and Exact Sciences, Universidad del Valle, Cali - Colombia

Corresponding author: apgarcia@udec.cl

ABSTRACT

H. pylori is associated as a predisposing factor for the development of gastric pathologies such as, peptic ulcers, non-cardiac gastric adenocarcinoma and gastric MALT lymphoma, being thus recognized by the International Agency for Research on Cancer and the World Health Organization (WHO) as category I carcinogen. The routes of transmission of this pathogen are not entirely clear, but a possible oral-fecal transmission and interactions with yeasts of the *candida* genus are postulated. The objective of this work was to establish the effect of the interaction between *H. pylori* and *C. albicans* in the reciprocal interconversion of the coccoid form to the bacillary state of the bacterium in order to advance in the understanding of microbial interactions between these two pathogens human. For that, several studies were performed using conventional techniques (bacterial viability assay: microbial cultures, Gram stain and urea test) and microscopic-based techniques (immunofluorescence detection assay and fluorescent light microscopy assay) were performed to mixture of bacteria (*H. pylori* ATCC J99 and ATCC 43504) and yeast (*C. albicans* ATCC 10231 and ATCC 14053). Results suggest the existence of a strong bacterium-yeast surface interaction between *H. pylori* and *C. albicans* that could be the result of stress conditions for *H. pylori*, which, depending of bacterial strain, permits the change from a bacillary to a coccoid state until the optimal conditions for the bacterium are restored.

keywords: *Helicobacter pylori*, *Candida albicans*, bacillary shape, coccoid shape, bacterial-fungi interaction.

1. INTRODUCTION

Helicobacter pylori is a Gram negative bacterium that colonizes 50 % of the human population (Mahnaz *et al.* 2015), it is adhered mainly to the gastric mucosa by various efficiently specialized and adapted pathogenicity mechanisms helping to survive the adverse conditions of the stomach, such as acidity, peristalsis, nutrient availability, innate and adaptive immunity of the host and competing microorganisms (Cover and Blaser, 2009). This bacterium can be considered as part of the transient human gastric microbiome because it can remain for decades interacting with the gastric mucosa without causing harm to the host (asymptomatic carriers) although it is not clear at all if its presence generates some positive effect directly or indirectly on the humans (Nardone and Compare, 2015). However, the presence of *H. pylori* is associated as a predisposing factor for the development of gastric pathologies such as gastritis, peptic ulcers, non-cardiac gastric adenocarcinoma and gastric MALT lymphoma (Atherton, 2006), being recognized by the International Agency for Research on Cancer and the World Health Organization (WHO) in 1994 as a category I carcinogen (Serrano *et al.*, 2009). The above is supported for its ability to produce ordered histological changes by an established sequence that originate inflammation, formation of non-atrophic gastritis, atrophy, intestinal metaplasia, dysplasia and gastric adenocarcinoma (Correa *et al.*, 2006).

For the eradication of *H. pylori*, it is usually used a treatment based on various antibiotics, achieving a successful effect in most cases while complying with the dose and time of administration suggested. However, a recurrent infection status has been demonstrated (Reshetnyak *et al.*, 2017), and explained due to reinfection process or as an effect resulting of bacterial strain that is resistant to antibiotics, and in consequence, it activates the mechanism of interconversion of its bacillary form, that is metabolically active, to its coccoid form (Kaprelyants *et al.*, 1993; Krzyżek *et al.*, 2018).

At present, structural changes in the interconversion from coccoid forms to the bacillary state, and vice versa, of *H. pylori* as well as their triggering factors are not fully understood (Reshetnyak *et al.*, 2017). However, previous researches have reported the identification of specific bacterial cytokines of *Mycobacterium tuberculosis*, *Mycobacterium avium*, *Micrococcus luteus* and *Rhodococcus rhodochrous*, which play an important role in the activation and reproduction of the latent state of the bacteria, showing that viable cells are able to secrete substances promoting the transition from dormant to active reproductive states (Shleevea *et al.*, 2002; Shleevea *et al.*, 2015; Palencia *et al.*, 2016; Reshetnyak *et al.*, 2017). In addition, between external inducers that have been identified are cyclic adenosine

monophosphate (cAMP), unsaturated fatty acids and resuscitation promoter factor (Rpf) which are obtained from the supernatant of mycobacterial cultures. In particular, this Rpf protein is a pheromone belonging to the group of bacterial cytokines with a molecular weight of 16-17 kDa. In addition, *H. pylori* cultures in the coccoid state have been found to retain oxidative metabolism at the same level as bacillary forms for several months (Shleeva *et al.*, 2002; Shleeva *et al.*, 2015; Palencia *et al.*, 2016; Reshetnyak *et al.*, 2017), with high levels of acidic and alkaline phosphatases, and a level of stable ATP that increases if an amount of nutritious fresh medium is added to the old crop (Gibbon *et al.*, 1995; Shleeva *et al.*, 2002; Reshetnyak *et al.*, 2017). But also, by immunocytochemistry techniques, the incorporation of a bromodeoxyuridine marker in the transformed forms have been demonstrated suggesting a continuous synthesis of DNA (Reshetnyak *et al.*, 2017).

Preliminary in vitro observations suggest that the interaction of *H. pylori*-specific strain ATCC 43504 and *C. albicans* ATCC 14053 promotes the reciprocal interconversion, that is, from the coccoid form to the bacillary state when the conditions of the environment are optimal for the bacteria, either when it is supplied with the required nutritional and physical requirements, or by the action of secondary metabolites produced by *C. albicans*. By the above, the objective of this work was to establish the effect of the interaction between *H. pylori* and *C. albicans* in the reciprocal interconversion of the coccoid form to the bacillary state of the bacterium in order to advance in the understanding of microbial interactions between these two human pathogens.

2. MATERIALS AND METHODS

2.1. Yeast strains and culture conditions

Two commercial strains of *C. albicans*, *C. albicans* ATCC 10231 (strain designation 3147) and *C. albicans* ATCC 14053 (strain designation NIH3172) were used. Each strain was seeded in Sabouraud Dextrose Agar (Oxoid, England), which is constituted by peptone, D-glucose and Agar with pH 5.3. They were incubated in aerobiosis at 37 °C for 24 hours.

2.2. Bacterial strains and culture conditions

As bacterial models were used two strains of *H. pylori*, *H. pylori* ATCC J99 (commercial strain isolated from a patient with duodenal ulcer) and *H. pylori* ATCC 43504 (commercial strain isolated from the human gastric antrum of a gastric cancer patient). They were grown on Columbia agar plates (Oxoid, England) supplemented with 7 % horse blood and incubated under microaerobic conditions in the presence of 5 % O₂, 10 % CO₂ and 85 % N₂ at 37 °C for

4 days. Once the bacterial growth was observed, Gram stain and the urease test were performed.

2.3. Preparation of the suspension of microorganisms

For the preparation of the suspension of yeasts and bacteria, colonies of *C. albicans* and *H. pylori* were taken with a bacteriological loop and dispersed, separately, in 10 ml of YPD broth (Difco™) until homogeneous suspensions were obtained. Subsequently, the dispersions were standardized to correspond to 0.5 on the McFarland scale (1.5×10^8 CFU/ml) by the measuring of the intensity of scattered light at a wavelength of 600 nm using UV-vis spectrophotometry.

2.4. Preparation of mixtures of microorganisms

Mixtures were made from the suspensions of bacteria and yeasts previously standardized, which consisted of 2 ml of each standard suspension of *H. pylori* and 2 ml of the suspension pattern of *C. albicans* in order to obtain the following mixtures: (a) *H. pylori* J99 - *C. albicans* 10231, (b) *H. pylori* J99 - *C. albicans* 14053, (c) *H. pylori* 43504 - *C. albicans* 10231 and (d) *H. pylori* 43504 - *C. albicans* 14053, with their respective controls.

2.5. Bacterial viability assay from mixtures between *H. pylori* and *C. albicans*

The mixtures were incubated at 37 °C in aerobiosis for a period of 18 days, then subcultures were performed on Columbia agar supplemented with 7% fetal bovine serum (FCS), plus urea at a concentration of 5 mM and incubated at 37 °C in microaerophilic for 4 days. Each culture was performed in fresh mount, Gram stain and urease test.

2.6. Immunofluorescence detection assay

Rabbit polyclonal antibodies, IgG were used anti- *H. pylori* labeled with Fluorescein-5-isothiocyanate (FITC) (Abcam, USA), at a concentration is 5,000 mg/ml, measured at a wavelength of 528 nm.

Then mixtures of cells (bacteria and yeast) with their respective controls were made in 1 ml of PBS 1X, corresponding to 1.5×10^8 CFU/ml. Subsequently, in a 96-well plate, 200 µl of each mixture was added in its respective well and 1 µl of anti-*H. pylori* antibodies were added labeled with FITC and incubated for one hour at room temperature and in the dark.

At the end of the incubation time, 10 µl of each sample was added to a coverslip and observed in the LSE NL confocal spectral microscope, LSM780, which has the Center for Advanced Microscopy (CMA) of the Universidad de Concepción. The objective used was the

Apochromatic Plan 63X NA 1.4 plus zoom up to 2X. The obtained fluorescent images correspond to a thick plane of 2-4 μm (Zen 2012 acquisition software).

2.7. Fluorescent light microscopy assay

After observing, through optical microscopy and immunofluorescence, the mixtures between *H. pylori* and *C. albicans*, the bacterial viability kit BacLight (Invitrogen, USA) was used, according to the manufacturer's instructions, to demonstrate the viability of *H. pylori* in mixtures with *C. albicans*, by means of fluorescence microscopy.

3. RESULTS Y DISCUSSION

3.1. Bacterial viability assay from mixtures between *H. pylori* and *C. albicans*



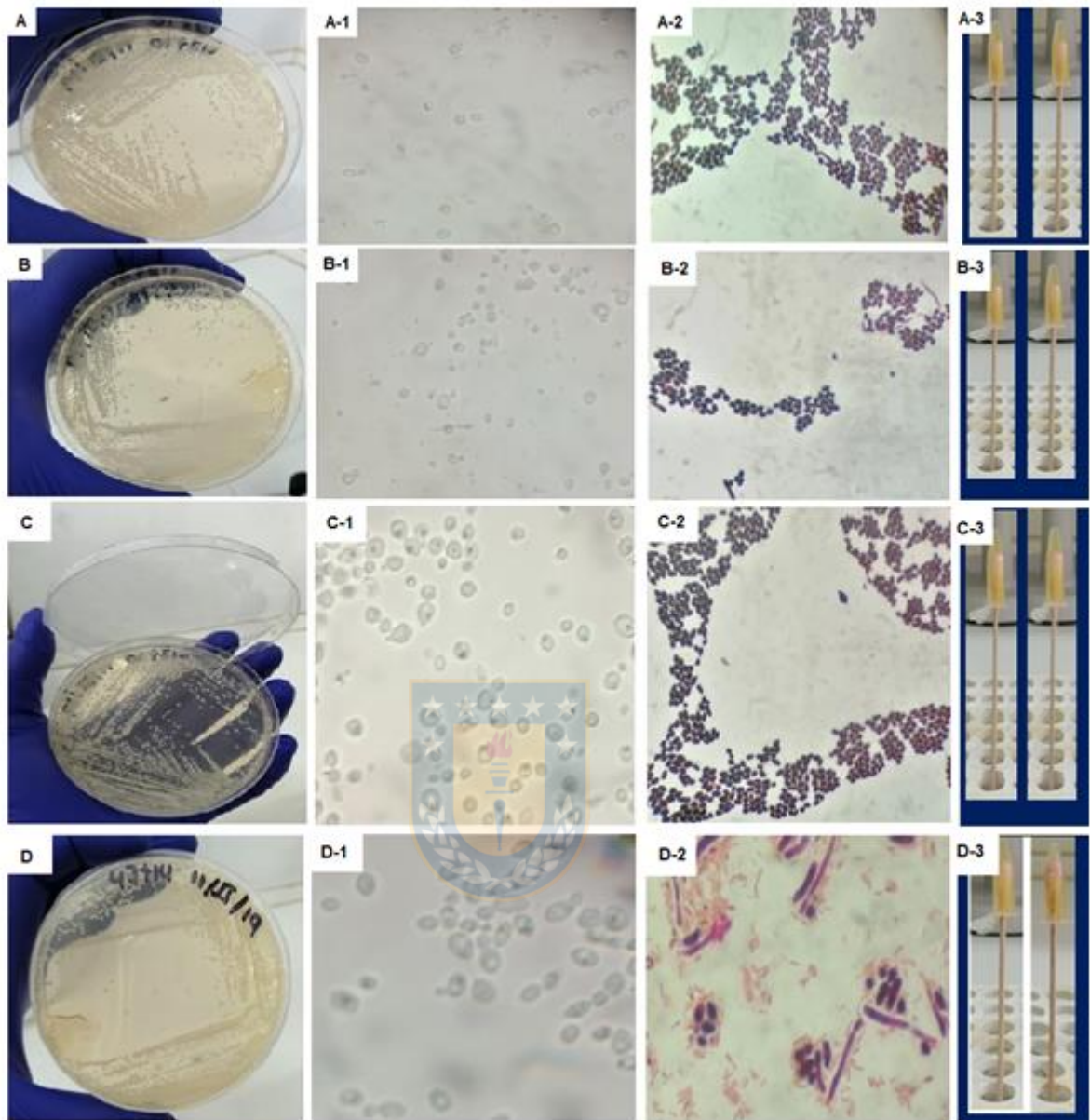


Figure 1. Images of the microorganism mixtures in YPD broth: *H. pylori* ATCC J99 + *C. albicans* ATCC 10231 (A), *H. pylori* ATCC J99 + *C. albicans* ATCC 14053 (B), *H. pylori* ATCC 43504 + *C. albicans* ATCC 10231 (C) and *H. pylori* ATCC 43504 + *C. albicans* ATCC 14053 (D), respectively. In addition, A-1, B-1, C-1 and D-1 are images in fresh of growth media observed by optical microscopy, at 40X. A-2, B-2, C-2 and D-2 are images of Gram stain, at 100X and A-3, B-3, C-3 and D-3 are images of respective urease tests.

In order to establish if *H. pylori* is able to remain viable in the presence of *C. albicans* strains even under unfavorable conditions such as those described above (aerobiosis and in YPD broth for 18 days of incubation), the mixtures were observed in fresh, through Gram stain and

applying the urease test (with negative result). Under these conditions, yeast and coccoid structures were observed that correspond to cells of *C. albicans* and *H. pylori*, respectively. This confirmed the nutritional and physical requirements of microaerophilic bacteria, such as *H. pylori* (Albertson *et al.*, 1998; Andersen *et al.*, 2000).

Subsequently, when sub-culturing under favorable conditions for *H. pylori* such as Columbia agar supplemented with 7 % fetal bovine serum, more urea at a concentration of 5 mM and incubated at 37 °C, in a microaerobic atmosphere for 4 days. Gram-negative structures corresponding to *H. pylori* were observed when performing Gram staining, which were observed co-aggregated to the periphery of the yeasts. The urease test was positive for the mixture of *H. pylori* strain ATCC 43504 in the presence of *C. albicans* strain ATCC 14053 (Figure 1).

On the other hand, the other mixtures of the other evaluated strain of *H. pylori* remained in their coccoid state, being negative urease. These results suggest that there is probably a specific interaction between the strain of *C. albicans* ATCC 14053 and *H. pylori* ATCC 43504 promoting the morphological transition from the coccoid state to the bacillary state of the bacteria. In this sense, it has been reported that *C. albicans* has the ability to reduce oxygen levels to values required by microaerophilic bacteria, and therefore, its presence can provide growth stimulating factors for bacteria in a manner analogous to those resulting from metabolism of nutrients (O'Sullivan *et al.*, 2000; Huang *et al.*, 2015; Xu *et al.*, 2015; Nobbs *et al.*, 2015). According to the above, a possible explanation of the result observed in the system *H. pylori* ATCC 43504 + *C. albicans* ATCC 14053 is that the strain of *C. albicans* ATCC 14054 has the capacity to generate microaerobic environments by reducing the levels of oxygen. However, the results obtained are also consistent with the fact that the coccoid form possesses a metabolism with the ability to synthesize DNA and certain enzymes such as acid phosphatase, alkaline phosphatase and catalase being capable to active the transition from the coccoid morphology to the bacillary (Koo *et al.*, 2018). In particular, catalase is of great importance for the bacteria to neutralize the effects of toxic oxygen species induced by an aerobic atmosphere in order to guarantee their survival under stress conditions, however, the coccoid form remained in *H. pylori* ATCC J99 + *C. albicans* ATCC 10231, *H. pylori* ATCC J99 + *C. albicans* ATCC 14053 and *H. pylori* ATCC 43504 + *C. albicans* ATCC 10231, suggesting that a more complex mechanism might be acting. Thus, our preliminary study of mixtures between *H. pylori* and *C. albicans* suggests that the observed morphological transition originates in specific interactions between this strain with *C. albicans* ATCC 14053. In order to advance in the understanding of *H. pylori* and *C. albicans* interactions several experiments were performed and these are shown below.

3.2. Immunofluorescence detection assay

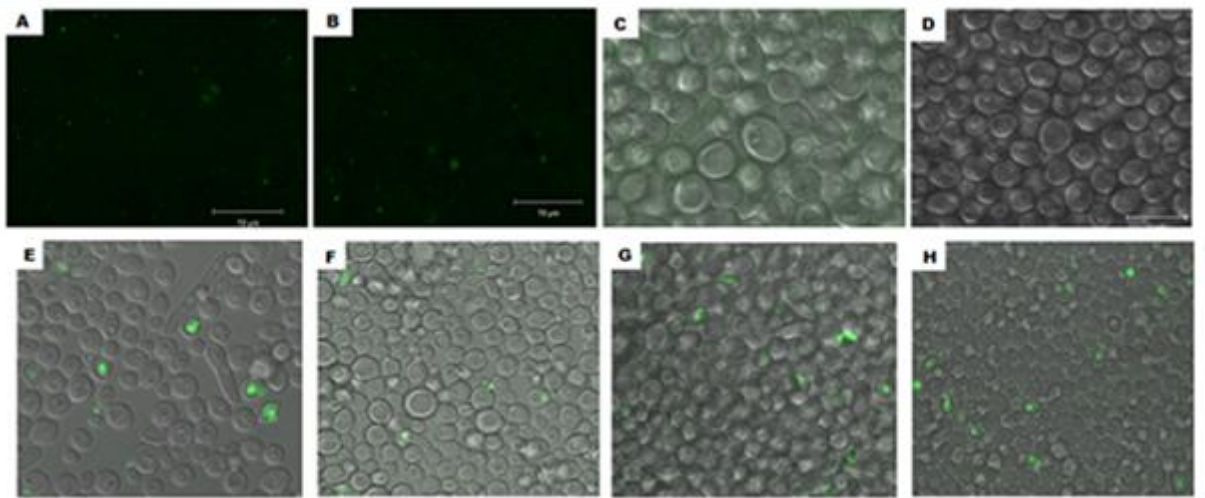


Figure 2. Image of immunofluorescence of mixtures of *H. pylori* and *C. albicans*. A, B, C and D correspond to the controls of *H. pylori* ATCC J99, *H. pylori* ATCC 43504, *C. albicans* ATCC 10231 and *C. albicans* ATCC 14053, respectively. Mixtures of four days of incubation at 37 °C in microaerophilia are identified to be *H. pylori* ATCC J99 + *C. albicans* ATCC 10231 (E), *H. pylori* ATCC J99 + *C. albicans* ATCC 14053 (F), *H. pylori* ATCC 43504 + *C. albicans* ATCC 10231 (G) and *H. pylori* ATCC 43504 + *C. albicans* ATCC 14053 (H).

From the immunofluorescence technique, mixtures of *H. pylori* and *C. albicans* were analyzed under the growth conditions described above, where a green fluorescence was observed, corresponding to *H. pylori*, which is observed in different parts of the yeast, with positions, centric (see Figure 2, image H), internal periphery and anchored on the external surface of the yeast (see Figure 2, image F) in its different stages, for example, in image E it is observed that *C. albicans* 10231 is in the budding state with two green fluorescence patterns located in each gem. The results suggest a close interaction between yeast and bacteria, because no external fluorescence was observed in the external environment. However, it is not possible to say exactly that the bacteria found in the intracellular space are located in an exclusive organelle such as the yeast vacuole, nor can it be ruled out that the bacterium is in an 'eclipse position', i.e., that the image corresponds to the fact that the bacteria could be located below or above the yeast, due to the fact that in the procedure the fixation was not carried out prior to incubation with the polyclonal antibody. Previous studies suggest that *H. pylori* has evolved to invade eukaryotic cells such as *C. albicans*, establish and remain viable within the yeast vacuole, as well as replicate and transmit to future generations, because it has developed strategies that allow it to interrupt the maturation of the normal endosome and the ability to fuse with the lysosome. In this context, and not conclusively, it has been proposed that the

bacteria-yeast symbiotic interaction is the result of a defense mechanism in environmental stress conditions, host immune system and antibacterial therapy (Zheng *et al.*, 1999; Saniee *et al.*, 2013).

It is important to consider that the mechanisms of interaction and internalization between *H. pylori* and eukaryotic cells with only cellular membrane, such as gastric epithelial cells, immunocytes, macrophages, among others, are better understood, whereas the internalization of *H. pylori* in cells of microorganisms with cell wall is still a matter of discussion. Several studies have reported that the bacterial-eukaryotic cell interaction is mediated by adhesins such as BabA and SabA, the latter having a role of great importance, because it stimulates G proteins, activates phagocytosis and the oxidative burst reactions of neutrophils and I get phosphorylation signaling, responsible for triggering the remodeling of the actin skeleton (Evans *et al.*, 1992; Dubois and Borén, 2007; Saniee *et al.*, 2013). In the case of the interactions between *H. pylori* and *C. albicans*, the internationalization hypothesis is clearly an extrapolation of the interaction by internalization of *H. pylori* - eukaryotic cells and amoebae characterized by having only a cell wall, aspects that contrast with the presence of wall in the *C. albicans* (Björkholm *et al.*, 2000; Mella *et al.*, 2016). Since cellular wall is understood to be a dynamic structure, in principle, arguments based on rigid nature of wall are not sufficient to eliminate the internationalization possibility (Alfatah *et al.*, 2017). Today, it is accepted that the wall has a specie-dependent plasticity allowing different cell morphologies, molecular remodeling and compositional changes as a result from adaptation to the surrounding environment (Lipke and Ovalle, 1998; Xie and Lipke, 2010; Skrebinska *et al.*, 2018), e.g., transglutaminase-type proteins (TGAm) are involved in the formation of covalent linkages associated with cell wall stability, differentiation, growth regulation, cellular adhesion, tissue integrity, and protection against environmental changes; however, the existence of TGAm is an example of the possibility to induce dynamic change in the wall of yeast by biochemical affecting. Inhibition of TGAm and affecting of wall and features associated with the functions of TGAm have been described (Xie and Lipke, 2010).

3.3. Fluorescent light microscopy assay

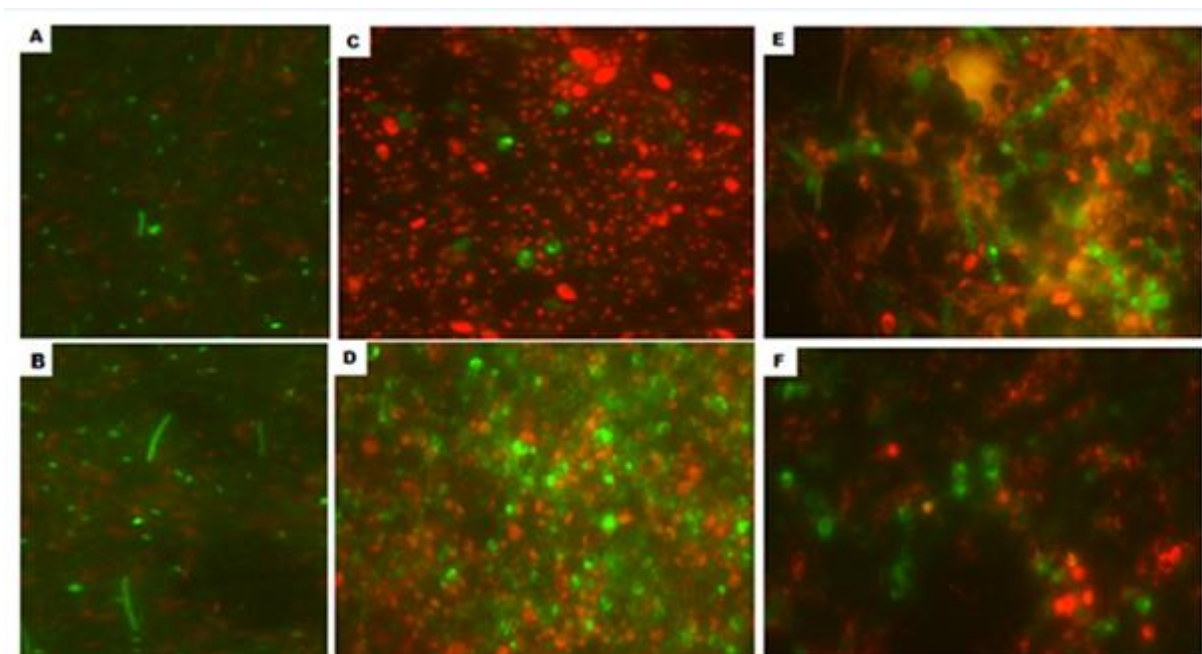


Figure 3. Images of fluorescent light microscopy of mixtures of *H. pylori* and *C. albicans*: Controls of *H. pylori* ATCC J99 y *H. pylori* ATCC 43504 (A and B, respectively) and mixtures of *H. pylori* ATCC J99 + *C. albicans* ATCC 10231, *H. pylori* ATCC J99 + *C. albicans* ATCC 14053, *H. pylori* ATCC 43504 + *C. albicans* ATCC 10231 and *H. pylori* ATCC 43504 + *C. albicans* ATCC 14053, (C, D, E and F, respectively).

The viability of the mixtures of *H. pylori* and *C. albicans* was evaluated using the Bac Light™ kit, which uses two nucleic acid dyes, SYTO® 9 that emits a green fluorescence and has the ability to penetrate both intact and damaged membranes, while propidium iodide emits a red fluorescence that reduces the green fluorescence emitted by SYTO® 9 by penetrating damaged membrane cells (Boulos *et al.*, 1999). The results obtained through the implementation of this technique are shown in Figure 3.

According to the basis of the technique, which uses as a criterion to differentiate between viable and dead bacteria cell and membrane integrity (Gregori *et al.*, 2001; Reyna-Beltrán *et al.*, 2018), a greater number of viable cells was observed in the samples D, E and F, whereas in C, the number of viable cells observed is lower, with dead cells predominating. However, in this context, it is important to indicate that the presence of cells that maintain their membrane being metabolically inactive is also possible since these only can lose the ability to grow in microbiological culture media (i.e., viable non-culturable cells or VBNC), and therefore, their description should be considered within the possible results of the technique (Cunningham *et al.*, 2009). On the other hand, in relation to cell morphology, the results show cells of larger size, oval and hyphal that correspond to *C. albicans*, while in their interior some have oval

structures of smaller size, possibly corresponding to *H. pylori* in a coccoid state, because the reduction in cell size and round appearance is commonly found in cells VBNC, as it has been reported for *Campylobacter* spp., *Burkholderia pseudomallei*, *Vibrio cholerae*, among others, and which is associated with a strategy to minimize energy requirements (Stiefel *et al.*, 2015). The previous approach is consistent with the fact that *H. pylori* is in unfavorable physical and environmental conditions, such as nutrient starvation (Laam *et al.*, 2014) and the presence of oxygen (Cook and Bolster, 2007).

The results suggest the existence of a close bacterium-yeast interaction that could possibly be established as a defense strategy against stress conditions for *H. pylori*, which would change from a bacillary to a coccoid state until the optimal conditions for the bacterium, such as nutrients and microaerobic atmosphere, are restored. Thus, the morphological interconversion between cellular states, that is, to pass from the coccoid state to a bacillary state, is found to be promoted by interactions between specific strains, such as *H. pylori* ATCC 43504 and *C. albicans* ATCC 14053 (see Figure 1, images D to D-3) and not necessarily a generalized interaction between these microorganisms. The above was confirmed by classical microbiological techniques: microbial cultures, Gram stain and urea test. Conversely, results obtained with the other strains of *H. pylori* and the same yeast shown by fluorescence microscopy that their cell membranes are not affected, but morphological interconversion at the cellular level was not evidenced.

4. CONCLUSIONS

The results suggest the existence of a strong bacterium-yeast surface interaction between *H. pylori* and *C. albicans* that could be the result of stress conditions for *H. pylori*, which, depending of bacterial strain, permits the change from a bacillary to a coccoid state until the optimal conditions for the bacterium are restored. In addition, interaction by internalization between *H. pylori* and *C. albicans* was not evidenced from SEM and TEM analyses, suggesting that the 'apparent internalization' observed by immunofluorescence detection assay and fluorescent light microscopy assay can be the result of surface anchoring on yeast surface that produces an optical overlap with the largest cell in the background.

ACKNOWLEDGMENTS. Authors thanks to project VRID-Enlace, N0291/18 by the funds for the performing of the project. Sixta L. Palencia thanks to CONICYT for doctoral fellowship.

REFERENCES

- Mahnaz, A.M., Chamanrokh, P., Whitehouse, C.A., Huq, A. 2015. Methods for detecting the environmental coccoid form of *Helicobacter pylori*. *Front. Public Health* 3, 147.
- Cover, T.L., Blaser, M.J. 2009. *Helicobacter pylori* in health and disease. *Gastroenterol.* 136,1863–1873.
- Nardone, G., Compare, D. 2015. The human gastric microbiota: Is it time to rethink the pathogenesis of stomach diseases? *United Eur. Gastroenterol. J.* 3, 255–260.
- Atherton, J.C. 2006. The pathogenesis of *Helicobacter pylori*-induced gastro-duodenal diseases. *Annual Rev. Pathol.: Mechanisms of Disease* 1, 63–96.
- Serrano, A., Hernández, C.M., De la Garza, S.J., Herrera, L.A. 2009. *Helicobacter pylori* y cáncer gástrico. *Cancerología* 4, 193–204.
- Correa, P., Piazzuelo, M.B., Camargo, M.C. 2006. Etiopathogenesis of gastric cancer. *Scandin. J. Surg.* 95, 218–224.
- Reshetnyak, V.I., Reshetnyak, T.M. 2017. Significance of dormant forms of *Helicobacter pylori* in ulcerogenesis. *World J. Gastroenterol.* 23, 4867–4878.
- Kaprelyants, A.S., Gottschal, J.C., Kell, D.B. 1993. Dormancy in non-sporulating bacteria. *FEMS Microbiol. Lett.* 10, 271–286.
- Krzyżek, P., Biernat, M.M., Gościński, G. 2018. Intensive formation of coccoid forms as a feature strongly associated with highly pathogenic *Helicobacter pylori* strains. *Folia Microbiol.* 64, 273 – 281.
- Palencia, S.L., Lagos, G., García, A. 2016. Fungi-bacterium interactions: *Helicobacter pylori* -*Candida albicans*. *J. Sci. Technol. Appl.* 1, 53–69.
- Shleeva, M., Kondratieva, T., Rubakova, E., Vostroknutova, G., Kaprelyants, A., Apt A. 2015. Reactivation of dormant “non-culturable” *Mycobacterium tuberculosis* developed *in vitro* after injection in mice: Both the dormancy depth and host genetics influence the outcome. *Microb. Pathog.* 78, 63–66.
- Shleeva, M.O., Bagramyan, K., Telkov, M.V., Mukamolova, G.V., Young, M., Kell, D.B., Kaprelyants, A.S. 2002. Formation and resuscitation of ‘nonculturable’ cells of *Rhodococcus rhodochrous* and *Mycobacterium tuberculosis* in prolonged stationary phase. *Microbiol.* 148,1581–1591.
- Gibbon, L.T., Barer, M.R. 1995. Oxidative Metabolism in Nonculturable *Helicobacter pylori* and *Vibrio vulnificus* Cells Studied by Substrate-Enhanced Tetrazolium Reduction and Digital Image Processing. *Appl. Environ. Microbiol.* 3379–3384.
- Andersen, L.P., Dorland, A., Kara, H. 2000. Possible Clinical Importance of the Transformation of *Helicobacter pylori* into Coccoid Forms. *Scandin. J. Gastroenterol.* 2000; 35, 897–903.
- Albertson, N., Wenngren, I., Sjöström, J.E. 1998. Growth and Survival of *Helicobacter pylori* in Defined Medium and Susceptibility to Brij 78. *J. Clinical Microbiol.* 36, 1232–1235.
- Huang, J.Y., Sweeney, E.G., Sigal, M., Kuo, C.J., Guillemin, K., Amieva, M.R. 2015. Chemodetection and Destruction of Host Urea Allows *Helicobacter pylori* to Locate the Epithelium. *Cell Host & Microbe* 18, 147–156.
- O’Sullivan, J.M., Jenkinson, H.F., Cannon, R.D. 2000. Adhesion of *Candida albicans* to oral streptococci is promoted by selective adsorption of salivary proteins to the streptococcal cell surface. *Microbiol.* 146, 41–48.
- Xu, H., Jenkinson, H.F., Dongari-Bagtzoglou, A. 2015. Innocent until proven guilty: mechanisms and roles of *Streptococcus* - *Candida* interactions in oral health and disease. *Mol Oral Microbiol.* 29, 99–116.
- Nobbs, A.H., Jenkinson, H.F. 2015. Interkingdom networking within the oral microbiome. *Microbes Infect.* 17, 484–492.
- Koo, H., Andes, D.R., Krysan, D.J. 2018. *Candida* – streptococcal interactions in biofilm-associated oral diseases. *PLOS Pathog.* 14, 1–7.
- Zheng, P.Y., Hua, J., Ng, H.C., Ho, B. 1999. Unchanged characteristics of *Helicobacter pylori* during its morphological conversion. *Microbios* 98, 51–64.
- Saniee, P., Siavoshi, F., Nikbakht, B.G., Khormali, M., Sarrafnejad, A., Malekzadeh, R. 2013. Localization of *H. pylori* within the Vacuole of *Candida* Yeast by Direct immunofluorescence Technique. *Arch. Iran. Med.* 16, 705–710.

- Saniee, P., Siavoshi, F., Nikbakht, B.G., Khormali, M., Sarrafnejad, A., Malekzadeh, R. 2013. Immunodetection of *H. pylori*-specific protein in oral and gastric *Candida* yeasts. *Arch. Iran. Med.* 16, 624–630.
- Dubois, A., Borén, T. 2007. *Helicobacter pylori* is invasive and it may be a facultative intracellular organism. *Cell Microbiol.* 9, 1108–1116.
- Evans, D.G., Evans, D.J., Graham, D.Y. 1992. Adherencia e internalización de *Helicobacter pylori* por células HEp-2. *Gastroenterol.* 102, 1557–1567.
- Björkholm, B., Zhukhovitsky, V., Löfman, C., Hultén, K., Enroth, H., Block, M., Engstrand, L. 2000. *Helicobacter pylori* Entry into Human Gastric Epithelial Cells: A Potential Determinant of Virulence, Persistence, and Treatment Failures. *Helicobacter* 5, 148–154.
- Mella, C., Medina, G., Flores-Martina, S., Toledo, Z., Simaluiza, R.J., Pérez-Pérez, G., Fernández, H. 2016. Interaction between zoonotic bacteria and free living amoebas. A new angle of an epidemiological polyhedron of public health importance? *Arch. Med. Vet.* 48: 1–10.
- Alfatah, M.D., Bari, V.K., Nahar, A.S., Bijlani, S., Ganesan, K. 2017. Critical role for CaFEN1 and CaFEN12 of *Candida albicans* in cell wall integrity and biofilm formation. *Scientific Reports* 7, 1–12.
- Skrebinska, S., Mégraud, F., Bessède, E. 2018. Diagnosis of *Helicobacter pylori* infection. *Helicobacter* 23(Suppl. 1), e12515.
- Lipke, P.N., Ovalle, R. 1998. Cell wall architecture in yeast: new structure and new challenges. *J. Bacteriol.* 180, 3735–3740.
- Xie, X., Lipke, P.N. 2010. On the evolution of fungal and yeast cell walls. *Yeast* 27, 479–488.
- Boulos, L., Prevost, M., Barbeau, B., Coallier, J., Desjardins, R. 1999. LIVE/DEAD (R) BacLight (TM): application of a new rapid staining method for direct enumeration of viable and total bacteria in drinking water. *J. Microbiol. Meth.* 37, 77–86.
- Reyna-Beltrán, E., Bazán, C., Iranzo, M., Mormeneo, S., Luna, J. The Cell Wall of *Candida albicans*: A Proteomics View. in: <https://www.intechopen.com/books/candida-albicans/the-cell-wall-of-candida-albicans-a-proteomics-view> DOI: 10.5772/intechopen.82348.
- Gregori, G., Citterio, S., Ghiani, A., Labra, M., Sgorbati, S., Brown, S., Denis, M. 2001. Resolution of Viable and Membrane-Compromised Bacteria in Freshwater and Marine Waters Based on Analytical Flow Cytometry and Nucleic Acid Double Staining. *Appl. Environ. Microbiol.* 4662–4670.
- Cunningham, E., O'Byrne, C., Oliver, J.D. 2009. Effect of weak acids on *Listeria monocytogenes* survival: Evidence for a viable but nonculturable state in response to low pH. *Food Control*, 1141–1144.
- Stiefel, P., Schmidt-Emrich, S., Maniura-Weber, K., Ren, Q. 2015. Critical aspects of using bacterial cell viability assays with the fluorophores SYTO9 and propidium iodide. *BMC Microbiol.* 15, 1–9.
- Laam, Li., Mendis, N., Trigui, H., Oliver, J.D., Faucher, S.P. 2014. The importance of the viable but non-culturable state in human bacterial pathogens. *Front. Microbiol.* 5, 1–20.
- Cook, K.L., Bolster, C.H. 2007. Survival of *Campylobacter jejuni* and *Escherichia coli* in groundwater during prolonged starvation at low temperatures. *J. Appl. Microbiol.* 103, 573–583.
- [39] Kana, B.D., Gordhan, B.G., Downing, K.J., Sung, N., Vostroktunova, G., Machowski, E.E., Mizrahi, V. 2008. The resuscitation-promoting factors of *Mycobacterium tuberculosis* are required for virulence and resuscitation from dormancy but are collectively dispensable for growth in vitro. *Molec. Microbiol.* 67, 672–684.
- Quaglia, N.C., Dambrosio, A. 2018. *Helicobacter pylori*: A foodborne pathogen? *World J. Gastroenterol.* 24, 3472–3487.

Capítulo VIII: Discusión

El estudio de microorganismos mediante cultivos axénicos fue un pilar esencial para el nacimiento de la bioquímica y la biología molecular moderna. Sin embargo, en la década de 1870 microbiólogos como Luis Pasteur, informaron fenómenos resultantes de las interacciones existentes entre comunidades de múltiples especies [33] que producen un amplio espectro de situaciones asociadas con la patogenicidad, nutrición, adquisición de genes, transporte, construcción de nichos y estructuras comunitarias, entre otras [34]. Siendo dichas situaciones diferentes en un estado planctónico, que es representado por el 1% de los microorganismos (**Artículo 2.** Polymicrobial Biofilms: Fundamentals, diseases, and treatments – A review).

Lo anterior, aumentó exponencialmente estudios multidisciplinarios asociados a las interacciones microbianas, que integraron el desarrollo de herramientas de biología molecular, genómica, ecología química y microbiana, biofísica y modelos ecológicos [35]. Las interacciones entre levaduras y bacterias son de gran importancia para el entendimiento de los distintos procesos que se desencadenan entre estos microorganismos, en condiciones reales de hábitat y colonización. La complejidad que surge por la presencia de estas interacciones hace que sea necesario describir las interacciones en diferentes niveles (biológicos, fisicoquímicos y bioquímicos) que en muchas ocasiones son interdependientes. Además, es claro que las interacciones deben ser descritas en términos de cada par o grupo de especies. En el caso particular de las interacciones entre *C. albicans* y *H. pylori*, no se dispone de una descripción completa sobre las interacciones que pueden tener lugar; además, los mecanismos de interacción que se han reportado son débilmente entendidos y estas basados sólo en la descripción de observaciones experimentales de un número relativamente pequeño de autores. De acuerdo a lo anterior, fue necesario avanzar en el estudio de las interacciones entre estos dos microorganismos (*C. albicans* y *H. pylori*) por su impacto en la salud humana, lo que implicó el desarrollo de nuevas estrategias para dichos estudios, en lo posible de aplicabilidad general (**Artículo 1,** Fungi-bacterium interactions: *Helicobacter pylori* - *Candida albicans*), es decir, no sólo describir los posibles tipos de interacciones desde un punto de vista ecológico, sino diseñar cómo medirlas, lo cual se convirtió a nivel científico en un reto metodológico y con gran impacto a nivel de las ciencias microbiológicas. En este contexto, se direccionó el presente trabajo a la integración interdisciplinaria de la microbiología y ciencia básica, como la química, con el firme propósito de aportar con nuevas herramientas y estrategias que permitieran vislumbrar los posibles

mecanismos moleculares implicados en las interacciones bacteria levadura (*H. pylori*- *C. albicans*).

La superficie de los microorganismos además de la función biológica habitual que cumplen, proporciona una interfaz vital para las interacciones patógeno-huésped y la interacción con otros microorganismos [36-37]. Existe un gran número de métodos para el estudio de superficies microbianas como: Microscopía Electrónica de Barrido (SEM), Microscopía Electrónica de Transmisión (TEM), Microscopía de Fluorescencia (FM) que requieren un pretratamiento “destrutivo” de la muestra y consigo, la alteración de la integridad celular y contaminación por componentes de membrana interna [38], produciendo pérdida de información valiosa sobre la composición real de la superficie, lo que genera un sesgo o “ventana oscura” que limita la posibilidad de una clara identificación estructural de las superficies microbianas, las cuales, son el pilar central y esencial para el estudio de interacciones. Es por ello que nos centramos en la selección y aplicación de un método no destructivo, rápido, fácil de usar y altamente sensible [39] como la Espectroscopia Infrarroja (espectroscopia IR) [40]. Sin embargo, sus mayores limitaciones son la alta similitud espectral entre los espectros de diferentes microorganismos, y la superposición y ensanchamiento de señales adyacentes [41]. Lo anterior, direccionó el desarrollo y aplicación de una potente herramienta analítica, llamada espectroscopia derivada funcionalmente mejorada (FEDS) [40 - 42] (Objetivo específico 1, capítulo IV y V), que se caracteriza por ser un método sencillo para obtener la desconvolución espectral y el aumento de la resolución espectral de las señales [43]. Lo cual permitió la caracterización del espectro vibratorio de la superficie exterior de *H. pylori* y *C. albicans* mediante el espectro vibratorio de infrarrojo medio (IR) y espectroscopia derivada funcionalmente mejorada (FEDS), obteniendo patrones característicos y claves de la composición superficial de la membrana externa de *H. pylori* y *C. albicans* [44-45].

Los resultados obtenidos en la caracterización de la superficie de *H. pylori* (ATCC 43504 y J99), a partir de espectroscopía de infrarrojo medio, evidenciaron señales similares a las descritas para diversos microorganismos en varias investigaciones [46- 47] y, aunque se puede obtener información importante de ellos, para el análisis específico de la superficie externa de *H. pylori* no son muy útiles, debido que para ambas cepas los espectros IR son muy similares, siendo el coeficiente de correlación (R^2) calculado alrededor de 0.9906, en consecuencia, la información diferenciadora contenida en los espectros es inferior al 10 %. Mediante un análisis clásico de los espectros IR, se podría concluir que las dos cepas en

estudio son las mismas. En consecuencia, este primer análisis permite señalar que no es posible diferenciar las cepas de *H. pylori* utilizando el método clásico para la interpretación de espectros IR. Sin embargo, está claro que algunas señales se pueden utilizar para la supervisión de los cambios de superficie, ya que éstos son fáciles y correctamente identificados. Es importante resaltar que la aplicación de FEDS a los espectros clásicos de IR, permitieron identificar vibraciones moleculares asociadas a los grupos funcionales S-H del aminoácido cisteína característico de las proteínas de membrana externa de *H. pylori* [48-49], que generalmente no se identifican en IR y fue posible constatar a través del análisis computacional de la teoría funcional de la densidad. Este es el primer trabajo a nivel mundial que utiliza la herramienta de FEDS para estudios microbiológicos, permitiendo establecer patrones de diferenciación entre las cepas de *H. pylori*. Aporte clave para el estudio de interacciones célula-célula y célula-superficie entre microorganismos, incluido el estudio de biopelículas polimicrobianas.

Por otra parte, se ha informado la co- existencia de *H. pylori* y *C. albicans* en biopsias gástricas de pacientes con gastritis, que inevitablemente impacta negativamente el éxito del tratamiento de úlceras gástricas bacterianas, pero también, podría tener implicaciones para la adaptabilidad de *H. pylori* en ambiente exgástrico, su prevalencia y patogenicidad [50 -52]. Para determinar los tipos de interacción entre *H. pylori* y *C. albicans* (Objetivo 2. Capítulo VI) se desarrolló e implementaron técnicas metodológicas de análisis, como espectroscopía infrarroja, análisis de desconvolución, microscopías electrónicas de transmisión y escaneo, microscopía óptica, dispersión dinámica de la luz, ángulo de contacto, electroforesis de gel de agarosa y amplificación genética, que hicieron posible identificar los múltiples mecanismos de interacción superficial que dirigen el anclaje, la co-agregación y la formación de biopelícula polimicrobiana entre *C. albicans* y *H. pylori*, mediadas por: (i) interacciones hidrofóbicas entre cadenas de péptidos no polares y estructuras lipídicas, (ii) enlaces de hidrógeno entre componentes superficiales de levadura y bacteria e (iii) interacciones superficiales mediadas por el grupo funcional thiol.

Estos resultados son un significativo aporte científico desde el punto de vista metodológico experimental, más aún ayuda a la comprensión de la patogénesis de *H. pylori* y a correlacionar la interacción como un posible causante del fracaso de los medicamentos utilizados para la erradicación de *H. pylori* en el ambiente gástrico [53- 54]. Si bien el campo de la investigación de biopelículas de *H. pylori* es bastante nuevo, se ha informado en

ensayos *in vitro* que *H. pylori* asociado a biopelículas es más resistente a la claritromicina, en comparación a su estado planctónico [55].

Para establecer si *H. pylori* es capaz de permanecer viable en presencia de cepas de *C. albicans* (Objetivo 3. Capítulo VII) generando condiciones desfavorables. Se realizó ensayo de viabilidad bacteriana de co-cultivos entre *H. pylori* y *C. albicans*, donde se realizó seguimientos seriados de montajes en fresco, tinción de Gram y la prueba de ureasa. Donde efectivamente se observó estructuras de levaduras y formas cocoides que corresponden a células de *C. albicans* y *H. pylori*, respectivamente; sin embargo, se evidenció la transición del estado cocoide a un estado bacilar en el co-cultivo correspondiente a la cepa de *H. pylori* ATCC 43504 y *C. albicans* ATCC 14053, al proporcionar condiciones favorables para la bacteria (agar columbia, suplementado al 7% con suero de caballo, 5 mM de urea e incubadas en un ambiente microaerofílico). Además, se observaron los fenómenos de anclaje y coagregación, mediante la tinción de Gram y microscopía electrónica de barrido, lo cual se correlacionó perfectamente con los resultados anteriormente expuestos en el capítulo VI, al indicar los procesos iniciales para la interacción superficial entre estos dos microorganismos. Sin embargo, no se logró establecer los posibles mecanismos involucrados que promovieron la interconversión o transición morfológica del estado cocoide al estado bacilar de cepas específicas (*H. pylori* ATCC 43504 y *C. albicans* ATCC 14053), mientras que los demás co-cultivos de las cepas en estudio, mantuvieron un estado cocoide y la prueba de ureasa negativa [56].

En los ensayos de detección por inmunofluorescencia se observó una fluorescencia verde, correspondiente a *H. pylori*, la cual se observa en diferentes partes de la levadura, con posiciones céntricas, periferia, interna y anclado en la superficie externa de la levadura. Sin embargo, no es posible decir con exactitud la ubicación de las bacterias, ni se puede descartar que la bacteria esté en 'posición de eclipse', es decir, que la imagen corresponde al hecho de que la bacteria pudo estar ubicada por debajo o por encima de la levadura, debido a que en el procedimiento no se realizó la fijación previa a la incubación con el anticuerpo policlonal. Estudios previos sugieren que *H. pylori* ha evolucionado para invadir células eucariotas como *C. albicans*, establecerse y permanecer viable dentro de la vacuola de levadura [57-58], diferentes estudios sugieren la remodelación del esqueleto de actina [59-60], plasticidad dependiente de la especie que permite diferentes morfologías celulares, remodelación molecular y cambios composicionales como resultado de la adaptación al entorno circundante [61-64].

Conclusiones

1. Nuestros resultados confirman la importancia de estudiar los microorganismos como parte de comunidades de especies mixtas en lugar de forma aislada, debido a que esto contribuirá a la comprensión de los diferentes tipos de interacción que se puedan establecer entre bacterias y hongos.
2. Además de las señales típicas asociadas con el espectro IR de microorganismos, por FEDS, se puede realizar una mejor y detallada descripción de la membrana externa de las biopelículas de *H. pylori*. En particular, IR+FEDS puede realizar satisfactoriamente la detección y monitoreo de proteínas ricas en cisteína.
3. La transformada de FEDS del espectro IR medio es una poderosa herramienta analítica para mejorar el análisis espectral por espectroscopía IR. En el caso particular de las biopelículas de *C. albicans*, se observó que es posible realizar la deconvolución de señales y lograr una mejor diferenciación de las mismas. Para su interpretación debe considerarse los modelos moleculares de unidades de serina, treonina, glicina, alanina, ácido glutámico, prolina y N-acetil-D-glucosamina, por ser los componentes principales en la pared celular de *C. albicans*. De esta manera, se encontró que el espectro vibratorio de las biopelículas de *C. albicans* se puede entender considerando sólo los componentes principales de la pared celular.
4. La formación del biofilm polimicrobiano entre *C. albicans* y *H. pylori* ocurre a través de la combinación de diferentes mecanismos a nivel de superficie: interacciones hidrofóbicas entre cadenas de aminoácidos no polares y estructuras lipídicas, formación de enlaces de hidrógeno y anclaje covalente a través de la formación de enlaces disulfuro. Nuestros experimentos no evidenciaron internalización bacteriana e interacciones electrostáticas.
5. Se sugiere la existencia de una fuerte interacción superficie bacteria-levadura entre *H. pylori* y *C. albicans* que podría ser el resultado de condiciones de estrés para *H. pylori*, que, dependiendo de la cepa bacteriana, permite el cambio de un estado cocoide a un estado bacilar, a partir de cepas interactuantes específicas (*H. pylori* ATCC 43504 y *C. albicans* ATCC 14053) al restablecerse las condiciones óptimas para *H. pylori*.

Proyecciones

El conocimiento de los mecanismos involucrados en las interacciones entre *C. albicans* y *H. pylori* permitirá comprender la patogénesis microbiana, además de vislumbrar nuevas estrategias para el control de la infección bacteriana, que implicará redireccionar un diagnóstico mixto para identificar no sólo a *H. pylori*, sino además a *C. albicans*, así como la implementación de agentes fúngicos en el tratamiento para la erradicación bacteriana.

Es fundamental continuar con el estudio de interacciones microbianas, mediante la aplicación de (IR +FEDS) en conjunto con técnicas microbiológicas y moleculares con el firme objetivo de identificar los mecanismos involucrados en interacciones superficiales de microorganismos patógenos y por ende, de interés para la salud pública.

REFERENCIAS

- [1] Mesquita Braga R, Nóbrega Dourado M, L Araújo W (2016) Microbial interactions: ecology in a molecular perspective. *Brazilian Journal of Microbiology*, 4:1. [https://doi: 10.1016 / j.bjm.2016.10.005](https://doi.org/10.1016/j.bjm.2016.10.005)
- [2] Tshikantwa T.S, Ullah M.W, He F, Yang G (2018) Current Trends and Potential Applications of Microbial Interactions for Human Welfare. *Front. Microbiol*, 9:1156. <https://doi.org/10.3389/fmicb.2018.01156>
- [3] Palencia S, Lagos G, García A (2016) Fungi-bacterium interactions: *Helicobacter pylori*-*Candida albicans*. *Journal of Science with Technological Applications*. 53–69
- [4] Faust K, Raes J. (2012) Microbial interactions: from networks to models. *Nat. Rev. Microbiol.*10, 538–550. <https://doi:10.1038/nrmicro2832>
- [5] Zhu J, Yan Y, Wang Y, Qu D (2019) Competitive interaction on dual-species biofilm formation by spoilage bacteria, *Shewanella baltica* and *Pseudomonas fluorescens*. *Journal of Applied Microbiology* 126 (4): 1175-1186. <https://doi: 10.1111 / jam.14187>
- [6] Feichtmayer J, Deng L, Griebler C (2017) Antagonistic Microbial Interactions: Contributions and Potential Applications for Controlling Pathogens in the Aquatic Systems. *Front Microbiol* 8: 2192. <https://doi.org/10.3389/fmicb.2017.02192>
- [7] Araújo A, Jansen A, Bouchet F, Reinhard K, Ferreira L (2003) Parasitism, the Diversity of Life, and Paleoparasitology. *Mem Inst Oswaldo Cruz, Rio de Janeiro Vol. 98(Suppl. I): 5-11.* <https://doi.org/10.1590/S0074-02762003000900003>
- [8] Deveau A, Bonito G, Uehling J, Paoletti M, Becker M, Bindschedler S, Wick LY (2018) Bacterial–fungal interactions: ecology, mechanisms and challenges. *FEMS Microbiology Reviews*, 42(3): 335–352. <https://doi:10.1093/femsre/fuy008>
- [9] Quigley EM (2013) Gut bacteria in health and disease. *Gastroenterol Hepatol (N Y)*. 9(9):560-569. PMID: 24729765; PMCID: PMC3983973
- [10] Wang B, Yao M, Lv L, Ling Z, Li L (2017) The Human Microbiota in Health and Disease. *Engineering* 71-82. <https://doi.org/10.1016/J.ENG.2017.01.008>
- [11] Hold GL, Smith M, Grange C, Watt ER., El-Omar EM., Mukhopadhyaya I (2014) Role of the gut microbiota in inflammatory bowel disease pathogenesis: what have we learnt in the past 10 years?. *World journal of gastroenterology* 20(5): 1192–1210. <https://doi:10.3748/wjg.v20.i5.1192>
- [12] Roy J, Albert CH, Choler P, Clément JC, Ibanez S, Lavergne S, Saccone P, Zinger L, Geremia RA (2013) Microbes on the cliff: alpine cushion plants structure bacterial and fungal communities. *Front. Microbiol.* 4: 64. <https://doi:10.3389/fmicb.2013.00064>
- [13] Chen T, Nan Z (2015) Effects of phytopathogens on plant community dynamics: A review. *Acta Ecologica Sinica*, 35(6), 177–183. <https://doi: 10.1016 / j.chnaes.2015.09.003>

- [14] Duan G, Christian N, Schwachtje J, Walther D, Ebenhöf O (2013). The Metabolic Interplay between Plants and Phytopathogens. *Metabolites* 3(1): 1–23. <https://doi:10.3390/metabo3010001>
- [15] Kostic AD, Howitt MR., Garrett WS (2013) Exploring host-microbiota interactions in animal models and humans. *Genes & development* 27(7): 701–718. <https://doi:10.1101/gad.212522.112>
- [16] Strutzberg-Minder K, Tschentscher A, Beyerbach M, Homuth M., Kreienbrock L. (2018) Passive surveillance of *Leptospira* infection in swine in Germany. *Porcine Health Management*, 4(1). <https://doi:10.1186/s40813-018-0086-5>
- [17] Flint JF, Garner MR (2009) Feeding beneficial bacteria: A natural solution for increasing efficiency and decreasing pathogens in animal agriculture. *The Journal of Applied Poultry Research*, 18(2): 367–378. <https://doi:10.3382/japr.2008-00133>
- [18] Frey-Klett P, Burlinson P, Deveau A, Barret M, Tarkka M, Sarguinet A (2011) Bacterial-Fungal interactions: hyphens between agricultural, clinical, environmental, and food microbiologists. *Microbiol Mol Biol Rev* 75(4):583–609. <https://doi:10.1128/MMBR.00020-11>
- [19] Méar JB, Kipnis E, Faure E, Dessein R, Schurtz G, Faure K, Guery B (2013) *Candida albicans* and *Pseudomonas aeruginosa* interactions: more than an opportunistic criminal association? *Med Mal Infect* 43(4):146-51. <https://doi:10.1016/j.medmal.2013.02.005>.
- [20] Brand A, Barnes JD, Mackenzie KS, Odds FC, Gow NAR (2008) Cell wall glycans and soluble factors determine the interactions between the hyphae of *Candida albicans* and *Pseudomonas aeruginosa*. *FEMS Microbiology Letters*, 287(1): 48–55. <https://doi:10.1111/j.1574-6968.2008.01301.x>
- [21] Peters BM, Jabra-Rizk MA, Scheper MA, Leid JG, Costerton JW, Shirliff ME (2010) Microbial interactions and differential protein expression in *Staphylococcus aureus*–*Candida albicans* dual-species biofilms. *FEMS Immunology & Medical Microbiology* 59(3): 493–503. <https://doi:10.1111/j.1574-695x.2010.00710.x>
- [22] Peters BM, Ovchinnikova ES, Krom BP, Schlecht LM, Zhou H, Hoyer LL, Henk JB, Henny C.M, Mary Ann JR, Shirliff, ME (2012). *Staphylococcus aureus* adherence to *Candida albicans* hyphae is mediated by the hyphal adhesin Als3p. *Microbiology* 158(12): 2975–2986. <https://doi:10.1099/mic.0.062109-0>
- [23] Silverman RJ, Nobbs AH, Vickerman MM, Barbour ME, Jenkinson HF (2010). Interaction of *Candida albicans* Cell Wall Als3 Protein with *Streptococcus gordonii* SspB Adhesin Promotes Development of Mixed-Species Communities. *Infection and Immunity* 78(11): 4644–4652. <https://doi:10.1128/iai.00685-10>
- [24] Bamford CV, Mello A, Nobbs A.H, Dutton LC, Vickerman MM, Jenkinson HF (2009) *Streptococcus gordonii* Modulates *Candida albicans* Biofilm Formation through Intergeneric Communication. *Infection and Immunity* 77(9): 3696–3704. <https://doi:10.1128/iai.00438-09>
- [25] Xu H, Jenkinson HF, Dongari-Bagtzoglou A (2014) Innocent until proven guilty: mechanisms and roles of *Streptococcus-Candida* interactions in oral health and disease. *Molecular Oral Microbiology* 29(3): 99–116. <https://doi:10.1111/omi.12049>
- [26] Tshikantwa, TS, Ullah MW, He F, Yang G (2018) Current Trends and Potential Applications of Microbial Interactions for Human Welfare. *Frontiers in microbiology*, 9: 1156. <https://doi:10.3389/fmicb.2018.01156>
- [27] O'Brien S, Fothergill JL (2017). The role of multispecies social interactions in shaping *Pseudomonas aeruginosa* pathogenicity in the cystic fibrosis lung. *FEMS Microbiology Letters*, 364(15): <https://doi:10.1093/femsle/fnx128>
- [28] Morales DK, Jacobs NJ, Rajamani S, Krishnamurthy M., Cubillos-Ruiz JR, Hogan DA. (2010) Antifungal mechanisms by which a novel *Pseudomonas aeruginosa* phenazine toxin kills *Candida albicans* in biofilms. *Molecular Microbiology*, 78(6): 1379–1392. <https://doi:10.1111/j.1365-2958.2010.07414.x>
- [29] Zheng H, Kim J, Liew M, Yan JK, Herrera O, Bok JW, Wang Y (2015) Redox Metabolites Signal Polymicrobial Biofilm Development via the NapA Oxidative Stress Cascade in *Aspergillus*. *Current Biology* 25(1): 29–37. <https://doi:10.1016/j.cub.2014.11.018>
- [30] Lambouij JM, Hoogenkamp MA, Brandt BW, Janus MM, Krom BP (2017) Fungal mitochondrial oxygen consumption induces the growth of strict anaerobic bacteria. *Fungal Genet Biol* 109:1–6. <https://doi:10.1016/j.fgb.2017.10.001>.

- [31] Walker AW (2015) The Human Microbiota and Pathogen Interactions. *Molecular Medical Microbiology* 347–356. <https://doi.org/10.1016/b978-0-12-397169-2.00019-6>
- [32] Juan SD, Clara SS (2017) From the intestinal flora to the microbiome. *Rev Esp Enferm Dig* 2018;110(1):51-56. <https://doi.org/10.17235/reed.2018.4947/2018>
- [33] Stubbendieck, Reed M.; Vargas-Bautista, Carol; Straight, Paul D. (2016). Bacterial Communities: Interactions to Scale. *Frontiers in Microbiology*. doi:10.3389/fmicb.2016.01234
- [34] P. Frey-Klett, P. Burlinson, A. Deveau, M. Barret, M. Tarkka, A. Sarguinet (2011). Bacterial-Fungal Interactions: Hyphens between Agricultural, Clinical, Environmental, and Food Microbiologists. *Microbiol. Molecular Biol.*
- [35] Deveau, A; Bonito, G; Uehling, J; Paoletti, M; Becker, M; Bindschedler, S; Hacquard, S; Hervé, V; Labbé, J; Lastovetsky, O A; Mieszkin, S; Millet, L J; Vajna, B; Junier, P; Bonfante, P; Krom, B P; Olsson, S; Elsas, J D van; Wick, L Y (2018). Bacterial - Fungal Interactions: ecology, mechanisms and challenges. *FEMS Microbiology Reviews*. doi:10.1093/femsre/fuy008
- [36] Scherlach, Kirstin; Graupner, Katharina; Hertweck, Christian (2013). Molecular Bacteria-Fungi Interactions: Effects on Environment, Food, and Medicine. *Annual Review of Microbiology*, 67(1), 375–397. doi:10.1146/annurev-micro-092412-155702
- [37] H. Shimomura, K. Hosoda, S. Hayashi, K. Yokota, Y. Hirai, (2012). J. Bacteriol. Phosphatidylethanolamine of *Helicobacter pylori* Functions as a Steroid-Binding Lipid in the Assimilation of Free Cholesterol and 3 β -Hydroxyl Steroids into the Bacterial Cell Membrane. doi: 10.1128/JB.00105-12
- [38] Anthony P. Moran (1995). Cell surface characteristics of *Helicobacter pylori* 10(3-4), 271–280. doi:10.1111/j.1574-695x.1995.tb00043.x
- [39] J. Ojeda, M. Dittrich in: *Microbial Systems Biology: Methods and Protocols*, Methods in Molecular Biology, Navid A. Springer Science, 2012.
- [40] Palencia, Manuel (2018). Functional transformation of Fourier-transform mid-infrared spectrum for improving spectral specificity by simple algorithm based on wavelet-like functions. *Journal of Advanced Research*, 14(), 53–62. doi:10.1016/j.jare.2018.05.009
- [41] Andreas Barth (2007). Infrared spectroscopy of proteins. 1767(9), 1073–1101. doi:10.1016/j.bbabi.2007.06.004
- [42] Palencia M, Garcés-Villegas V, Restrepo DF, *et al.* (2020). Functionally-enhanced derivative spectroscopy (FEDS): a powerful tool to increase of spectral resolution in the mid-infrared advanced analysis of complex samples—a mini review. *J Appl Biotechnol Bioeng*. 7(1):43–46. doi: 10.15406/jabb.2020.07.00214
- [43] E Benitez, T Lerma, Alexander Córdoba (2017) Making of porous ionic surfaces by sequential polymerization: polyurethanes+ grafting of polyelectrolytes. *J. Sci. Technol. Appl* 2, 44-53
- [44] M. Palencia, S. Palencia, A. García. Vibrational spectrum characterization of outer surface of *helicobacter pylori* biofilms by functionally-enhanced derivative spectroscopy (feds) (2020). *J. of the Chilean Chemical Society*.
- [45] S. Palencia, M. Palencia, A. Gracia (2021). Mid-infrared vibrational spectrum characterization of outer surface of *Candida albicans* by Functionally-Enhanced Derivative Spectroscopy (FEDS). *J. Appl. Spectr.*
- [46] W. Jiang, A. Saxena, B. Song, *et al* (2004) Elucidation of functional groups on gram-positive and gram-negative bacterial surfaces using infrared spectroscopy. *Langmuir: the ACS Journal of Surfaces and Colloids*. doi: 10.1021/la049043+
- [47] G. J Thomas, Jr. Benevides, J. M. Overman, S. A. Ueda, T., Ushizawa, K. Saitoh, M. Tsuboi (1995). Polarized Raman spectra of oriented fibers of A DNA and B DNA: anisotropic and isotropic local Raman tensors of base and backbone vibrations. *Biophysical journal*, 68(3), 1073–1088. [https://doi.org/10.1016/S0006-3495\(95\)80282-1](https://doi.org/10.1016/S0006-3495(95)80282-1)
- [48] P. Mittl, L. Luthy, L. P. Hunziker, M. Grutter (2000). The Cysteine-rich Protein A from *Helicobacter pylori* a Lactamase. *Journal of Biological Chemistry*, 275(23), 17693–17699. doi:10.1074/jbc.M001869200.
- [49] Zanotti, Giuseppe (2014). Structural and functional aspects of the *Helicobacter pylori* secretome. *World Journal of Gastroenterology*, 20(6), 1402–. doi:10.3748/wjg.v20.i6.1402.
- [50] Garcia A, Salas-Jara MJ, Herrera C, González C (2014) Biofilm and *Helicobacter pylori*: From environment to human host. *World Journal of Gastroenterology* 20, 5632-5638. doi: 10.3748/wjg.v20.i19.5632.

- [51] Yonezawa H, Osaki T, Kamiya S (2015) Biofilm Formation by *Helicobacter pylori* and Its Involvement for Antibiotic Resistance. Biomed Research International 914791. doi: 10.1155/2015/914791.
- [52] Hathroubi S, Servetas SL, Windham I, Merrell DS, Ottemann (2018) *Helicobacter pylori* Biofilm Formation and Its Potential Role in Pathogenesis. Microbiology and Molecular Biology Review 82, e1-18. doi: 10.1128/MMBR.00001-18
- [53] A. Marqués, J M. Vítor, A. Santos, M. Oleastro, F. Vale (2020) Trends in *Helicobacter pylori* resistance to clarithromycin: from phenotypic to genomic approaches. doi.org/10.1099/mgen.0.000344.
- [54] Hua-Xiang Xia, Martin Buckley', Conor T. Keane, Colm A. O'Morain (1996) Clarithromycin resistance in *Helicobacter pylori*: prevalence in untreated dyspeptic patients and stability *in vitro*. J. Antimicrob. Chemother
- [55] S. Hathroubi, S. Servetas, I. Windham, D. Scott, K Ottemann (2018) *Helicobacter pylori* Biofilm Formation and Its Potential Role in Pathogenesis. Microbiol Mol Biol Rev
- [56] L. Andersen, A Dorland, H. Kara (2000). Possible Clinical Importance of the Transformation of *Helicobacter pylori* into Coccoid Forms. Scand. J. Gastroenterol.
- [57] P. Siavoshi, F., Nikbakht, B.G., Khormali, M., Sarrafnejad, A., Malekzadeh, R (2013). Localization of *H. pylori* within the Vacuole of *Candida* Yeast by Direct immunofluorescence Technique. Arch. Iran. Med.
- [58] P. Siavoshi, F., Nikbakht, B.G., Khormali, M., Sarrafnejad, A., Malekzadeh, R. 2013. Immunodetection of *H. pylori*-specific protein in oral and gastric *Candida* yeasts. Arch. Iran. Med.
- [59] A. Dubois, T. Borén (2007). *Helicobacter pylori* is invasive and it may be a facultative intracellular organism. Cell Microbiol.
- [60] D. Evans, D. Evans, D. Graham (1992). Adherencia e internalización de *Helicobacter pylori* por células HEp-2. Gastroenterol.
- [61] M. Alfatah, V. Bari, A. Nahar, S. Bijlani, K. Ganesan (2017). Critical role for CaFEN1 and CaFEN12 of *Candida albicans* in cell wall integrity and biofilm formation. Scientific Reports
- [62] P. Lipke, R. Ovalle (1998). Cell wall architecture in yeast: new structure and new challenges. J. Bacteriol.
- [63] X. Xie, P. Lipke (2010). On the evolution of fungal and yeast cell walls. Yeast.
- [64] S. Skrebinska, F. Mégraud, E. Bessède (2018). Diagnosis of *Helicobacter pylori* infection. Helicobacter 23(Suppl. 1)